
Environmental
Studies
Research
Fund

208-2

**Regional Assessment of Seabed Geohazard Conditions
Canadian Beaufort Outer Shelf and Upper Slope:
Legacy Data Synthesis**

**Évaluation régionale des géorisques du fond marin,
plate-forme continentale externe et talus supérieur de la
portion canadienne de la mer de Beaufort :
synthèse des données existantes**

Canada

August 2016

**REGIONAL ASSESSMENT OF SEABED GEOHAZARD CONDITIONS
CANADIAN BEAUFORT OUTER SHELF AND UPPER SLOPE:
LEGACY DATA SYNTHESIS**

SECTION 2

**GEOPHYSICAL AND GEOLOGICAL
DATA COMPILATION
OUTER SHELF AND UPPER SLOPE
SOUTHERN BEAUFORT SEA:
A HANDBOOK OF GEOHAZARD CONDITIONS**

REPORT DOCUMENT NO. 20110068-RPT-001 REV 2

**Woodworth-Lynas, C., S. Blasco, D. Duff, J. Fowler, E.B. İşler, J. Landva,
E. Cumming, A. Caines and C. Smith**

Prepared for: Environmental Studies Research
Funds
ESRF Secretariat
Natural Resources Canada
14th Floor, 14-C3-4
580 Booth Street
Ottawa, Ontario
K1A 0E4

2	CRN-969	C.W-L	J. Fowler	E.C	22 July 2016
1	Issued as Final	C.W-L	J. Fowler	E.C	4 December 2015
0	Issued as Final	C.W-L	L. Williams	E.C	14 September 2015
Draft C	Issued for Review	C.W-L	L. Williams	E.C	15 April 2015
Draft B	Issued for Review	C.W-L	D.D.	E.C	31 May 2013
Draft A	Issued for Review	C.W-L	D.D./J.F.	E.C	15 April 2013
Rev	Description	Prepared	Checked	Approved	Date

ABSTRACT

This handbook reviews a wide range of geological, acoustic and seismic geophysical data collected in the southern Canadian Beaufort Sea since the 1970's up to and including 2010. The purpose has been to analyze these data and to produce a basic reference that describes and interprets features and anomalies that represent potential geohazards on the modern seafloor, and beneath it to a depth of approximately 1000 m. Examples of each type of geohazard are illustrated. The focus has been on delineating geohazards on the continental slope, a region which was largely unknown prior to the early 2000's. The handbook also discusses the problem of subsea permafrost on a section of the Beaufort Shelf extending from the shelf margin landwards to the Amauligak F-24 discovery well. At this location in 1988 a geotechnical borehole was drilled to a depth of 468 m below seafloor, which is to this day the only fully sampled borehole through ice-bearing sediments on the shelf. Features on and beneath the outer Mackenzie Trough and Yukon Shelf are also described. The relatively well known Late Quaternary development of the continental shelf, together with new knowledge of the continental slope is combined in an evolutionary chronostratigraphic framework (see Enclosure 9 for synthesis).

A variety of potential geohazards are documented, some for the first time in public literature. Continental slope seafloor and near-seafloor geohazards include:

- *Slope Failures*, including the large Ikit Slump
- *Seafloor Offsets/Faults*
- *Fluid escape features (FEFs)*, large-scale mounds associated with eruptive flows
- *Pockmarks*
- *Seafloor Erosion*, in a linear region on the upper slope
- *Paleo-Scour Zone*, a shelf-parallel region of buried relict ice keel scour marks on the upper slope
- *Sheet-like and Ribbon-like mass transport deposits (MTDs)*
- *Mega-Scale Glacial Lineations*.

Potential geohazards more than 100 m below seafloor include:

- *Buried Mass Transport Deposits*
- *Faults*
- *Amplitude Anomalies*, associated with possible gas
- *Gas Hydrates*.

Continental shelf (Beaufort and Yukon Shelves and Mackenzie Trough) seafloor and near-seafloor geohazards include:

- *Acoustic Permafrost*
- *Shallow Water Flow Potential*, based on end of well drilling reports
- The *FEF Zone*, a narrow belt of small-scale, positive relief fluid escape features along the shelf margin

- *Water Column Anomalies*, caused by escaping methane along parts of the shelf margin
- *Shelf FEFs*, isolated features landward of the FEF Zone
- *Relict Ice Scour Marks*
- *Paleo-Scour Zones* on the margins of Mackenzie Trough, and buried beneath the Trough
- *Modern Ice scour*
- *Seafloor Erosion* along the western flank of Mackenzie Trough
- *Pockmarks*.

Continental shelf potential geohazards more than 100 m below seafloor include:

- *Amplitude Anomalies*, associated with possible gas
- *Gas Hydrates*.

ACKNOWLEDGEMENTS

Funding for producing the Southern Beaufort Sea: A Handbook of Geohazard Conditions was provided by the Environmental Studies Research Fund (ESRF), Program of Energy Research and Development (PERD), and the Beaufort Regional Environmental Assessment program (BREA). Data for the study were contributed by Natural Resources Canada, Earth Science Sector, Geological Survey of Canada; ArcticNet Seabed Mapping Project; ION Geophysical, GX Technology; BP Exploration Company; Imperial Oil Resources Ventures Ltd.; Chevron Canada Ltd.; ConocoPhillips Canada Resources Corp. Special thanks are due to Patrick Campbell (Canadian Seabed Research Ltd.) for assistance with data requests and to the Inuvialuit Game Council for advice and support during this project.

We gratefully acknowledge the helpful input and comments provided on the draft report by the ESRF Technical Advisory Group comprising Linda Graf and Karen Muggeridge (ConocoPhillips), Kevin Hewitt (Chevron), Jim Thompson (BP Exploration Company), George Reid (Imperial Oil Resources Ventures Ltd.), Ben Seligman (Shell), Shannon Vossepoel (Arctic Institute of North America) and Hugh Bain (ESRF).

The draft report has benefitted from a critical review by Brian MacLean and Gordon Cameron (Geological Survey of Canada-Atlantic). We especially thank the Scientific Authority for this study, Mr. Steve Blasco, for his help, guidance and useful discussions.

Requests for data used in this study should be directed to one of the following:

Geological Survey of Canada-Atlantic
Bedford Institute of Oceanography
P.O. Box: 1006
Dartmouth, Nova Scotia B2Y 4A2
Canada
Phone: (902) 426-2730
Fax: (902) 426-1466

BP Exploration Company
240 4th Avenue SW
Calgary, Alberta T2P 2H8
Canada
Phone: (403) 233-1313

ConocoPhillips Canada
P.O. Box 130, Stn. M
401 9th Avenue SW
Calgary, Alberta T2P 2H7
Canada
Phone: (403) 233-3323



Beaufort Sea Exploration Drilling Program
Imperial Oil Resources Ventures Limited
385 Quarry Park Blvd. S.E.
P.O. Box 2480, Station M
Calgary, Alberta T2P 3M9
Canada

CONTENTS

	Page
1. INTRODUCTION	1-1
1.1 Purpose and Scope	1-1
1.2 Geodetics	1-2
2. DATABASE	2-1
2.1 Legacy Geophysical Data	2-1
2.2 Digital Geophysical Data	2-1
2.2.1 Multibeam Bathymetry Data	2-1
2.2.2 Seismic Data	2-2
2.2.3 Sub-bottom Profiler Data	2-2
2.3 Geotechnical Data	2-2
2.3.1 Radiocarbon Dates	2-3
2.4 Offset Well Data	2-3
3. REGIONAL SETTING	3-1
3.1 Regional Structure and Stratigraphy	3-1
3.1.1 Yukon Shelf	3-2
3.1.2 Mackenzie Trough	3-2
3.1.3 Beaufort Shelf	3-6
3.1.4 Continental Slope	3-8
3.1.5 Late Quaternary Evolution of the Southern Beaufort Sea	3-10
3.2 Regional Seismicity	3-11
4. REGIONAL FRAMEWORK AND CORRELATIONS	4-1
4.1 Stratigraphic Nomenclature	4-1
4.2 Correlations	4-1
4.2.1 Yukon Shelf and Mackenzie Trough	4-1
4.2.2 Yukon Shelf, Mackenzie Trough and Beaufort Shelf	4-2
4.2.3 Mackenzie Trough and Continental Slope	4-5
4.2.4 Beaufort Shelf and Continental Slope	4-5
4.3 Correlation Difficulties	4-7
5. SEAFLOOR CONDITIONS AND GEOHAZARD FRAMEWORK	5-1
5.1 Continental Slope Bathymetry and Morphology	5-1
5.1.1 Slope Failures	5-1
5.1.2 Seafloor Offsets/Faults	5-3
5.1.3 Seafloor Gradient	5-3
5.1.4 Expressions of Buried Topography	5-3
5.1.5 Large-scale FEFs	5-5
5.1.6 Streamlined FEFs	5-6
5.1.7 Seafloor Erosion	5-7
5.1.8 Pockmarks	5-8
5.1.9 Paleo-Scour Zone	5-8
5.2 Beaufort Shelf Bathymetry and Morphology	5-10
5.2.1 FEF Zone	5-11

5.2.2	Water Column Anomalies	5-12
5.2.3	Shelf FEFs	5-12
5.2.4	Relict Ice Scour Marks	5-12
5.3	Mackenzie Trough/Yukon Shelf Bathymetry and Morphology	5-13
5.3.1	Modern Ice scour	5-13
5.3.2	Paleo-Scour Zone	5-14
5.3.3	Seafloor Erosion	5-14
5.3.4	Pockmarks	5-14
5.4	Anthropogenic Seafloor Features	5-14
6.	GEOLOGIC CONDITIONS AND GEOHAZARD FRAMEWORK: UPPER ~100 M BSF	6-1
6.1	Continental Slope	6-1
6.1.1	Sheet-like MTDs	6-1
6.1.2	Ribbon-like MTDs	6-2
6.1.3	Seafloor Offsets/Faults	6-2
6.1.4	Mega-Scale Glacial Lineations	6-3
6.1.5	Slope FEFs	6-3
6.1.6	Paleo-Scour Zone	6-4
6.2	Beaufort Shelf	6-4
6.2.1	Acoustic Permafrost	6-4
6.3	Mackenzie Trough/Yukon Shelf	6-11
6.3.1	Mackenzie Trough Unconformity	6-11
6.3.2	Shallow Stratigraphy	6-12
6.3.3	Paleo-Scour Zones	6-14
6.4	Shallow Water Flow Potential	6-14
6.4.1	Background	6-14
6.4.2	Assessment of SWF Potential in the Study Area	6-15
7.	GEOLOGIC CONDITIONS AND GEOHAZARD FRAMEWORK: ~100 m to ~1000 m BSF	7-1
7.1	Continental Slope	7-1
7.1.1	Buried Mass Transport Deposits	7-2
7.1.2	Stratified Sediments	7-3
7.1.3	Faults	7-3
7.1.4	Slope FEFs	7-3
7.1.5	Amplitude Anomalies	7-4
7.1.6	Gas Hydrates	7-4
7.2	Beaufort Shelf	7-5
7.2.1	Permafrost	7-5
7.2.2	Gas Hydrates	7-5
7.3	Mackenzie Trough/Yukon Shelf	7-6
7.3.1	Amplitude Anomalies	7-6
8.	GEOHAZARD OVERVIEW	8-1
8.1	Slope Failure	8-1
8.2	Shallow Water Flow	8-2
8.3	Faults	8-2
8.4	Seafloor Gradient	8-3

8.5	Fluid Escape Features	8-3
8.6	Seafloor Erosion	8-4
8.7	Ice Keel Turbates	8-4
8.8	Boulders and Ice-Rafted Debris	8-4
8.9	Acoustic Permafrost	8-5
8.10	Shallow Gas and Hydrate Potential	8-5
8.11	Wellbore Instability and Tight Spots	8-5
8.12	Seismicity and Tsunamis	8-5
8.13	Anthropogenic Features	8-6
9.	DISCUSSION AND RECOMMENDATIONS	9-1
9.1	Data Gaps	9-1
10.	REFERENCES	10-1

LIST OF TABLES

Table 2.1:	2D and 3D seismic data sources	2-2
Table 2.1:	Source for C₁₄ dates	2-3
Table 2.3:	Regional offset wells, southern Beaufort Sea	2-5
Table 3.1:	Mackenzie Trough seismostratigraphy	3-3
Table 3.2:	Updated Mackenzie Trough seismostratigraphy	3-4
Table 6.1:	Cores used for calculating average slope sedimentation rates	6-16
Table B.1:	C₁₄ dates for cores located within the Beaufort Sea	19
Table B.2:	Sedimentation rates for cores located within undisturbed strata	22

LIST OF APPENDICES

A	Methodology: Radiocarbon Age Calibration
B	Calibrated C₁₄ Dates and Sedimentation Rates

LIST OF PLATES

SECTION 1:

- 1.1 Regional Setting and Location Map, Southern Beaufort Sea

SECTION 3:

- 3.1 Deep crustal structure across the centre of the Beaufort Shelf
 3.2 Plio-Pleistocene stratigraphy of the Beaufort Shelf/Mackenzie Trough
 3.3 Legacy sub-bottom profile, line 80-507 from Mackenzie Trough
 3.4 Zoomed in legacy sub-bottom profile, line 80-507 from Mackenzie Trough
 3.5 Beaufort Shelf schematic north-south stratigraphic cross-section
 3.6 Colour-coded onshore/offshore chronostratigraphic correlation
 3.7 Sub-bottom profile line 0302_2010_260_1430 illustrating continental slope units/horizons

- 3.8 2D cross-slope seismic profile
- 3.9 Earthquake Epicentres and Magnitudes

SECTION 4:

- 4.1 Correlation between slope stratigraphies developed by Fugro and the Geological Survey of Canada
- 4.2 Stratigraphic relationships, southern Beaufort Sea
- 4.3 Shelf to slope schematic cross-section
 - 4.4 Mackenzie Trough and Yukon Shelf transition
- 4.5 Mackenzie Trough schematic cross-section
- 4.6 Mackenzie Trough and Beaufort Shelf transition
- 4.7 Sub-bottom Profile, Line 0037_2004_185_1741_0003kHz_Ch0_0_utm, in Mackenzie Trough
- 4.8 Schematic, shelf to slope cross-section showing the most recent Geological Survey of Canada model
- 4.9 Sub-bottom Profile, Line 0139_2010_257_0708, across Kugmallit Channel on the Upper Slope
- 4.10 Sub-bottom Profile, Line 0099_2010_254_0445, showing basal ice scour mark topography

SECTION 5:

- 5.1 The Ikit Slump, a large retrogressive slope failure
- 5.2 Retrogressive slope failure on the middle slope
- 5.3 Perspective and cross-sectional profile views of gullied topography on the mid-slope region
- 5.4 Perspective and longitudinal profile views of gullied topography on the mid-slope region
- 5.5 Illustration of curved and coalescing gullied topography on the lower slope
- 5.6 Sub-bottom Profile, Line 0052_2010_250_0601, showing grooves on the H5 horizon
- 5.7 Perspective and profile view showing seafloor expression of grooves on the horizon H5
- 5.8 Multibeam image of a large FEF
- 5.9 Sub-bottom profile, Line 092571951, through a large FEF
- 5.10 Illustration of streamlined FEFs
- 5.11 Sub-bottom Profile, Line 042081227, illustrating truncated Unit 1 sediments
- 5.12 Perspective and profile views of a group of pockmarks
- 5.13 Perspective view of the Paleo-Scour Zone
- 5.14 Perspective and profile view of the FEF Zone showing coalesced cones
- 5.15 Sub-bottom Profile, Line 0085_2010_252_0953, showing two distinct buried scour marks
- 5.16 The Paleo-Scour Zone as interpreted by Hill *et al.* (1982)
- 5.17 Sub-bottom Profile, Line Cone_2009_250_23_27_41, showing the interpreted Paleo-Scour Zone
- 5.18 MBES perspective view towards the southeast showing seafloor “wrinkles” in the FEF Zone
- 5.19 Water column anomalies at the shelf margin
- 5.20 Water column plume
- 5.21 Perspective view of an FEF that has grown through an ice scour mark

- 5.22 Perspective view of an ice scour mark cutting across a subdued FEF
- 5.23 Perspective and profile views of a 7 km-long ice scour mark on the Beaufort Shelf
- 5.24 Dendritic valley network, outer Mackenzie Trough
- 5.25 Chute-like valley network below 1000 m water depth

SECTION 6:

- 6.1 Time slices of 3D seismic data
- 6.2 Sub-bottom Profile, Line 092780111, showing an example of buried MTD's
- 6.3 Example of a single, ribbon-like buried MTD in Unit 2 sediments
- 6.4 Sub-bottom Profile, Lines 092571339 & 092571436, showing gas pillars above a buried MTD
- 6.5 Illustration of small-scale faults that offset the seafloor
- 6.6 2D seismic profile through a large FEF
- 6.7 Sub-bottom Profile, Line 092580826, through a slope FEF
- 6.8 Example of buried FEF flows around a slope FEF
- 6.9 Photographs of core PC-31
- 6.10 Log of core PC-31
- 6.11 Sub-bottom profile north of Amauligak borehole 3F-24
- 6.12 High-resolution multichannel seismic profile showing acoustic permafrost
- 6.13 Map of depth to fully frozen ice-bearing permafrost in the Beaufort Mackenzie Basin
- 6.14 Location of GSC Amauligak 3F-24 borehole and regional 2D seismic lines
- 6.15 Velocity logs, lithology and ice content of the Amauligak 3F-24 borehole
- 6.16 Examples of P-cable data comparisons with high resolution 2D and reprocessed 3D data
- 6.17 P-cable data comparison
- 6.18 Sample images from Zhu *et al.* (2011)
- 6.19 Location map of the Mallik 3D survey
- 6.20 Mackenzie Trough/Yukon Shelf multibeam bathymetry and profile
- 6.21 Current-formed comet marks affect the Unit MT2 relict ice scour surface
- 6.22 Example of the calculation of sedimentation rates (core BP10-PC02)

SECTION 7:

- 7.1 Cross-shelf 2D seismic profile
- 7.2 Downslope seismic profile
- 7.3 2D cross-slope seismic profile
- 7.4 Example of cross-slope 2D seismic profile
- 7.5 Unconformities and buried topography
- 7.6 2D seismic profile showing possible spreading blocks in a near-surface MTD
- 7.7 2D seismic profile across Outer Mackenzie Trough
- 7.8 2D seismic profile from Yukon Shelf to the Continental Slope
- 7.9 2D seismic profile in the Amauligak discovery region
- 7.10 Example of scanned 2D seismic profile from the Mackenzie Trough

SECTION 8:

- 8.1 DND Legacy Sites, Southern Beaufort Sea



LIST OF ENCLOSURES

- 1 Multibeam Bathymetry Map, Southern Beaufort Sea
- 2 Survey Trackplot Map, Southern Beaufort Sea
- 3 Multibeam Bathymetry, Core and Borehole C₁₄ Dates Map, Southern Beaufort Sea
- 4 Sub-bottom and 2D Seismic Profiles, Line 80-507, Southern Beaufort Sea
- 5 Seafloor Gradient Map, Southern Beaufort Sea
- 6 Ikit Slump Scarp Repetitive Mapping 2006-2009
- 7 Seismic Profile Across Yukon shelf-Outer Mackenzie Trough-Continental Slope-Beaufort Shelf-Amauligak 3F-24 Borehole, Southern Beaufort Sea
- 8 2D and 3D Seismic Profile Comparisons, Southern Beaufort Sea
- 9 Late Quaternary Evolution of the Southern Beaufort Sea

LIST OF ABBREVIATIONS

APF	Acoustic permafrost
ASTIS	Arctic Science and Technology Information System
BP	Before Present (cal years BP refers to calibrated radiometric dates)
BSF	Below Seafloor
BSS	Below Sea Surface
C ₁₄	Radiocarbon
CMP	Common Mid-point
CSR	Canadian Seabed Research
DND	Department of National Defence
EL	Exploration Lease
ESRF	Environmental Studies Research Fund
FEF	Fluid Escape Feature
FGP	Frontier Geoscience Program
Fugro	Fugro GeoSurveys, a division of Fugro Canada Corp.
GoM	Gulf of Mexico
GSC	Geological Survey of Canada
GSC-A	Geological Survey of Canada – Atlantic
IBPF	Ice-Bearing Permafrost
IRD	Ice-Rafted Debris
JAMSTEC	Japan Agency for Marine Earth Science and Technology
LGM	Last Glacial Maximum
MBES	Multibeam Echosounder
MGL	McGregor Geoscience Ltd.
MSCL	Multi-Sensor Core Logger
MSGL	Mega-Scale Glacial Lineations
MTD	Mass Transport Deposit
Myr	Million years
NAD	North American Datum
PLF	Pingo-like Feature
SBP	Sub-Bottom Profile
SPZ	Saturated Paleo-Scour Zone
SSZ	Saturated Scour Zone
SWF	Shallow Water Flow
TAP	Tarsiut-Amauligak Pull-Apart
UTM	Universal Transverse Mercator
UXO	Unexploded Ordnance
U/C	Unconformity
VSP	Vertical Seismic Profile
2D	2-Dimensional
2DHR	2-Dimensional High Resolution
3D	3-Dimensional
3DSO	3-Dimensional Short Offset

1. INTRODUCTION

1.1 Purpose and Scope

The Environmental Studies Research Fund (ESRF) in collaboration with industry participants and the Geological Survey of Canada (GSC) commissioned a synthesis project of legacy data for the southern Canadian Beaufort Sea. The purpose of the project was to locate, catalogue, digitize, database and analyze geophysical, geological and geotechnical data collected over the Beaufort Sea outer continental shelf and slope (Plate 1.1). A detailed report on the state of knowledge of geohazards on and beneath the Beaufort Shelf has been published by the GSC (Blasco *et al.* 2011). The present study is a companion to the GSC work focusing primarily on the continental slope, but including parts of the outer Mackenzie Trough and Yukon shelf that fall within the study area. In addition a review of the difficulties and potential solutions to permafrost mapping on the Beaufort Shelf is presented.

Fugro GeoSurveys, a division of Fugro Canada Corp. (Fugro) was contracted to review legacy geological and geophysical data in order to evaluate and update the regional geological framework with the prime objective of identifying and assessing potential geohazards and their distribution in the southern Beaufort Sea. A geohazard can be defined as “a geological state that represents or has the potential to develop further into a situation leading to damage or uncontrolled risk” (e.g. Piper, 2012). Seafloor and sub-seafloor geohazards have been identified and the potential processes and formation mechanisms associated with each type of hazard are described. A second objective is to link stratigraphies and associated depositional and erosive processes of the shelf and Mackenzie Trough to the continental slope, and to provide a glacial chronostratigraphic framework for geohazard assessment.

Data reviewed were acquired in water depths ranging from 60 m to 1500 m between the years 1980 and 2010. Particular features, such as regions of slope failure, fluid escape features (FEFs) and shallow gas, are described and illustrated. Seafloor and sub-seafloor features are described, and discussed in terms of the potential constraints to oil and gas exploration. In particular, an understanding of seafloor/sub-seafloor stability is essential in the design of seabed-based facilities, such as anchors, wellhead assemblies and pipelines.

The geohazards analysis integrated existing public and proprietary information, and included assessments of:

Seafloor Conditions (e.g. Seafloor topography, lithology, dips, direct and indirect indicators of geotechnical properties of seafloor sediments, and associated potential seafloor hazards).

Near-surface Conditions (e.g. Shallow faulting/slumping, gas escape structures, major shallow lithologic/unit boundaries, relic features such as slumping/faulting, direct and

indirect indicators of geotechnical properties of near-surface sediments, and other shallow sub-seafloor hazards).

Deeper Conditions (e.g. Deeper unit boundaries, evidence of shallow gas, faulting, direct and indirect indicators of geotechnical properties of deeper sediments, and other deeper sub-seafloor hazards).

The following report sections describe the datasets used in the compilation, the regional geological setting, the seafloor, shallow and subsurface geological conditions, and identified drilling hazards and constraints, as well as recommendations. Page-size plates are inserted at the end of each report section. References, appendices and large-scale map enclosures are included at the back of the report. The digital version of the report contains all text and illustrations in Adobe Acrobat PDF document format.

1.2 Geodetics

Results are presented using NAD83, CSRS, UTM Zone 8 as the horizontal datum. Details are given below.

Horizontal Datum

Reference Ellipsoid: GRS80

Datum Name: NAD83 CSRS

Semi-Major Axis: 6 378 137.000 metres

Semi-Minor Axis: 6 356 752.314 metres

Flattening: 1/298.257222101028

Mapping Projection

Projection: Universal Transverse Mercator

Zone: 8

Central Meridian: 135° W

False Easting: 500 000 metres

False Northing: 0 metres

Scale at the CM: 0.9996

350000

425000

500000

575000

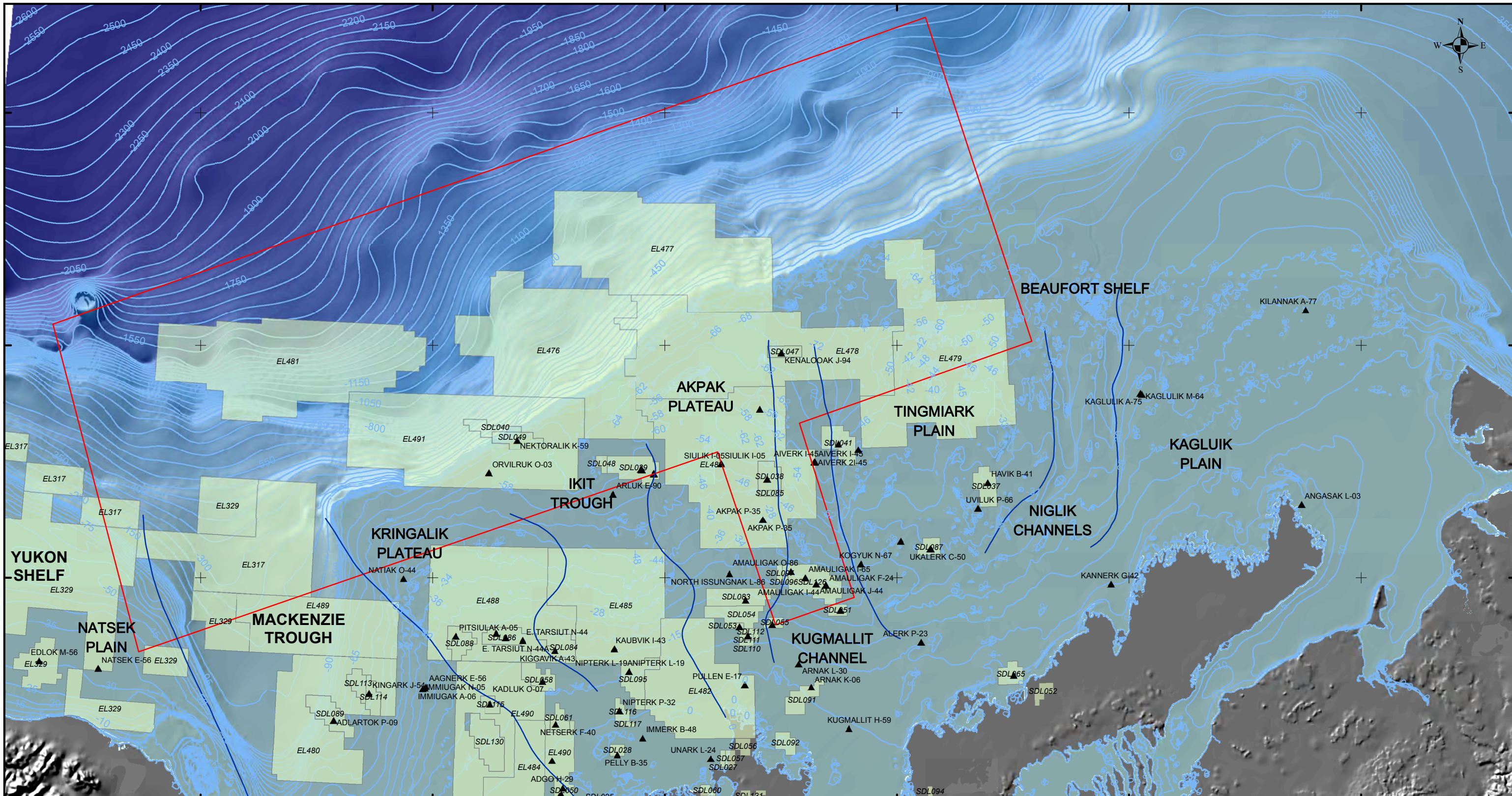
650000

725000

7925000

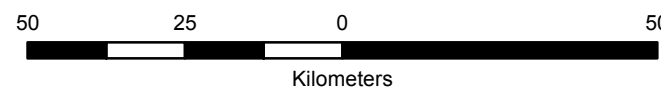
7850000

7775000



NAD83 UTM ZONE 8

DWG No.: 20110068-LOC-BEAU-P11-0



- ▲ EXISTING WELLS
- GEOLOGY PHYSIOGRAPHIC REGIONS
- BATHYMETRY CONTOURS

- ▭ STUDY AREA
- ▭ LEASE BLOCKS



**REGIONAL SETTING AND LOCATION MAP
SOUTHERN BEAUFORT SEA**

2. DATABASE

2.1 Legacy Geophysical Data

A large database of seismic and acoustic profiles has been collected from the Beaufort Shelf and upper slope region since the initial surveying voyage of CSS *Hudson* during its circumnavigation of the Americas in 1970 (e.g. Edmonds, 1973). Most of these datasets were collected on the continental shelf by the oil and gas industry.

Much of the legacy geophysical seismic and sub-bottom profiler data are in the form of paper records. The Arctic Science and Technology Information System (ASTIS) which is maintained by the University of Calgary, was contracted to compile the Beaufort Sea legacy database. ASTIS completed the database prior to the start of this study and have catalogued legacy data that are now documented in an Excel spreadsheet.

Initially, the present study was intended to review (on a prioritized basis within the established budget) all available legacy hard copy and digital data. However it was quickly appreciated that wholesale scanning of legacy (hard copy) data would require a disproportionate amount of time and available funding. Additionally, XY navigation data were unavailable for the majority of legacy data, such that the relocation of track lines could not be performed. Ultimately it was decided in consultation with the Scientific Authority and the ESRF Technical Advisory Group that this study would focus on the digital data available and supplement these where necessary with legacy hard copy data.

In particular, one hard copy legacy seismic and concurrent sub-bottom profile line (80-507), collected in 1980 provided by the GSC-A, was scanned. This particular line, although situated along the southern margin of the study area, was selected because it includes a complete NE-SW profile across the Mackenzie Trough and onto the Beaufort and Yukon shelves. Both the 80-507 seismic and sparker sub-bottom profiles are co-registered and have been used as the basis for key regional interpretations by previous researchers (O'Connor and Blasco, 1982; 1986).

2.2 Digital Geophysical Data

2.2.1 Multibeam Bathymetry Data

Multibeam bathymetry data has been collected in the southern Canadian Beaufort Sea by both the Geological Survey of Canada and University of New Brunswick as part of the ArcticNET program. Data used for this study were collected between 2001 and 2010, generally concurrently with sub-bottom profiler data acquisition from the research vessels CCGS *Amundsen* and CCGS *Nahidik*. Vertical resolution varies with water depths and between collection systems but generally ranges from ± 0.5 m on the Beaufort and Yukon shelf regions to as much as ± 5 m at slope water depths of ~ 1000 m. The datasets have been combined and compiled as a single bathymetric image with a horizontal resolution of 20 m (Enclosure 1).



2.2.2 Seismic Data

Numerous 2D and some 3D seismic programs have been completed in the southern Canadian Beaufort Sea. A selection of digital and scanned 2D seismic reflection profiles and a 3D volume were made available for this study from a variety of different sources (see Table 2.1). For the present study all seismic profiles included data to a depth of 750 m below seafloor. Data quality and resolution vary amongst the different datasets, with the poorest generally being associated with the legacy scanned data. The BeaufortSPAN East dataset, provided by ION Geophysical, was of excellent quality and has been used to display most examples of geological structure and regional framework for this study. The locations of the survey lines and of representative profiles are shown on Enclosure 2. Comparisons between representative BeaufortSPAN, GSC 2D and legacy profiles and corresponding selected 3D profiles are reproduced on Enclosure 8. The BeaufortSPAN and corresponding 3D profiles are comparable in terms of vertical and horizontal resolution and are the most useful for analysis of geological conditions and geohazard framework below ~100 m BSF (Enclosure 8 panels A and B). A typical legacy profile although partially resolving key reflectors lacks stratigraphic detail revealed by the corresponding 3D line (Enclosure 8 panel C). GSC lines tuned to focus on large scale, deep seated crustal structure are of poorer horizontal resolution compared to BeaufortSPAN and 3D profiles (Enclosure 8 panel D)

All lines have been reviewed during this study, however only select lines have been interpreted. Representative 3D seismic data in lease block EL 476 were made available by Imperial Oil.

Table 2.1: 2D and 3D seismic data sources

Source	Year Data Collected	Number of Lines Available
Geological Survey of Canada (2D)	1980 – 2010	32
ION GXT: BeaufortSPAN East (2D)	2006-2009	19
Imperial Oil (3D)	2009	volume

2.2.3 Sub-bottom Profiler Data

An extensive database of sub-bottom profiler data exists for the southern Canadian Beaufort Sea (Enclosure 2). Data were collected using Knudsen and boomer sub-bottom profiler systems aboard the CCGS *Amundsen* and CCGS *Nahidik* between 2001 and 2010. In 2009 and 2010, a dense grid of survey data was acquired to the northeast of Mackenzie Trough on the continental slope and shelf margin. Much of the remainder of the study area has sparse coverage, in the form of regional survey lines. A potentially useful dataset from the Mackenzie Trough, collected jointly by the Japan Agency for Marine Earth Science and Technology (JAMSTEC) and GSC in 2002 could not be used due to problems with corrupted data files.

2.3 Geotechnical Data

Numerous piston, trigger weight and box cores have been collected in the southern Canadian Beaufort Sea from 1980 to 2010. A total of 47 cores, boreholes and wells with

available radiometric age dates were selected for use in this study (Table 2.2), comprising 25 industry and 22 GSC/ArcticNet datasets.

Table 2.1: Source for C14 dates

Source	Number of radiometric dates	Number of cores, boreholes or wells
GSC/ArcticNet	58	22 cores and boreholes
Imperial Oil	23	13 piston cores
BP	15	10 piston cores
Dome Texaco <i>et al.</i>	1	1 well (Uviluk P-66)
Gulf Canada <i>et al.</i>	1	1 well (Tarsiut N-44)

2.3.1 Radiocarbon Dates

A total of 98 calibrated C₁₄ dates from 47 cores, boreholes and wells were used to help correlate and constrain the age relationships between acoustic and seismic stratigraphies on the shelf, slope and in the Mackenzie Trough (Enclosure 3). The datasets include two uncalibrated dates from the Dome Gulf Hunt Kopanoar I-44 well; these dates could not be calibrated because the original laboratory sheets indicating how the uncalibrated dates were derived could not be sourced.

All radiocarbon (C₁₄) ages compiled were converted to calibrated years BP (cal years BP) using the IntCal Marine 09 curve (Reimer *et al.* 2009) applied within Calib Rev 6.0.0 software (Stuiver and Reimer, 1993; Stuiver *et al.* 2005), with its default mean global reservoir correction of 408 yr. A local reservoir age correction (ΔR) of 420 \pm 40 was used for the study area (McNeely *et al.* 2006; Coulthard *et al.* 2010). As per Stuiver and Reimer (op. cit.) results are rounded to the nearest 10 years for samples where standard deviation in the radiocarbon age is greater than 50 years (e.g. 8015 \pm 63 cal years BP = 8020 \pm 63 cal years BP). The calibration procedure is given in Appendix A and C₁₄ dates are given in Appendix B.

2.4 Offset Well Data

A significant number of exploratory wells have been drilled on the Beaufort Shelf, mostly landward of the study area (Plate 1.1). Drilling histories and geological reports for 26 exploratory wells located on the Beaufort Shelf have been reviewed to identify previously encountered tophole drilling hazards and constraints. A synopsis of wells reviewed for the present investigation is provided in Table 2.3. The wells were drilled between 1976 and 1989, in water depths from 26 m to 64 m. Lithologies encountered in the shallow section typically consisted of clays/claystones with interbeds of unconsolidated sand/sandstone.

Discontinuous permafrost of varying thickness was encountered in many of the wells. Observed depths to base of permafrost ranged from ~150 m BSF to 776 m BSF. A common condition was the presence of elevated gas content in porous sand/sandstone below the discontinuous permafrost boundary. It appears that the permafrost forms a cap that traps upward migrating gas which is abnormally pressured. In their analysis of well



data Weaver and Stewart (1982) report that 99.5% of formation gas in the upper 2000 m of sediment is methane.

Wellbore stability problems due to Shallow Water Flow (SWF) forced abandonment of the Kopanoar D-14 well, after penetrating overpressured saturated sand at 503 m BSF. Shallow overpressures were not observed in most wells. Wellbore stability problems were also experienced at Aiverk I-45 within permafrost-bearing unconsolidated sands, causing abandonment of the well.

Reports of loss of circulation were rare, although when they did occur it generally corresponded with the base of permafrost.

Table 2.3: Regional offset wells, southern Beaufort Sea

Well	UWI	Operator and Year	Easting	Northing	Water Depth (m)	Total Depth (m)	Drilling Hazards and Constraints
Dome Aiverk I-45 Kugmallit Channel	300I45703013 3300	Dome Petroleum Ltd. 1982	548637.86	7812248.76	64	730	Permafrost sand section became washed out and well was abandoned. Unconsolidated sand with clay encountered between 240-270 m BSL.
Akpak P-35 Akpak Plateau	300P3570201 34000	Gulf 1984-1985	531817.00	7793554.00	41	5169	Base of permafrost reported at 715 m BSF: Background gas increased from 0.4 to 4.8% at 769 m due to pocket of gas at the base of the permafrost
Akpak 2P-35 Akpak Plateau	302P3570201 34000	Gulf 1985	531820.63	7793739.50	41	3673	Base of permafrost was reported at 731 m BSF with corresponding spike in background gas values
Dome Hunt Irkaluk B-35 Akpak Plateau	300B3570401 34000	Dome Petroleum Ltd. 1982	530785.10	7831292.24	56	4860	Discontinuous permafrost from 40-100 m BSF.
Dome Hunt Kenalooak J(N)-94 Kugmallit Plateau	300N7050133 300	Dome Hunt 1979	538002.70	7847256.51	68	184	Abandoned due to mechanical difficulties: Permafrost from 37-99 m BSF.
Hunt Dome Kopanoar D-14 Ikit Trough	300D1470301 35000	Lamar Hunt 1976	496555.37	7808661.83	57	1077	Abnormally pressured water sand encountered at 503 m BSF: Water migrated from 503 m to the seafloor

**GEOPHYSICAL AND GEOLOGICAL DATA COMPILATION: SOUTHERN BEAUFORT SEA
A HANDBOOK OF GEOHAZARD CONDITIONS**



							enlarging the well boring causing the wellhead to lean and necessitate abandonment of the well
Dome Kopanoar I-44 Ikit Trough	30002300000 00000	Dome Petroleum Ltd. 1980	492504.39	7810028.76	59	649	Loss of circulation material at 309-312 m BSF which corresponded with the bottom of submarine permafrost. Hole abandoned due to mechanical failure
Dome Gulf Hunt Kopanoar L -34 Ikit Trough	300L3470301 35000	Dome Petroleum Ltd. 1979	492537.02	7809793.40	58	2015	Loss of circulation at 458-464 m BSF. Casing subsided in hole and hole was abandoned
Dome Hunt Kopanoar M - 13 Ikit Trough	300M1370301 35000	Hunt International Petroleum 1979	496524.39	7808474.31	57	4281	None documented.
Dome Hunt Nektoralik K-59 Ikit Trough	300K5970301 36001	Dome Petroleum Ltd. 1977	452232.16	7819497.70	64	2790	None documented.
Dome Nerlerk J-67 Tingmiark Plain	300J6770301 33000	Dome Petroleum Ltd. 1984	562467.5	7816355.1	45	4904	None documented.
Dome Nerlerk M-98 Tingmiark Plain	300M9870133 000	Dome Petroleum Ltd. 1982	556115.84	7818275.41	49	4940	None documented.
Gulf Aagnerk E-56 Mackenzie Trough	300E5669501 36450	Gulf Canada Corporation 1986	422817.02	7739756.19	33	1100	Well kick at 305 m. The cause was gas associated with a coal seam that extended from 300- 305 m.
Dome Natiak O-44 Kringalik Plateau	300O4470101 37000	Dome Petroleum	415487.8	7774758.4	44	4650	None documented.

**GEOPHYSICAL AND GEOLOGICAL DATA COMPILATION: SOUTHERN BEAUFORT SEA
A HANDBOOK OF GEOHAZARD CONDITIONS**



		Ltd. 1983					
Amauligak 2F-24 Kugmallit Channel	302F2470101 33300	Gulf Canada Resources Ltd. 1988	552030.6	7772559.5	32	4260	Tight hole conditions occurred from 1297- 846 m MD, and 1790-1290 m MD.
Amauligak 2F-24A Kugmallit Channel	302F2470101 33301	Gulf Canada Resources Ltd. 1988	552030.6	7772562.6	32	3760	None documented in the tophole section. Cement stringer encountered at 3229 m BSF.
Amauligak 2F-24B Kugmallit Channel	302F2470101 33302	Gulf Canada Resources Ltd. 1988	552034.6	7772568.8	32	4477	None documented.
Amauligak 2F-24BST Kugmallit Channel	302F2470101 33303	Gulf Canada Resources Ltd. 1988	552034.6	7772568.8	32	4577	None documented.
Immiugak N-05 Mackenzie Trough	300N0569501 37000	Gulf Canada Resources Ltd. 1989	421769.7	7739083.3	32	397	Well kick at 310 m. Lost circulation at 368 m. Well kick at 397 m. A high pressure gas zone was encountered. The well was then abandoned with small volumes of gas still emanating from the well.
North Issungnak L-86 Akpak Plateau	300L8670101 34000	Gulf Canada Resources Inc. 1982	520947.7	7776266.9	26	4771	Permafrost reported at two locations within the top 776 m BSF.

3. REGIONAL SETTING

3.1 Regional Structure and Stratigraphy

The Canadian Beaufort Shelf is approximately 1100 km in length, with an area of roughly 110000 km². It extends from Point Barrow, US, in the west to the Amundsen Gulf in the east. The shelf is divided into three regions: the narrow western shelf (Yukon shelf), the broad eastern shelf (Beaufort Shelf), and the Mackenzie Trough which serves as a divide between the western and eastern shelf regions (Plate 1.1).

The Beaufort-Mackenzie Basin is a sub-basin of the Canadian Arctic Passive Margin, a geological province that formed during the Late Jurassic to Mid-Cretaceous, associated with seafloor spreading which created the Canada Basin. Various concepts concerning the opening of the Arctic Ocean and an associated framework have been based on the continued collection of better quality seismic reflection data, as described by Lane (1997). However, deep 2D seismic reflection data (BeaufortSPAN, collected in 2006 and 2007 by ION Geophysical Corporation) suggest to Dinkelman *et al.* (2008) and Helwig *et al.* (2011) a return to the early hypothesis of rotational opening of the Canadian Basin and a northerly orientation of the paleo-spreading centre near the mouth of the Mackenzie River.

Normal faults accommodated northwestward extension leading to continent margin formation in Late Cretaceous time (ca. 95 Myr) (Lane, 2002). The faults are best developed beneath the Mackenzie Delta and Tuktoyaktuk Peninsula, and trap significant oil and gas accumulations, of which the Amauligak oil field, discovered in 1984, is the largest, with estimated recoverable reserves of 235 million barrels (NEB, 1998). The half-graben Tarsiut–Amauligak Pull–Apart (TAP) system accommodated 7 km of downfaulting in Oligocene to Mid-Miocene time (Helwig *et al.* 2011) (Plate 3.1). A variety of complex deformation processes from folding, thrusting, strike-slip faulting, extension, basin inversion and gravity-induced loading all operated in a narrow time frame during this period (Dinkelman *et al.* 2008).

Cenozoic deltaic sediments were deeply eroded during the Early Pliocene, creating a well-developed shelf-wide regional angular unconformity that passes laterally into a disconformity at the margins of the Beaufort-Mackenzie Basin (e.g. Blasco *et al.* 1990). Folds and faults are truncated by the unconformity, which marks the end of significant tectonism. Above the unconformity more than 3500 m of Pliocene to Pleistocene sediments of the Iperk and Shallow Bay Sequences have accumulated. The depocentre, containing the thickest sediment accumulation, is located in the region northeast of Kugmallit Channel (Blasco *et al.* 1990).

The Iperk Sequence records the gradual filling of the Beaufort-Mackenzie Basin by initial deep water prograding muds that grade up into slope, outer shelf and mid-shelf fine-grained sediments. These in turn pass up into Pleistocene outer and inner shelf clays, silts and sands and ultimately into fluvial and fluvio-glacial sediments (Blasco *et al.* 1990; Dixon *et al.* 1984; McNeil *et al.* 1982; Jones *et al.* 1980). The Iperk Sequence is unconformably capped by the relatively thin Shallow Bay Sequence, which comprises

predominantly fine-grained transgressive to open shelf shallow marine sediments of the Late Pleistocene and Holocene.

A regional seismic and chronostratigraphic framework for the Pliocene and Pleistocene succession has been developed and updated over the years with the analysis of biostratigraphic data and geophysical logs made available from a number of exploration wells (e.g. Dixon and Snowdon, 1979; Jones *et al.* 1980; McNeil *et al.* 1982; Dixon *et al.* 1984). Blasco *et al.* (1990) summarized previous work and provided higher resolution detail of the Pliocene to Pleistocene succession, particularly the uppermost portion from ~150 m below sea level to the modern seafloor. They drew on seismic and shallow acoustic stratigraphy and on carbon dates from industry exploration wells (e.g. Hill *et al.* 1985).

A geological model for the uppermost 100 m of the continental shelf, originally proposed by the Geological Survey of Canada, was expanded in 1980 and 1982 (O'Connor, 1980; O'Connor and Blasco, 1982) with the recognition of nine distinct physiographic regions. The model included new understandings about the nature and distribution of permafrost in sediments beneath the seafloor (O'Connor, 1981a), and an analysis of shelf edge morphology (O'Connor, 1981b). An analysis of the large industry geotechnical database provided information on soil type and condition on the shelf (O'Connor and Blasco, 1984). A synthesis of all available data on seafloor sediments and coastal morphology on the shelf and upper slope was presented in The Marine Science Atlas of the Beaufort Sea (Pelletier, 1984), and a companion geological and geophysical atlas followed in 1987 (Pelletier, 1987a). A further geological atlas (Dixon, 1996) synthesized knowledge of the Beaufort-Mackenzie Basin from a number of sources including marine seismic and well data.

3.1.1 Yukon Shelf

Above the well defined Early Pliocene unconformity, Upper Iperk Sequence strata form a wedge of sediments thickening northwards from ~100 m near the coastline to >700 m beneath the shelf margin (Lewis and Meagher, 1991; Blasco *et al.* 1990) (Plate 3.2 and Enclosure 4). Ten regression/transgression cycles are recognized in this sequence, and the upper erosive surfaces of several cycles are characterized by channels. Channels cut into the upper three cycles (from seafloor downwards, Units I, II and III), are oriented to the northeast, implying cross-shelf drainage in that direction during subaerial exposure. Progressively younger Upper Iperk Sequence strata are encountered towards the shelf margin and a single thermoluminescence date of >53000 cal years BP was recorded within Unit I (youngest) sediments (Blasco *op.cit.*). There are no Late Wisconsinan sediments on the shelf and Unit I, II and III sediments are either exposed at the seafloor or are covered by a thin veneer of Holocene sediments reworked from the underlying units.

3.1.2 Mackenzie Trough

The 150 km by 75 km north-northwest to south-southeast oriented Trough is submerged below sea level and cuts across the broad, flat continental shelf. The Trough was formed



during late Upper Iperk Sequence times and is easily recognizable in seismic profiles as a regional angular unconformity (Enclosure 4). On both margins the unconformity passes either conformably or disconformably into Upper Iperk Sequence strata beneath the Yukon and Beaufort shelves. The Trough was incised ~500 m into Upper Iperk Sequence and pre-Early Pliocene sediments probably by the action of glacial ice streams during the Early Wisconsinan (Blasco *et al.* 1990; 2007; 2011; Plate 3.2). The Trough is partially filled by more than 300 m of Quaternary sediments. Analysis of newly acquired 2D seismic reflection profiles by Batchelor *et al.* (2012) suggested evidence for two Quaternary ice advances by north-flowing ice streams in the Mackenzie Trough.

A synthesis of previous work and analysis of a grid of several seismic lines and sub-bottom profiles by MGL (1987) formalized the seismic stratigraphy of Mackenzie Trough into four units, for which sparse borehole data provided lithological information (Table 3.1). A further analysis of more recent seismic data led MGL (1992a) to identify thirteen units and seven regional unconformities within five sequences above the unconformity at the base of the Mackenzie Trough to account for lateral variation in facies and seismic character across and along the Trough (Table 3.2). The five sequences correlate with the four seismostratigraphic units originally defined by O'Connor and Blasco (1986) and MGL (1987).

A line of legacy seismic and sub-bottom profiler data collected in 1980 across the Trough shows the four units and highlights the two principal difficulties with attempts to tie the seismic stratigraphy to the adjacent shelf areas (Enclosure 4). The difficulties are that geological depositional environments and processes in the Trough and on the shelf were quite different, with thick accumulations of Trough sediment thinning to the point of being irresolvable on the shelf. In addition, permafrost in shelf sediments below Unit B masks stratigraphy in sub-bottom profiles, and velocity inversions in seismic data make correlations between unfrozen Trough and frozen shelf units very difficult.

**Table 3.1: Mackenzie Trough seismostratigraphy
(adapted from MGL, 1987)**

Unit Name	Lithology
MT1a	Clay
MT1b	Clay and silt
MT2	Clay and silt mud
MT4	Sand with organic layers
MT5	No data

Note: Unit MT3 of O'Connor & Blasco (1986) on the western side of Mackenzie Trough is an anomalous interval, now included in MT4 and is no longer used (e.g. MGL, 1987).



Table 3.2: Updated Mackenzie Trough seismostratigraphy (adapted from O'Connor and Blasco, 1986 and MGL, 1987; 1992a). Lithology is generalized with most data derived from boreholes and wells south of the study region. U/C = Unconformity.

Unit Name	Lithology	Sequence Number	Southern Trough	Eastern Trough	Central Trough	Western Trough	Northern Trough	North Slope of Yukon Shelf
MT1a	Clay	5	S20	S20	S20	S20	S20	S20
			U/C12					
MT1b	Clay & silt	4	S19					
			U/C11					
			S18	S18				
			U/C10					
MT2	Clay & silt mud	3	S17	S17	S17	S17	S17	S17
			U/C9a					
MT4	Sand with organic layers	2	S16	S16	S16			
			U/C9					
MT5	No data	1	S15	S15				
			U/C8					
MT4	Sand with organic layers	2	S14	S14	S14		S14c S14b S14a	
			U/C7					
MT4	Sand with organic layers	2	S13c	S13c	S13c	S13c		
					S13b	S13b		
MT4	Sand with organic layers	2			S13a		S13a	
			U/C7				S12?	
MT5	No data	1						S11
					S10?	S10?		S10
MT5	No data	1		S9	S9		S9	
					S8		S8	
MT5	No data	1					S7	
			U/C1					

For ease of description the simplified four stratigraphic units are used in this report, and are described in sequence from the seafloor down.

Unit MT1

Unit MT1 is the youngest unit in the Mackenzie Trough and extends between the top of Unit MT2 and the seafloor. The unit thins northwestwards from ~100 m south of the study region, and within the study area thins northwards from approximately 25 m to 20 m. Within the study area the unit is thinnest in the centre of the Trough and thickens along both Trough margins to a maximum of 120 m along the eastern margin against the Kringalik Plateau onto which it can be traced (Enclosure 4). The unit pinches out or is eroded at the seafloor along the western margin of the Trough. The unit is subdivided into lower (MT1b) and upper (MT1a) sub-units.

MT1a is distinguished from underlying Unit MT1b by a high amplitude reflection (Plate 3.4). MT1a comprises well developed parallel reflectors that drape and gradually mute topography inherited from the ice keel turbated upper surface of MT2 and from individual scour marks buried within MT1a (see Section 6.1.1). The clays of this sub-unit were deposited in open marine conditions (MGL, 1987), and the draped topography is progressively muted so that at the seafloor it has been almost completely erased. The unit can be traced northeastwards to the Kringalik Plateau of the Beaufort continental shelf where it onlaps the top of Unit MT2 on the eastern Trough margin before pinching out. Near the northeastern margin of the Trough a buried zone of hummocky and diffractive reflectors marks a thin interval of disturbed sediments interpreted as an ice keel turbate (Plate 3.3; see Section 4.2.2).

South of the study area Unit MT1b comprises interbedded sand, silt and clay deposited as clinoform reflectors of a prograding delta, formed during a sea level lowstand (Moran *et al.* 1989). The well defined delta front terminates immediately south of the study area. In the study area, Unit MT1b comprises a well developed series of parallel to slightly disconformable reflectors, likely of clay and silt, which drape the hummocky ice keel turbated surface of Unit MT2. Biostratigraphic analysis (Burden, 1986) indicates that MT1b was deposited in marginal marine conditions, presumably becoming progressively more open marine with distance northwards, away from the delta front. The draped topography of the ice scoured surface of underlying Unit MT2 is propagated upwards through the unit and into sub-unit MT1a. Distinct v-shaped notches truncate reflectors within sub-unit MT1b. The notches, interpreted as buried ice keel scour marks, have apparent widths of 50 m to 150 m, exceptionally 500 m, and are between 5 m and 10 m deep. Reflectors typically drape the notched topography.

Unit MT2

This seismically transparent to poorly stratified unit is between 80 m and 100 m thick and occurs at an average depth of 220 m BSS (MGL, 1987). Lithologically the unit comprises clay, and clay and silt with minor sand, as represented in the Aagnerk E-56 exploration well (40 km southeast of the study area southern boundary). Its upper surface is characterized by a high amplitude hummocky and diffractive reflection. The surface is resolved on SBP as highly irregular with relief of 2 m to 5 m, and is interpreted in this

study as an ice keel scoured surface representing the top of an ice keel turbate (Plates 3.3 and 3.4). O'Connor and Blasco (1982) noted the presence of buried scour marks and scoured surfaces in this unit from their analysis of legacy sub-bottom profile line 80-507 (shown on Plates 3.3 and 3.4 and Enclosure 4).

Unit MT4

Poorly stratified Unit MT4 occurs at an average depth of 280 m BSS. Borehole samples from Adlartok P-09 and Aagnerk E-56 exploration wells, ~40 km southeast of the study area, indicate sandy sediments. High resistivity logs suggest the presence of permafrost. Non-marine conditions prevailed during deposition, and the relative paucity of pollen suggests deposition during a glacial retreat before land vegetation was established and subaerial exposure to allow development of permafrost (MGL, 1987). Seismic stratigraphic facies analysis led Batchelor *et al.* (2012) to conclude that the unit is a glacial till deposited beneath an ice stream. Along the eastern margin of the Mackenzie Trough, the top of MT4 appears to become parallel to reflections above and below and continues onto the continental shelf beneath the Kringalik Plateau at an average depth of ~125 m BSS (MGL, 1987). A unit designated MT3 was described by O'Connor and Blasco (1986) but due to its restricted occurrence and its more likely interpretation as a zone of deformation in the upper part of Unit MT4, it is no longer used (MGL, 1987).

Unit MT5

This unsampled unit is restricted in occurrence to a deep, buried sub-valley within the Trough and comprises irregular reflectors that cause diffractions (O'Connor and Blasco, 1986; MGL, 1987). The thickness of MT5 increases northwards from 0 m to 100 m over a distance of 70 km (MGL, 1987). From seismic data the unit has been interpreted as a glacial till (Shearer, 1971; O'Connor and Blasco, 1986; Batchelor *et al.* 2012). Alternatively the unit may represent *in situ* sediments disturbed by overriding glacial ice.

3.1.3 Beaufort Shelf

The deep stratigraphy of the Beaufort Shelf comprises pre-Early Pliocene sediments affected by tectonic folds and faults overlain by Pliocene-Pleistocene sediments of the Iperk and Shallow Bay Sequences (Plate 3.2 and Enclosure 4). Tectonic subsidence resulted in thick accumulations (4 km) of Iperk strata beneath the central shelf (Dietrich *et al.* 2011). The Mackenzie Trough was cut into Iperk strata during the Pleistocene by glacial ice and is filled with more than 300 m of Quaternary sediments (Blasco *et al.* 1990; Blasco *et al.* 2011).

The upper 100 m of sediment on the shelf was deposited in the last ~27000 years during which time sea level rose at least 140 m (Hill *et al.* 1985). Five stratigraphic units can be interpreted in this interval (Plate 3.5 and Enclosure 7). From the seafloor down these are Units A and B (part of the Shallow Bay Sequence) and Units C, D and E (part of the Upper Iperk Sequence) (e.g. Blasco *et al.* 2011; O'Connor, 1980; O'Connor and Blasco, 1982).

Unit A

Unit A comprises recent silts and clays transported by the Mackenzie River and deposited in water depths >10 m following the Holocene sea level rise (O'Connor, 1980). This unit ranges in thickness from a few centimetres in the east to 10 m in the west increasing to as much as 15 m to 20 m in Ikit and Kugmallit Channels and Mackenzie Trough. The clays are mostly illite, and geotechnically the unit is characterized by low undrained shear strength, high compressibility and moderate to high apparent overconsolidation ratios (Blasco *et al.* 2011).

Unit B

Unit B has a gradational upper contact with Unit A silts and clays and comprises a transgressive sequence of sand, silt and soft marine clay deposited in littoral, deltaic, and lagoonal environments during the last sea level rise, 6000 to 9000 cal years BP (Blasco *et al.* 2011; Hill *et al.* 1991). Sharp variations in undrained shear strength occur between the interbedded silts and soft clays. The unit ranges in thickness from little to none in the west to ~10 m in the east, and fills the large, shelf-crossing channels, such as Kugmallit Channel, which cut into the top of the underlying Unit C (Plate 3.5). The channels were cut during a 70 m low-stand of sea level at ~18000 cal years BP (Blasco *et al.* 1990).

Unit C

Unit C comprises 40 m of fine- to medium-grained, very dense, well sorted sand with gravel, silts and clays representing a broad coastal outwash plain (Blasco *et al.* 2011). High-angle acoustic clinoform reflectors in Unit C indicate the presence of laterally migrating fluvial channels (e.g. Hill *et al.* 1985; Blasco *et al.* 1990). The undulose top surface of Unit C is a well developed high amplitude reflector and is an unconformity/disconformity that formed during subaerial erosion ~18000 cal years BP. The hummocky surface is in part the result of thermokarst development during which ephemeral ponds and lakes formed and in which peat deposits accumulated. The surface was further modified by erosion during marine transgression 6000 to 9000 cal years BP (Hill *et al.* 1991; Blasco *et al.* 2011) when Unit B marine sediments were being deposited. The top of Unit C marks the upper stratigraphic limit of permafrost on the shelf, the overlying Units A and B being deposited under transgressive and fully marine conditions preventing further permafrost development (Plate 3.5). There are places on the shelf where Units B and C are laterally contemporaneous (Hill *et al.* 1985).

Unit D

Unit D disconformably overlies Unit E although the contact is not well resolved on seismic reflection profiles due to a lack of impedance contrast. Unit D comprises up to 40 m of silt and clay deposited in a delta-margin or inner-shelf marine setting. A peaty mud sample from the bottom of Unit D at the Uviluk well gave a radiocarbon age of 21620 ±630 cal years BP (Hill *et al.* 1985; Plate 3.5). Unit D was deposited during a marine transgression between ~21000 cal years BP and the Late Wisconsinan.

Unit E

Unit E, a medium- to fine-grained sand of unknown thickness lies below Unit D and appears to form a series of pro-delta depositional lobes, and represents an early glacial outwash deposit (Blasco *et al.* 2011). The environment of deposition indicates alternating

sub-aerial delta plain and near-shore marine (Blasco *et al.* 1990) similar to Unit C. At the Tarsiut N-44 well a peat sample from 141 m below sea surface (120 m below seafloor) in this unit gave an age of 27380 ±470 cal years BP (Hill *et al.* 1985).

A regional erosion surface has been correlated from onshore Richards Island to the offshore shelf (Plate 3.6). The surface is interpreted by Murton *et al.* (2010) to be the result of a catastrophic outburst flood from glacial Lake Agassiz at ~13000 cal years BP associated with the northern hemisphere Younger Dryas cooling event. The flood is thought to have flowed towards the northeast across Richards Island, the interfluvium between the East Channel and Middle Channel of the Mackenzie delta, inundating it to a water depth of at least 10 m (30 m above modern sea level). Picard *et al.* (2012) suggest that glacial outburst events in the Beaufort Sea could have resulted in up to 2 km of shelf edge progradation in single events of short duration. Murton *et al.* (*op. cit.*) interpreted that at its peak, floodwaters were directed across the shelf along Kugmallit Channel to the shelf margin. A second outburst flood event occurred at ~9300 cal years BP. However, these dates do not coincide with the two globally identified meltwater pulses (MWP 1A and 1B) that occurred at ~14000 cal years BP and 11300 cal years BP, respectively (e.g. Bard *et al.* 2010). Two later meltwater pulses between ~8500 and ~8200 cal years BP are linked to drainage events of glacial lakes Agassiz and Ojibway (Törnqvist and Hijma, 2012), but with no indication of pathway taken to the ocean. Analysis of oxygen isotope data from three cores collected in the Mackenzie Trough in 2002 by Schell *et al.* (2008) led them to conclude that evidence for a meltwater pulse from Lake Agassiz is unlikely and that a much weaker signal from an Agassiz-like event was more likely to be the result of meltwater from the Russian shelf.

3.1.4 Continental Slope

Until very recent investigations, information on the continental slope has been largely restricted to the shelf edge and upper slope. O'Connor (1981a and b) described the distribution of acoustic permafrost (APF) extending to the shelf edge, and showed evidence for mass wasting processes and deposits on the uppermost continental slope. Hill *et al.* (1982) described evidence for creep deformation on the slope using high resolution sub-bottom profiler data and geotechnical test results from a number of piston cores. They noted evidence for the truncation of reflectors at the seafloor, suggesting erosion or progradation. Their findings are discussed in more detail in Section 6.1.6.

Since at least the Neogene, the continental slope has been the locus of a continuous cycle of deposition and subsequent removal of sediment via downslope mass transport events. These events evolved downslope into turbidity currents that flowed for hundreds of kilometres across the abyssal plain of the Canada Basin towards the North Pole (Mosher *et al.* 2011). Continuous, flat-lying reflections within these distal deposits are evidence that there has been no reworking or disturbance of these sediments since they were deposited. A very large (132000 km²) buried mass transport complex, up to 700 m thick and likely comprising several failure events, forms a vast lobe stretching over 800 km north from the slope and Mackenzie Trough (Mosher *et al.* 2012). Immediately seaward of the shelf margin the continental slope to at least 1000 m water depth

comprises stratified surficial units, punctuated by buried mass transport deposits (MTDs), all of marine origin. Three surficial units can be identified to ~90 m BSF, the approximate limit of sub-bottom profiler penetration. Beneath these units 2D seismic reflection profiles reveal deeper sequences of stacked MTDs and stratified sediments. From the seafloor down, the surficial slope stratigraphy comprises four informally named units which are described below.

Unit 1

This unit ranges in thickness from 5 m near the bottom of the slope to ~45 m at the shelf margin. The unit comprises acoustically well stratified pelagic muds of silty clay. Within Unit 1 a regional acoustic horizon, H1a, is characterized by sandy and gravelly ice rafted debris (IRD). Dated core samples yield a C_{14} calibrated age of ~13000 cal years BP for the H1a horizon (Appendix B). The base of Unit 1 is defined by seismic horizon H2 with an approximate age of 16000 cal years BP extrapolated from C_{14} dates (Plate 3.7).

Unit 2

Acoustically well stratified Unit 2 likely comprises pelagic muds of silty clay. The unit is 5 m to 60 m thick, and is thickest (40-60 m) beneath the middle slope. On the upper slope the entire thickness of the unit has been reworked into an ice keel turbate in the paleo-scour zone. The turbate ranges in thickness from 25 m to 30 m, exceptionally 40 m, and pinches out along its northern margin in water depths between 250 m and 400 m. The paleo-scour zone is described in more detail in Section 6.1.6.

Horizon H3 marks the top of a region-wide interval of acoustically massive to poorly stratified sediments interpreted as sand-prone turbidites and/or MTDs (Plate 3.7). The interval is generally between 5 m and 25 m thick, and rests on horizon H4, a regional unconformity marking the base of Unit 2 sediments (Plate 3.7). The interval is thickest (15-25 m) beneath the mid-slope region. Within the unit the H3 horizon has a well-developed hummocky topography that is expressed at the modern seafloor through the overlying Units 1 and 2 strata, as downslope-oriented ridges and gullies in the mid-slope region with wavelengths 0.5 km to 2 km, and trough-to-ridge heights of 2 m to 10 m (described in Section 5.1.4). The H3 to H4 interval is interpreted as an erosive and depositional event, or series of events, resulting from regional sheet flows emanating from the shelf margin. Morphologies resemble type I and type IV gullies of the glacially influenced continental slope of west Antarctica (Gales *et al.* 2013). The gullied interval has been mostly eroded by other buried MTDs in the region of license block EL476 (see Plate 1.1 for location and Enclosure 1).

Discrete, downslope-oriented MTDs occur within Unit 2 sediments as linear ribbon-like deposits up to 5 km wide, 30 m thick and 40 km long. All MTDs are internally acoustically structureless with well defined margins that truncate adjacent stratigraphy. The ribbon-like MTDs are morphologically distinct from the regional H3 to H4 turbidite/MTD interval, and are interpreted as discrete events, initiating as point sources on the upper slope and shelf margin, and are likely sand-prone. The uppermost regions of most of the MTDs appear to be truncated along the northern pinchout margin of the paleo-scour zone. It is speculated either that initial MTD failures were precipitated by ice keel grounding events, or that failures originated upslope at the shelf margin, and these regions were subsequently

overprinted by the paleo-scour zone turbate. Ribbon-like MTDs are described in more detail in Section 6.1.2.

Unit 3

This unit is bounded by two regional unconformities, horizons H4 and H5, both characterized by undulatory surfaces (Plate 3.7). The unit comprises acoustically massive to poorly stratified sediments that are likely sand prone turbidites and/or MTDs similar to those in the overlying H3 to H4 interval. Within the penetration limits of the sub-bottom profiler data the unit ranges in thickness from <1 m to 35 m. The unit thins downslope and in places below water depths of ~725 m it is completely eroded where H4 cuts down onto the H5 surface.

The H4 unconformity originated in part from erosion by turbiditic or mass transport flow mechanisms. However, in deeper water both the H4 and H5 unconformity are of possible glacial origin. Between water depths of ~600 m and 700 m, both surfaces are modified by ridges and grooves with ~1 m to 7 m of relief and apparent widths of ~300 m (see section 6.1.4 for description). Although buried beneath ~50 m to 60 m of Unit 1 and 2 pelagic drape these features can be seen at the modern seafloor oriented at 045°. The ridges and grooves are interpreted as mega-scale glacial lineations (MSGL) made by grounded ice moving parallel to slope contours. Coarse material, possibly including boulders, may be associated with Unit 3 sediments.

Units 4 to 7

2D seismic data allows for the identification of deeper strata, which has been divided into Units 4 to 7 (Plate 3.8). The base of Unit 4 is defined by seismic horizon H10, the base of Unit 5 with seismic horizon H50, the base of Unit 6 with seismic horizon H60 and the base of Unit 7 with seismic horizon H80. Without the benefit of borehole data, the units were identified based on the mapping of strongly reflective seismic horizons that could be traced over long distances along and across the slope.

3.1.5 Late Quaternary Evolution of the Southern Beaufort Sea

A synoptic chronostratigraphic model of the Beaufort Shelf and continental slope from Late Quaternary to present is shown on Enclosure 9. It is based on the results of previous work, mostly on the shelf, by the Geological Survey of Canada and others, and on data presented in this study. The model starts at approximately 30000 years BP and describes, in 8 panels with notes, the key events and depositional units described in the present study. It represents a model for a tectonically subsiding glaciated margin characterized by aggradation and progradation of the shelf, punctuated by marine transgression and regression. The development of a landward-thickening zone of permafrost is characteristic of a periodically exposed and actively prograding and aggrading margin. The slope is characterized by thick sequences of rapidly accumulated stratified pelagic sediment underlying and overlying the rough paleo-topography of mass transport deposits, the preserved evidence of periodic slope failures.

3.1.5.1 Sea Level History

The history of global sea level rise during the Late Quaternary has been summarized by several authors, and two sea level curves by Chappell and Shackleton (1986) and Rohling *et al.* (1998) are used for discussion purposes here. These together with the Beaufort Sea regional curve of Hill *et al.* (1985) are shown on Enclosure 9. The curve of Rohling *et al.* (1998) in particular serves as a good reference for the duration of lowstands and shows a LGM minimum of approximately -120 m, based on data from the Red Sea. This agrees well with the curve of Chappell and Shackleton (1986) based on raised coral terraces on the Huon Peninsula, New Guinea which shows a slightly lower stand at approximately -130 m. The salient feature of both curves is that sea level rise was continuous and rapid from the -120/-130 m lowstand through most of Holocene time. The regional sea level curve for the Beaufort Sea also shows the same general trend with sea level passing -120 m during the LGM but implying that this level was reached, and passed without halting, during a continuous period of rapid sea level rise from a minimum depth of at least -140 m that began before 27 000 years BP (Hill *et al.* 1985). The only other feature in the Beaufort Sea curve that differs from the general global trend is a period, between 12000 and 15000 years BP, when sea level fell from approximately -40 m to -70 m, based on buried erosion surfaces identified in acoustic data. A “nick point” has been inferred on the seabed between 70 m and 80 m water depth linked to this fall (Pelletier, 1987b). A minor contour-parallel channel-like feature at these depths on the shelf edge on the northeastern margin of the Mackenzie Trough does not appear to be true “nick point”, and no other evidence for a shoreline has been found during the present study.

In summary, sea level rise was continuous and rapid since at least LGM times and, with the possible exception of the inferred sea level fall, there was no pause during which a strand line was developed above -120 m.

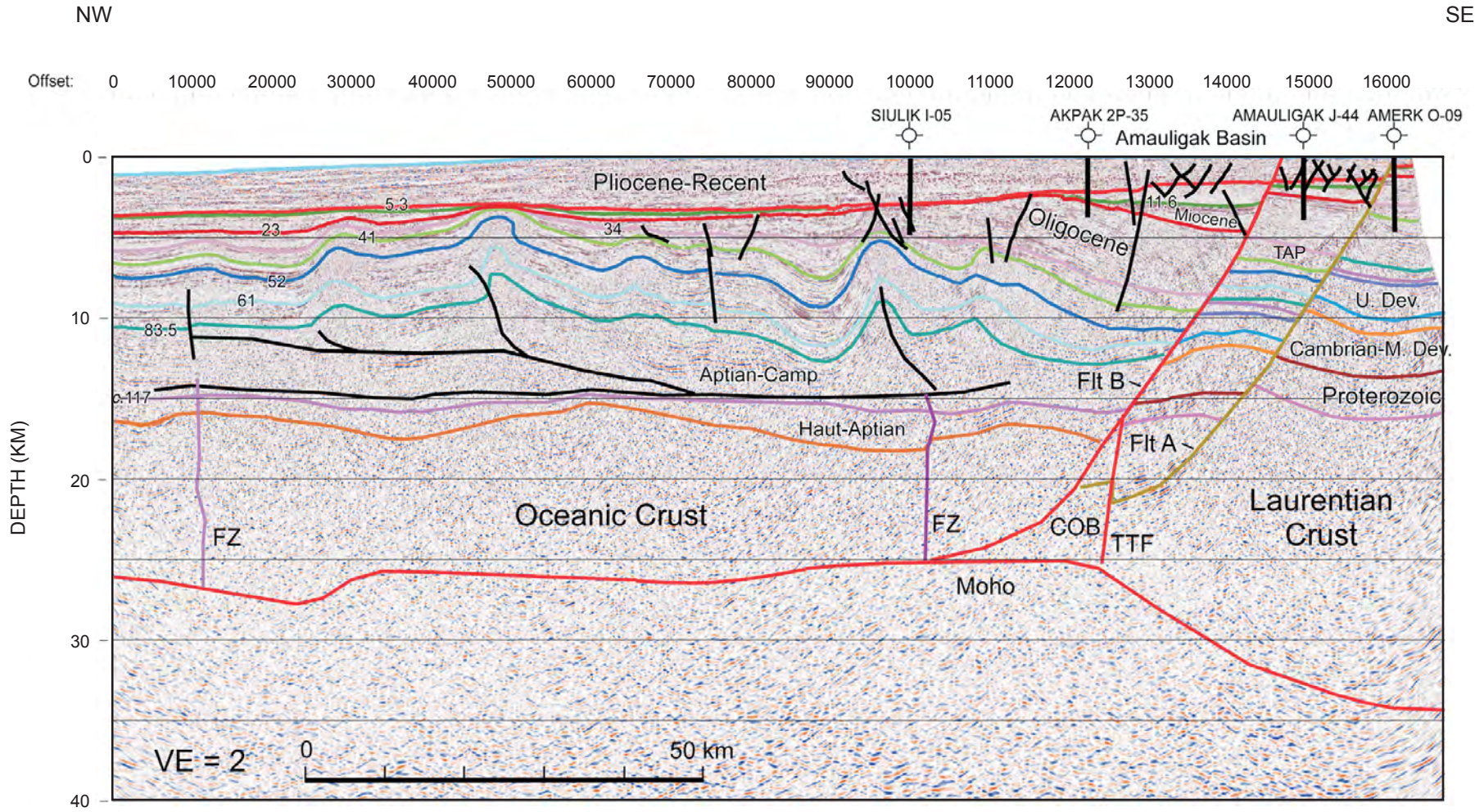
3.2 Regional Seismicity

The southern Beaufort Sea is underlain by oceanic crust and experiences episodic seismic activity (Dixon *et al.* 1992). The largest earthquake magnitude reported is M 6.5 (Dixon *et al.* 1992). Seismicity on this part of the rifted continental margin is thought to be related principally to tectonic processes at the lithosphere/asthenosphere boundary, and possibly to post-glacial isostatic rebound (Dixon *et al.* 1992). A number of historical earthquakes beneath the Beaufort Sea margin to the north of the Mackenzie Delta have occurred in a cluster mostly on the continental slope between the 200 m to 2500 m bathymetry contours (Plate 3.9). Within the southern Beaufort region, there is approximately one earthquake of M > 4 per year, and one M > 5 expected roughly every 10 years (Hasegawa *et al.* 1979). Only two large earthquakes in the Beaufort Sea have been studied, the M 6.5 event in 1920 and an M 5.5 event in 1975 (Hasegawa *et al.* 1979). Adams and Atkinson (2003) consider seismicity potential to be moderate.

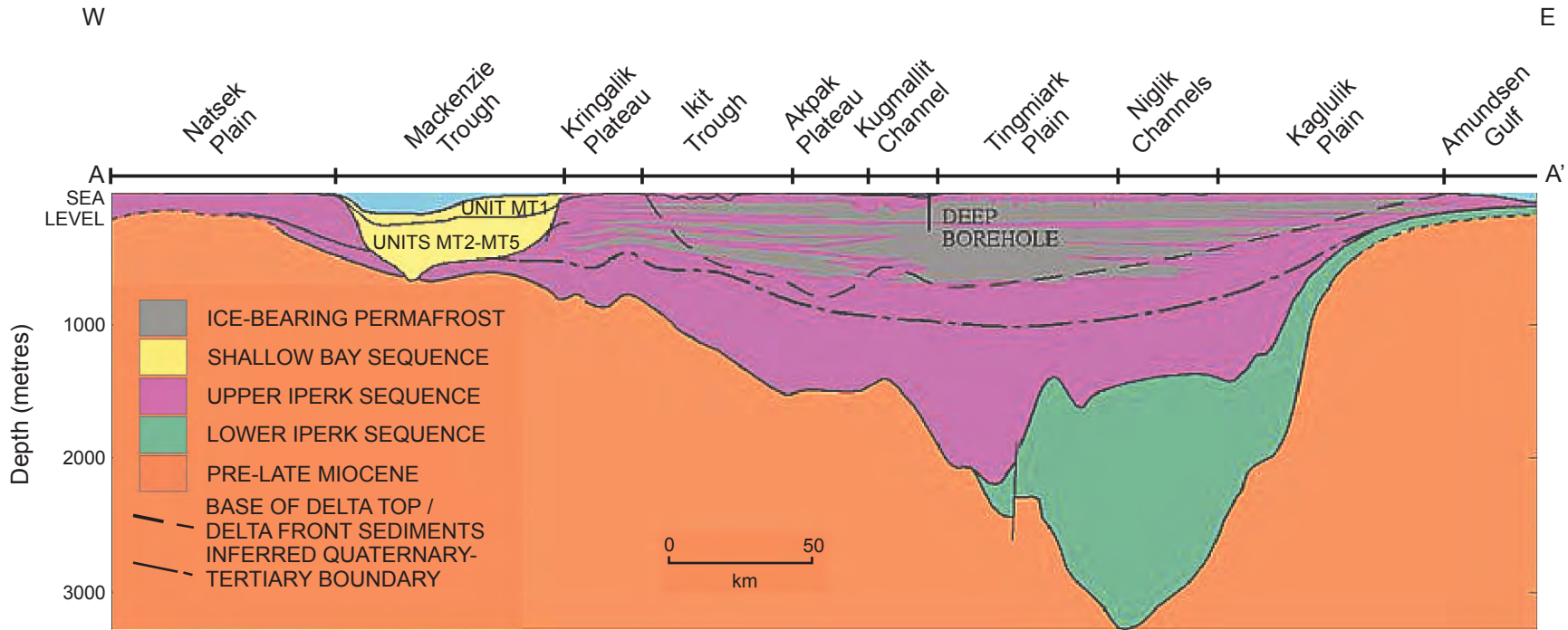
Ground motion in the Beaufort Sea appears to be a combination of normal and strike-slip faulting. One model for the origin of regional seismicity is gravitational loading of oceanic lithosphere beneath the outer Mackenzie Delta (Lane, 2002), caused by geologically rapid

sediment aggradation. Postglacial rebound may also be a contributing factor. Ground motions may be substantially modified by soil conditions, especially the low-consolidation sediments of the Mackenzie Delta and Mackenzie River valley (Hyndman *et al.* 2005). For strong shaking on similar deep soft soil deposits elsewhere, high frequencies are usually somewhat attenuated but low frequencies are substantially increased in amplitude.

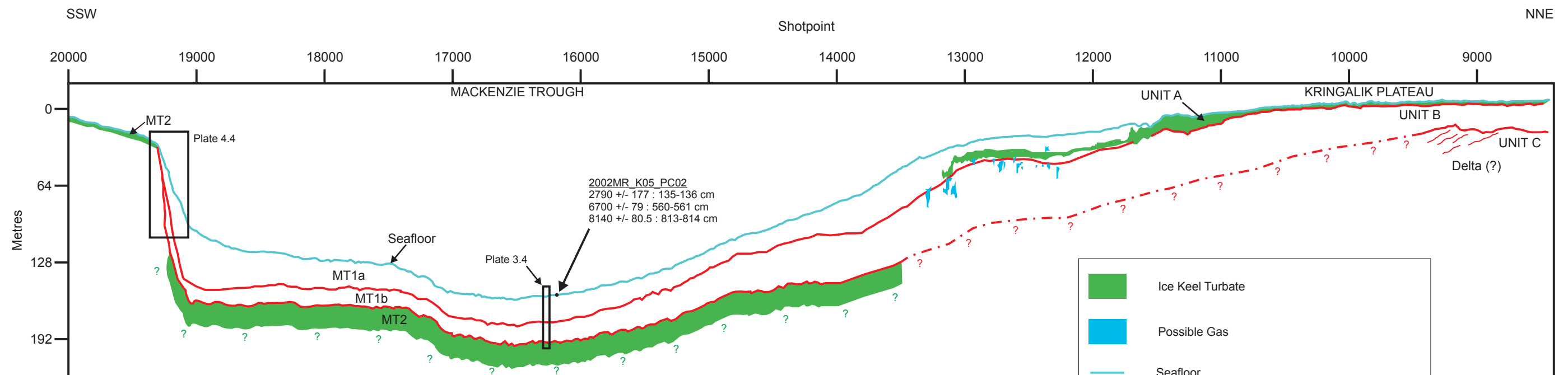
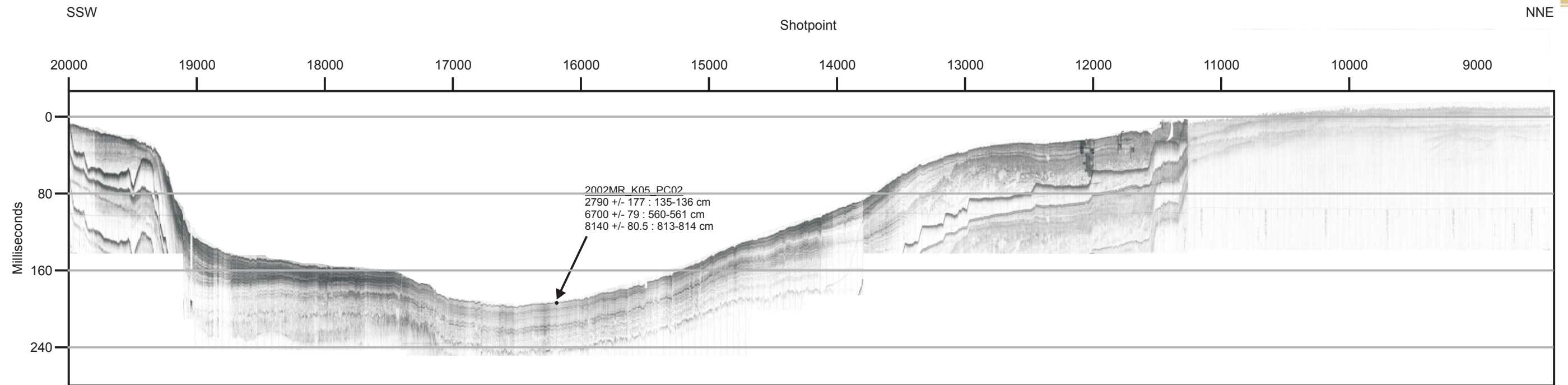
Very little is known about the tsunami history of the Beaufort-Mackenzie region (Leonard *et al.* 2010). There is only a very recent written history and very limited tide gauge monitoring. Tsunami risk is likely much less significant than on both the Pacific and Atlantic coasts, particularly as the presence of extensive sea ice is expected to attenuate tsunami waves. Tectonically-generated tsunamis are unlikely but Hyndman *et al.* (2005) suggest the potential for large thrust earthquakes beneath the Mackenzie Delta that could act as a trigger. Mosher (2009) considered that the tsunami-generating potential of the Ikit Slump (Saint-Ange *et al.* 2014) was potentially high (see Enclosure 1 for location).



Deep crustal structure across the centre of the Beaufort Shelf to 40 km depth. The Tarsiut-Amauligak Pull-Apart (TAP) half-graben has accommodated 7 km of downfaulting in Oligocene to Mid-Miocene time. The continent-ocean boundary (COB) is interpreted to be at the Tuktoyuktuk transform fault zone (TTF). Flt A = Amauligak Fault; Flt B = Amerk Fault; FZ = fracture zones in oceanic crust; Moho = Mohorovicic discontinuity. From Helwig *et al.* (2011).

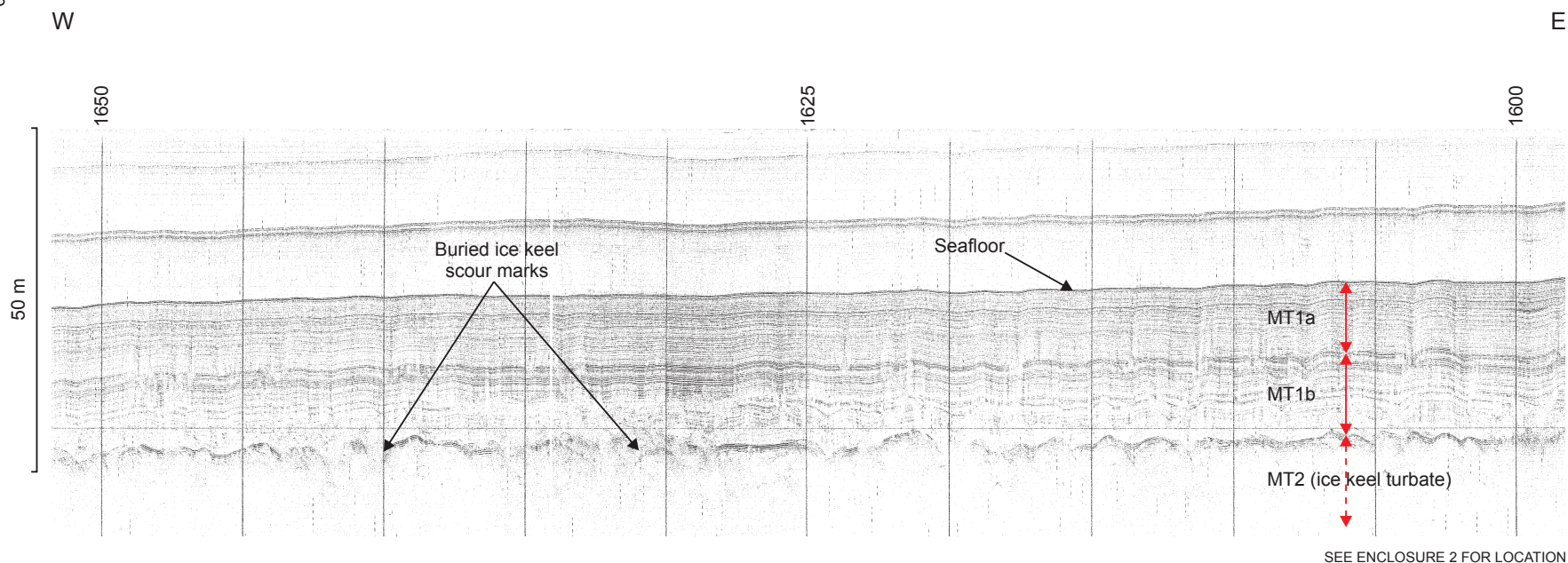


Plio-Pleistocene stratigraphy of the Beaufort Shelf/Mackenzie Trough. This schematic east-west cross-section between 30 m and 50 m water depth shows that the depocentre, with the thickest accumulation (~3500 m) of post Late Miocene Iperk Sequence sediments, is located beneath the central shelf. Subsea permafrost is shown extending to ~700 m below seafloor (Modified from Blasco et al. 1990).

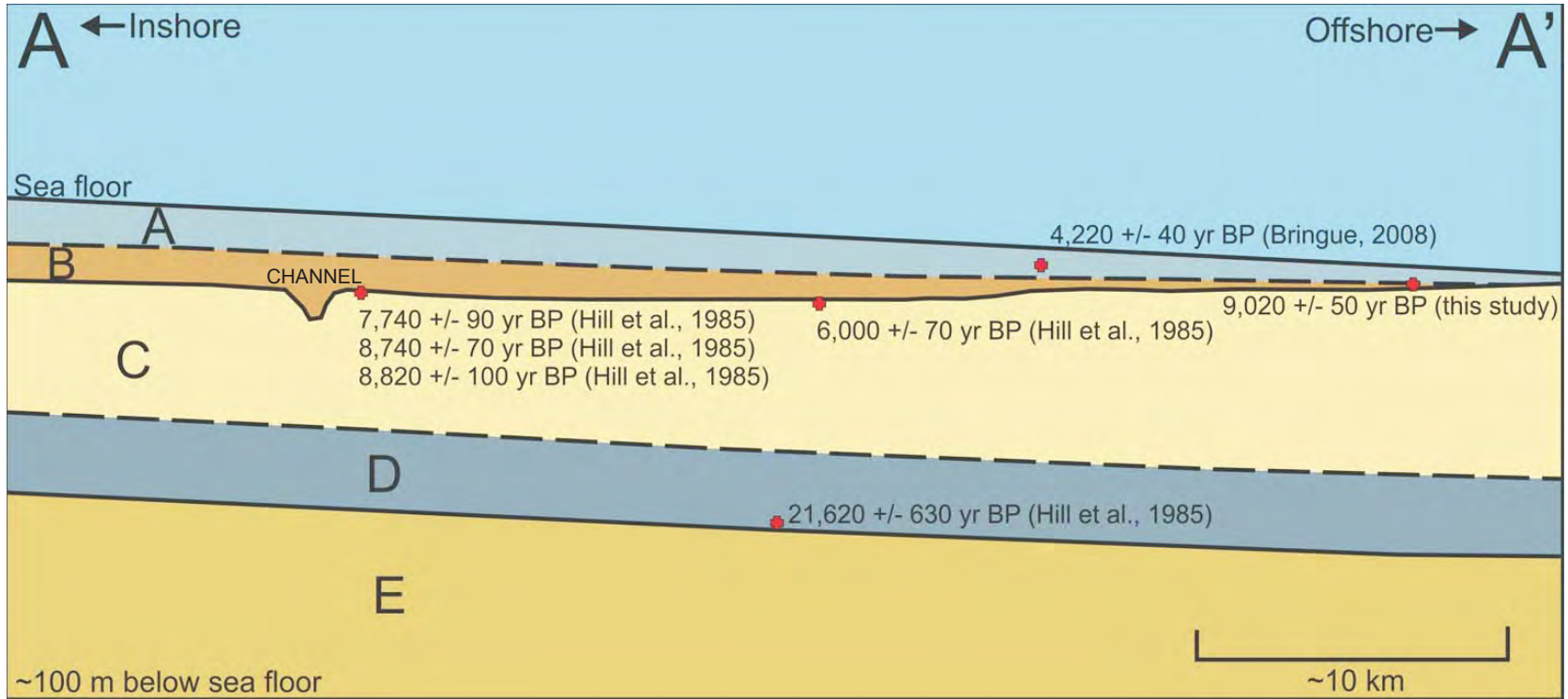


SEE ENCLOSURE 2 FOR LOCATION

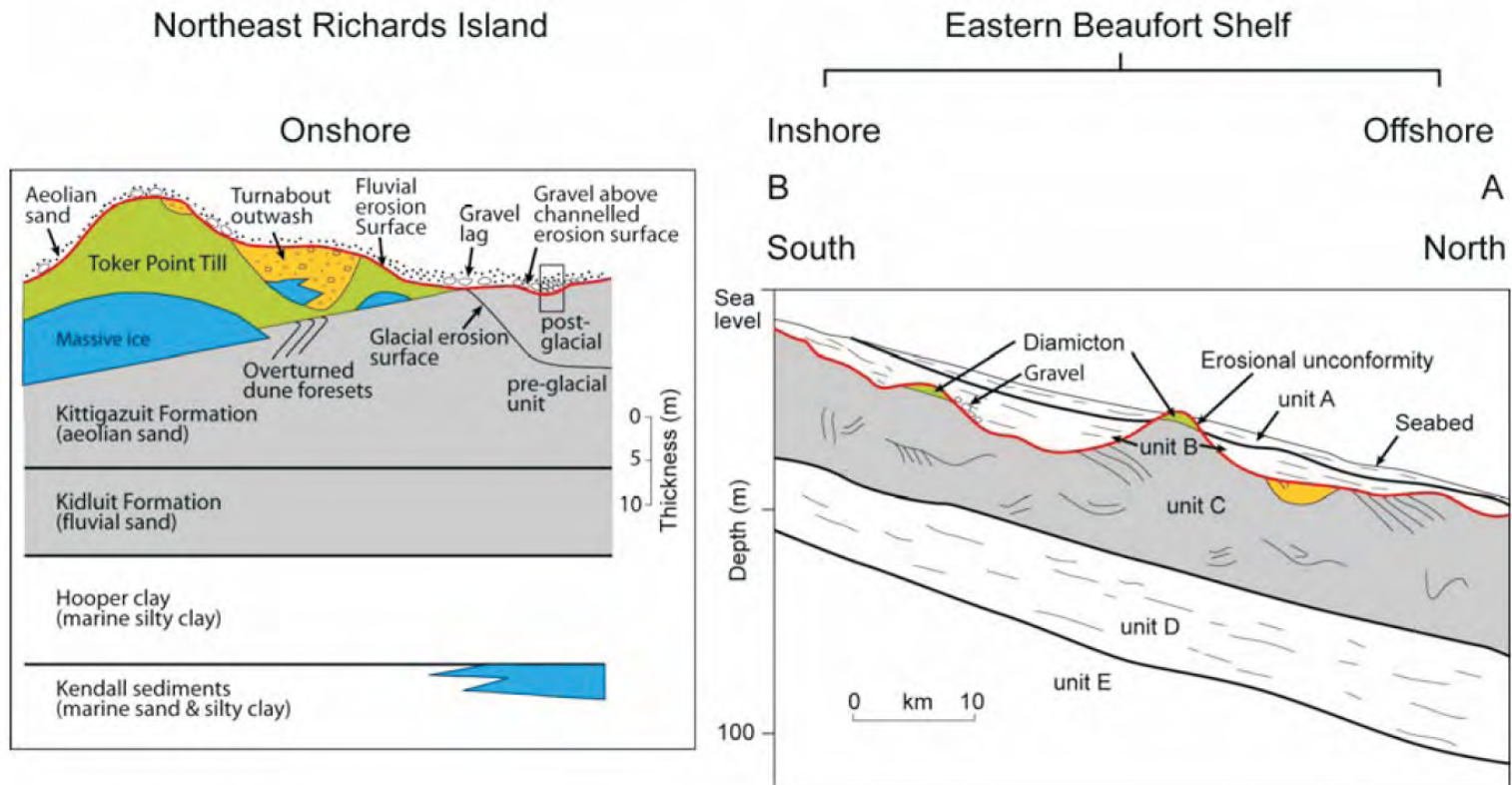
Legacy sub-bottom DOME/GSC profile line 80-507 from Mackenzie Trough. Sparker profile (top) and interpretation (bottom). The profile shows the aerial extent of two buried ice keel turbates (solid green): Unit MT2 beneath the Trough and within Unit MT1a on the northeast margin of the Trough. The profile highlights the difficulties of tracing stratigraphic units from the Trough to shelf.



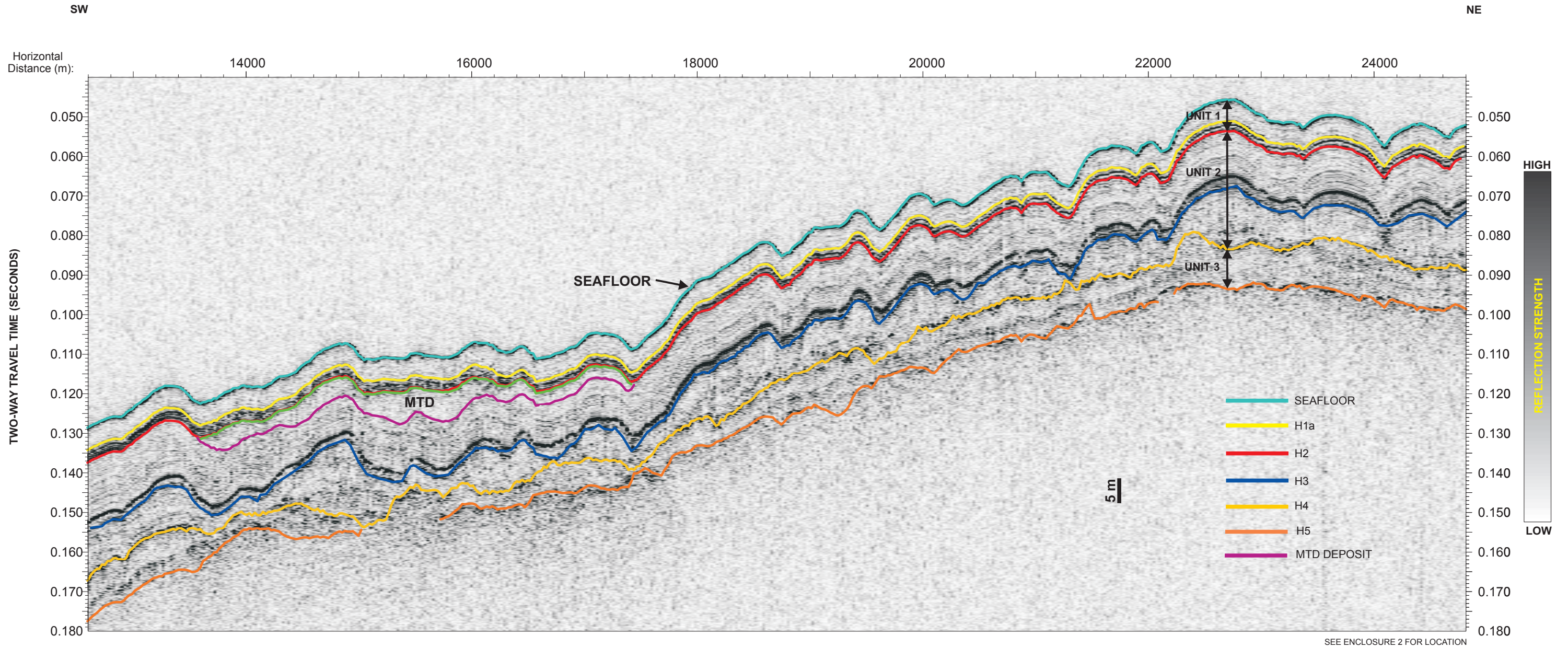
Zoomed in legacy sub-bottom profile, Line 80-507 from Mackenzie Trough. The profile shows the top of Unit MT2 and the hummocky ice-scoured surface which forms the base of Unit MT1. Note the ice scoured surface is propagated upwards through pelagic silty muds of unit MT1b, and rarely through overlying Unit MT1a to the modern seafloor.



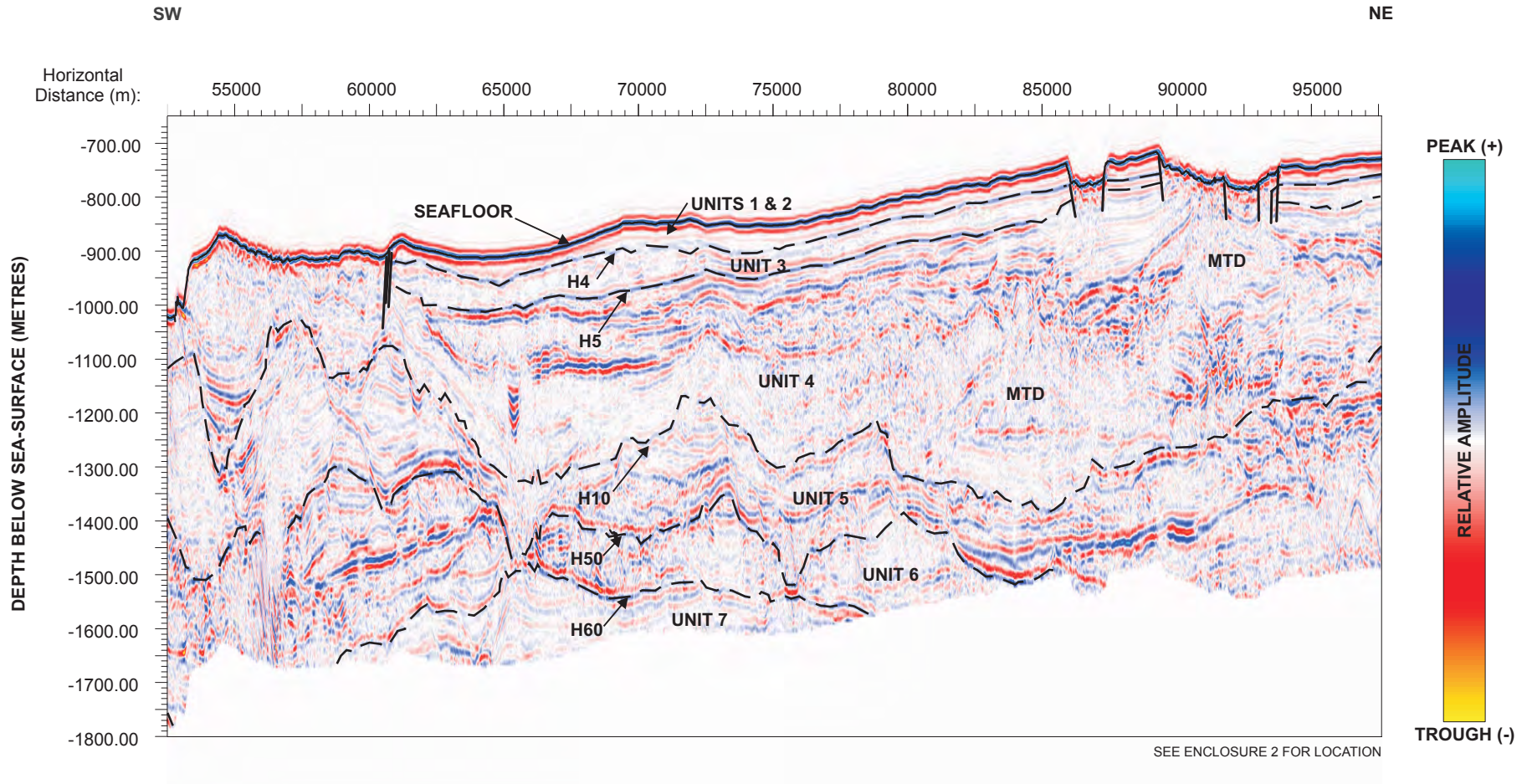
Beaufort Shelf schematic north-south stratigraphic cross-section of the upper ~100 m. Units A and B comprise the Shallow Bay Sequence. Units C, D and E are part of the uppermost Iperk Sequence. (From Blasco *et al.* 2011).



Colour-coded onshore/offshore chronostratigraphic correlation. A regional erosion surface (red line) was formed by a catastrophic outburst flood from Glacial Lake Agassiz ~13,000 years BP. Units A and B comprise the Shallow Bay Sequence. Offshore units C, D and E are part of the uppermost Iperk Sequence. Adapted from Murton *et al.* (2010).



Sub-bottom profile line 0302_2010_260_1430 illustrating continental slope units/horizons. In this example, the H3 to H4 sub-unit has thinned to as little as 5 m and the buried topography of H3 (blue) is propagated to the seafloor, where it is seen as the ridged and fluted topography on multibeam imagery. Note how poorly stratified sediments below H3 bury the topography on H4 (gold). The vertical scale bar is based on an assumed acoustic velocity in sediment of 1600 m/s.



2D cross-slope seismic profile. BeaufortSPAN Line BE2-5450 courtesy of ION Geophysical Corporation.

350000

425000

500000

575000

650000

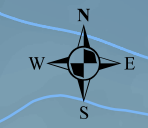
725000

7925000

7860000

7775000

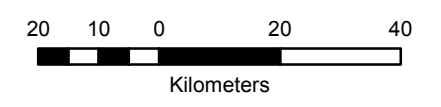
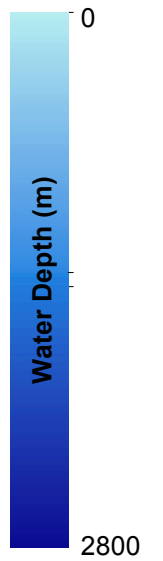
7700000



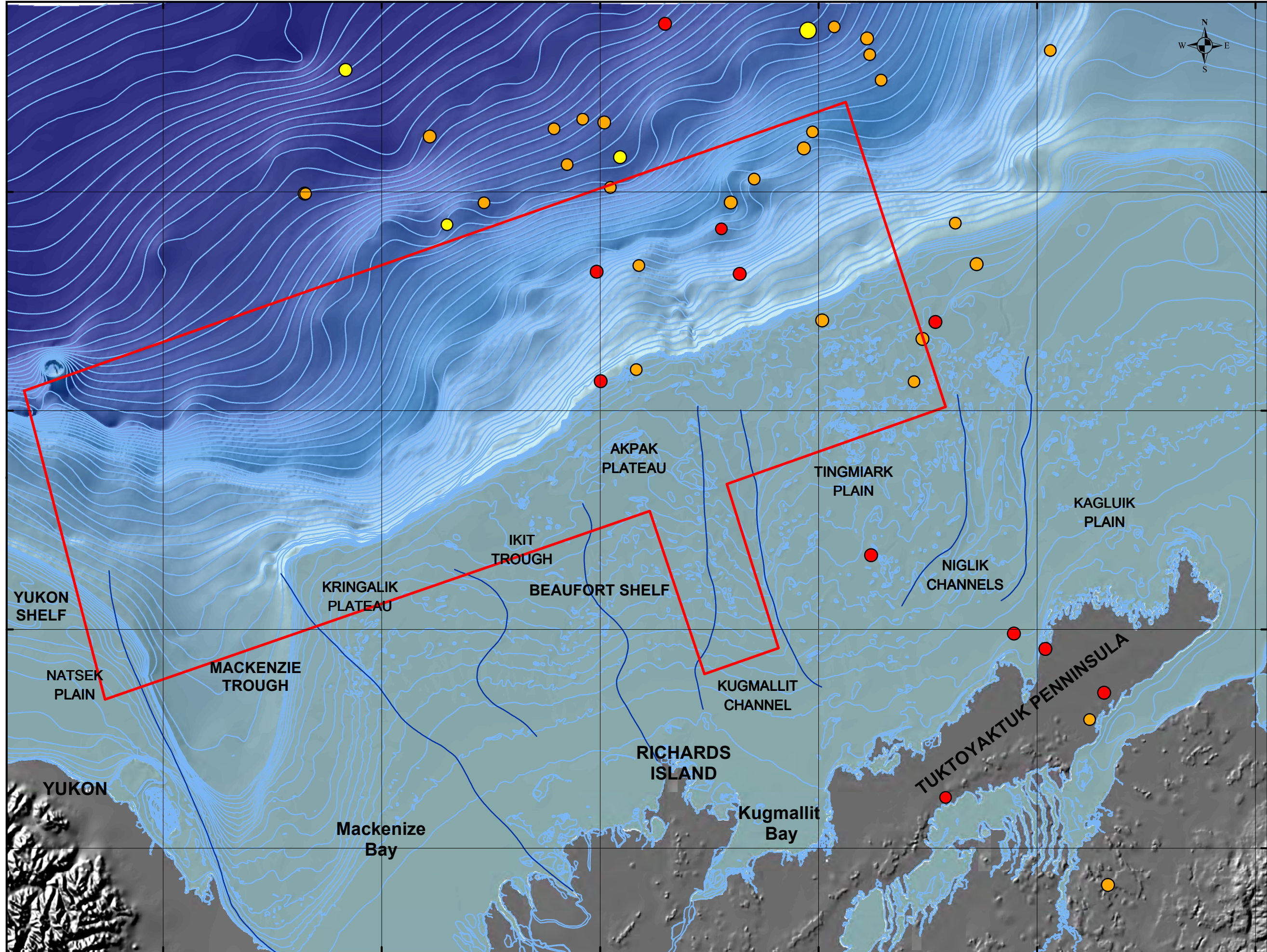
MAGNITUDE

- 1.0 - 1.9
- 2.0 - 2.9
- 3.0 - 3.9
- 4.0 - 4.9
- 5.0 - 5.9
- 6.0 - 6.9
- 7.0 - 7.8

- SEISMICITY DEPTH: 0 - 15 km
- SEISMICITY DEPTH: 15 - 30 km
- SEISMICITY DEPTH: 30 - 45 km
- BATHYMETRY CONTOURS
- PHYSIOGRAPHIC REGIONS
- SITE INVESTIGATION AREA



EARTHQUAKE EPICENTRES AND MAGNITUDES



4. REGIONAL FRAMEWORK AND CORRELATIONS

4.1 Stratigraphic Nomenclature

Since 1970 different stratigraphic nomenclatures have been developed to describe the Quaternary sediments beneath the Yukon shelf, Mackenzie Trough, Beaufort Shelf, and continental slope. To assist with visualizing the deeper stratigraphy, a 365 km-long 2D seismic profile is provided on Enclosure 7. The profile is combined from six ION GXT lines and extends from the Yukon shelf across the outer Mackenzie Trough, turns parallel to the slope before traversing the Beaufort Shelf to the Amauligak 3F-24 geotechnical borehole. Stratigraphies and nomenclature are briefly described below.

Surficial and older units of the less well studied Yukon shelf comprise Units I, II and III (Lewis and Meagher, 1991). Mackenzie Trough stratigraphy comprises Units MT1 to MT5 of O'Connor and Blasco (1986), and these units are used throughout this report. The units were sub-divided and renamed into Units S7 to S20 by MGL (1992a).

Beaufort Shelf Quaternary sediments comprise Units A, B, C, D, E and F and unconformities U/C1 and U/C2 mark the bases of Units A and B, respectively (O'Connor and Blasco, 1980).

From the seafloor down, the continental slope stratigraphy as proposed here comprises Unit 1 (with basal seismo-acoustic horizon H2), Unit 2 (with basal unconformity, seismo-acoustic horizon H4) and Unit 3 (with basal unconformity, seismo-acoustic horizon H5), and is partially constrained by C₁₄ dates from piston cores (Plate 4.1). These units approximately equate in vertical extent with the informal stratigraphic Units S1 (equivalent to Unit 1), S2 and S3 (equivalent to Unit 2) and S4 (equivalent to Unit 3) of the Geological Survey of Canada (Rankin *et al.* 2010; 2011; 2013). Deeper horizons identified in the 2D seismic data comprise Units 4 to 7 (Section 3.1.4).

4.2 Correlations

In this section the stratigraphic correlation of units beneath the Beaufort and Yukon shelves, Mackenzie Trough and continental slope is described based on acoustic and seismic data and radiometric dates from cores and boreholes. Plate 4.2 shows the stratigraphic relationships between these four regions, and plate 4.3 is a schematic showing proposed shelf to slope correlations.

4.2.1 Yukon Shelf and Mackenzie Trough

Mid to Late Wisconsinan sediments are absent on the Yukon shelf, and Upper Iperk Sequence strata rise very close to the seafloor (<2 m) with sediments of >53000 cal years BP located just 5 m BSF in borehole GSC-1 (Blasco *et al.* 1990; Enclosure 3). Upper Iperk sediments are unconformably overlain by a very thin veneer of reworked Iperk and marine silts and clays of the Shallow Bay Sequence, deposited during and after the regional Holocene transgression that flooded both the Beaufort and Yukon shelves.

Lateral facies changes, due to differences in depositional processes, make it difficult to correlate shallow acoustic and seismic stratigraphy between the Trough and the continental shelf on both margins. In addition, seafloor multiples mask the shallow subsurface stratigraphy in the shallow waters of the eastern and western Trough margins. However, Blasco *et al.* (1990) made the general correlation between Trough Unit MT1 and Beaufort Shelf Units A and B, and mapped the base of Unit MT1 at ~40 m BSF. Palynological evidence suggests that the base of MT1 may be 12000 to 14600 years old leading Blasco *et al.* (1990) to interpret the presence of a glacial ice stream that overrode Unit MT2 before retreating by 14000 cal years BP.

Units MT1 and MT2 can be traced to the western margin of the Mackenzie Trough. Here, from limited data, Unit MT1b appears to have pinched out so that sediments of Unit MT1a rest directly on the hummocky paleo-scoured surface of MT2. At the edge of the Yukon shelf Unit MT1a sediments have been completely eroded and the ice scoured MT2 surface is exposed at the seafloor (Plate 4.4). As it rises towards the Yukon shelf the base of Unit MT2 can be seen to truncate horizontally stratified sediments, and where it becomes conformable with these underlying sediments on the shelf, the bottom surface of MT2 becomes hummocky. The stratified sediments are interpreted to be much older Iperk sequence strata and thus at this location the base of MT2 represents the base of Trough unconformity which is ~20 m below seafloor.

4.2.2 Yukon Shelf, Mackenzie Trough and Beaufort Shelf

Plate 4.5 is a schematic cross-section of the Mackenzie Trough showing correlations beneath the Yukon shelf and Beaufort Shelf (Kringalik Plateau) as interpreted during this study. The deepest imaged Trough unit is MT2, interpreted as an ice keel turbate. Shallow stratigraphy in the outer Mackenzie Trough comprises acoustically well stratified clays and silts of Units MT1 and MT2 (Plates 3.3 and 4.6).

Sub-bottom data reveal structures in both near-surface Units MT1a and MT2. Notably, the top of Unit MT2 is characterized as an undulatory surface with ~2 m to 5 m relief often associated with bow-tie acoustic diffraction artifacts. The hummocky topography of this surface is draped with acoustically well stratified sediments of Unit MT1, and the topography is propagated upwards through overlying strata, though progressively muted, to at least the MT1a/MT1b boundary and in places to the modern seafloor (Plate 3.4) where they can be seen as curvilinear grooves on multibeam imagery. Immediately beneath the hummocky surface Unit MT2 is either acoustically structureless or characterized by numerous overlapping acoustic diffractions.

The base of Unit MT2 is below the maximum acoustic depth of penetration and cannot be seen. However, as the undulatory upper surface is traced to the north-northwest down the axis of the Trough, a deeper, similarly roughened surface can be seen rising up towards the upper MT2 surface. The two surfaces, separated by a region of acoustically structureless to poorly stratified sediments, eventually merge at ~350 m water depth (approximately 395 m BSS, Plate 4.7).

On the northeast margin of Mackenzie Trough a similar, but thinner and aurally restricted chaotic zone bounded by hummocky reflectors occurs immediately above the base of Unit MT1a. The base of the chaotic zone coincides approximately with the base of MT1a (Plate 4.6). Towards the shelf (Kringalik Plateau) the upper boundary of the zone rises towards and reaches the modern seafloor where active scouring by ice keels is occurring.

Interpretation

MT1 and MT2 are distal, fine-grained deposits of the Mackenzie River that can be traced upslope to the south outside the study area, where they merge into a well-developed clinof orm sequence of the Mackenzie delta (e.g. MGL, 1992a; Jenner & Blasco, in prep.). The hummocky upper and lower surfaces that bound the acoustically structureless/diffractive region at the top and bottom of Unit MT2 are characteristic of buried ice keel turbate deposits. In places, hummocky topography of the upper MT2 surface is propagated to the modern seafloor through overlying pelagic drape sediments of Unit MT1 where it is revealed, although muted, as curvilinear ice keel scour mark grooves on multibeam imagery. The hummocky lower and upper surfaces are thus interpreted as the initial and final ice scour events, respectively, of a period of intense ice keel turbation, represented by the structureless/diffractive stratigraphic Unit MT2 in between. It is possible that the turbate is equivalent in age to the paleo-scour zone on the upper slope (see section 5.1.9), the end of scouring occurring between 16000 cal years BP and 12000 cal years BP. This association cannot be proven without C₁₄ dates for Unit MT2.

Intense mechanical reworking by ice keels has likely altered the original physical sediment properties of Unit MT2. Additionally Unit MT2 may contain coarse-grained ice-rafted debris, possibly ranging from sand to boulders, deposited from floating ice.

Three cores obtained in 2002 from the Mackenzie Trough area sampled Unit MT1 "plumites", distal deposits of the Mackenzie River plume (Jenner and Blasco, in prep.; Scott *et al.* 2009; Schell *et al.* 2008). C₁₄ dates from rhythmically laminated silts and clays (likely annual deposits) near the base of one of these cores (PC01 in 671 m water depth) record sedimentation rates of 16.1 mm/yr from distal outwash as the Laurentide Ice Sheet retreated inland. Cores PC02 and PC03 record much lower sedimentation rates ranging between 0.5 mm and 1.8 mm/yr (Jenner and Blasco, in prep.; see Enclosure 3 for core locations).

The aurally restricted chaotic zone seen against the eastern margin of the Trough within Unit MT1a is also interpreted as an ice keel turbate (Plates 3.3 and 4.6). However, the turbate appears to be diachronous, which is likely a function of rising sea level during the late Holocene. The buried portion of the turbate thus represents a saturated paleo-scour zone and the turbate associated with the modern scour regime on the shelf is the saturated scour zone of O'Connor and Blasco (1982).

At the edge of the Yukon shelf the bottom of Unit MT2 is interpreted as an ice scoured surface affecting flat-lying sediments of the Upper Iperk Sequence. The scoured Upper Iperk surface is interpreted to represent the basal Mackenzie Trough unconformity.

Beneath the eastern margin of the Trough the top of MT2 is inferred to correlate with the top of shelf Unit C, an erosive undulatory surface truncating gently dipping clinoforms. If the MT2/Unit C correlation is valid then there is a significant lateral facies change between the submerged ice keel turbate of MT2 and outwash plain delta foresets of Unit C. The top surface of Unit MT2 and Unit C thus represents the end of major ice keel scouring in the Trough and delta top erosion on the shelf margin. Unit MT1b represents a period of pelagic sedimentation, well stratified sediments draping and partially smothering the underlying ice keel scoured surface of Unit MT2. Solitary ice scour marks are preserved in well stratified Unit MT1b sediments in the Trough. Unit MT1b pinches out laterally towards the Yukon shelf so that Unit MT1a lies directly on Unit MT2. On the Beaufort Shelf margin Unit MT1b is correlated with Unit B, deposited during Holocene transgression.

Uninterrupted pelagic sedimentation of well stratified sediments continued throughout Unit MT1a to the modern seafloor, and in places the muted topography of buried ice keel scour marks on the upper MT2 surface is visible at the seafloor. During deposition of Unit MT1a a period of ice keel scouring commenced on the eastern Trough margin. The resulting ice keel turbate is diachronous, the top surface gradually rising to the modern seafloor on the Kringalik Plateau and merging with the modern saturated scour zone of shelf Unit A (Plate 4.6). On the western Trough margin a period of seafloor erosion has removed ~55 m of Unit MT1a sediments resulting in exposure of the relict MT2 upper ice scoured surface (described in section 6.3.2). As it is traced onto the Yukon shelf the relict MT2 surface is gradually buried beneath a thin cover of late Holocene sediments which are affected by modern ice scour marks.

The transgressive and post-transgressive Beaufort Shelf Units A and B have been tentatively correlated with Mackenzie Trough Unit MT1 and the thin surficial Holocene sediments above Unit I on the Yukon shelf (Blasco *et al.* 1990). Sands of Beaufort Shelf Unit C may correlate with Unit MT1b of the Mackenzie Trough (Blasco *et al. op. cit.*). Very tentative general correlations were made by Blasco *et al. (op. cit.)* between Beaufort Shelf Units C and D, Mackenzie Trough Units MT2 to MT5, and Yukon shelf Units I to III. These combined units are inferred to be early Wisconsinan and younger in age but apart from the work of Hill *et al.* (1985; 1993) who reported dates from the Beaufort Shelf no older than 25890 ±867 cal years BP, the ages of potential correlative units from the Yukon shelf, Mackenzie Trough and continental slope have yet to be confirmed.

Although the distinction between shelf Unit B and underlying Unit C is apparent on acoustic profiles, the boundary is diachronous. Deposition of shelf Unit C began ~21000 cal years BP (Blasco *et al.* 2011), and ended with the deposition of uppermost glacio-fluvial outwash sediments ~6800 cal years BP (Hill *et al.* 1985), contemporaneous with the deposition of transgressive Unit B, which continues to be deposited today in water depths <10 m (Blasco *et al.* 2011).

The erosion surface above shelf Unit C was gradually transgressed during the Holocene after a significant depositional hiatus (Blasco *et al.* 2011). A depositional hiatus is not necessarily implied in the Mackenzie Trough, which in the study area is mostly below 70 m water depth, and therefore has been continuously submerged. Marine deposition of

Units MT1a and MT1b continued during transgression of the higher elevation Beaufort Shelf.

Results of the present study confirm the correlation between Beaufort Shelf Units A and B and Mackenzie Trough Units MT1a and MT1b (Plates 4.2 and 4.5; see Section 6.3.2). A tentative correlation is made between the irregular unconformity marking the top of Beaufort Shelf Unit C clinoforms on the eastern margin of the Mackenzie Trough and the buried ice keel scoured surface marking the top of Mackenzie Trough Unit MT2 (Plates 4.5 and 4.6). The top of Unit C is interpreted by Blasco *et al.* (1990) as an erosional or non-depositional surface, formed during the 70 m sea level low stand at the LGM ~19000 cal years BP (Blasco *et al.* 2011), and thus the scour events that created the final upper MT2 surface were made at this time.

4.2.3 Mackenzie Trough and Continental Slope

There is a lack of SBP data from the mouth of Mackenzie Trough to the continental slope (Enclosure 2). However, Mackenzie Trough Units MT1a and b, MT2 and the top of MT4 can be traced from 350 m water depth in the centre of the Trough where their combined thickness is ~55 m, to 700 m water depth where combined thickness is ~45 m immediately above the headwall scarp of a slump (Enclosure 1). Although this stratigraphy is disrupted in the slumped regions, in water depths of 900 m to 1400 m the units reappear draped above older, buried topography that is propagated to the modern seafloor. However, the correlation at these depths is tentative due to the lack of survey coverage.

Shallow stratigraphic ties between the portion of the slope near the mouth of the Mackenzie Trough, and the remainder of the slope in the northeastern part of the study area are not possible owing to a large swath of disrupted seafloor, informally named the Ikit Slump by Saint-Ange *et al.* (2014), that separates the two areas by a minimum distance of 40 km. In this region, SBP data show acoustically structureless sub-seafloor sediments, and thus no direct stratigraphic ties can be made between Units MT1 and MT2 and slope Units 1 and 2. However, 2D seismic data have allowed the identification and tentative tracing of deeper units (Units 4 to 7) both along and across the slope, and from the slope into the Mackenzie Trough (see Sections 7.1 and 7.3). At the seafloor and in the sub-seafloor the Trough to slope transition is abrupt and a thick succession of slumped and MTD sediments at the transition prohibits the positive correlation between these disturbed and complex slope sediments with the relatively well stratified Trough units and Iperk Sequence strata beneath the base of Trough unconformity.

4.2.4 Beaufort Shelf and Continental Slope

Plate 4.3 schematically illustrates shelf and slope correlations from the present study. The shallow slope stratigraphy (Units 1 to 3) is based solely on the interpretations of sub-bottom profiler data. Deeper stratigraphy on the slope and shelf are based on 2D seismic profiles and on groundtruthing from well logs (e.g. Fortin and Blasco, 1990; Blasco *et al.* 2011), and in particular to the Amauligak 3F-24 borehole which provided a continuous

stratigraphy from seafloor to 468.45 m BSF (Ruffell *et al.* 1990; Blasco, 2012). Data from the core samples and from downhole logging instruments enabled the definition of a detailed stratigraphy with evidence for eight regression/transgression cycles (Blasco, 2012). The borehole passed through shelf Units A to E (described in Section 3.1.3) and fourteen subsequent lithological units (Units F through S).

A BeaufortSPAN 2D seismic line passes within 50 m of the 3F-24 borehole location, and possible correlations between borehole stratigraphy and seismic horizons are shown on Enclosure 7. A tentative pick for the base of Unit C, known to have a weak amplitude response, has been extrapolated to the upper slope, where the horizon occurs some distance beneath slope horizon H5 indicating a possible correlation with slope Unit 4 (Enclosure 7). The correlation should be regarded as speculative, given the inherent difficulties with interpreting seismic reflection data in permafrost-affected sediments (see Section 6.2.1).

Plate 4.8 illustrates the most recent model developed by the Geological Survey of Canada (Blasco, pers. comm.) modified slightly from the original model reported in Rankin *et al.* (2010; 2011; 2013). Plate 4.3 shows the combined acoustic and seismic stratigraphy for the continental slope and shows the correlations with the Geological Survey of Canada model. Correlations are explained in the following paragraphs.

A regional correlation is made between the erosional/non-depositional surface above shelf Unit C and the unconformity that defines the top of slope Unit 3 (horizon H4). Both the shelf and slope regional unconformities above Unit C and Unit 3, respectively, have been modified by incision of the Kugmallit Channel. On the shelf this occurred when sea level fell to 70 m during the LGM (Blasco *et al.* 1990; 2011) at ~19000 cal years BP, and thus the incision of the Kugmallit Channel into the top of Unit 3 on the slope is interpreted to be chronostratigraphically equivalent. The margins of the Kugmallit Channel on the shelf rise up to and merge with the shelf-wide unconformity above Unit C, and on the upper slope the Channel margins rise up to and merge with horizon H4, the slope-wide unconformity above Unit 3 (Plate 4.9). On the slope horizon H4 also approximates the bottom surface of the paleo-scour zone (Plate 4.10). However, the Geological Survey of Canada model (Plate 4.8) uses dates from the shelf to infer a possible LGM age (~19000 cal years BP) for the base of Unit C beneath the shelf, the location of which has not yet been identified beneath the slope.

The erosive styles of the regional unconformities above shelf Unit C and slope Unit 3 suggest unconfined, sheet-like erosive flow across the shelf and shelf margin and onto the slope. Such a flow regime is consistent with the general hummocky regional unconformity at the top of shelf Unit C, and with the interpretation of upper Unit C as a broad glacial outwash plain (Blasco *et al.* 1990) delivering distributed flow to the continental shelf margin possibly via a system of broad braided rivers. On the slope, sheet-like flow is further implied by the slope-wide topography of horizon H3, the top surface of Unit 3 MTD/turbidites, which takes the form of downslope-oriented gullies (see Sections 5.1.4 and 6.1.1), likely indicative of slope-wide, down-slope density current flow.

As sea levels fell to 70 m, sheet-like flow across the shelf would have become unsustainable and the down cutting of discrete channels began. Kugmallit Channel thus

became a conduit for meltwater flow that delivered sediment directly onto the upper slope at a point source. As Kugmallit Channel became active, sheet-like flow on the shelf ceased thus terminating the period of regional deposition of Unit 3 MTD/turbidites on the slope.

Correlation of the unconformities above shelf Unit C and slope Unit 3 implies that combined shelf Units A and B correspond with combined slope Units 1 and 2. Shelf Unit B comprises sediments reworked from underlying Unit C as sea level rose during the Holocene transgression. Transgression on the shelf is inferred to equate with development of the paleo-scour zone in slope Unit 2. The upper surface of the paleo-scour zone is diachronous, with the youngest scour marks formed on the mid-slope at ~16000 cal years BP, and on the upper slope prior to 12190 ±192 cal years BP, consistent with a rising sea level. 12000 cal years BP is approximately when sea level began rising from the 70 m low stand interpreted by Hill *et al.* (1985). Thus, a correlation between shelf Unit B and slope Unit 2 is likely. Post-transgressive marine clays and silts of shelf Unit A therefore correspond to slope Unit 1 sediments above horizon H1a, and represent the interval after the zone of active scouring had migrated onto the shelf.

Slope Units 1 to 3 can be identified on the 2D seismic lines, as well as a sequence of deeper slope seismostratigraphic units (Units 4 to 7). However, shelf units (Units A to E and deeper) are difficult to resolve (see Section 7.2). All of the slope units represent laterally discontinuous packages of MTDs sandwiched between well to poorly stratified pelagic sediments. Seismic horizons that define these units range from unconformities to unconformities, and represent the buried and often rugged topography of former seafloor positions resulting from slope failures. Within the units numerous unconformities that also may be truncated by other erosion surfaces are also identified. As a whole, Units 1 through 7 record a complex and heterogeneous stratigraphic history of continuous deposition represented by stratified intervals and MTDs. Erosion and downslope transport of these stratified deposits and earlier MTDs is represented by unconformities and unconformities that mark the basal surfaces of slope failures and of channels that served as conduits for MTDs and more fluidized flows.

4.3 Correlation Difficulties

A number of problems have complicated the development of a regional stratigraphy for uppermost units of the Quaternary section in the southern Beaufort Sea. These include the difficulties in tracing shallow (~100 m BSF) seismic units and horizons from the Mackenzie Trough beneath the Beaufort and Yukon shelves, and the lack of radiometric dates from deep boreholes. The acoustic stratigraphic continuity problem is due largely to pinchout or erosion of Mackenzie Trough units against both the Beaufort and Yukon shelf margins. The problem is compounded by the base of Trough unconformity, the surface of which can be clearly discerned in seismic profiles as an angular unconformity beneath the central Trough, but which curves gradually into disconformable concordance with much older Iperk sequence strata beneath both shelves (Enclosure 4).

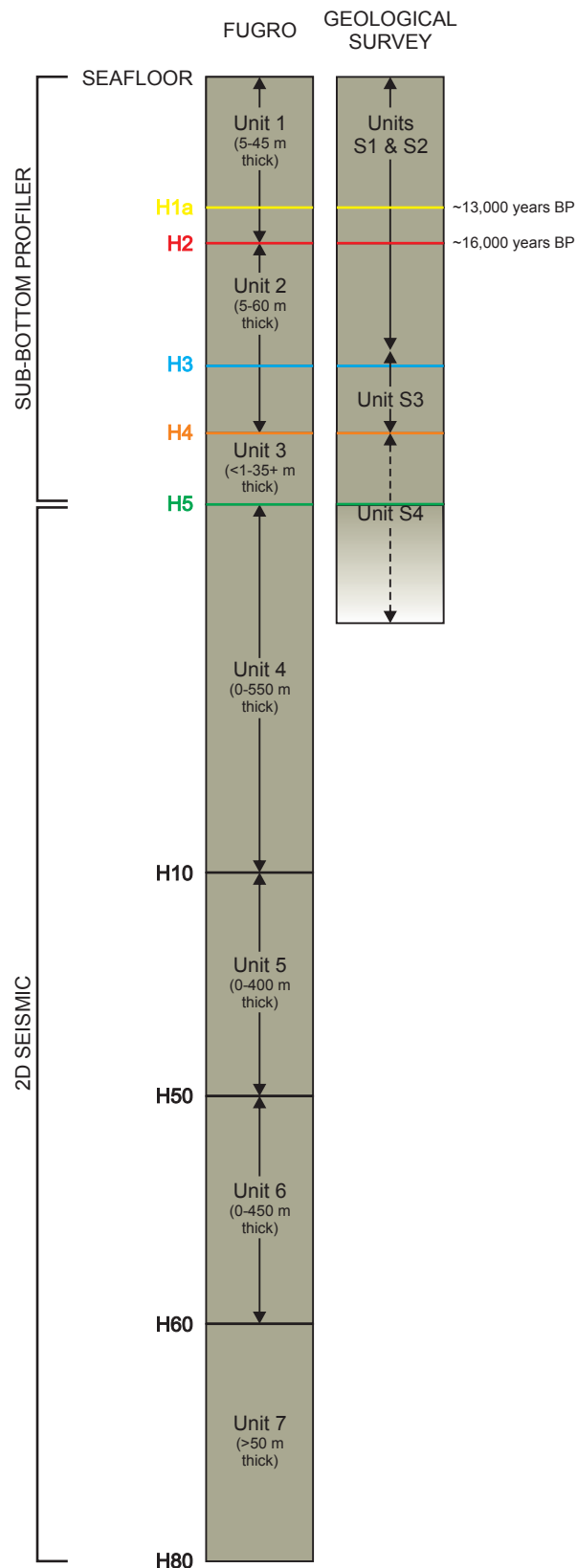
Difficulties with stratigraphic correlation also arise on the eastern Beaufort Shelf due to the presence of acoustic permafrost (APF) which overprints, enhances or partially masks stratigraphy to depths up to ~700 m below the modern seafloor. The APF is additionally problematic because permafrost does not uniformly affect the entire vertical profile of the shelf, and repetitive layers of poorly frozen sediment are frequently encountered sandwiched between frozen sediments. The vertical alternation between well frozen and poorly frozen sediments results in a sequence of velocity inversions that makes the creation of a coherent seismic velocity model difficult (e.g. MGL, 1992b). Acoustic permafrost is discussed in detail in section 6.2.1. Lateral changes in APF over tens of metres to kilometres add further complications (Pelletier, 1987a). The only shelf units unaffected by APF are the transgressive and post-transgressive Holocene sediments of Units A and B.

There are also difficulties with correlations between stratigraphies of the Beaufort Shelf and continental slope. Despite a large network of sub-bottom profiler data recently acquired across the shelf/slope boundary, the nature of the stratigraphic transition from shelf to slope units is constrained because of rapid facies changes between relatively thin, often acoustically structureless units on the shelf, to rapidly downslope-thickening, well-stratified units on the slope. Quaternary shelf stratigraphy is punctuated by periods of deposition and erosion during cyclical submergence and exposure whereas the slope records long periods of uninterrupted deposition, punctuated by discrete MTD and turbidite packages and erosion surfaces.

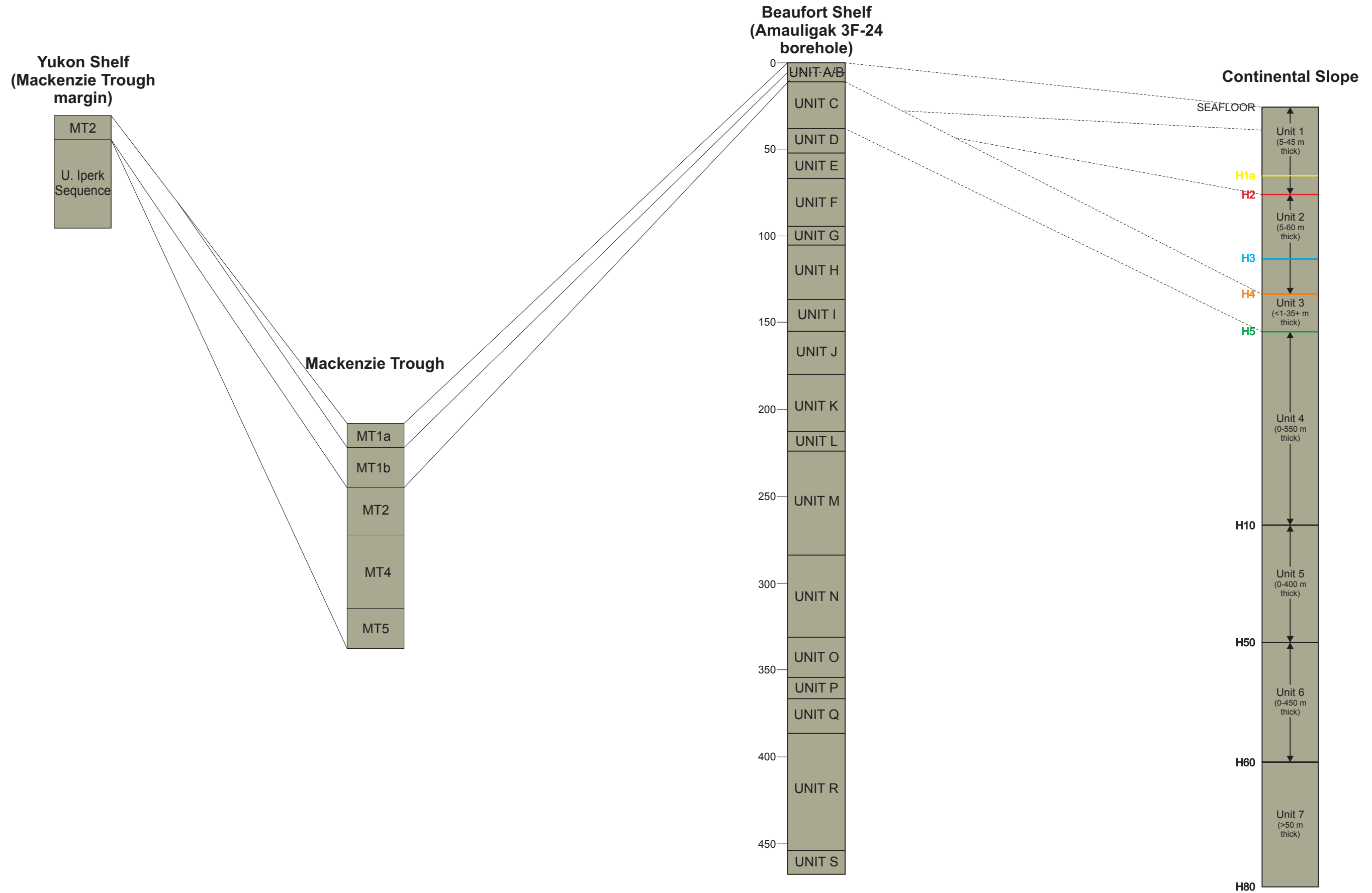
Shelf/slope correlation is additionally hampered by the shelf margin FEF Zone. The 1.5 km to 5 km wide zone is a region where diapiric FEFs have disrupted local stratified sediments of the uppermost slope and outermost shelf, and subsidence moats around the FEFs have within them their own, local stratified fill that complicates regional stratigraphy. Additionally, the FEFs are typically resolved as acoustic diffractions on sub-bottom profiles, and the presence of disrupted sediments and gas beneath them results in complete acoustic wipeout so that little or no stratigraphy can be resolved. As a result, stratigraphic transitions in the region where shelf and slope strata merge are generally not discernible.

A large area of the slope is disrupted by recent failure of the Ikit Slump that has resulted in the complete obliteration of internal acoustic stratification in a region 30 km to 50 km wide. The slumped region has effectively separated the slope stratigraphy into a well surveyed northeastern region, and a poorly surveyed southwestern region between which acoustic units cannot be correlated.

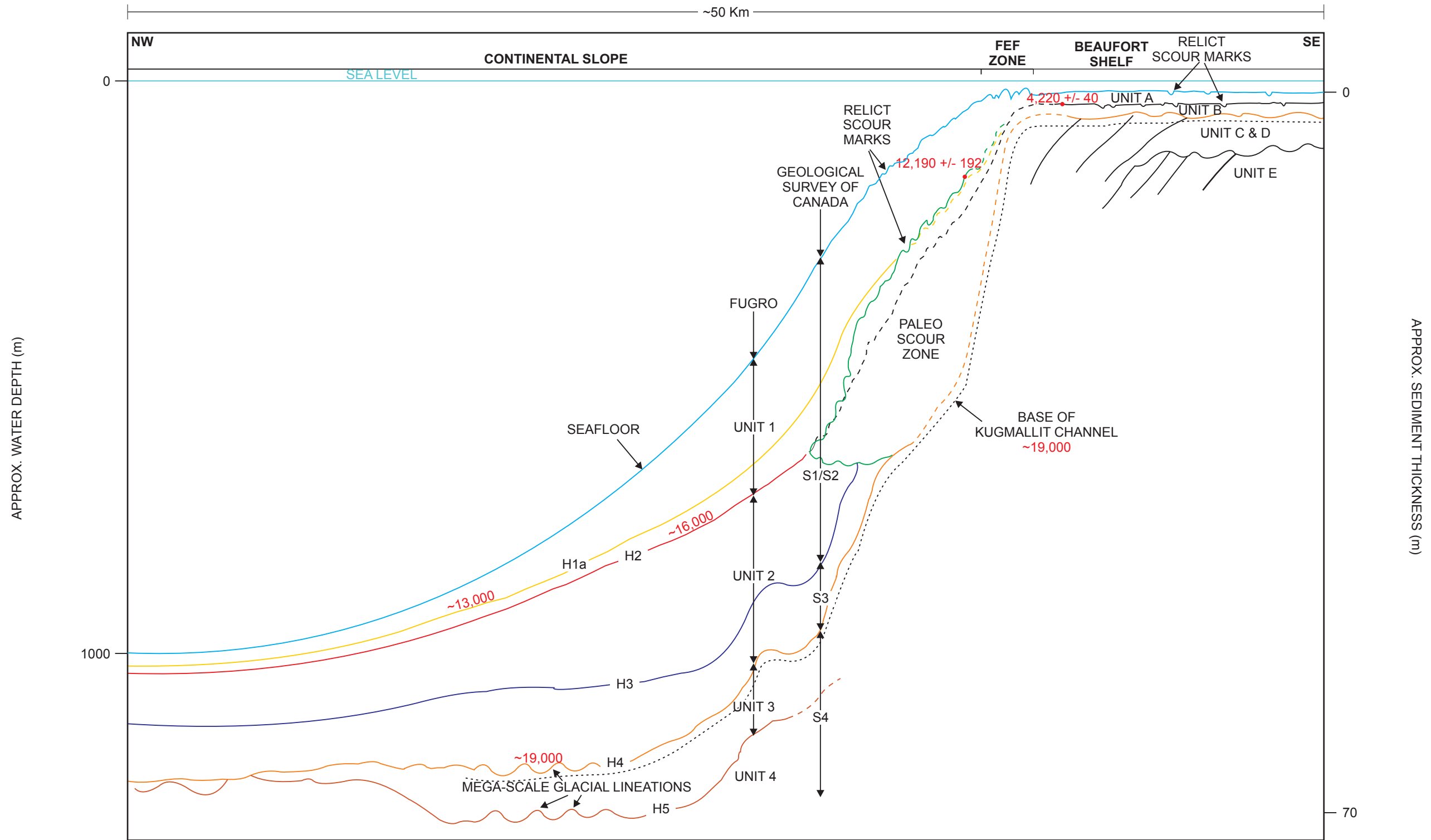
Stratified sediments of the Mackenzie Trough can be traced out onto the slope and matched to a well-defined Trough stratigraphy. However, the stratigraphy is truncated to the north by a network of valleys below ~1000 m water depth that are likely the superficial expression of buried MTDs and turbidites, and to the east by the Ikit Slump.



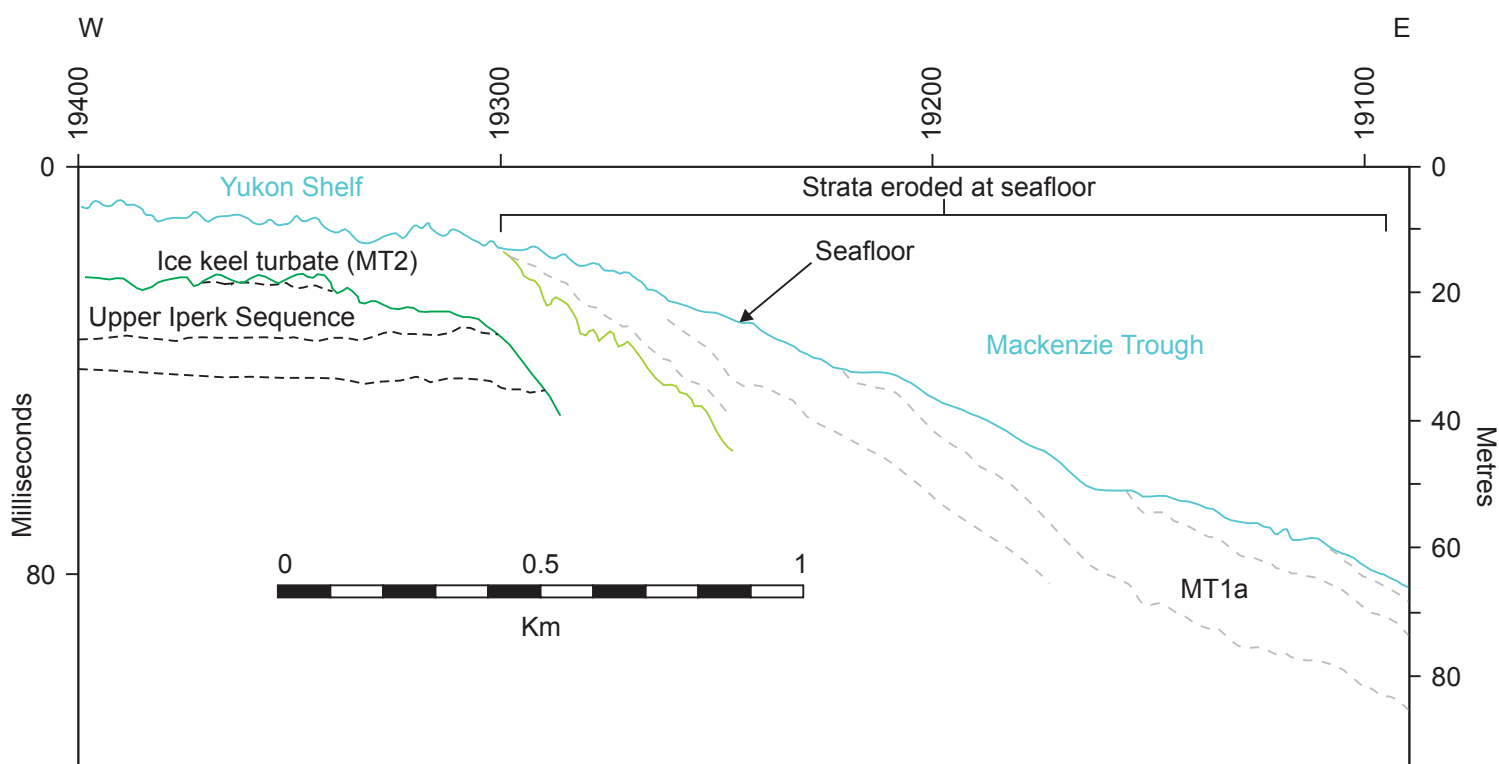
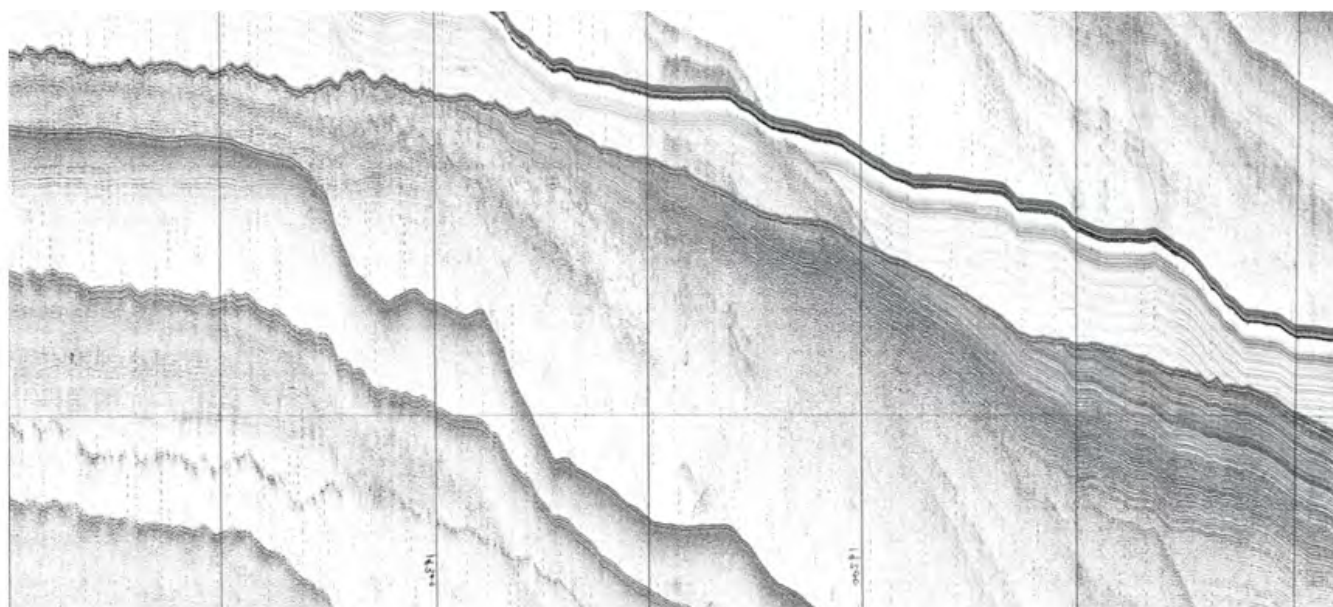
CORRELATION BETWEEN SLOPE STRATIGRAPHIES DEVELOPED BY FUGRO AND THE GEOLOGICAL SURVEY OF CANADA (GSC).



**STRATIGRAPHIC RELATIONSHIPS
SOUTHERN BEAUFORT SEA**

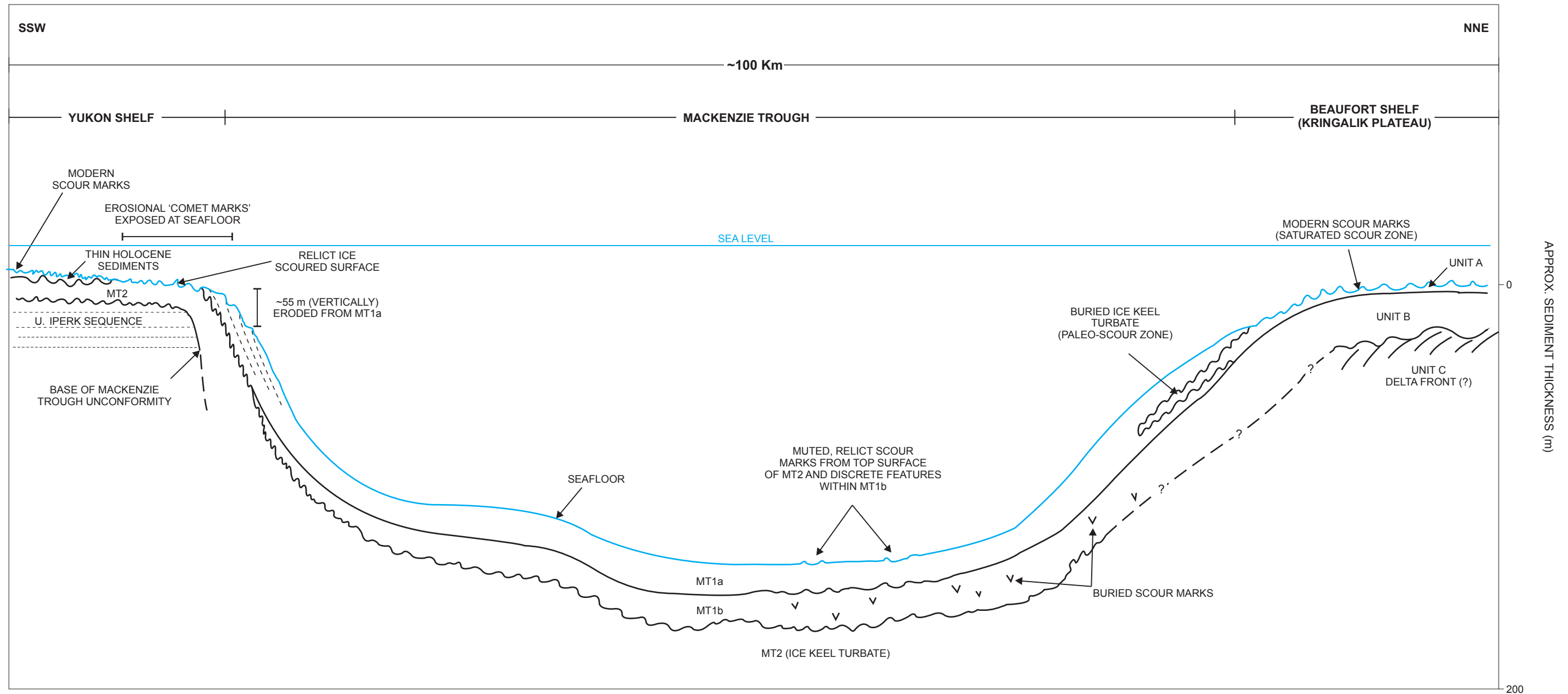


Shelf to slope schematic cross-section. This schematic illustrates the proposed correlations between shelf and slope stratigraphic units.

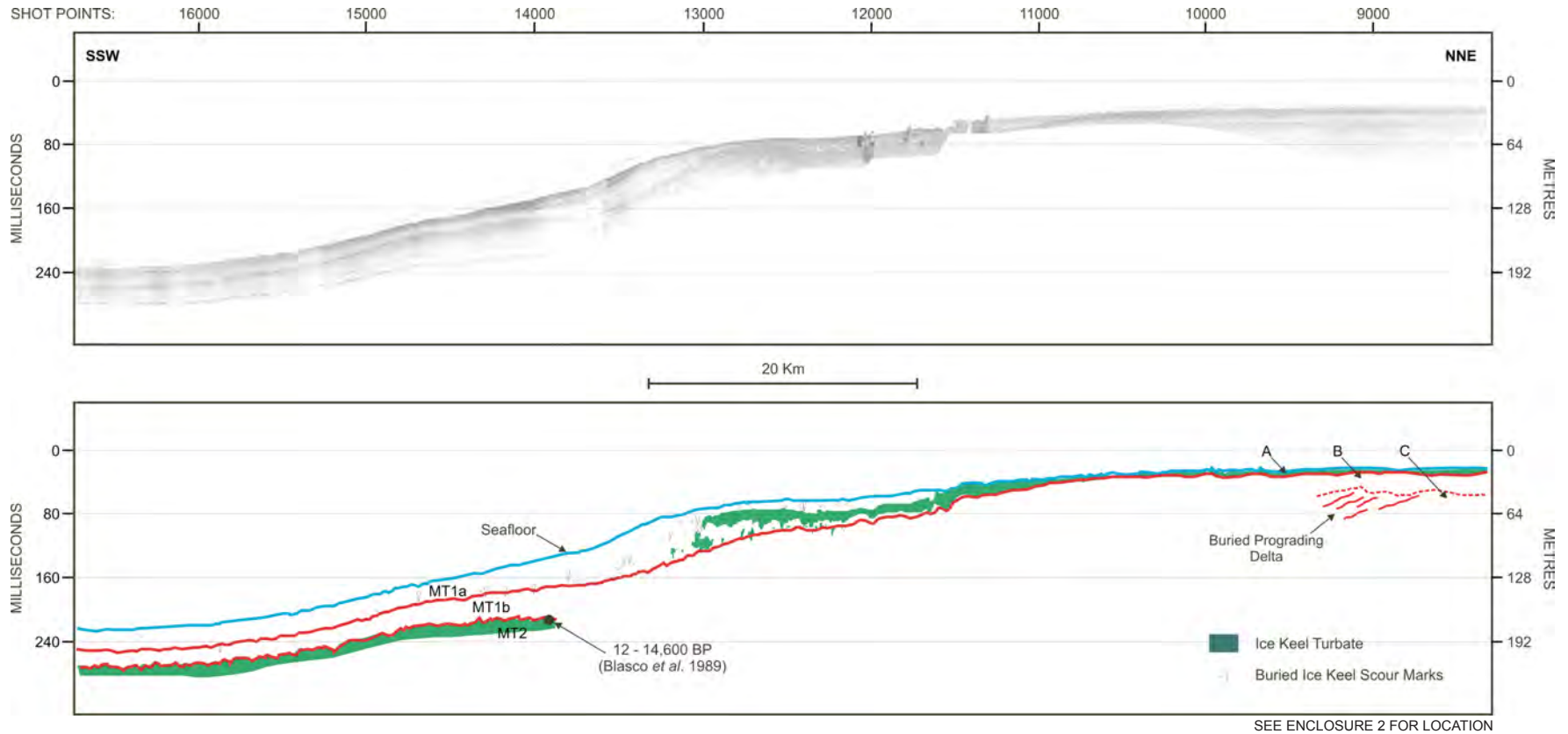


SEE ENCLOSURE 2 FOR LOCATION

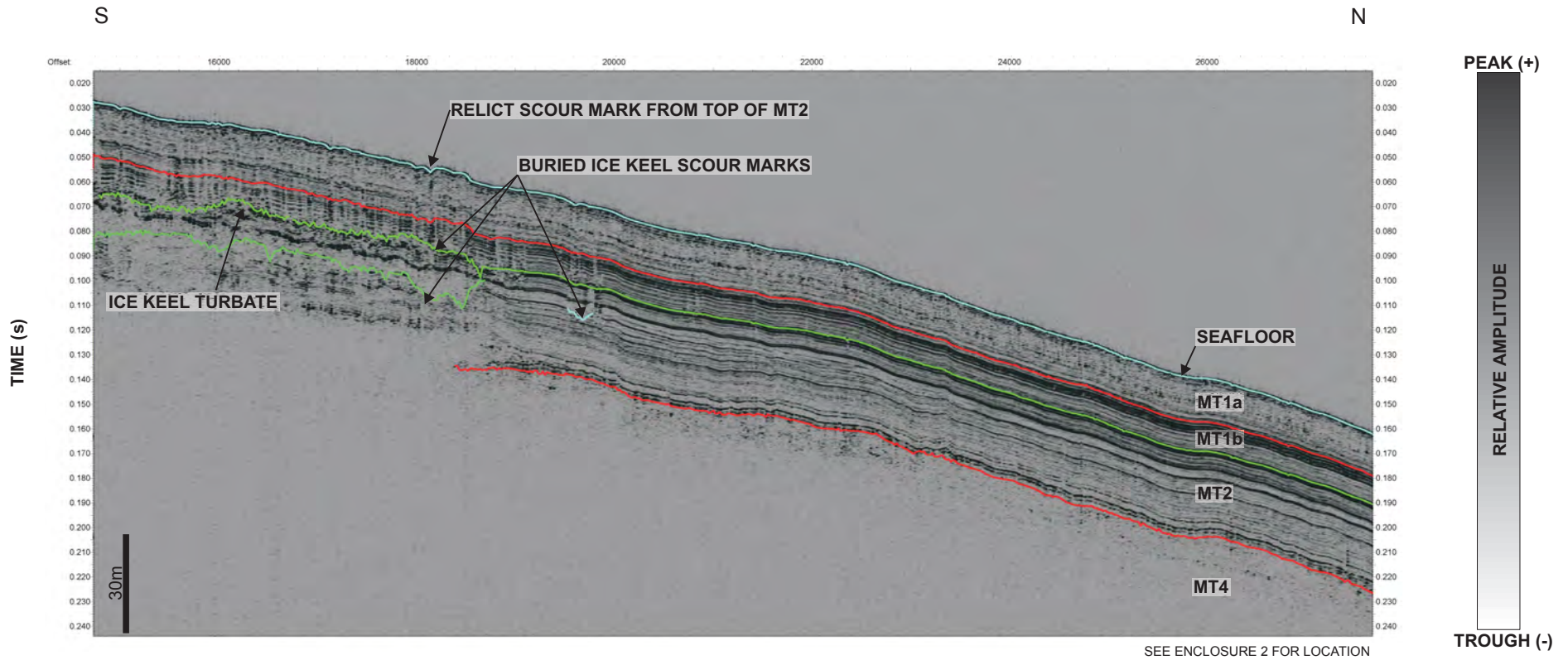
Mackenzie Trough and Yukon Shelf transition. Sparker SBP profile (Line 80-507) and interpretation of the transition from the western margin of Mackenzie Trough to the Yukon Shelf. Truncation of strata show that ~55 m of Unit MT1a has been eroded to re-expose relict scour marks of Unit MT2 at the seafloor on the Yukon Shelf. The base of MT2 truncates much older, horizontally stratified Upper Iperk sequence sediments. The hummocky surface at the base of MT2 likely represents relict scour marks incised into Upper Iperk sediments.



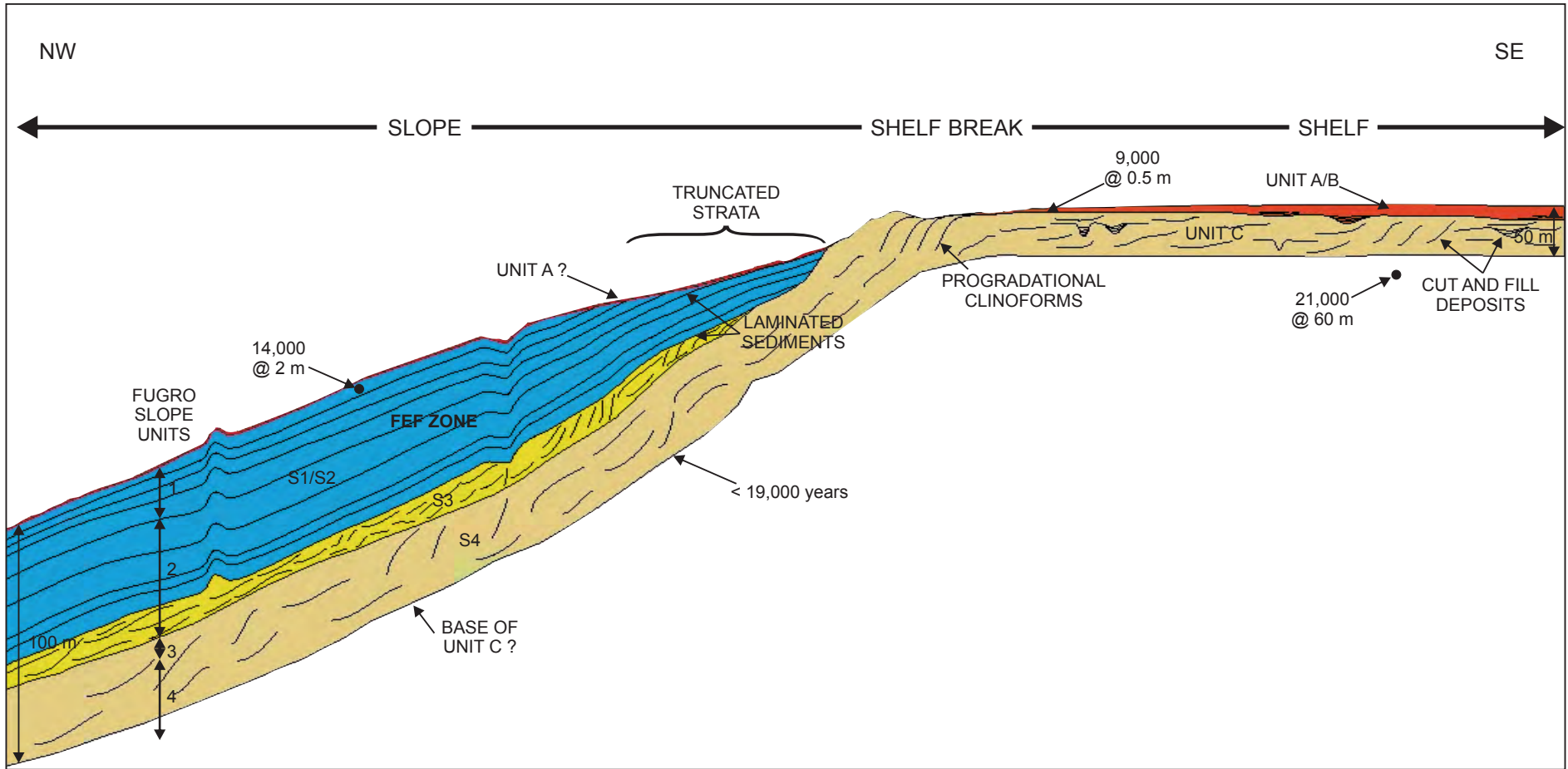
Mackenzie Trough schematic cross-section. This section illustrates the correlations between units in the Mackenzie Trough and beneath the Yukon Shelf and Beaufort Shelf based on sub-bottom profiler legacy data.



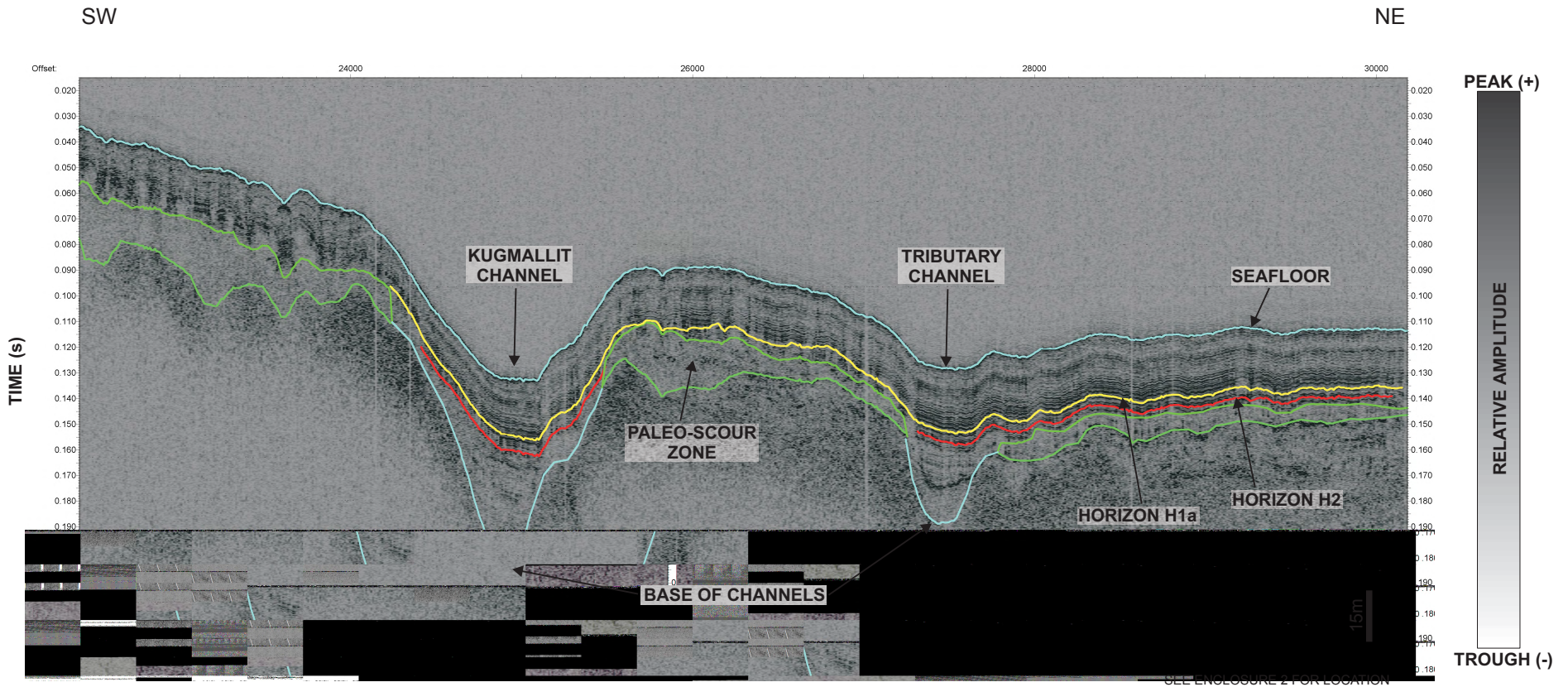
Mackenzie Trough and Beaufort Shelf transition. SBP sparker profile (line 80-507) and associated interpretation show the correlation between Mackenzie Trough and Beaufort Shelf Units.



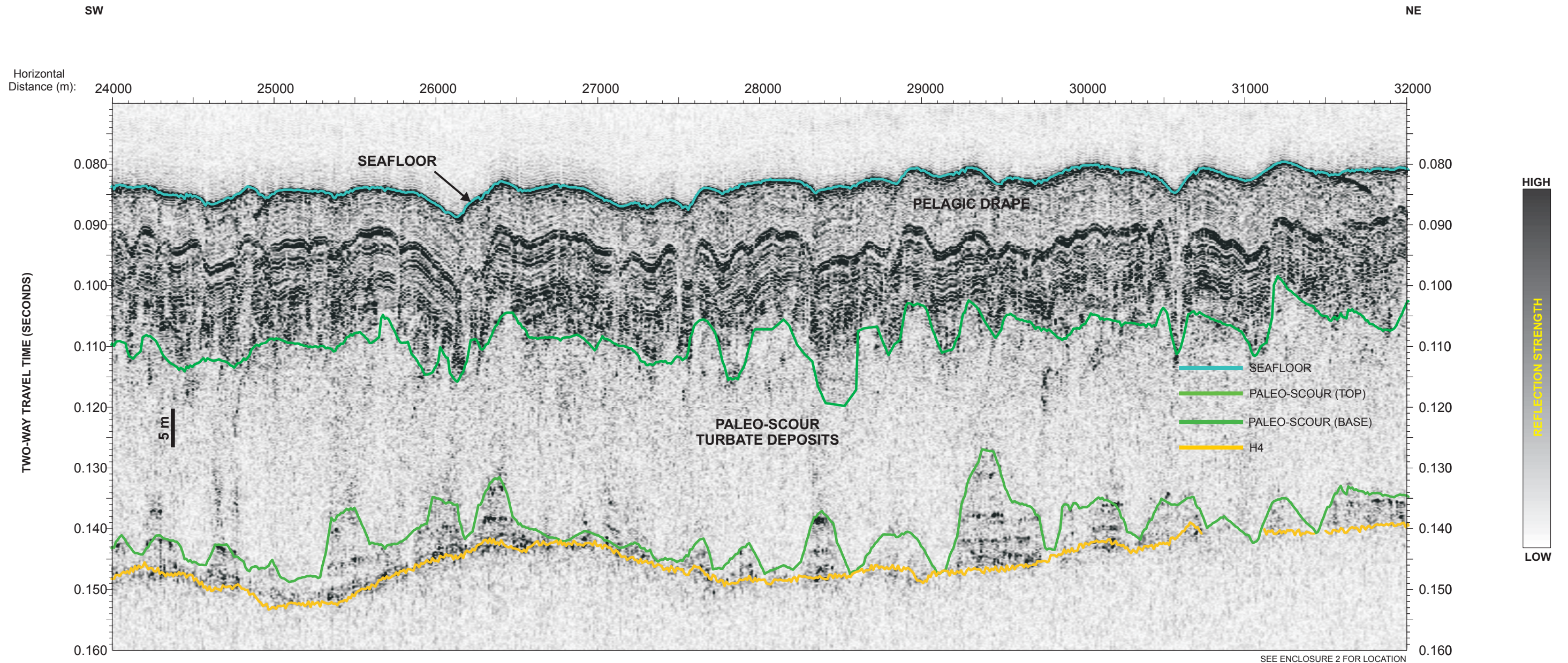
Sub-bottom Profile (Line 0037_2004_185_1741_003kHz_Ch0_0_utm) in Mackenzie Trough. The profile shows the interpreted Unit MT2 ice keel turbate where it pinches out in a water depth of ~350 m.



Schematic, shelf to slope cross-section showing the most recent Geological Survey of Canada model. The base of S4 is tentatively correlated with the bottom of shelf Unit C and is tentatively assigned a LGM age of ~19,000 BP. The Fugro slope unit stratigraphy is shown on the left side of the model. Correlations between the two models are shown in more detail in Plate 4.8. (Adapted from Rankin *et al.* 2011).



SBP Profile (Line 0139_2010_257_0708_LF_utm) across Kugmallit Channel on the Upper Slope. The main channel is on the left and a tributary channel on the right. The bases of the two channels merge with the bottom of the paleo-scour zone (green horizons), which is stratigraphically equivalent to horizon H4 marking the unconformity at top of slope Unit 3. On the Beaufort Shelf the Kugmallit Channel is cut into the top of shelf Unit C, an erosive event dated at ~19,000 years BP at the LGM. Assuming the base of the channel on the slope is time equivalent then the horizon H4, a regional unconformity on the slope, is also ~19,000 years BP. The extrapolated age of the horizon H2 (red) is ~16,000 years BP from C₁₄ dates in younger sediments above, and the C₁₄ age of horizon H1a (yellow) above is ~13,000 years BP.



Sub-bottom Profile (Line 0099_2010_254_0445) showing basal ice scour mark topography (envelope display). The lower green horizon marks the base of the Paleo-Scour Zone which penetrates to H4 (gold) and preserves the original hummocky topography of the earliest scour marks to have been formed. The isolated "islands" between the scour mark troughs preserve traces of originally stratified sediments. The hummocky green upper horizon marks the top of the Paleo-Scour Zone, and is diachronous between horizon H2 in deeper water and the younger H1a near the shelf margin. The hummocky upper surface preserves the topography of the last scour marks to have been formed, and this has been propagated to the seafloor through overlying pelagic drape sediments of unit 1. The vertical scale bar is based on an assumed acoustic velocity in sediment of 1600 m/s.

5. SEAFLOOR CONDITIONS AND GEOHAZARD FRAMEWORK

In this section seafloor geohazards are identified and described. For ease of description the bathymetry and morphology of associated geohazards in the study area is divided into three general regions: the Continental Slope, Beaufort Shelf and Mackenzie Trough/Yukon shelf. Bathymetry of the ESRF study area is illustrated on Enclosure 1. A seafloor gradient map, produced from the multibeam bathymetry data, is shown on Enclosure 5.

5.1 Continental Slope Bathymetry and Morphology

5.1.1 Slope Failures

Areas of slope failure that affect the modern seafloor are found only on the continental slope. Large portions of the seafloor on the slope show morphological evidence of failure in a series of irregular, downslope oriented channels and valleys, examples of which are shown in Plates 5.1 and 5.2. They range from 10 km to 50 km wide, up to at least 65 km long and merge downslope into very large, continuous regions of deformed seafloor sediments. Seafloor topography in these regions is typically hummocky in cross-slope profiles, and smoother in downslope profiles.

The failure zones exhibit scalloped headwall regions below which are step-like terraces of displaced but coherent slide blocks of sediment that have moved only short distances from their original location (Plates 5.1 and 5.2; Enclosure 1). The terrace steps have relatively flat, undisturbed upper surfaces. Just below the headwall scarp, terraces commonly exhibit a rotational dip of $\sim 2^{\circ}$ - 3° , toward the headwall. The terraced zones are generally 0.5 km to 5 km wide and downslope become progressively more muted merging into a zone characterized by lobate flow-like structures, and then into a generally flatter surface with small-scale channel-like features that meander downslope. Alternatively the terraces may merge into indistinct regions of downslope-oriented ridges and grooves, which become muted and merge with relatively smooth seafloor in the centre of the slumped region. Ridges and grooves have relief of 1 m to 2 m, and may indicate the flow direction of sediment moving downslope from the terraced region.

A particularly large slumped region, the Ikit Slump (Saint-Ange *et al.* 2014), extends from the shelf margin down the continental slope (Enclosure 1). The upper limit is marked by a headwall scarp, which is almost straight and oriented northeast-southwest, parallel to and cutting into the shelf margin. The scarp is 10 m to 20 m high, and dips 15° to 25° to the northwest in water depths ranging between 90 m and 175 m, over a distance of at least 40 km to the southwestern limit of multibeam coverage. In places, the scarp curves northwest into deeper water, delineating discrete basins containing slumped seafloor sediments.

Similar terraced geometries beneath prominent headwall scarps that merge into downslope-oriented ridges and grooves, channel-like features and lobate flows have been

described for other large submarine landslides, such as the retrogressive slump of the 1929 Grand Banks earthquake (Piper *et al.* 1999), the Storegga slide (e.g. Hafliðason *et al.* 2004) and Trænadjupet slide (Laberg and Vorren, 2000). Similar morphologies are documented in buried slides from the Ursa Basin of the Gulf of Mexico (Sawyer *et al.* 2009) and the Caspian Sea (Richardson *et al.* 2011). The downslope transitions of seafloor morphology are generally interpreted to represent changes in process from retrogressive rotational slumping, to debris flow and turbidity currents during a single failure event. Downslope movement may be perpetuated by continuous feeding of sediment from retrogressive slumping, over a period of hours or days (e.g. Piper *et al.* 1999), and through the process of "ignition", a mechanism whereby sediment-rich density currents achieve sufficient velocity to erode underlying sediment thereby increasing flow size and velocity (Parker, 1982). Areas of retrogressive slumping on the Beaufort continental slope likely developed following the failure and evacuation of sediment from an initial failure zone located downslope of the terraced region (e.g. Piper *et al.* 1999; Laberg and Vorren, 2000; Sawyer *et al.* 2009), and is the mechanism attributed by Saint-Ange *et al.* (2014) to the formation of the Ikit Slump.

5.1.1.1 Frequency and Age of Slope Failures

A comparison of overlapping imagery from a seafloor rendering of 3D seismic data collected in 2008 (gridded at 20 m) and two repeat multibeam bathymetry surveys in 2006 (gridded at 10 m) and 2009 (gridded at 15 m) was used to assess the stability of part of the headwall scarp above the Ikit Slump over the four-year period of observation. The positions of the headwall scarp, and scarps of the uppermost terraces in the rotational slump region were traced digitally and their positions compared between surveys (Enclosure 6). Although there is minor, variable offset between the mapped edges of the scarps at different locations, these are generally within the resolution limits of the overlapping datasets, thus between 2006 and 2009, the headwall scarp and upper terraces of the Ikit Slump are interpreted to have been stable.

In all cases where sub-bottom profiler data have been collected over the disturbed regions of seafloor below the headwalls, evidence of acoustic stratification has been lost. In addition there is no evidence for the accumulation of post-slump deposition of stratified sediments above the disturbed seafloor implying that all of the slumped regions are at least late or post-Unit 1 in age. This interpretation is supported by C_{14} dates obtained from surface sediments in cores CL04 and CL03 on the upper Ikit Slump of 1322 ± 44 and 1314 ± 43 BP (93-100 cm and 125-129.5 cm BSF respectively). Whether sediments above these elevations are of post-slump age cannot be stated with certainty. Saint-Ange *et al.* (2014) interpret the Ikit Slump event to have occurred approximately 1000 years ago based on C_{14} dates from a core in undisturbed sediments adjacent to the Slump and interpretation of sub-bottom profile data. Higher resolution age dating from cores on the upper slump will refine its age. The youngest date from core CL41, located on the flat floor of the lower slump is 5760 ± 78 BP for the interval 39-41 cm BSF, and below this the ages are inverted indicating that the core likely comprises disturbed sediment throughout.

Elsewhere, cores BP10-PC21 and BP10-PC22 from the headwall regions of two deeper slumps produced ages of 15701.5 ± 32.5 BP and 16310 ± 431.5 BP (96-104 cm and 111-

119 cm BSF respectively) (see Enclosure 3 for core locations). These dates approximately correspond with the age for the base of Unit 1 (see section 5.1.9) which is acoustically stratified and 3 m to 8 m thick in this region. However, Unit 1 sediments are truncated at the headwalls of both slumps, and there are no stratified Unit 1 sediments draping the failure zones beneath. Therefore the cores sampled older, disturbed sediments, and the slumps are likely of similar age to the Ikit Slump.

Mosher (2009) considers submarine land-sliding on the Beaufort continental slope as a significant potential hazard because of earthquake potential in combination with slope angles, thick sediment accumulation and rapid sedimentation rates in the Mackenzie River delta region.

5.1.2 Seafloor Offsets/Faults

In places, small-scale normal faults offset the modern seafloor from <1 m to 10 m. There are two types: those associated with slumped regions (see Section 6.1.3) and others associated with concentric subsidence around large-scale FEFs (see Section 5.1.5).

5.1.3 Seafloor Gradient

Immediately beyond the Beaufort Shelf the regional gradient increases to between 4° and 6° to the northwest on the upper continental slope, decreasing to between <1° and 2° on the middle and lower slope (Enclosure 5). Significant local increases in gradient of between 15° and 25° occur along the headwall regions of the Ikit Slump and other slumped and disturbed regions located on the continental slope (Enclosure 5).

At the shelf edge, the Kugmallit Channel, which has little seafloor morphological expression on the outer shelf, emerges on the upper slope as a well-defined, deeply incised channel that is 40 m to 50 m deep (Enclosure 1). The 1.2 km to 1.5 km wide channel can be traced downslope for at least 30 km to 750 m water depth. Two tributaries join it at low angles on its eastern bank at downslope distances of 20 km and 21.5 km from the shelf margin, in water depths of 500 m and 540 m respectively. The downslope gradient of the channel floor and its two tributaries is between 1° and 2° (Enclosure 5). Sidewall slopes generally range between 3° and 6°, and exceptionally up to 15°. Three small slumps <1 km long have affected the channel sides, between 20 km and 26 km downslope.

5.1.4 Expressions of Buried Topography

Gullies

In license block EL477, and in the northeast portion of EL476 (see Plate 1.1 for location and Enclosure 1), the continental slope is generally smooth, but with a network of subtle low relief gullies in the mid-slope region which are oriented downslope to the northwest. From the edge of the paleo-scour zone in water depths between ~360 m and 380 m the gullied terrain extends downslope for distances between 8 km to 12 km, before dying out between approximately 500 m and 580 m water depth (Enclosure 1). In cross-section, the

gullies are of variable width, ranging from 0.5 km to 2 km, and in depth from 2 m to 10 m (Plates 5.3 and 5.4). Slope angles of the gully margins are no greater than the average regional slope of $\sim 1.5^\circ$. The gullies represent topography inherited from a buried surface (horizon H3) 30 m to 40 m BSF (see Section 6.1.1).

Gullies reappear in deeper water between approximately 580 m and 700 m, and can be traced downslope to approximately 900 m water depth where they either die out or are truncated by the headwalls and sidewalls of the slumps (Enclosure 1). The gullies coalesce downslope and feed into wide but subtle swales, except where truncated by slumps. In cross-section, the gullies are of variable width, ranging from 0.2 km to 1 km, and in depth from 2 m to 6 m (Plate 5.5). Slope angles of the gully margins is no greater than the average regional slope of $\sim 1.5^\circ$. Like the straight gullies on the mid-slope, this population also represents topography inherited from the same buried surface (horizon H3) 15 m to 20 m BSF.

On the upper slope in the central and southwestern portion of EL476, a number of large, coalescing channel-like features merge downslope towards the northwest. They are 0.75 km to 2 km in width and can be traced 25 km downslope from their apparent origin at the seaward edge of the FEF Zone. The flat channel floors are generally 5 m to 10 m lower in elevation than the undisturbed margins, but with the same regional seafloor dip of 1° to 2° . The surface expression of the channels becomes progressively muted downslope until they can no longer be identified on the multibeam image beyond about 800 m water depth (Enclosure 1). Like the gullies in EL477 these seafloor features also represent inherited buried topography, in this case from buried Pleistocene ribbon-like mass-transport deposits described in Section 6.1.2.

Buried Ridges and Grooves

A portion of the base of Unit 3 (horizon H5), imaged in sub-bottom profiler data, is characterized by small-scale hummocky topography, often with associated "bowtie" acoustic artifacts. The hummocky surface is between ~ 650 m and at least 710 m BSS, and confined to an irregular northeast-southwest oriented linear region approximately 2 km to 5.5 km wide and 30 km long in the centre of license block EL477. Relief of features associated with "bowtie" artifacts is too small to measure, but two or three prominent dips on the H5 surface can be traced between several SBP lines indicating that they are ridges and grooves (Plate 5.6). The grooves have vertical relief of ~ 1 m to 7 m and apparent widths of 400 m to 500 m and can be traced upwards through ~ 50 m to 60 m of overlying pelagic drape to the seafloor (Plate 5.6). At the seafloor they appear as very subtle, straight-sided troughs oriented 045° but with reduced width (~ 300 m) and relief (1 m to 2 m) (Plate 5.7) and are more fully described in Section 6.1.4. The grooves are also seen on 3D seismic data from block EL477 where they form a striking set of straight, parallel lineations (Plate 6.1A). Sub-bottom profiler data show that the hummocky H5 surface can be traced southwest into license block EL476 for approximately 6 km (see Plate 1.1 for location and Enclosure 1). Within block EL476 the same surface is seen on 3D data, where it is identified between ~ 710 m and ~ 820 m BSS. The grooves here are between 5 m and 10 m deep and 200 m to 350 m wide and also oriented at 045° . The difference in observed groove elevation is probably due to acoustic attenuation of SBP data, the grooves likely continuing into deeper water beyond limit of the penetration. Thus the

grooves extend over a distance of at least 63 km parallel to the shelf margin, and their full elevation range is probably between ~650 m and ~820 m BSS.

Within the limits of the 3D volume in license block EL476, seismic profiles show both the H5 grooves and a second grooved surface stratigraphically 10 m and 30 m higher at the top of Unit 3 (horizon H4). These younger grooves have similar dimensions and the same orientation as those on the H5 surface and are located between ~700 m and ~800 m BSS. Within the H4 groove population a few are >300 m and one or two >600 m wide and these larger features are between 10 m and 15 m deep. The H4 horizon observed in SBP data to the northeast has small scale irregular topography but it is too subtle, and line spacing too great, for a grooved surface to be definitively identified and mapped.

Interpretation

The straight, uniformly-oriented buried ridges and grooves at the base and top of Unit 3 are interpreted as mega-scale glacial lineations (MSGSL) based on their consistent, unidirectional parallel orientation and dimensions (e.g. Clark, 1993; Spagnolo *et al.* 2013). In the Arctic ocean several generations of MSGSL have been mapped on and beneath the seafloor across large areas on the Alaskan slope, Chukchi Borderland and East Siberian continental slopes in modern water depths between 250 m and 1200 m (Engels *et al.* 2008; Niessen *et al.* 2013), as well as on Lomonosov Ridge (Jakobsson *et al.* 2008), Arlis Plateau and Mendeleev Ridge (e.g. Niessen *et al.* 2013). These MSGSL features are signatures of grounded glacial ice sheets extending far offshore from the modern coastlines, and occurred during earlier glaciations at least as far back as the middle Pleistocene or earlier (Niessen *et al.* 2013; Brigham-Grette, 2013). East-west oriented MSGSL extend along 640 km of the Alaskan Beaufort Sea margin are interpreted by Engels *et al.* (2008) as evidence for a large, west-moving, partially grounded ice shelf. They interpret this event to have occurred between Marine Oxygen-Isotope Stages 4 and 5b (~40000 to 70000 cal years BP).

Unfortunately the age range for the Unit 3 grooves is not known but they are likely much younger than MSGSL elsewhere in the Arctic Ocean. Thus both the H5 and H4 surfaces are tentatively linked to the movement of a very large and persistent late Pleistocene ice mass that grounded at least at the base and top of Unit 3, and possibly during Unit 3 deposition. Taking the lowest late Pleistocene eustatic global sea level to be -120 m at the Last Glacial Maximum (e.g. Rohling *et al.* 1998; Peltier, 2002; Peltier and Fairbanks, 2006) an ice mass capable of producing grooves across this depth range must have had a draft thickness on the order of at least 530 m to 700 m. The ice mass, possibly a melange of glacial and very thick sea ice, is inferred to have moved towards the southwest.

5.1.5 Large-scale FEFs

To date, seven large-scale FEFs have been discovered on the continental slope. These are not individually described, but general attributes, with examples, are discussed.

Slope FEFs are considerably larger than those in the shelf margin FEF Zone and occur as isolated features in water depths between 280 m and 1075 m (Enclosure 1). They are generally flat-topped conical features without summit craters, 5 m to 30 m high, with base diameters between 0.45 km and 1.1 km and side slopes of 5° to 10°. Two exceptions to this general morphology are a large-scale pockmark-like depression and a peaked cone with vents. Parasitic cones may be associated with FEFs in the form of adjacent flat-topped cones or as shallow craters on the flank of the main cone.

FEFs may be surrounded by a moat, and may comprise up to three overlapping cones (Plate 5.8). Moats are generally 0.6 km to 3 km in diameter, and are <5 m to as much as 30 m below the level of the surrounding seafloor. The margin of the moat surrounding the largest FEF is defined by a series of concentric ring faults with normal throws of 5 m to 10 m (Plates 5.8 and 5.9). A series of concentric step-like terraces 75 m to 100 m wide are created by the normal faults.

Where present, sub-bottom profiles show the ring faults offsetting the modern seafloor; however visual ROV observations reveal that recent pelagic sedimentation has completely masked exposed fault scarp surfaces. Sub-bottom profiles show no evidence of recent stratified pelagic drape on the cones. Water column anomalies may be present in multibeam data above the FEFs, likely related to seafloor fluid expulsion.

The variation in morphology between the FEFs is striking, and may be related to the stage of development and relative maturity of each feature. Studies of deep sea FEFs of similar scale off Barbados and along the Mediterranean Ridge accretionary complex suggest that conical features with craters may be indicative of mid-stage development, that evolve into flat-topped cones and encircling moat-like depressions during late stage development (e.g. Robertson and Kopf, 1998). In their analysis of several FEFs from different marine settings, Evans *et al.* (2008) describe characteristic "moat and pedestal" features of similar dimensions to those on the Beaufort continental slope. They interpret fault-bounded moats as calderas related to subsidence following eruption of fluidized sediments from the shallow subsurface. The flat-topped "pedestals" represent late stage eruptions, smaller in volume and presumably more cohesive than the earlier caldera-filling sediments (Evans *et al.* 2008). The presence of deep, vertical gas "chimneys" beneath the Beaufort continental slope FEF cones likely masks the feeder conduits that bring material to the surface from depth.

Fluidized material expelled from the FEFs forms distinct flows that can be mapped downslope in the sub-surface. FEF flows are described in more detail in Section 6.1.5.

5.1.6 Streamlined FEFs

On the upper slope immediately seaward of the main FEF Zone, in the vicinity of the western side of Kugmallit Channel where the shelf margin curves from northeast to southeast, lies a group of small FEFs (Enclosure 1). The FEFs occur in a 1.5 km by 5 km region between ~125 m and 250 m water depth within a belt of eroded seafloor sediments (see Section 5.1.7) and are typically 2 m to 5 m high with base diameters of 60 m to 90 m.

They are characteristically streamlined with steeper west-facing slopes of 5° to 10° and shallower, elongated east-facing slopes of 2° to 4° (Plate 5.10). Streamlining is probably the result of east-flowing bottom currents redistributing sediments onto the shallow lee slopes of the FEFs (see Section 5.1.7).

5.1.7 Seafloor Erosion

Unit 1 strata are truncated at very low angles at the seafloor in a semi-continuous, irregular belt on the upper slope, immediately seaward of the FEF zone in water depths between ~125 m and 250 m, and which in places extend to depths up to 600 m (Plate 5.11). The belt of truncated strata is at least 95 km long and typically 1 km to 2 km wide, but may be as narrow as 0.5 km and locally as wide as 10 km. By extrapolating eroded/non-deposited strata above the seafloor, an estimated thickness between 8 m and 20 m of Unit 1 sediment is missing along the upper slope. The large Ikit Slump has eroded any potential evidence of the former extent of truncated strata to the southwest. Erosion or non-deposition of Unit 1 sediments is restricted to the modern seafloor implying that the process responsible is recent and likely operated during Holocene times.

Interpretation

Truncation of strata at the seafloor is interpreted to be the result of two possible scenarios:

Holocene Marine Transgression. In this scenario erosion of Unit 1 began as temperatures warmed during late glacial times and the protective sea ice canopy deteriorated. With open water conditions, storm wave action and possible deeper longshore currents caused erosion of the soft muds of Unit 1 as sea level rose from the LGM 70 m lowstand.

Modern Erosion/Toplap. The pinch out of upper Unit 1 strata towards the shelf edge reflects an energetic environment where either deposition has been inhibited (toplap) or active erosion has removed stratified sediments. The agent responsible for erosion or non-deposition could be the narrow (15 km to 20 km) east-flowing shelf margin jet, located between 100 m and 200 m water depth, that brings Pacific-origin water into the Beaufort Sea (e.g. Forest *et al.* 2012; Nikolopoulos *et al.* 2009; Mathis *et al.* 2007; Spall *et al.* 2008; Pickart *et al.* 2004). Maximum mean peak shelf jet velocities are on the order of 20 cm/s and occur during spring (Christensen and Melling, 2010; Spall *et al.* 2008). In this scenario the streamlining of FEFs is interpreted to be the result of sediment deposition from the east-flowing jet on the sheltered, east-facing lee slopes. The jet could inhibit deposition in places and cause active erosion in others. However, the presence of truncated strata in water depths greater than 200 m suggests another mechanism that is or was operating over a wider area of the upper slope.

Both scenarios are considered plausible. The presence of eroded strata in water depths below the influence of the modern shelf margin jet suggests that active erosion of upper Unit 1 strata during the Holocene transgression when sea level was lower is a likely explanation. As sea level transgressed onto and across the shelf and slowed, modern

oceanographic conditions stabilized. The east-flowing shelf margin jet developed and erosion or inhibited deposition continued along the upper slope to the present day.

5.1.8 Pockmarks

A small number of pockmarks occur in groups on the upper slope, in the vicinity of the Kugmallit Channel immediately below the FEF Zone at the shelf margin. These upper slope pockmarks, are typically 40 m to 50 m in diameter and 0.5 m to 3 m deep, with sidewall gradients between 2° and 4° (Plate 5.12).

5.1.9 Paleo-Scour Zone

The seafloor of the uppermost continental slope between water depths of ~150 m and 400 m, is characterized by numerous straight to sinuous grooves that are approximately parallel to regional contours (Plate 5.12). The grooves are all located immediately seaward of the shelf margin FEF Zone, and intersect at low angles. Their distinctive topography can be traced southwest from license blocks EL477 and EL478 into EL476 where they are more subdued in relief (see Plate 1.1 for location and Enclosure 1). The grooved zone is between 3 km and 15 km wide and at least 175 km long. The zone is truncated at its southwestern end by the headwall scarp of the Ikit Slump (Enclosure 1). The grooves range from 0.3 km to 8 km long, 75 m to 100 m wide and 0.5 m to 3 m deep. Sidewall slopes are between 3° and 6° (Enclosure 5). The grooves are generally oriented sub-parallel to the shelf margin but may meander to intersect and cross-cut one another at low angles (Plates 5.13 and 5.14).

At the downslope margin of the grooved zone horizon H2 merges with a diffuse hummocky horizon between 5 m and 45 m BSF and cannot be traced any further upslope as a coherent reflector. The hummocky horizon is difficult to pick because it marks the boundary between an acoustically structureless zone beneath, and initially poorly stratified sediments above (Plate 5.15). The horizon is between 100 m and 450 m below modern sea level, and the hummocky topography is mimicked by overlying pelagic drape of Unit 1 strata that propagates this topography upwards to the seafloor. At the seafloor, the hummocky topography seen in SBP profiles is resolved in the multibeam image as numerous straight to sinuous grooves. In one or two places individual isolated grooves developed in acoustically stratified sediments are preserved in cross-section just beyond the deep water margin of the grooved zone (Plate 5.15). These buried grooves are relatively deep features with vertical relief up to 20 m, and widths (measured from multibeam seafloor imagery) up to 125 m.

The base of the acoustically structureless zone can be traced as a diffuse to distinctly hummocky surface approximately equivalent to horizon H4. Where it is well resolved the hummocky basal topography has relief of 2 m to 7 m above horizon H4 (Plate 4.10). The top of the grooved zone and base of the associated underlying acoustically structureless zone, together define a distinct acoustic unit affecting Unit 1 and 2 sediments. The thickness of the structureless zone ranges from 0 m at the downslope margin of the grooved zone, where it is approximately 450 m BSS. The zone thickens upslope to

between 25 m and 30 m, exceptionally 40 m, and thinning again towards the shelf margin FEF Zone.

Using sub-bottom profiler data, Hill *et al.* (1982) described the buried hummocky surface of the grooved zone and the overlying stratified deposits in terms of a regular undulating fold geometry. They described this geometry as a series of connected half waves, on the order of 30 m, with broad rounded crests and narrow troughs, and observed what they believed to be minor displacements along faults associated with the synform-like troughs (Plates 5.16 and 5.17). They described the acoustically structureless zone beneath the hummocky surface as a zone of chaotic reflectors. They inferred deformation in the underlying structureless region to have been contemporaneous with deposition and folding of the overlying stratified unit. Hill *et al.* (1982) interpreted their findings of this upper slope region to be the result of deposition and downslope creep of stratified sediments causing contemporaneous deformation by folding. They reasoned that accumulated creep strain caused the development of faults, and that relative displacement deformed the sediments at the lower boundary of the mass to form a decollement zone. However, in a discussion about the identification of creep deformation from sub-bottom profiles on submarine slopes, Piper (2005) noted that distinguishing such structures from pelagic drape on a rough surface, such as a mass transport deposit, is very difficult.

Interpretation

Multibeam data, collected in 2009 and 2010, now reveal the direct association between the buried hummocky surface and the intersecting linear seafloor grooves. Together, the basal hummocky H4 horizon, the acoustically structureless zone above, and the buried grooves on the upper surface are interpreted as an ice keel turbate, and are collectively referred to as the paleo-scour zone (Plates 4.3, 5.15 and 5.17).

The hummocky basal topography is interpreted as the remnant of the initial ice keel scoured surface, its relief (2 m to 7 m) indicative of the depth of scouring by the first seafloor-touching ice keel events. The overlying acoustically structureless zone is interpreted as an ice keel turbate, formed in the time period between H4 and H1a during which pelagic sediments were being continuously deposited and simultaneously mechanically reworked by scouring ice keels. Sediments were being continuously deposited during this time as is indicated by the undisturbed stratigraphy between H4 and H1a downslope of the paleo-scour zone. The upper grooved horizon is interpreted as a buried ice keel scoured surface, preserving intact the last-formed ice keel scour marks at the top of the ice keel turbate. These grooves are expressed at the seafloor through overlying Unit 1 sediments (e.g. Plates 5.13 and 5.15).

Ice keel scouring in the paleo-scour zone terminated at approximately horizon H2, approximately 15500 cal years BP. However, at core location PC-25 a radiocarbon date from immediately above the ice keel turbate indicates an age of 12190 ±192 cal years BP (Enclosure 3), approximately time equivalent to horizon H1a, and suggesting that the termination of ice scouring may have been diachronous. Isolated buried scour marks in deeper water just beyond the deep water margin of the paleo-scour zone are interpreted

as extreme scour events with measured incision depths of up to 20 m and widths (measured from the multibeam image) up to 125 m (Plate 5.15).

It is possible that deep-drafted icebergs originating from the terminus of an ice stream in the Amundsen Gulf were at least in part responsible for creating the ice keel turbate. The ice stream flowed northwestwards across the seafloor out into the Arctic Ocean reaching its furthest extent during the late glacial maximum (MacLean *et al.* 2015; Lakeman *et al.* 2012; Stokes *et al.* 2006). At this time the ice flowed out of the western Gulf into the Beaufort Sea becoming ungrounded between approximately 400 m and 500 m modern water depth (MacLean *et al.* 2015). The ice stream began final, rapid retreat at ~13000 cal years BP and had receded to eastern Amundsen Gulf by 12500 cal years BP (MacLean *et al.* 2015; Lakeman *et al.* 2012). Icebergs originating from the grounding line and drifting westwards in the Arctic gyre would have had sufficient draft to touch and plough the seafloor of the upper continental slope in the present study area

It is possible that the Unit MT2 ice keel turbate in the Mackenzie Trough (see section 4.2.2) is time equivalent to the paleo-scour zone described above. The deepest scour marks in Unit MT2 are at ~395 m BSS, 55 m shallower than the deepest features in the paleo-scour zone (see Plate 4.7). This depth difference could be accounted for by the more distal location of Mackenzie Trough from the proposed Amundsen Gulf iceberg source with respect to the paleo-scour zone on the slope, and to the effects of bathymetric sheltering by the northwest edge of the Kringalik Plateau.

5.2 Beaufort Shelf Bathymetry and Morphology

The Beaufort Shelf is essentially flat-lying, with gradients of $<0.5^\circ$ (Enclosure 5), and within the study area boundaries is generally <100 m below sea level (Enclosure 1). However, the shelf margin is not well defined and is represented by a gradually deepening transitional region of slightly convex slope between the flat seafloor of the continental shelf and the upper continental slope. The shelf-to-slope transition ranges between ~90 m and 120 m water depth in the east, and between ~100 m and 160 m water depth in the west (Enclosure 1).

The transition zone is straddled by a zone of fluid escape features (FEFs). Landward of the FEF Zone, the seafloor is characterized by numerous cross-cutting linear, to curvilinear ice keel scour marks extending to maximum water depths of ~112 m. A number of isolated FEFs occur on the shelf behind the main FEF Zone, their crests rising to as little as 19 m below sea surface.

The shelf is crossed by Kugmallit Channel, a northward-trending, shelf-crossing, flat-bottomed channel, partially filled by transgressive Holocene muds (O'Connor and Blasco, 1982). The channel extends from the vicinity of Kugmallit Bay, where its seafloor morphological expression is almost completely muted by thick (>20 m) Holocene fill, to the shelf edge where it merges with a relatively deeply incised downslope-meandering channel on the continental slope (see Sections 5.1.3 and 4.2.4). In the mid-shelf region between 20 m and 60 m water depth the channel has an asymmetric profile, the western

edge typified by barely perceptible gradients of much less than 0.1° and the eastern side being deeper with a slightly steeper margin against the Tingmiark Plain.

5.2.1 FEF Zone

A linear zone of numerous small-scale conical mounds and occasional pockmarks, interpreted as fluid escape features, straddles the shelf-slope transition between water depths of 75 m to 200 m. The FEF Zone is generally between 1.5 km and 5 km in width and is at least 130 km long (Plate 5.14 and Enclosure 1). It is discontinuous and narrows to as little as 0.3 km wide in the region where the Kugmallit Channel reaches the shelf margin (Enclosure 1). As it is traced to the southwest along the shelf margin, the FEF Zone is truncated by the pronounced shelf edge-parallel headwall scarp of the Ikit Slump (Enclosure 1).

FEFs are characterized by convex slopes with angles between 15° and 20° , occasionally approaching 30° . The base diameter of the mounds ranges from 70 m to 180 m and heights above seafloor range from 5 m to 25 m. The mounds are often clustered in coalesced groups, typically with a curvilinear trend either parallel or oblique to the shelf edge (Plate 5.14). A small number of pockmarks, small seafloor depressions generally <25 m in diameter and <1 m deep, occur dispersed throughout the FEF zone.

The FEF Zone is characterized in places by shelf edge-parallel seafloor “wrinkles” that occur between 75 m and 100 m water depth on the landward side of the main FEF zone (Plate 5.18). The wrinkles are subtle, curvilinear ridge-and-groove features, approximately 10 m to 20 m wide. Individual ridges and grooves can be traced for distances of <100 m to 500 m and have crest-to-trough relief that is typically <1 m.

Interpretation

It is almost certain that FEFs on the shelf and in the shelf margin FEF Zone are underlain by permafrost which at the shelf margin is at depths of ~100 m BSF (e.g. Morack *et al.* 1983; Taylor *et al.* 2013). The FEF zone represents the approximate seaward limit of permafrost. FEFs formed as the result of overpressure in shallow sediments caused by decomposing methane gas hydrates (Paull *et al.* 2011; 2007). The presence of depressed temperatures in sub-seafloor permafrost means that hydrates may be stable to depths as shallow as ~120 m (Paull *et al.* 2007). As the hydrate decomposes, gas is released creating overpressures that cause sediment expansion. Weaknesses in the overlying permafrost, such as buried taliks and thaw lakes that formed during sub-aerial exposure, allow the gradual upward extrusion of sediment to the seafloor where it forms characteristic conical FEFs and from which gas bubbles may escape into the water column. As sediment is gradually extruded to the surface, concentric collapse depressions or moats, form around the FEFs due to subsurface sediment volume loss (Paull *et al.* 2007). The absence of water column anomalies in multibeam data collected in 2009 and 2010 indicating free gas above FEFs in the FEF Zone suggests that these features may no longer be active.

5.2.2 Water Column Anomalies

In 2009 at least 41 water column plumes possibly related to seafloor fluid and/or gas expulsion, were observed in multibeam data (Plates 5.19 and 5.20). Most of these were observed in a 20 km by 3 km area (Paull *et al.* 2011; Saint-Ange *et al.* 2014) of relatively smooth seafloor at the shelf margin above the Ikit Slump headwall (Enclosure 1). Results from free gas and sediment sample analysis showed that the anomalies are related to methane seeps. C_{14} dates from the gas of ~50000 years suggest that the methane possibly originates from permafrost and/or gas hydrate decomposition in deep sediments (Paull *et al.* 2011). In 2010, only three water column anomalies were observed above individual FEFs on the continental shelf.

5.2.3 Shelf FEFs

A number of isolated FEFs occur on the shelf behind the main FEF Zone (Enclosure 1). The crests of isolated FEFs rise to as little as 19 m below sea surface. In 2010, an ROV dive was made on a shelf FEF above which water column anomalies possibly related to fluid and/or gas expulsion were observed in multibeam data. During the dive a small crater ~2 m in diameter was identified on the flank of the FEF cone that may have been the point of fluid/gas eruption. In addition a number of seafloor features were identified on the seafloor of the FEF cone that may be attributed to the action of bottom-feeding marine mammals.

The shelf FEFs are located in the region affected by relict ice keel scour marks (see below). Their age relationship to the scour marks appears to be time transgressive. In places, FEF cones clearly overprint scour marks (Plate 5.21), as seen at the FEF described above. In other places scour marks occur on the cone flanks, indicating that the FEF is older (Plate 5.22).

Large numbers of pockmarks occur in the Kugmallit Channel in water depths of ~9 m, where sediments are thickest, in a region 20 km offshore (Blasco *et al.* 2011). The pockmarks are associated with gas escape from beneath the seafloor. Repetitive mapping indicates that new features are presently forming (Blasco *et al.* 2011).

5.2.4 Relict Ice Scour Marks

On the continental shelf landward of the FEF Zone in water depths up to ~112 m, the seafloor is characterized by numerous cross-cutting linear to curvilinear ice keel scour marks (e.g. Plate 5.14). They generally range from 0.5 km to 7.4 km in length, 50 m to 620 m in width and 0.5 m to 3 m in depth (Plate 5.23). The widest scour marks are generally shallow features, evidently formed by wide, relatively flat keels with multiple small protrusions that created 'multiple' scour marks (e.g. Weber *et al.* 1989). The scour marks have sidewall slopes generally between 1° and 3°, exceptionally reaching 5° to 10° (Plate 5.23).

The maximum water depth in which new scour marks have been recorded is 60 m (Blasco *et al.* 2011) suggesting that most of the shelf margin scour marks are a relict population still visible at the seafloor. The scour marks are formed in post-transgressive soft muddy sediments of shelf Unit A. Much of Unit A shows little or no internal acoustic stratigraphy, and this has been interpreted as the result of mechanical reworking by scouring ice keels (O'Connor and Blasco, 1982).

The volume of scour-affected Unit A sediments is referred to by O'Connor and Blasco (1982) as a saturated scour zone (SSZ). For the region located in water depths between ~52 m and ~112 m, where Unit A is clearly affected only by relict scouring, the scour-affected sediments are referred to as a saturated paleo-scour zone (SPZ). In places where Unit A rests directly above it, the underlying dense and largely frozen sands of Unit C are believed to act as a physical barrier that restricts ice keel penetration to the unfrozen sediments above (e.g. Blasco *et al.* 2011).

5.3 Mackenzie Trough/Yukon Shelf Bathymetry and Morphology

The Mackenzie Trough is a broad, north-northwest oriented submerged asymmetric linear valley. It is approximately 150 km long, 75 km wide and is the seaward extension of the broad, flat Mackenzie delta. The Trough bisects the continental shelf, separating the Yukon shelf in the west from the Beaufort Shelf in the east. Bathymetrically the Trough extends from the -10 m to the -400 m contour where it merges with the east-northeast to west-southwest-oriented continental slope (Enclosure 1). The seafloor of the central axis of the Trough dips very gently to the north-northwest at an average of 0.17° (Enclosure 5). Slopes of the western margin against the Yukon shelf are typically $\sim 1^\circ$ (exceptionally 2.5°) to the east-northeast, and slopes of the eastern margin against the Kringalik Plateau are about 0.08° to the west-northwest (MGL, 1992a; Enclosure 5).

Seaward of the Trough between 800 m and 1000 m water depth a crude dendritic network of small, meandering tributary valleys, 5 km to 10 km long, 250 m to 750 m wide and 15 m to 50 m deep, dissects the otherwise featureless seafloor of the continental slope (Plate 5.24). Slope angles range between 8° and 20° (Enclosure 5). At a regional break in slope at ~1000 m water depth the valleys merge at the heads of wider but generally shorter valleys that flare downslope widening from ~0.5 km to 2.5 km. Some of these valleys are chute-like, from 40 m to 200 m deep separated by sharp-crested interfluves, the flanks of which are characterized by small, rill- and gully-like tributaries (Plate 5.25). At ~1200 m water depth the chute-like valleys coalesce and flatten out into a region of meandering, downslope-oriented ridges and grooves. In places the ridged and grooved terrain is punctuated by long, broad interfluves 3 km to 10 km long and up to 2 km wide, the flanks of which are characterized by rills and gullies.

5.3.1 Modern Ice scour

The Mackenzie Trough, now partially filled with more than 300 m of Quaternary sediments, is heavily scoured by modern ice keels in water depths <16 m, but the frequency of modern scouring decreases rapidly in water depths >33 m. Two extreme

scour events (penetration depths of 3.3 m) have been documented that were created in the last 18 years in water depths between 14 m and 17 m (Carr *et al.* 2010). From sub-bottom profile data, Comfort *et al.* (1990) interpreted the presence of sub-scour deformation beneath several modern scour marks, the deformation zone averaging 1.6 times greater than the incision depth of the scouring keels that formed them.

5.3.2 Paleo-Scour Zone

Between the southern edge of the study area at ~250 m and the 350 m bathymetric contour the smooth seafloor of the Mackenzie Trough is characterized by a population of curvilinear, intersecting grooves, similar in appearance to those in the paleo-scour zone on the continental slope (see Section 5.1.9). The grooves are more randomly oriented than those on the slope but are similarly interpreted as the seafloor expression of a buried ice keel scoured surface at the top of Unit MT2. Scour marks are not seen below ~350 m water depth.

5.3.3 Seafloor Erosion

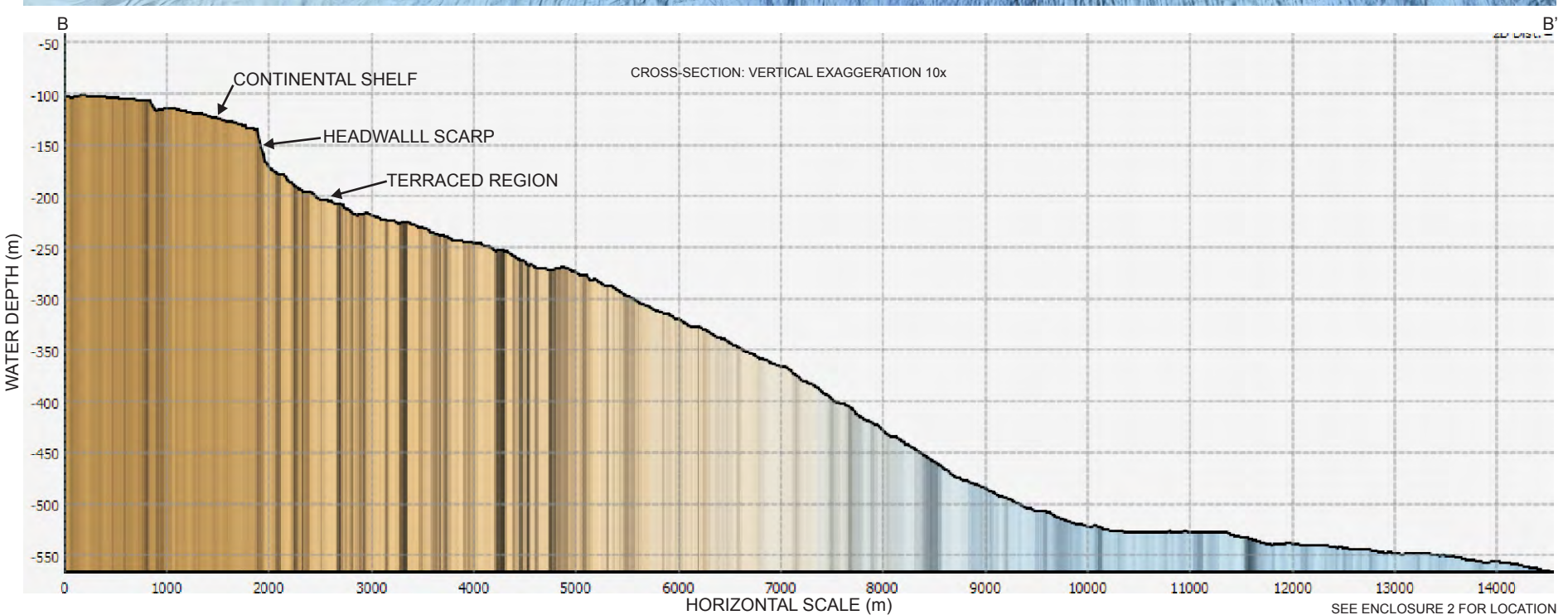
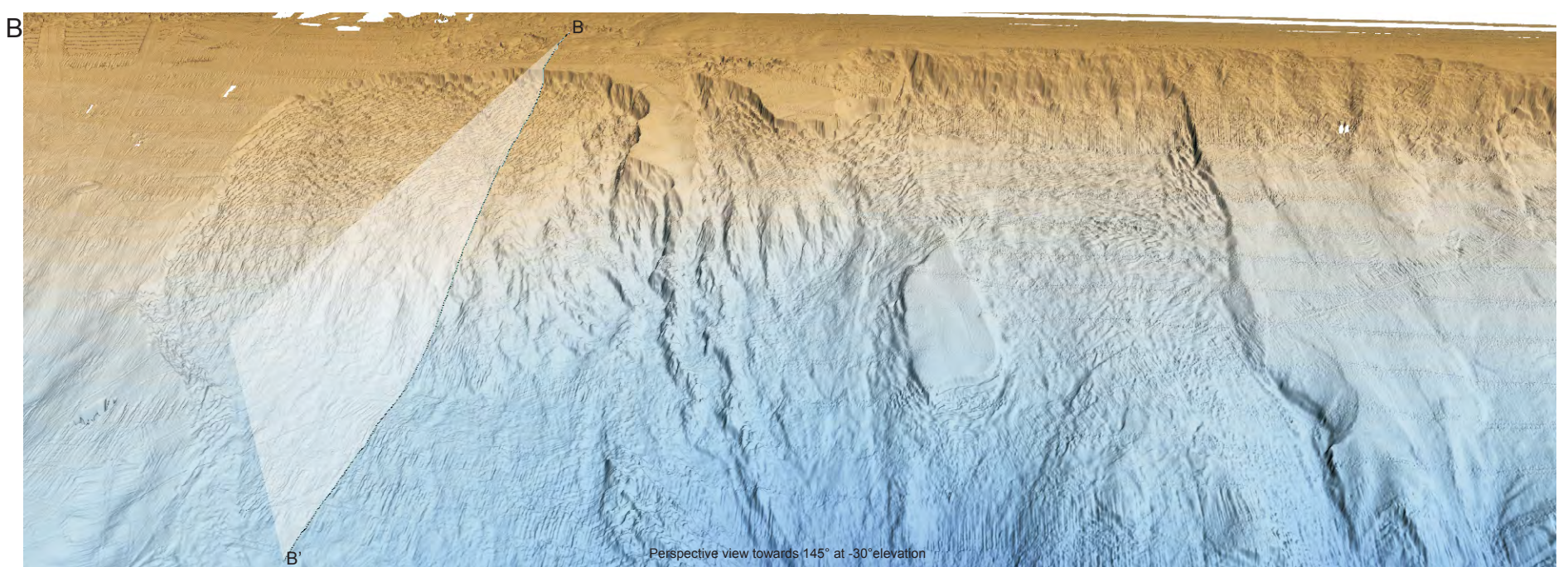
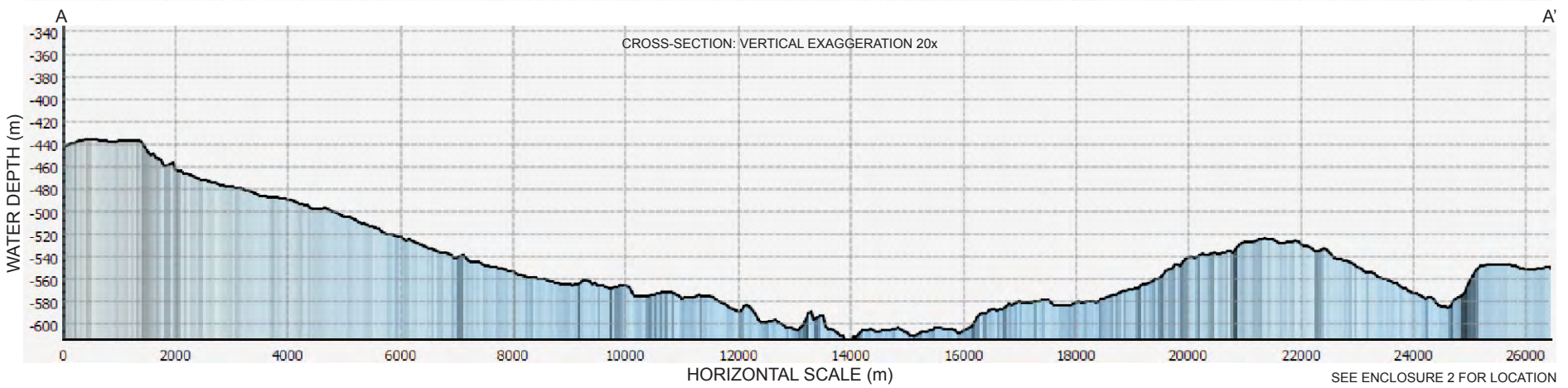
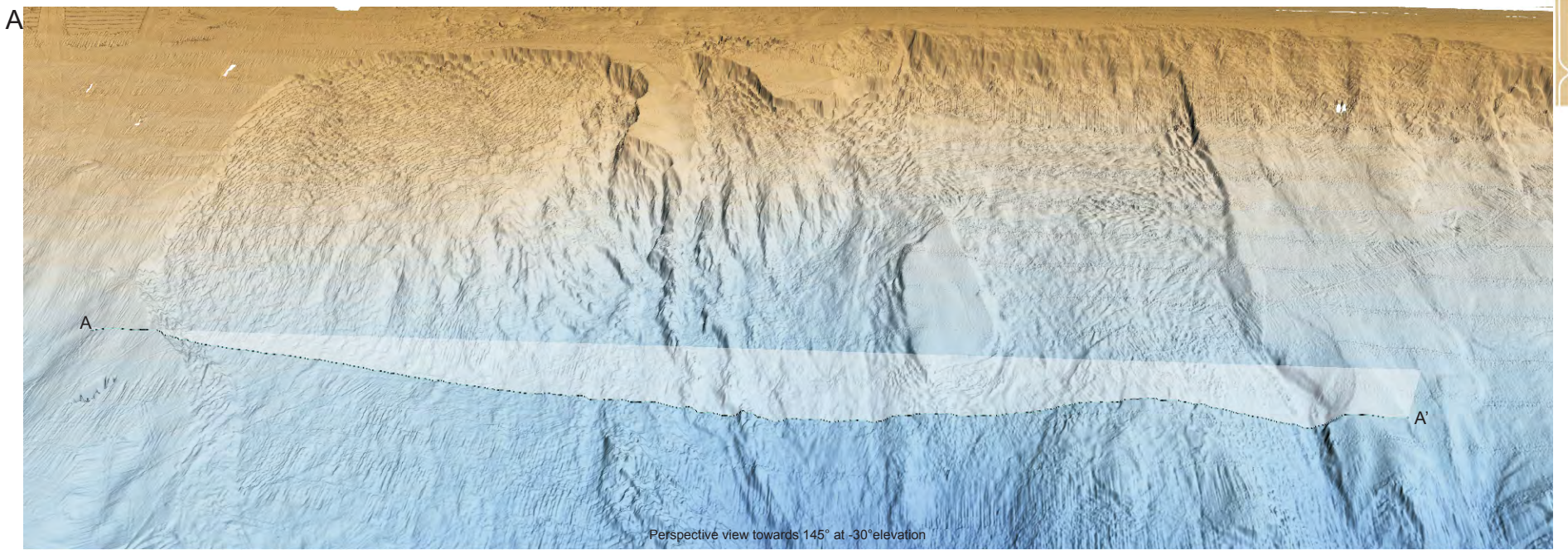
A belt of deeply eroded sediments has been identified along the western flank of the Mackenzie Trough and eastern margin of the Yukon shelf (see Section 4.2.1 and detailed discussion in Section 6.3.2). In this region all of Unit MT1a has been eroded to expose the ice scoured surface of Unit MT2. Strong currents have sculpted exposed sediments into comet marks (Werner *et al.* 1980) on the seafloor in this region. It is uncertain whether the strong current flow that formed these features is a modern process, and related to the erosion of sediments and exposure of the relict ice scour marks, or whether the comet marks are relict features on the exposed surface.

5.3.4 Pockmarks

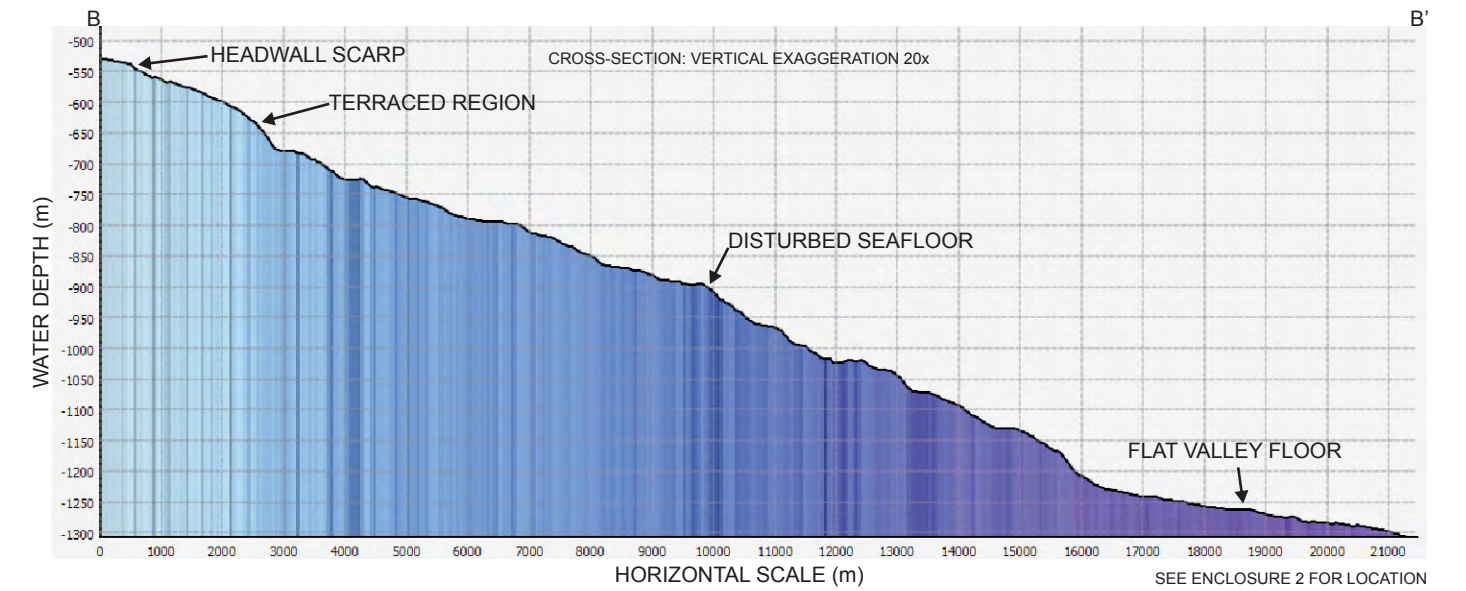
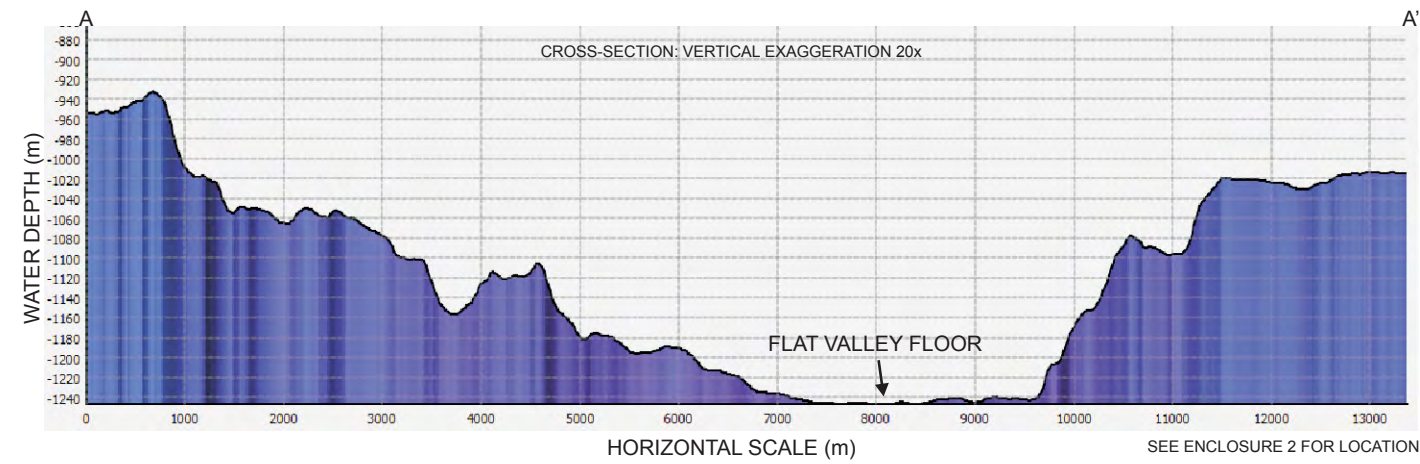
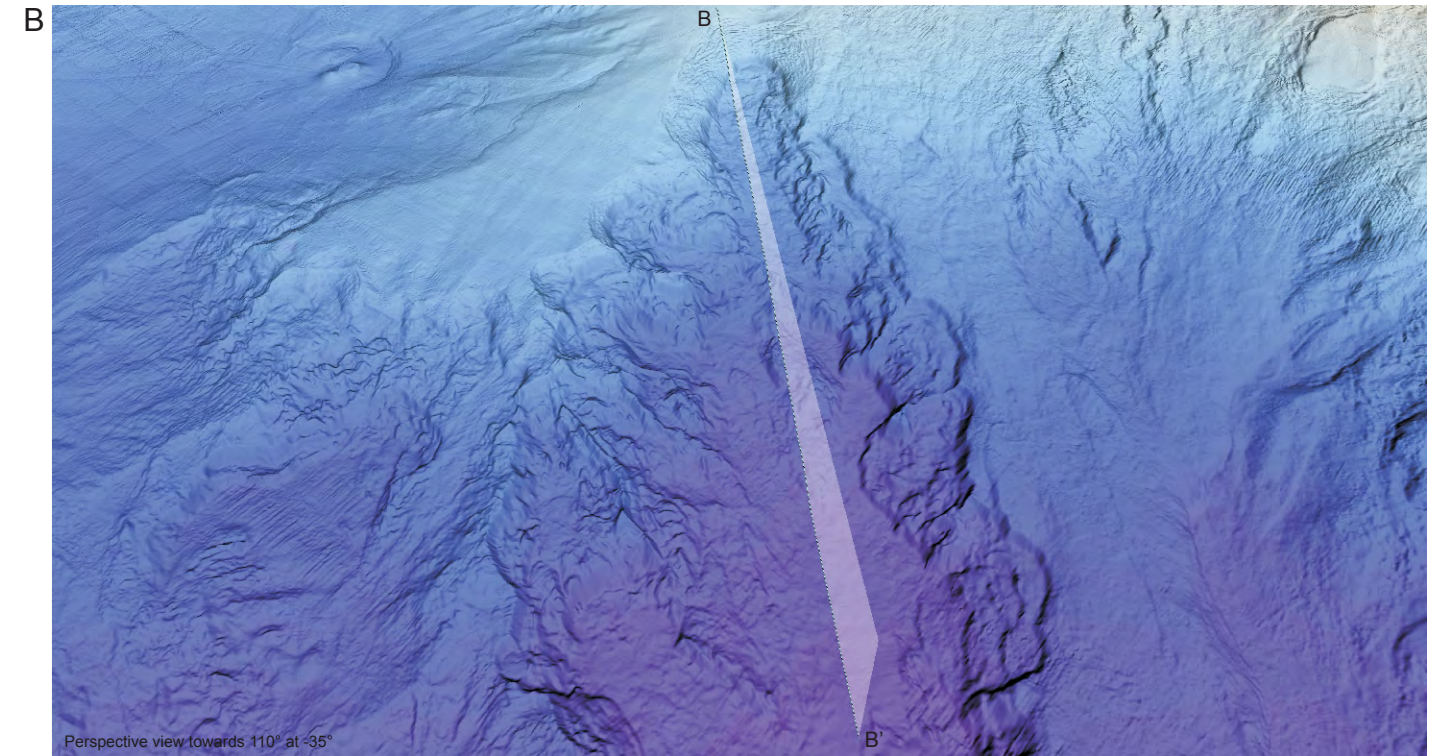
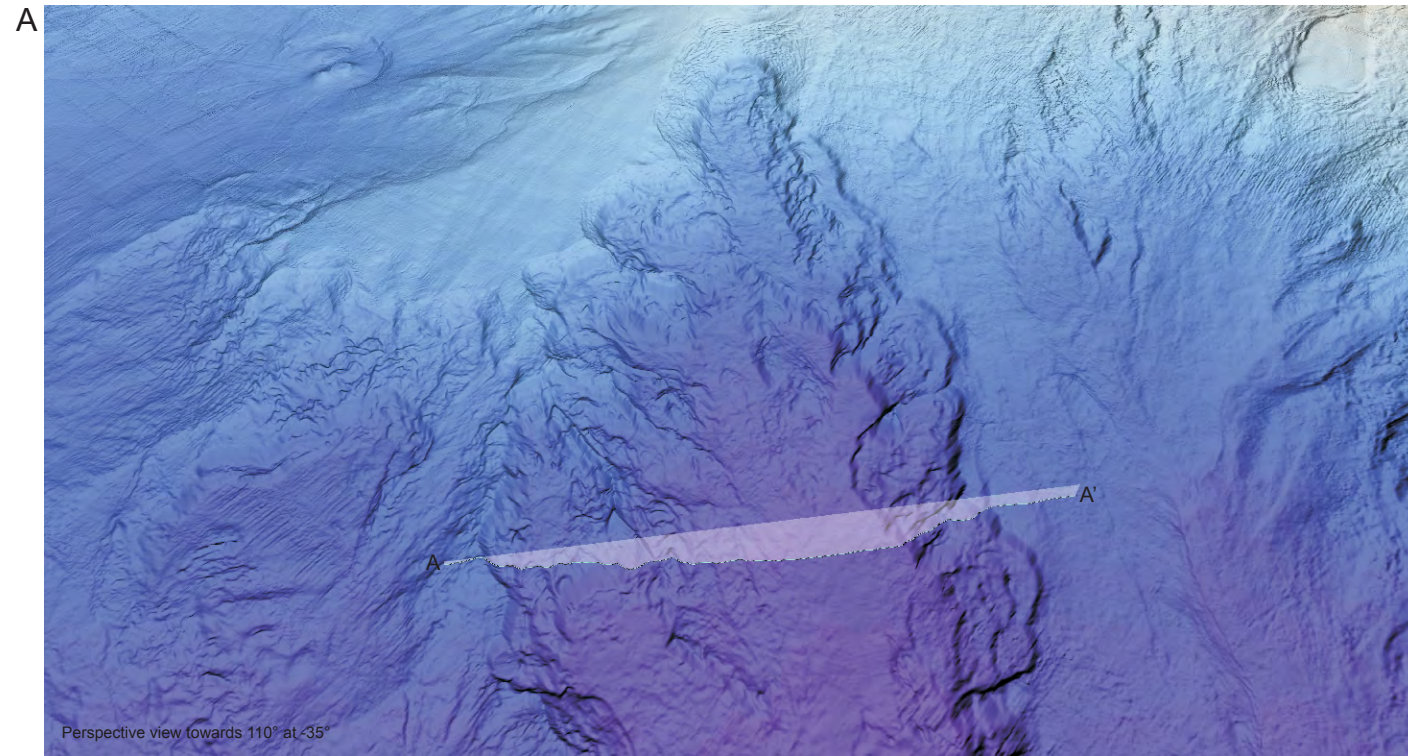
Pockmarks occur on the eastern margin of Mackenzie Trough, but these are located south of the investigation area and are described in detail by Blasco *et al.* (2011).

5.4 Anthropogenic Seafloor Features

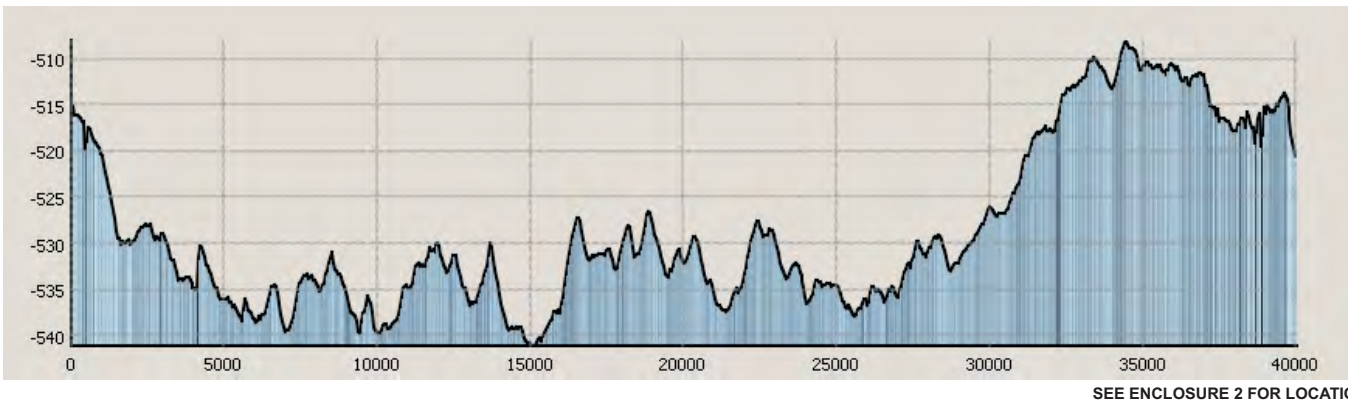
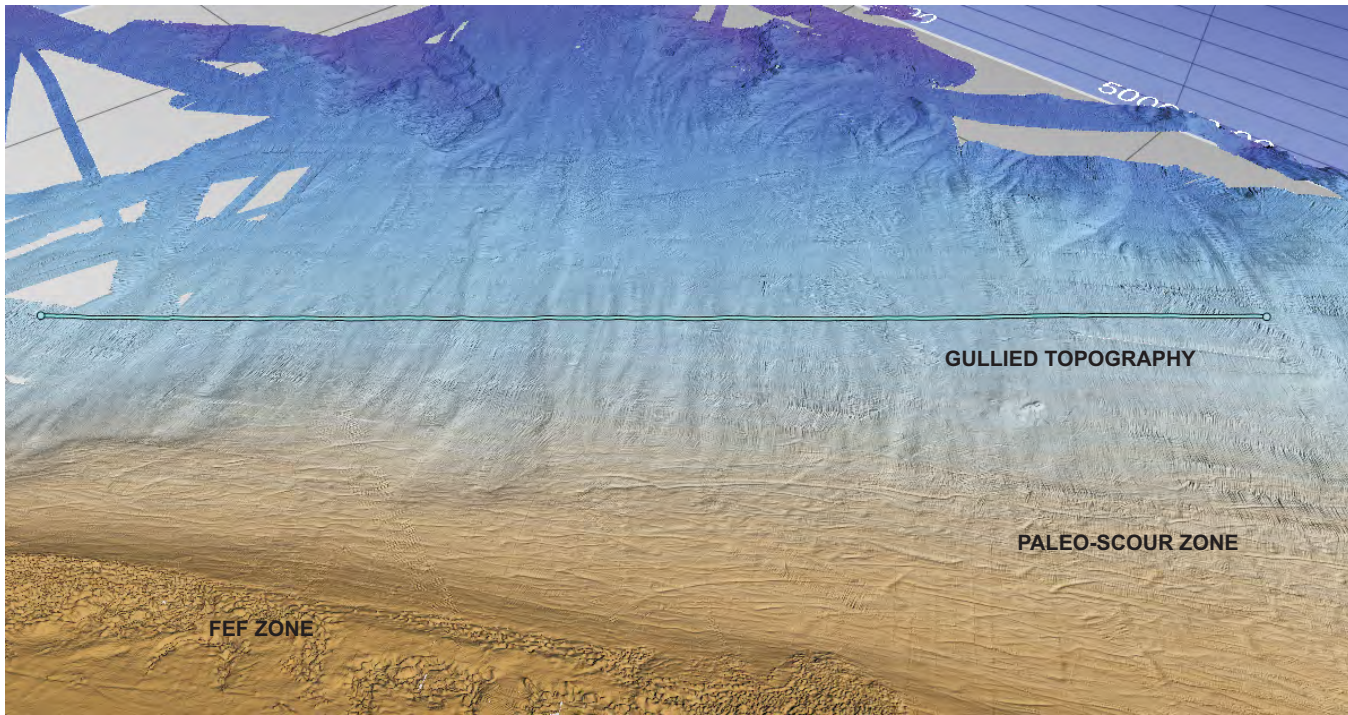
Within the investigation area, no anthropogenic features were observed from multibeam, sub-bottom profiler or 2D seismic data reviewed during the study.



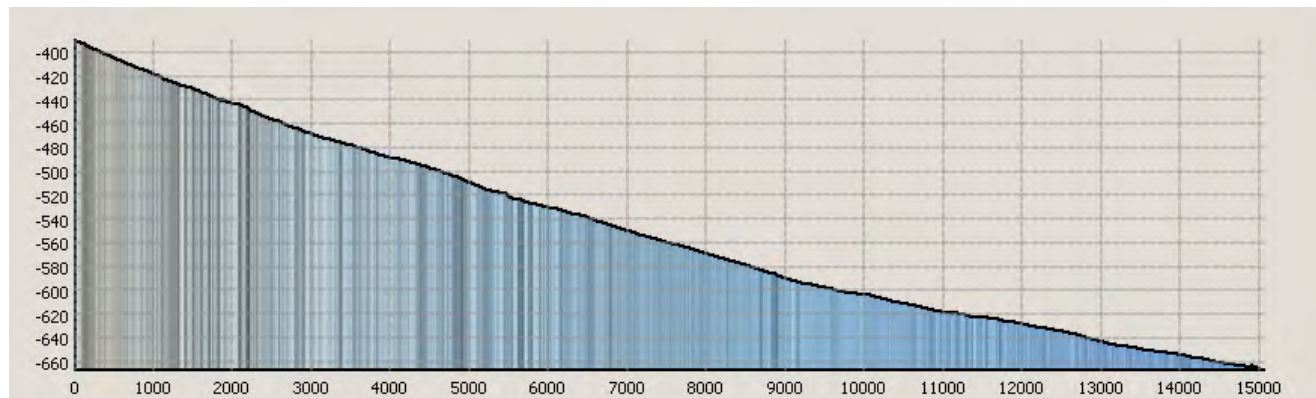
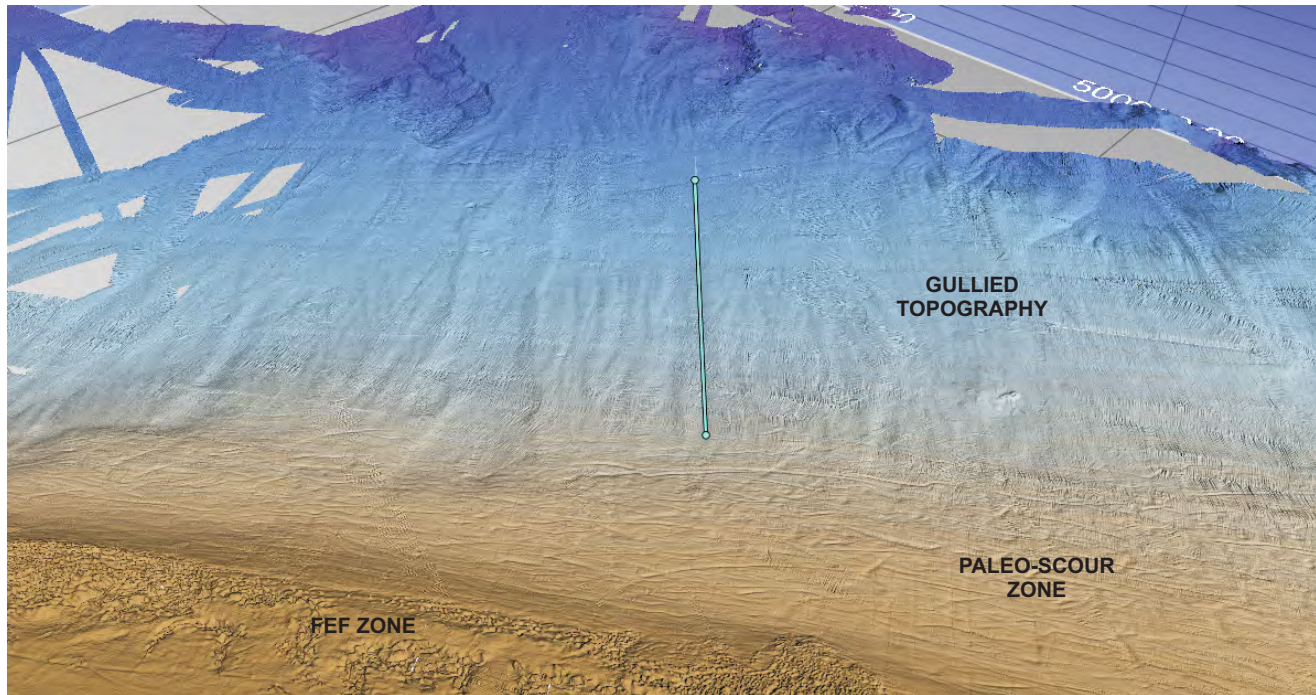
The Ikit Slump, a large retrogressive slope failure. The upper limit of the slump (brown region) is marked by a headwall scarp, 10 m to 20 m high, and with slopes of 15° to 25°, and can be traced northeast-southwest for at least 40 km in water depths between 90 m and 175 m. The scarp is almost straight in places where it cuts into the edge of the Beaufort shelf. Beneath the headwall, step-like terraces commonly exhibit a rotational dip of ~2° to 3°, toward the scarp. The terraces are coherent blocks of sediment that have moved only relatively short distances from their original location. As they are traced downslope to the northwest (into the blue region) the terraces become progressively muted merging into a zone of lobate flow-like structures, and then into a generally flatter surface with small-scale channel-like features that meander downslope. This kind of slump, similar to others on the Laurentian slope, Norwegian slope and to buried slumps in the Gulf of Mexico and Caspian Sea is thought to be the result of a single, retrogressive failure event. A-A' and B-B' show cross-section and long-section profiles of the slump zone, respectively.



Retrogressive slope failure on the middle slope. This slope failure is characterized by well developed scalloped headwall regions, some with terraces beneath, that pass rapidly into a deep valley. The flat floor of the valley may coincide with a formerly buried stratigraphic surface, over which sediments that originally occupied the slumped region slid downslope to the northwest and onto the lower slope. A-A' and B-B' show cross-section and section profiles of the valley, respectively.

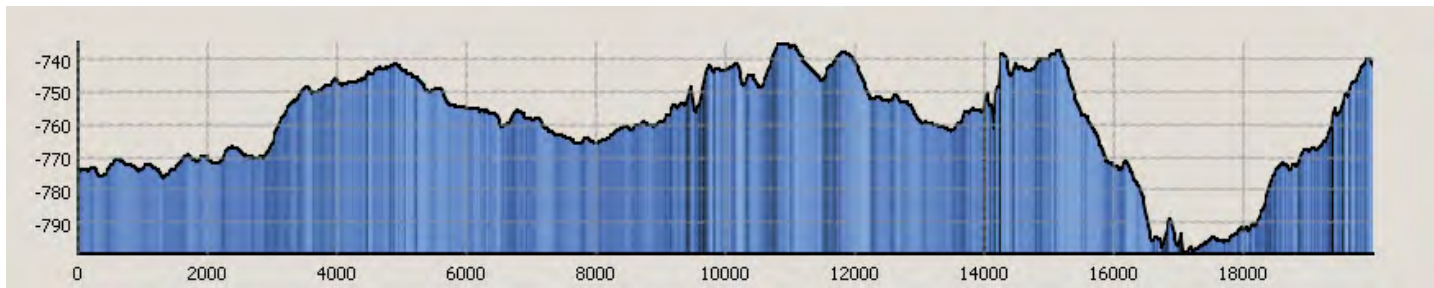
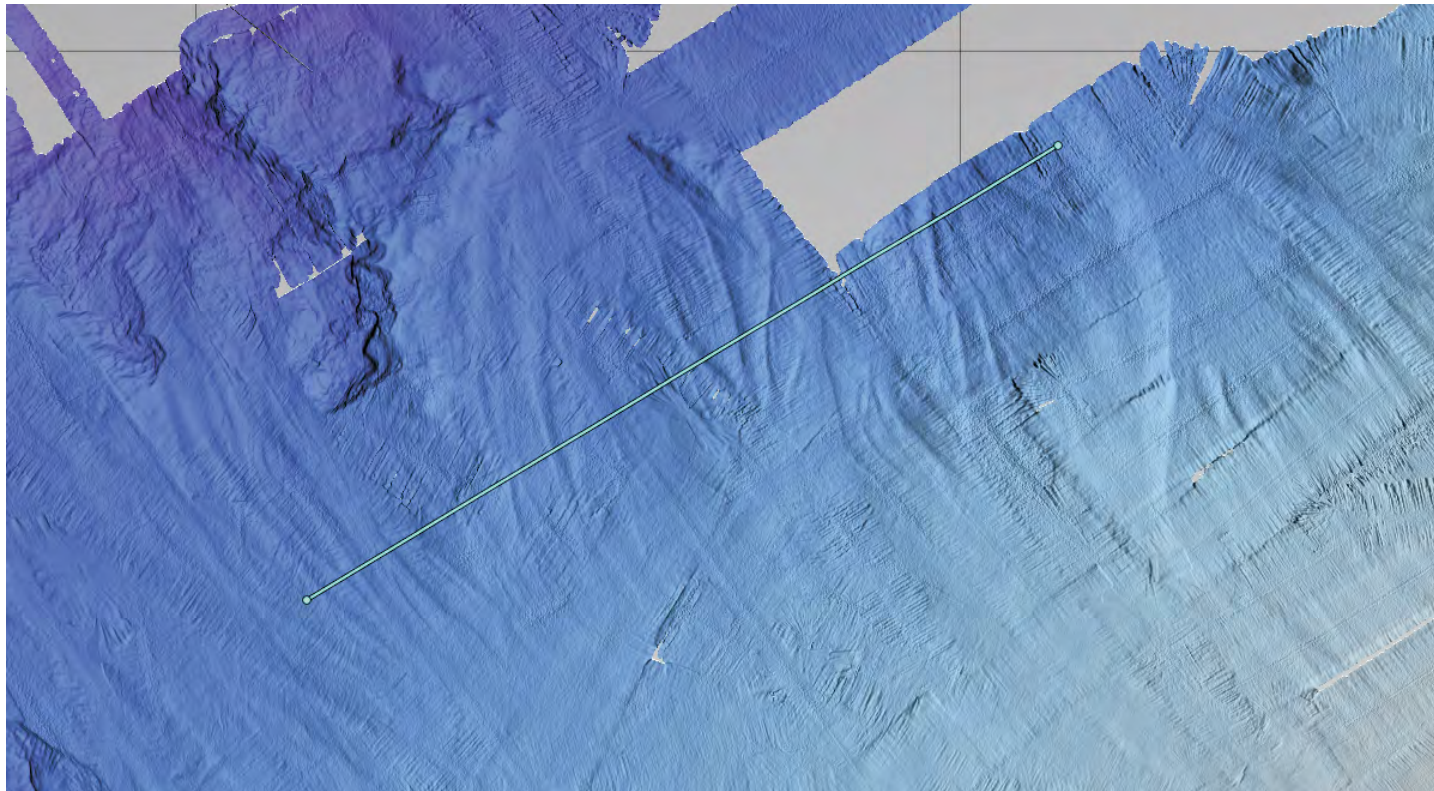


Perspective and cross-sectional profile views of gullied topography on the mid-slope region. Gullies, oriented towards the northwest, begin immediately downslope from the Paleo-Scour Zone in the foreground. View to the northwest at 45° elevation. A profile across the gullies (blue line in top image) is shown below (vertical exaggeration 300:1, scale in metres).



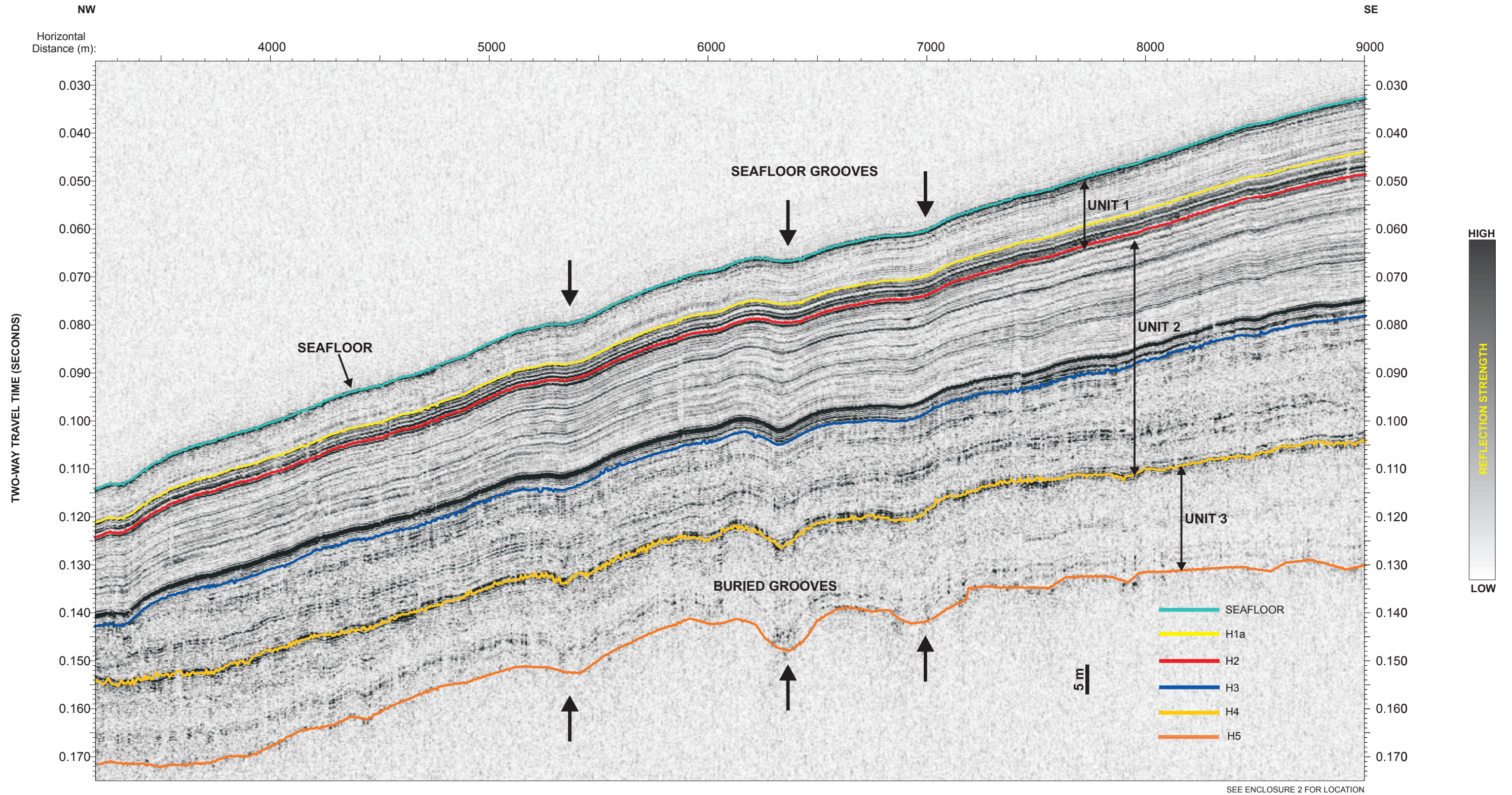
SEE ENCLOSURE 2 FOR LOCATION

Perspective and longitudinal profile views of gullied topography on the mid-slope region. Same view as in Plate 5.3 but profile is oriented downslope, parallel to gullies. Note smoothness of slope in this orientation. View to the northwest at 45° elevation. Profile (blue line in top image) is shown below (vertical exaggeration 15:1, scale in metres).

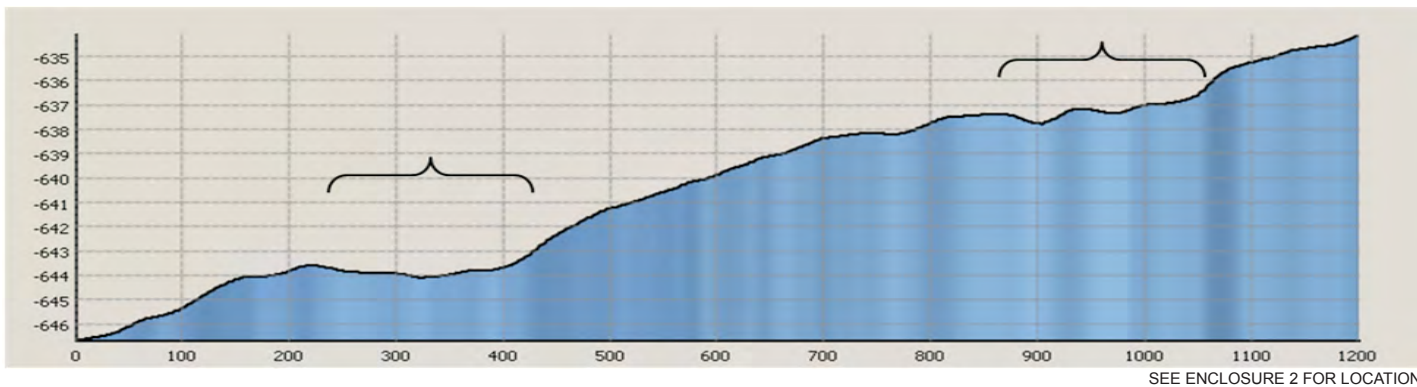
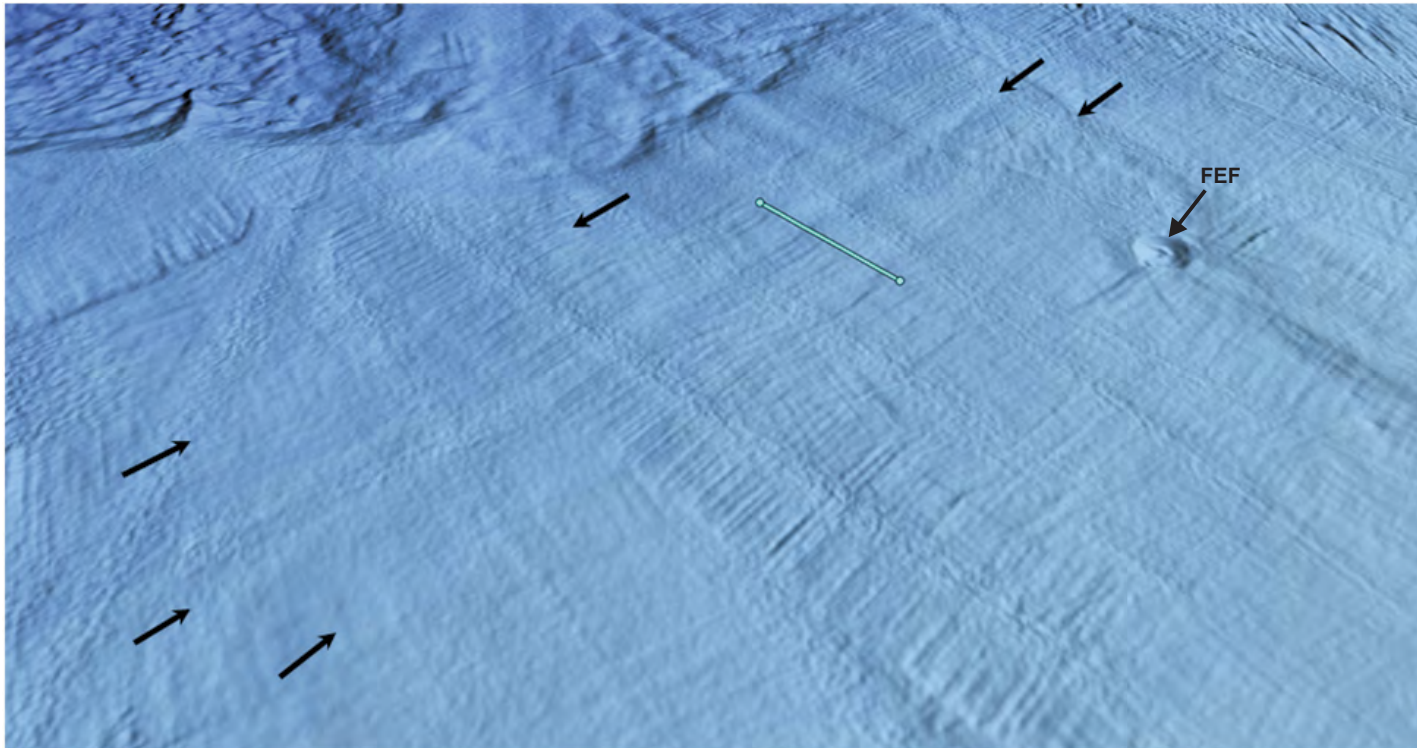


SEE ENCLOSURE 2 FOR LOCATION

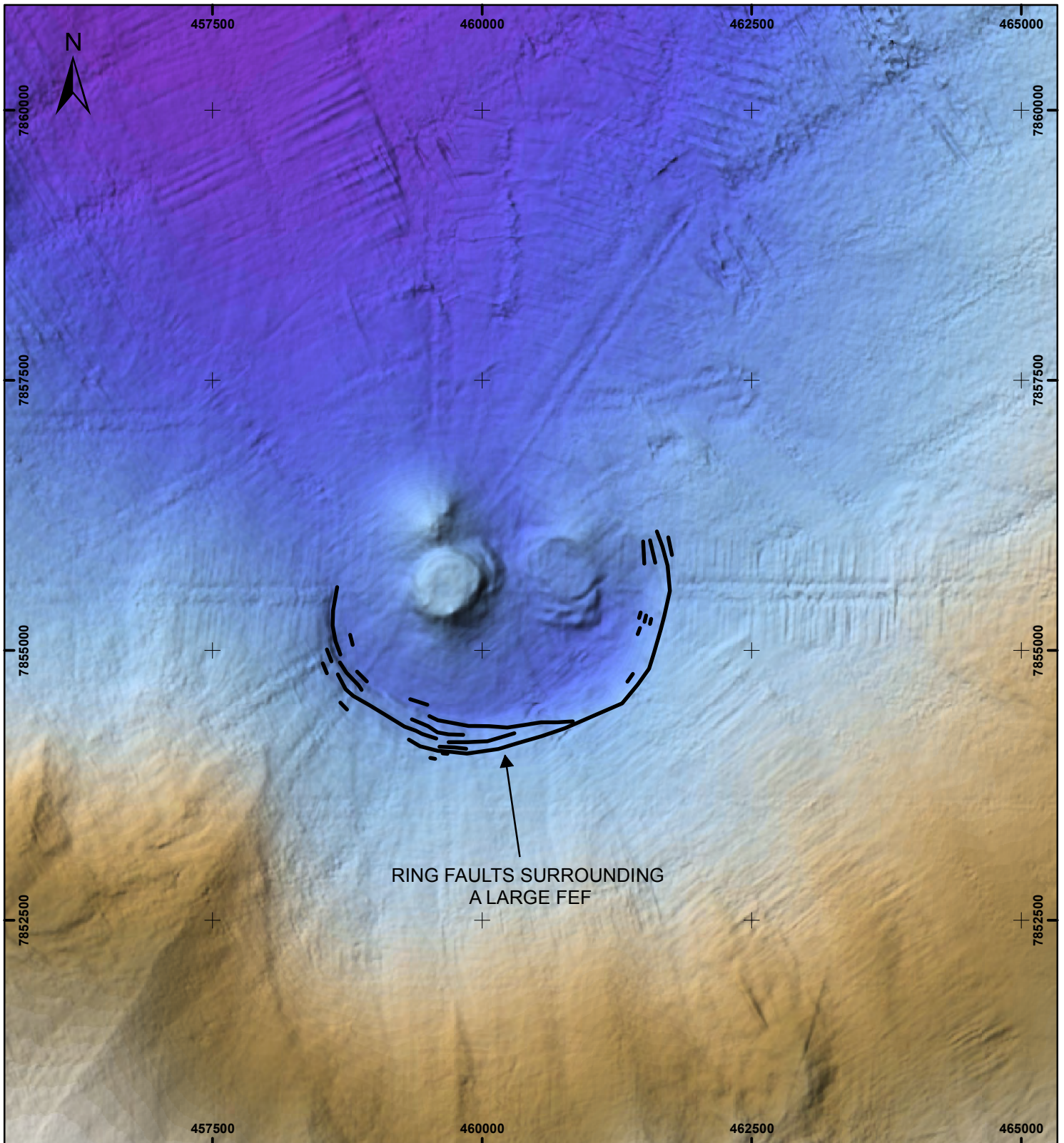
Illustration of curved and coalescing gullied topography on the lower slope. Vertical view, north up (top image). A cross-sectional profile across the gullies (blue line in top image) is shown with vertical exaggeration of 50:1, scale in metres).



Sub-bottom Profile (Line 0052_2010_250_0601) showing grooves on the H5 horizon. Prominent grooves on H5 (orange) can be traced upwards through 60 m of overlying pelagic drape to the seafloor (black arrows). The vertical scale bar is based on an assumed acoustic velocity in sediment of 1600 m/s.



Perspective and profile view showing seafloor expression of grooves on the horizon H5. The grooves (between black arrows) are oriented 45° and are the seafloor expression of features developed on buried horizon H5, 60 m below seafloor. View to the north at 45° elevation. The circular crater at centre right is an FEF. The profile (blue line in top image) shows that at the seafloor the grooves (curly brackets) are 200 m to 300 m wide and 1 m to 2 m deep (bottom image, vertical exaggeration 30:1, scale in metres).



RING FAULTS SURROUNDING
A LARGE FEF

NAD83, UTM ZONE 8

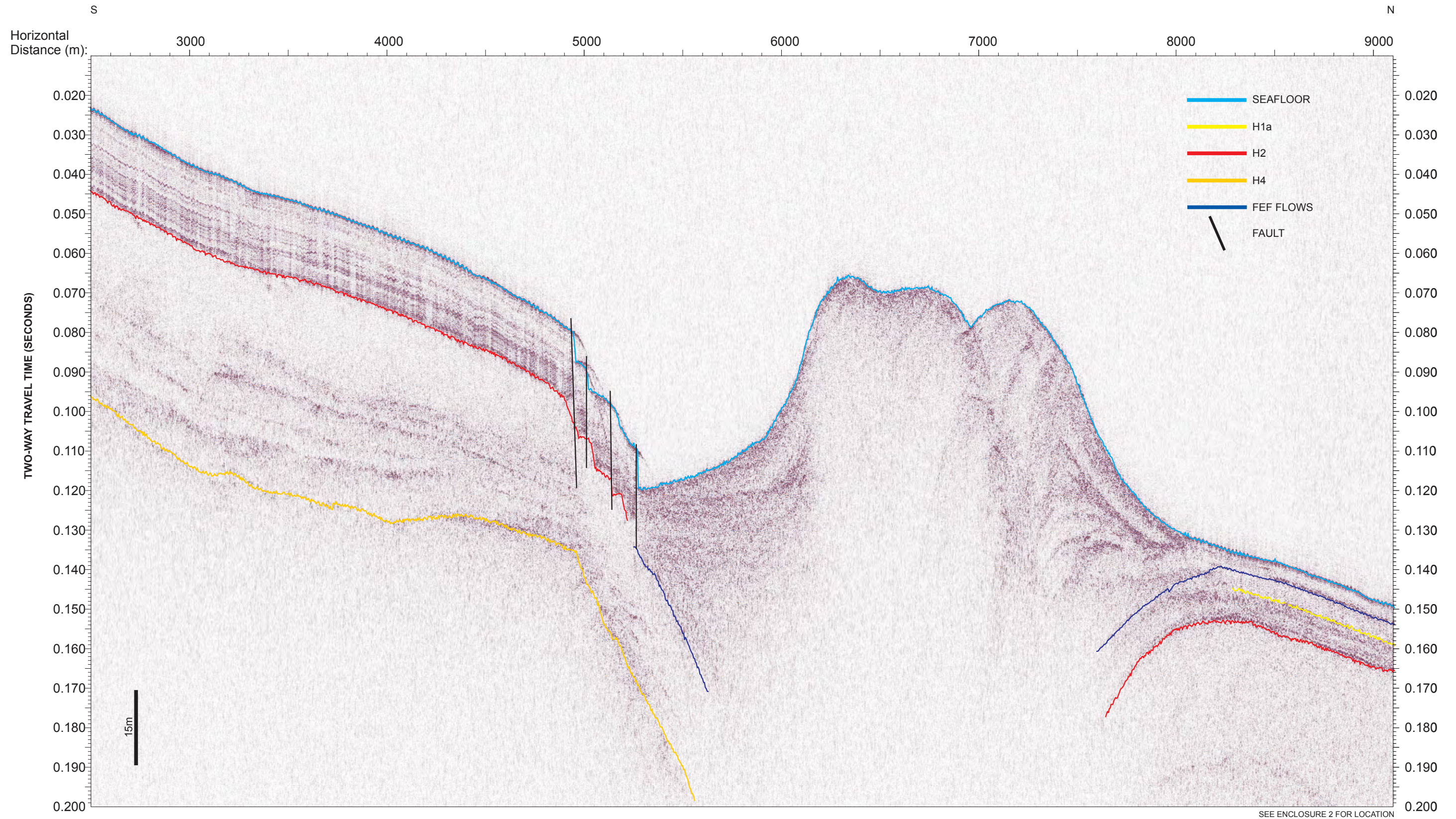


DWG No : 20110068-MBB-FEF-P58-0
Project No. 20110068

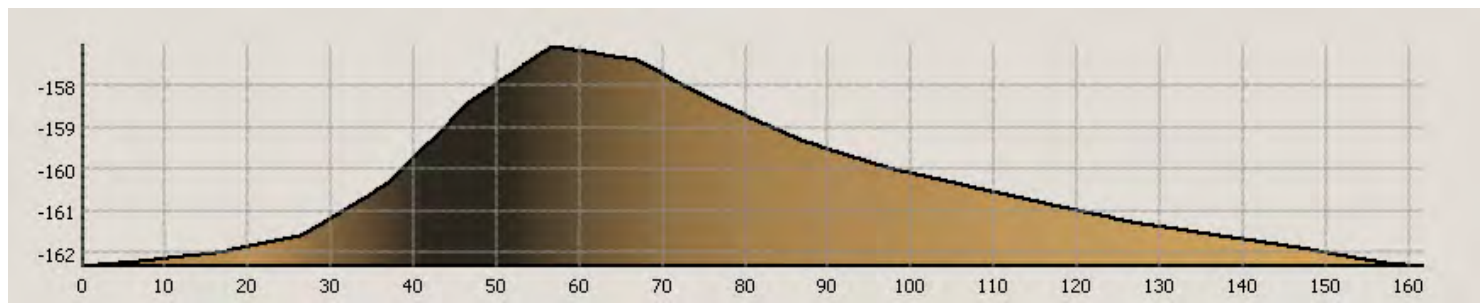
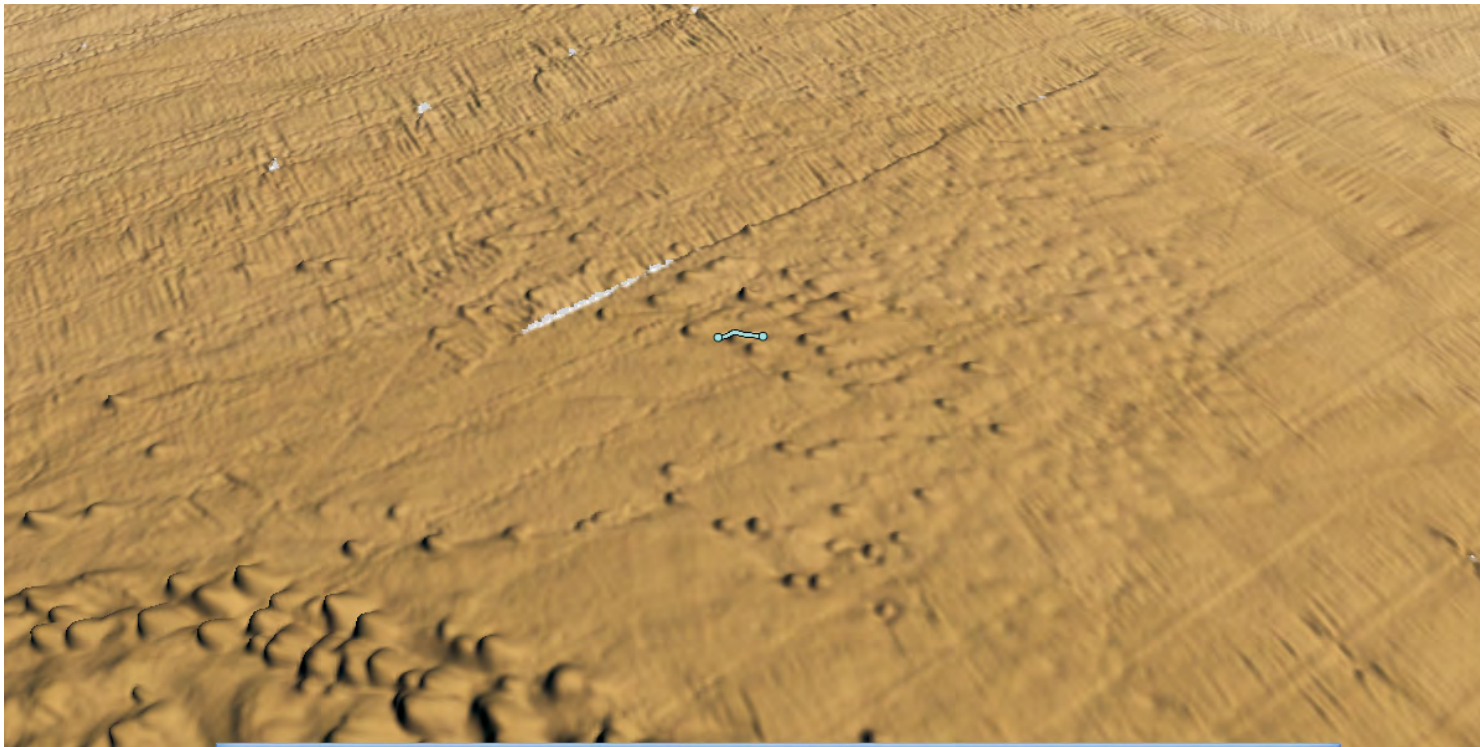


Multibeam image of a large FEF. The main cone and two parasitic cones are visible. Concentric ring faults, with throws of 5 m to 10 m, define part of the moat rim.



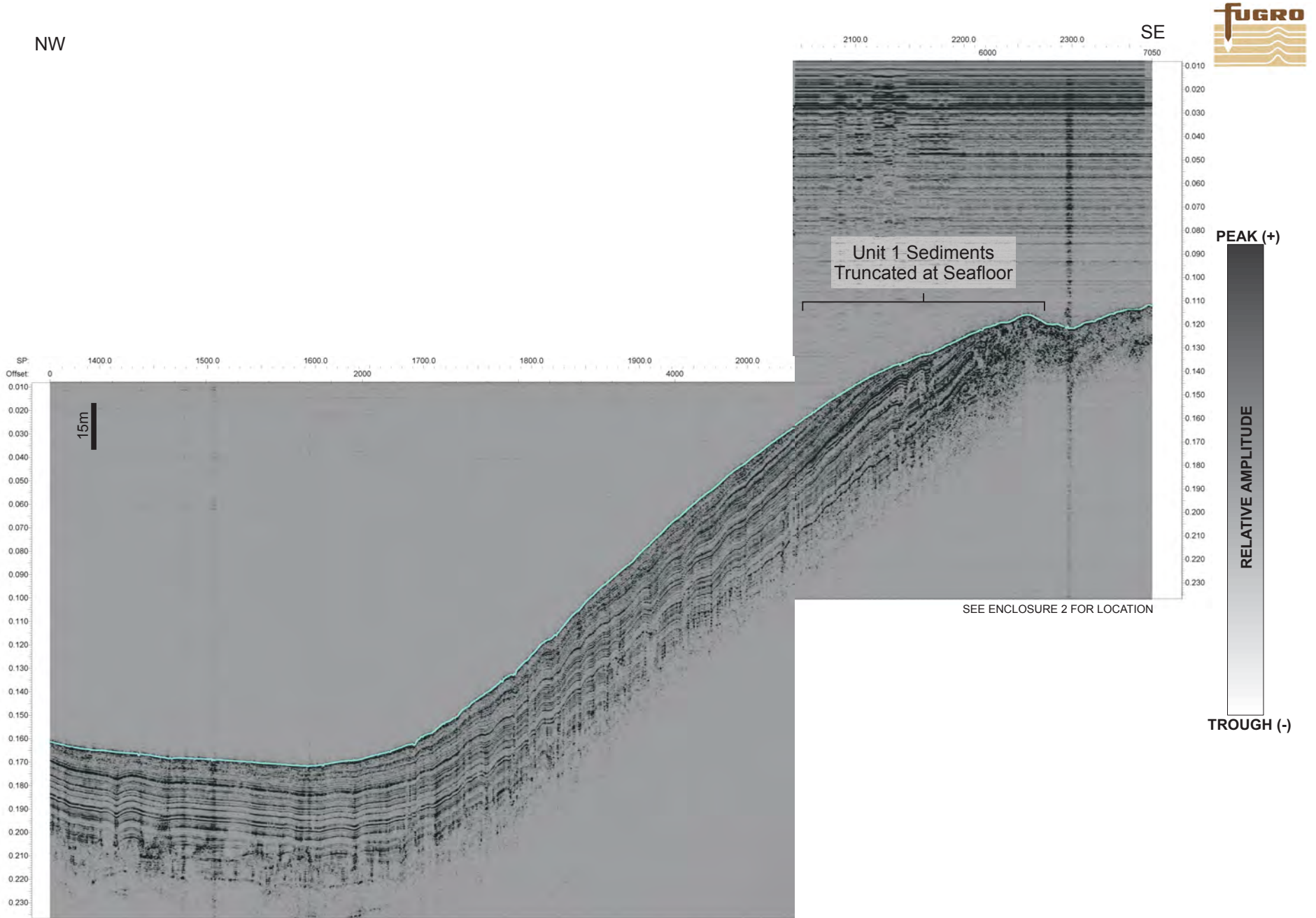


Sub-bottom Profile (Line 092571951) through a large FEF. With a base diameter between 800 m and 900 m, this FEF cone stands 30 m above the surrounding seafloor, and is located in a circular moat-like depression, ~ 3000 m in diameter, in water depths between 750 m to 795 m. Concentric ring faults, with throws of 5 m to 10 m, offset the seafloor and define the southern rim of the moat. Strongly reflective flow horizons can be seen filling the moat between the cone and the ring faults.

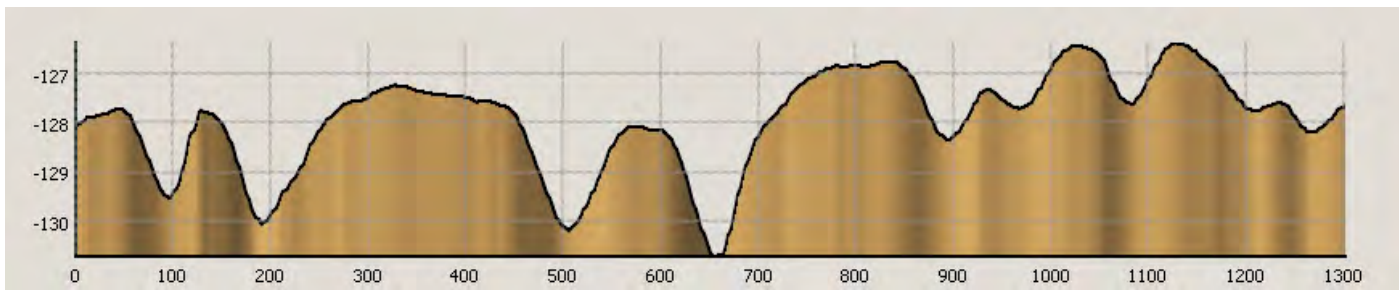
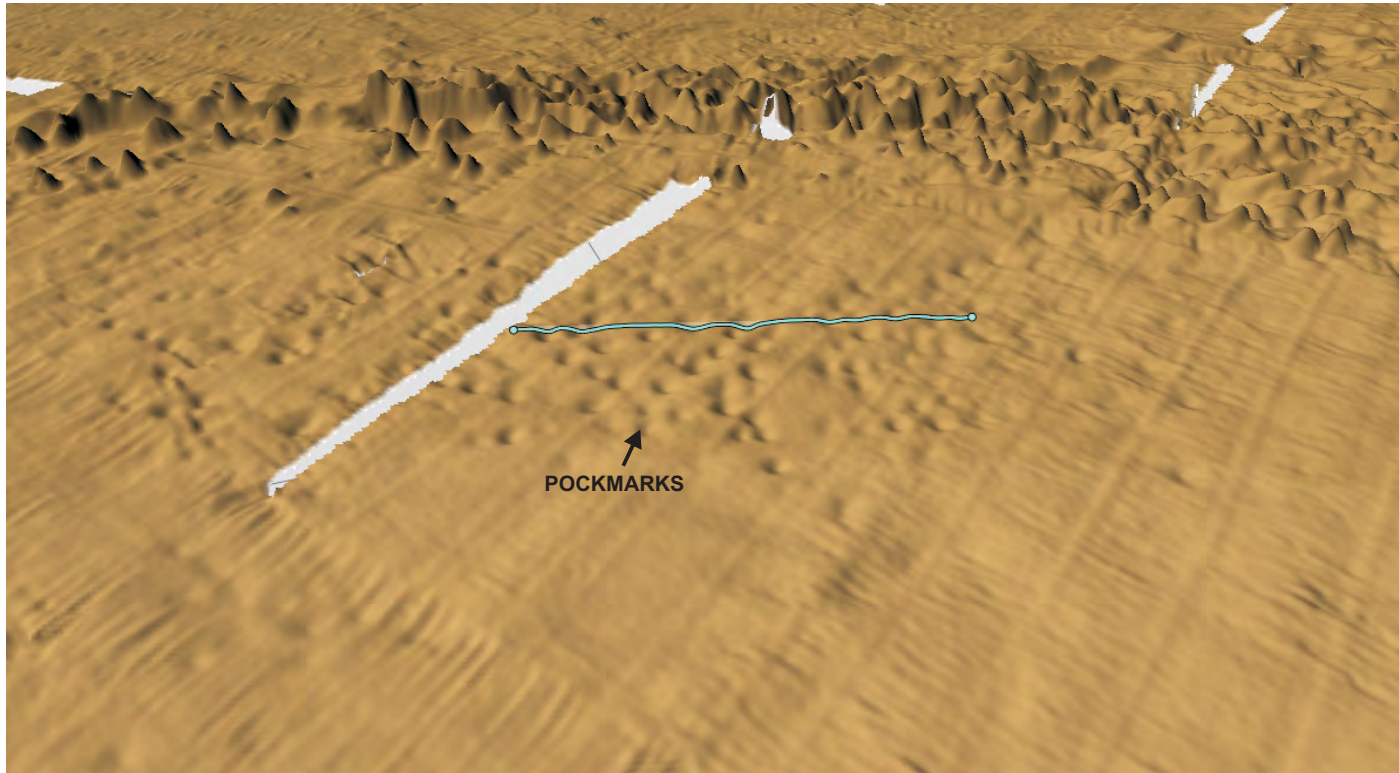


SEE ENCLOSURE 2 FOR LOCATION

Illustration of streamlined FEFs. This group of FEFs lies just north of the main FEF Zone on the upper continental slope. View to the north at 60° elevation. Profile of a single FEF (blue line in top image) shows a steep, west-facing slope and gentle east-facing slope (vertical exaggeration 5:1, scale in metres).

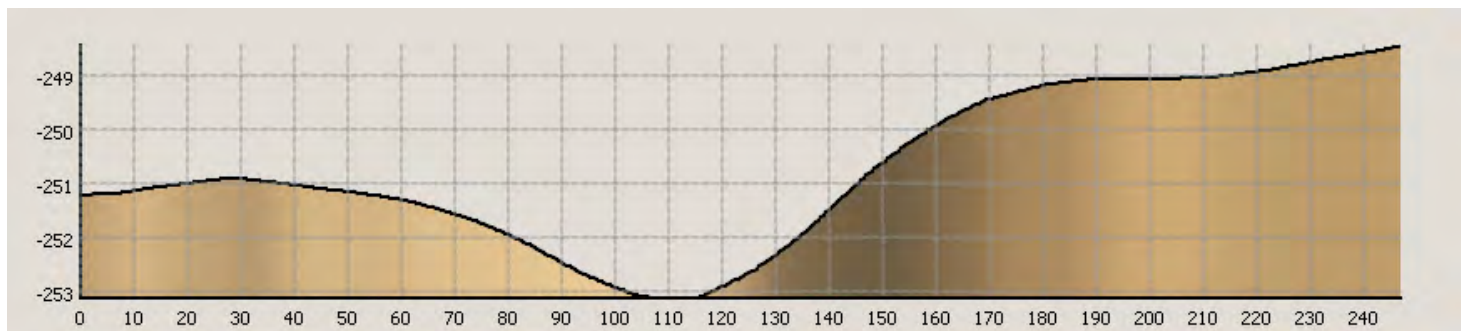


Sub-bottom Profile Line 042081227, illustrating truncated Unit 1 sediments. Up to 20 m of strata are estimated to have been eroded in places along the uppermost slope.



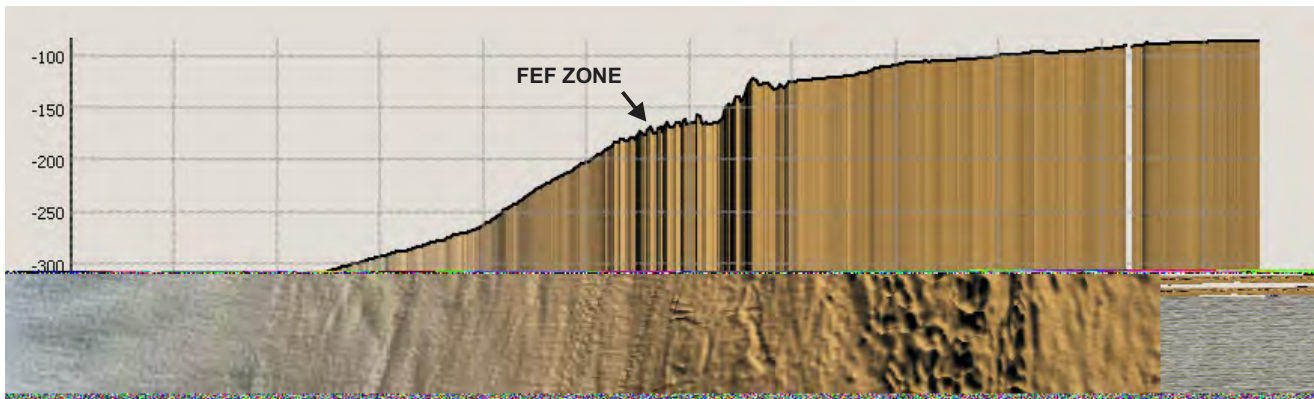
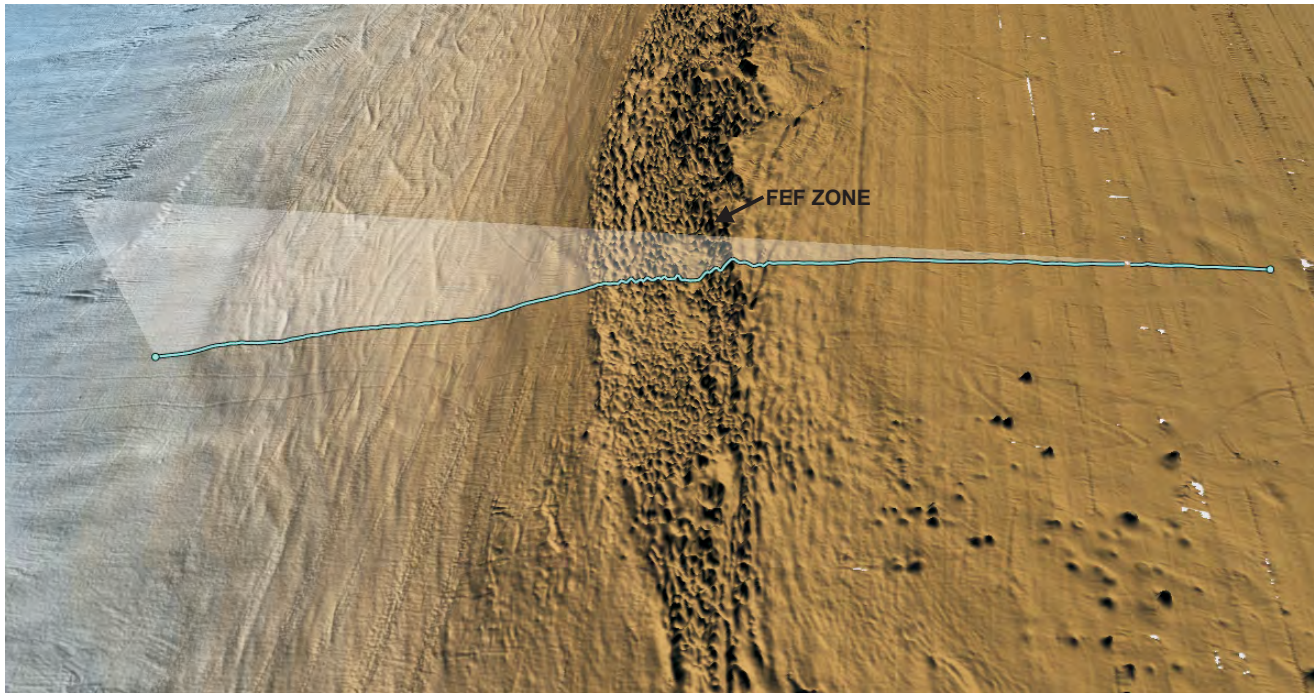
SEE ENCLOSURE 2 FOR LOCATION

Perspective and profile views of a group of pockmarks. Pockmarks, in the foreground, occupy the uppermost part of the continental slope in front of the FEF Zone (background). View towards 200° at an elevation of 35°. The profile below (blue line in top image) shows pockmark depths up to 3 m in this group profile (vertical exaggeration 50:1, scale in metres).



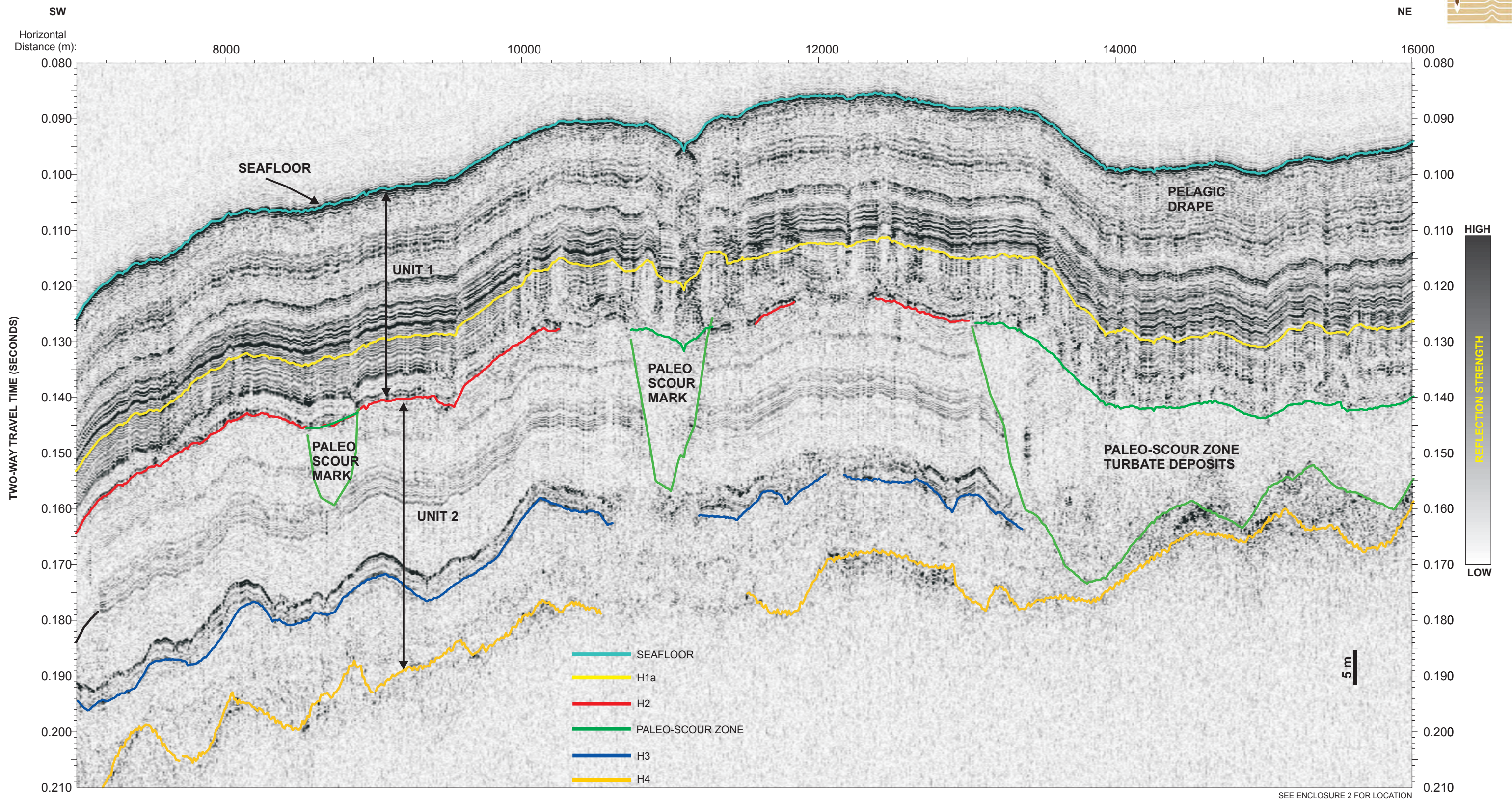
SEE ENCLOSURE 2 FOR LOCATION

Perspective view of the Paleo-Scour Zone (top image). Note how the intersecting and cross-cutting linear grooves are mostly sub-parallel to the shelf margin. View to the north at 45° elevation. The profile of one groove (blue line in top image) is shown below (vertical exaggeration 10:1, scale in metres).

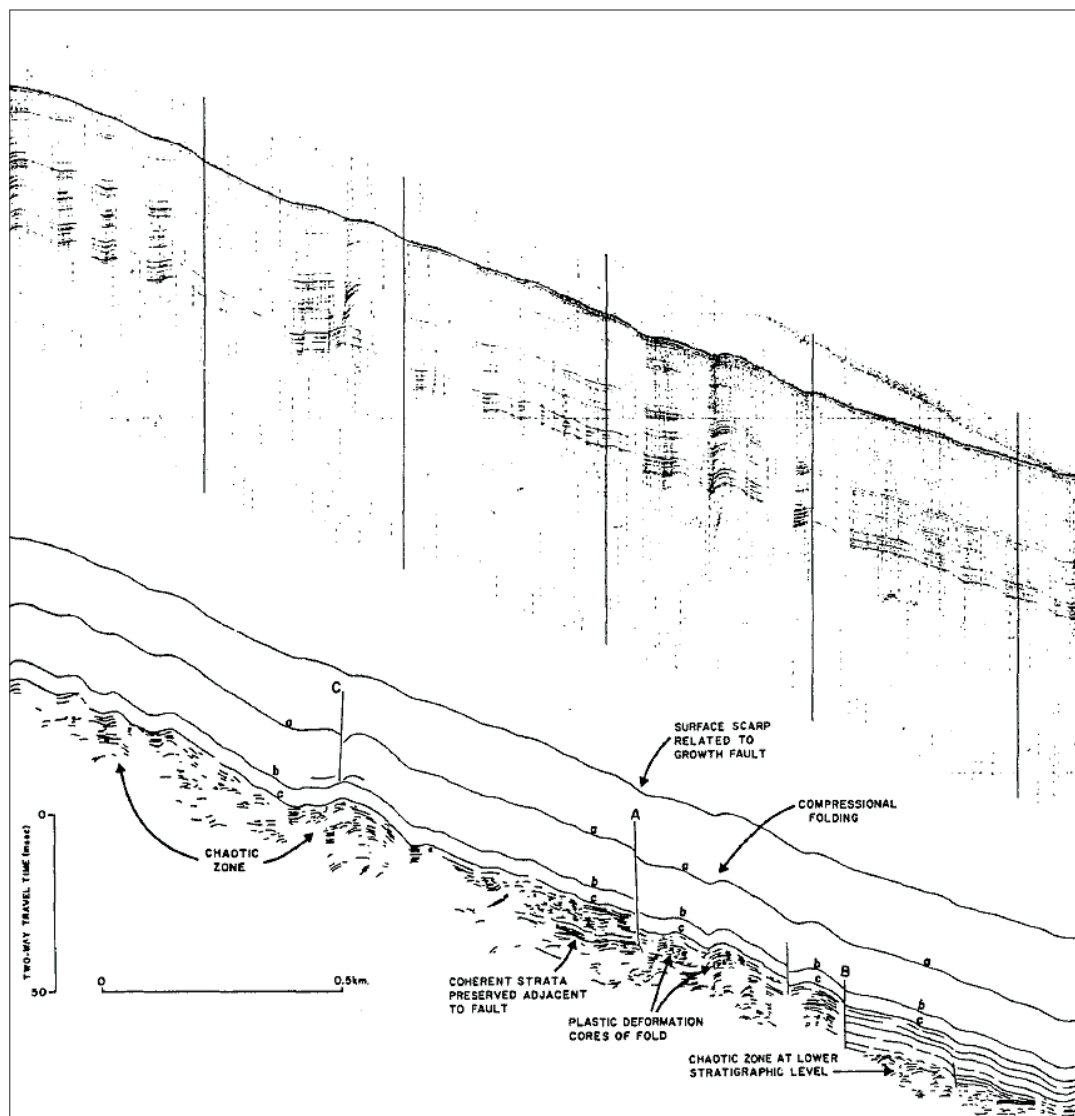


SEE ENCLOSURE 2 FOR LOCATION

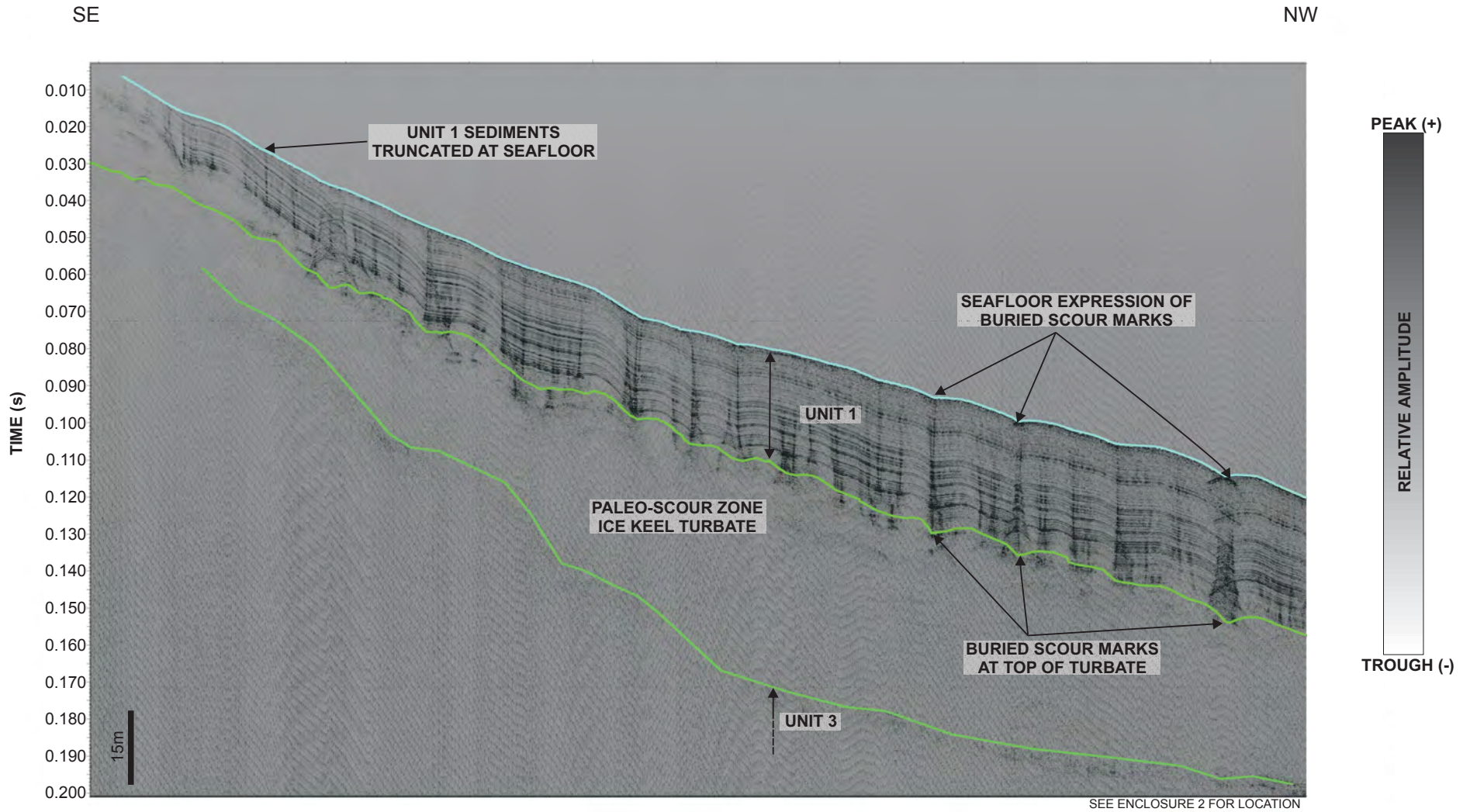
Perspective and profile view of the FEF Zone showing coalesced cones. The Beaufort Shelf with visible ice keel scour marks is to the right (landward) of the FEF Zone, and the Paleo-Scour Zone on the upper continental slope is visible to the left. View to the northeast at 45° elevation. Profile (blue line in top image) is shown below (vertical exaggeration 10:1, scale in metres).



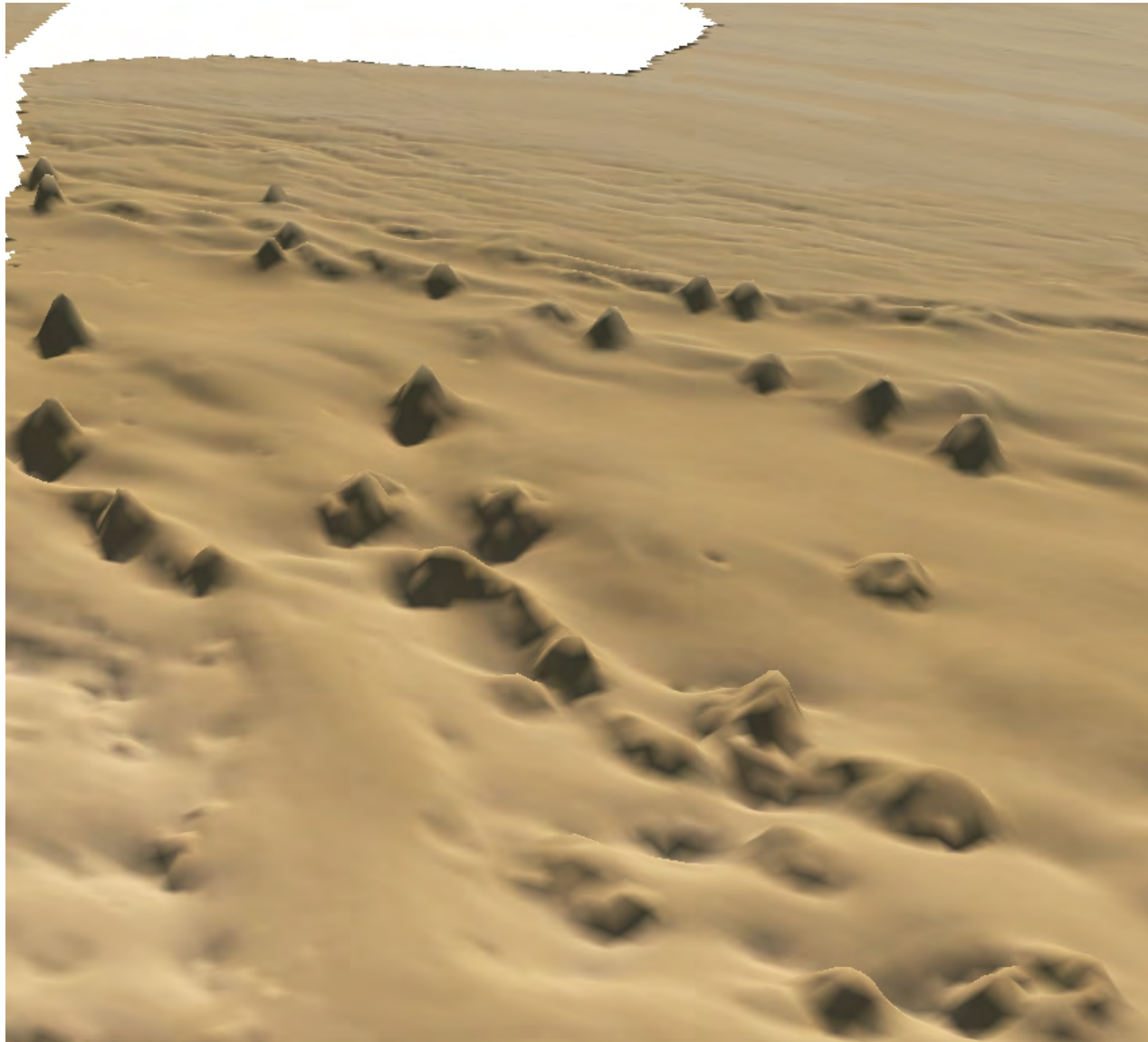
Sub-bottom Profile (Line 0085_2010_252_0953) showing two distinct buried scour marks. The cross-sectional view of two scour marks can be seen on the left (green horizons), and the continuous Paleo-Scour Zone to the right. The larger of the two scour marks is approximately 20 m deep. Its muted topography can be seen at the seafloor where its original incision depth is much reduced and its width is measured as 125 m. The vertical scale bar is based on an assumed acoustic velocity in sediment of 1600 m/s.



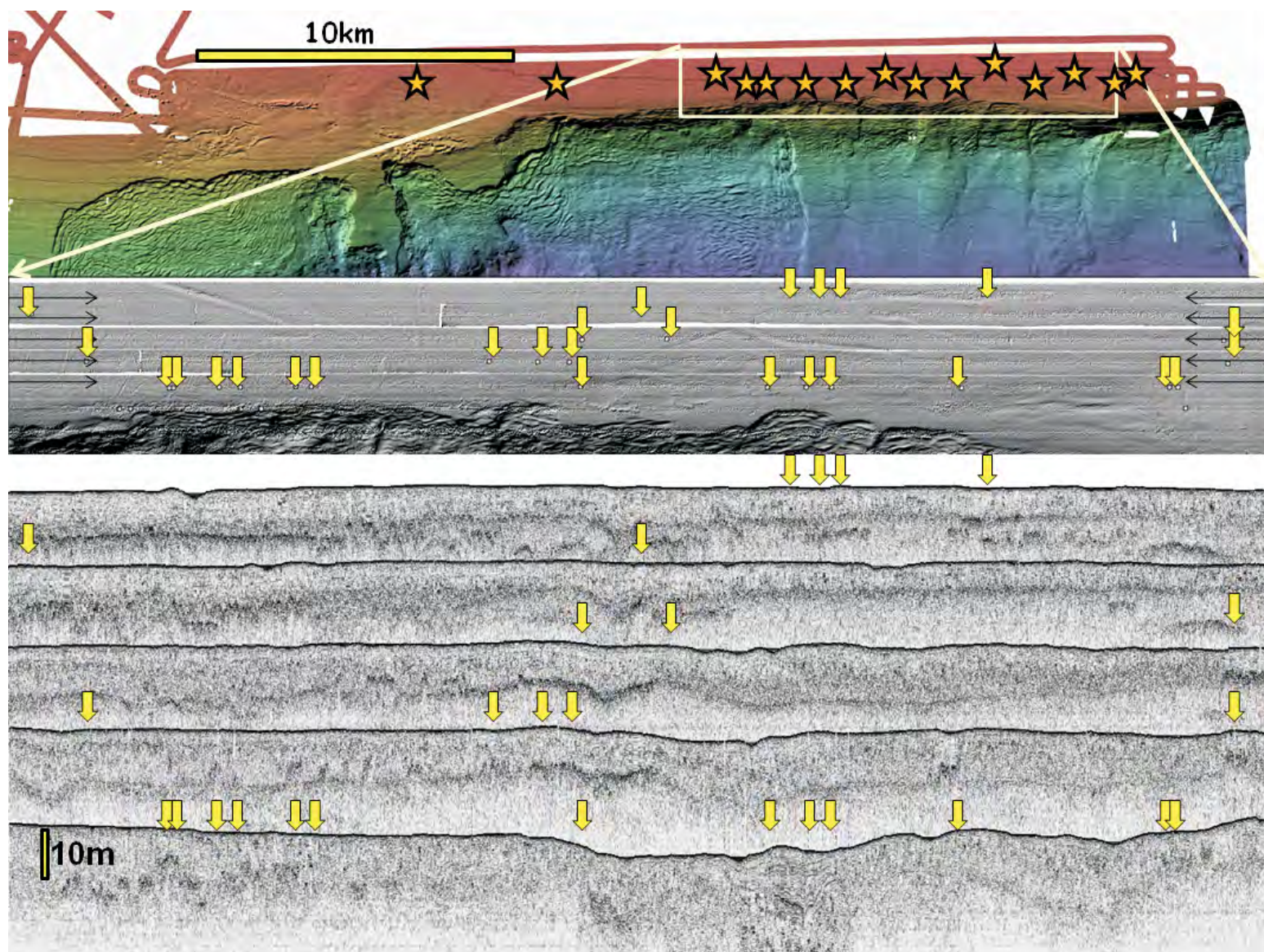
The Paleo-Scour Zone as interpreted by Hill *et al.* (1982). The ice keel turbate is illustrated in this figure as "chaotic zone". "Compressional folds" are the expression of rough topography on the upper turbate surface propagated vertically to the modern seafloor through acoustically well stratified pelagic drape. The buried rough topography is revealed at the seafloor on multibeam imagery as a network of intersecting grooves. From Hill *et al.* (1982).



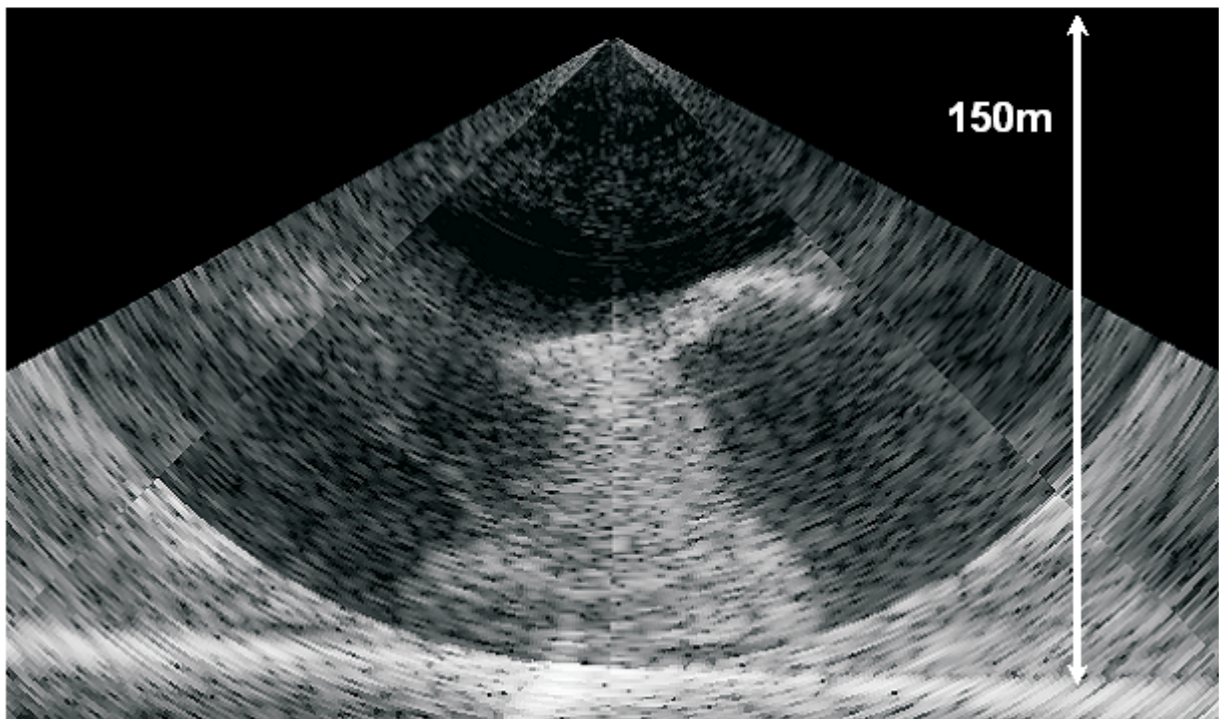
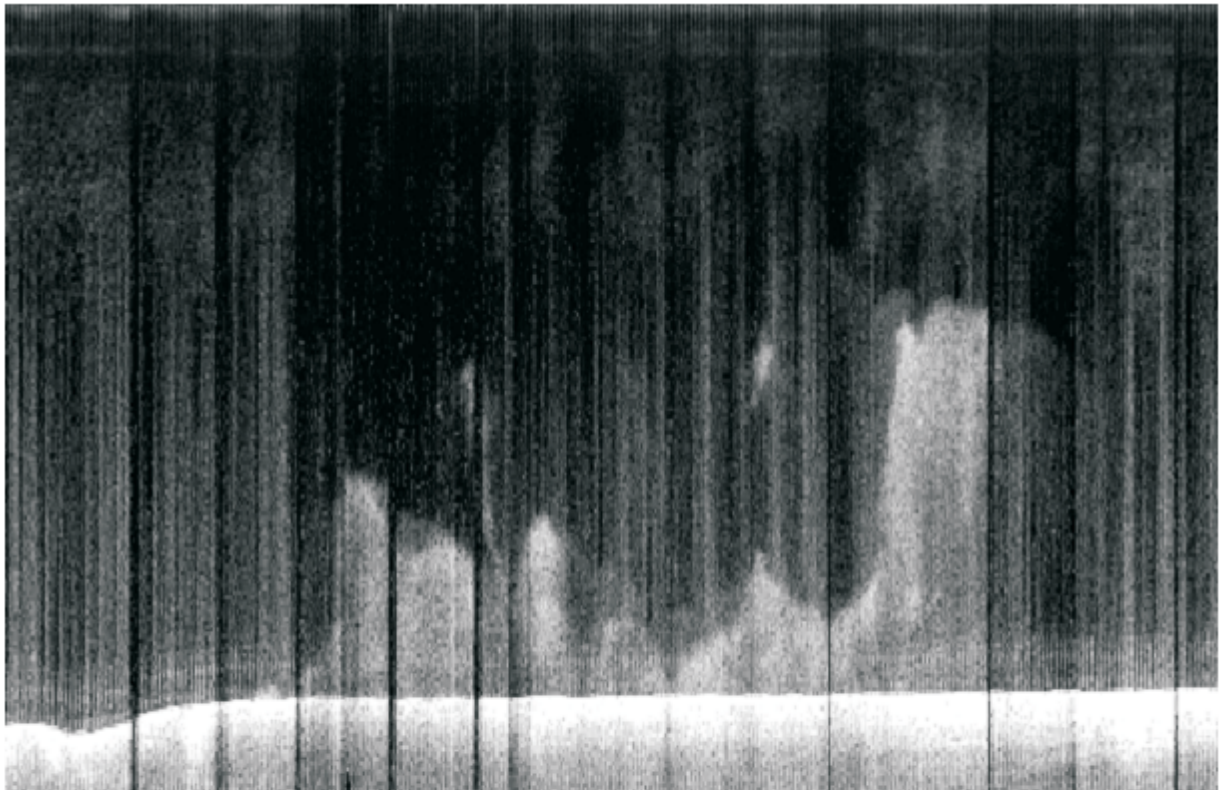
Sub-bottom Profile (Line Cone_2009_250_23_27_41) showing the interpreted Paleo-Scour Zone. This line is in the same vicinity of the line illustrated in Plate 6.11.



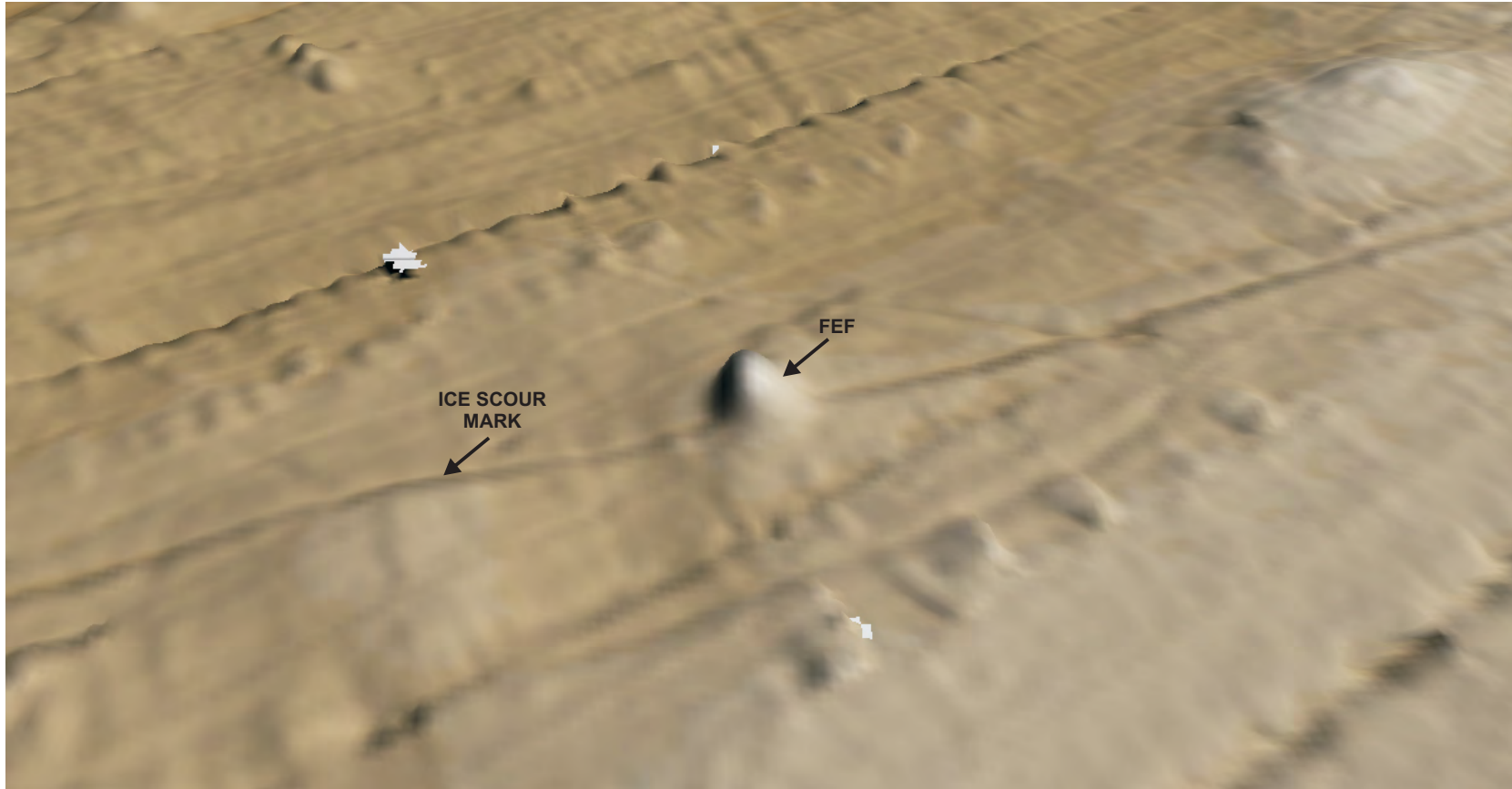
MBES perspective view towards the southeast showing seafloor “wrinkles” (near top of image) in the FEF Zone (scale in metres). The FEFs occur seaward (north-northwest) of the wrinkle field. View towards 135°, viewing elevation 15°, vertical exaggeration 5x.



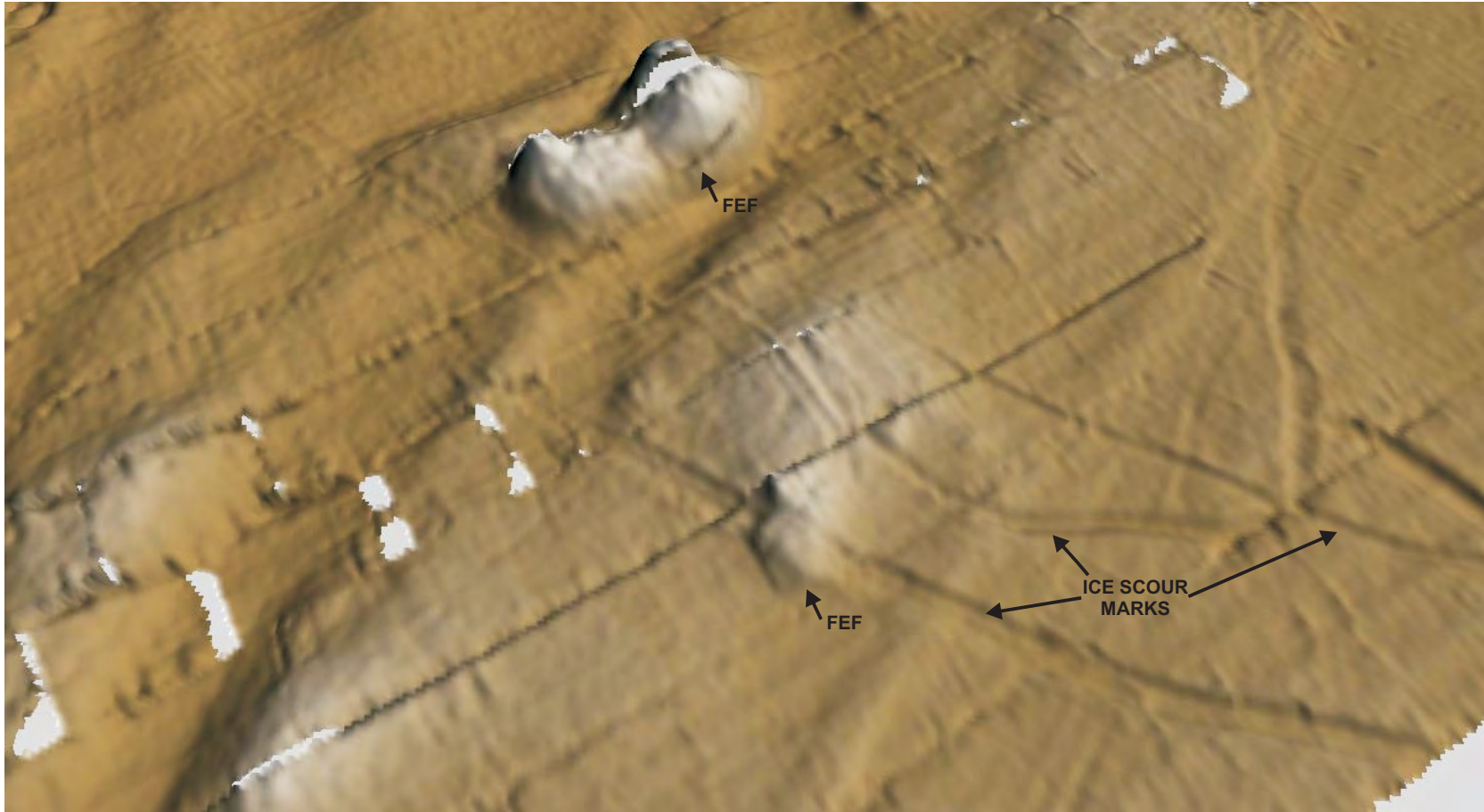
Water column anomalies at the shelf margin in September 2009. Yellow stars on the coloured multibeam rendering at top show the approximate location of anomalies observed in multibeam data. More precise locations are shown by yellow arrows in the enlarged grey-scale multibeam image (centre), and the associated centreline multibeam profiles (bottom). Illustration courtesy of John Hughes Clarke, University of New Brunswick Ocean Mapping Group.



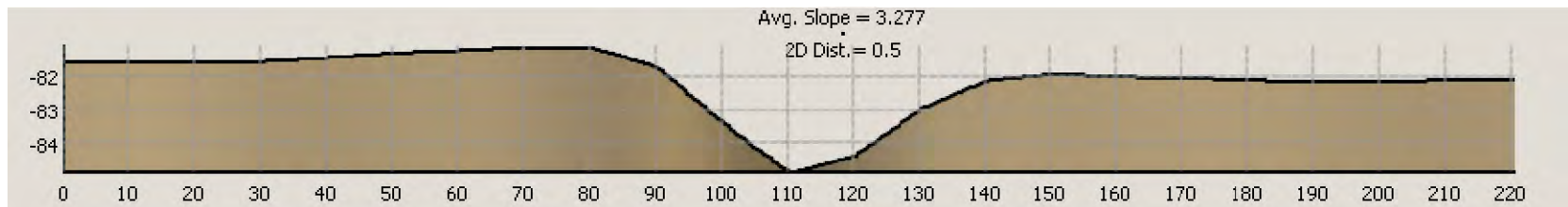
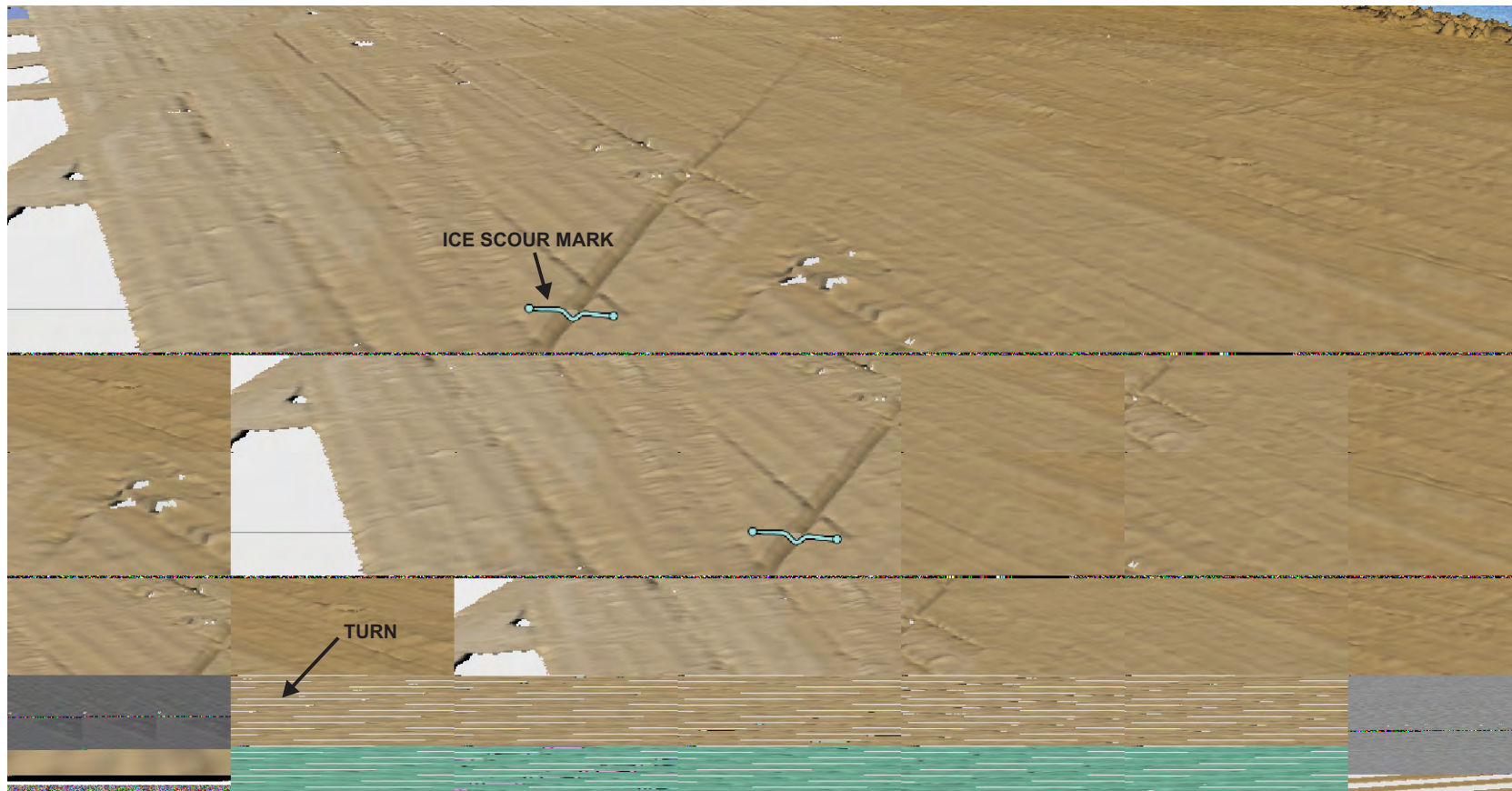
Water column plume. Example of MBES water column data showing plume (possible gas) emanating from the seafloor at the continental shelf/slope break. TOP: along-track image of plume structure; BOTTOM: sample cross-track image from the same plume (images courtesy of John Hughes Clarke, University of New Brunswick Ocean Mapping Group).



Perspective view of an FEF that has grown through an ice scour mark. The FEF (centre) rises ~7 m above the scour mark (trending obliquely across image). View to the north at 45° elevation.

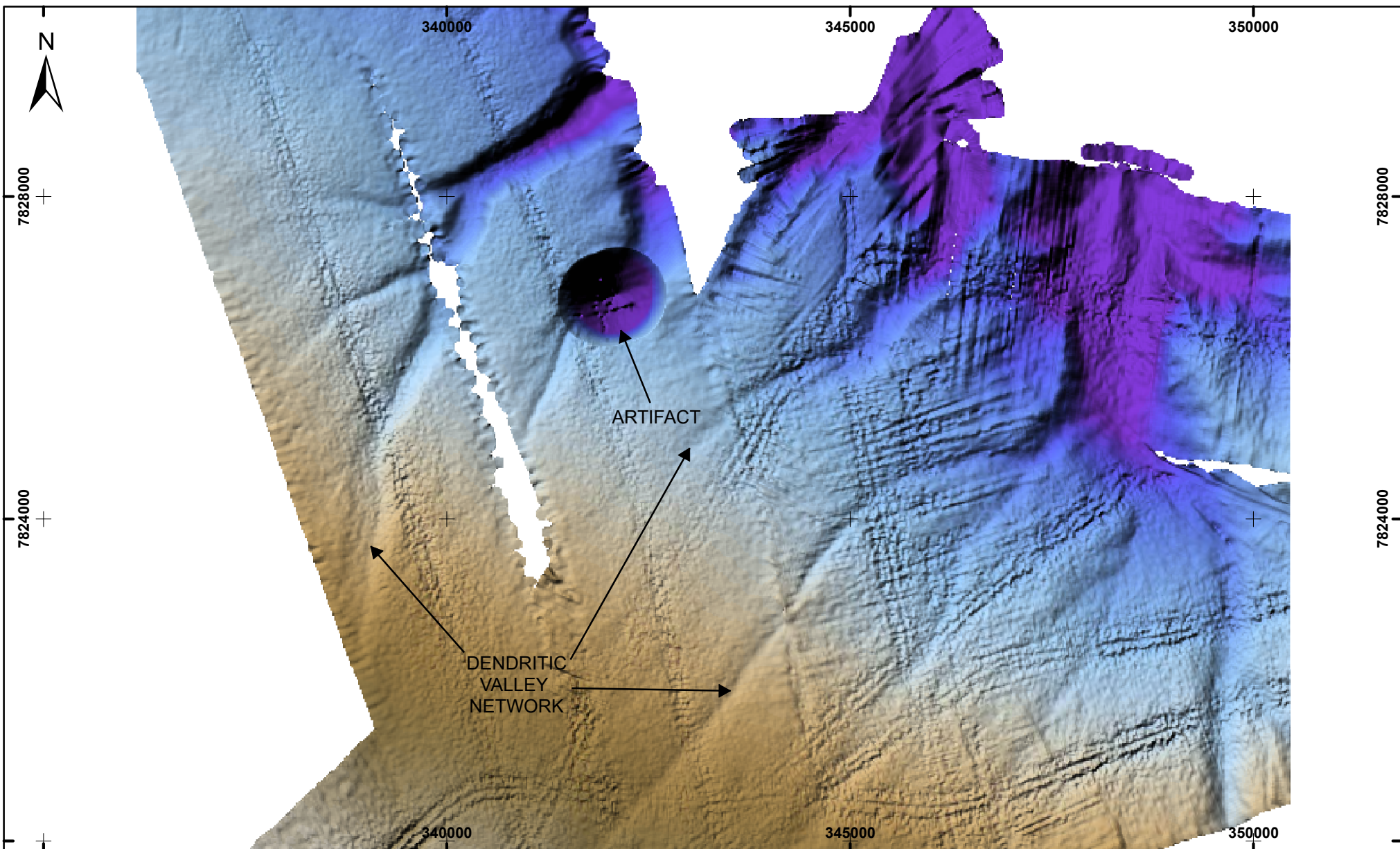


Perspective view of an ice scour mark cutting across a subdued FEF. The scour mark (foreground) rises up 8 m over the crest of the FEF mound (centre). View to the north at 60° elevation.



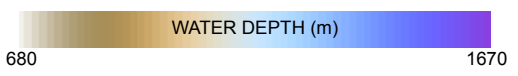
SEE ENCLOSURE 2 FOR LOCATION

Perspective and profile views of a 7 km-long ice scour mark on the Beaufort Shelf. The perspective view is towards 270° at 30° elevation, and shows a long, straight scour mark with a maximum depth of 3 m and sidewall slopes between 5° and 10°. Blue line shows profile location and profile is shown below. Profile scale in metres. Measured from its end point in the far distance (86 m water depth), this scour mark is 5.8 km long to the sharp turning point in the foreground and another 1.2 km long to its termination point in 82 m water depth.



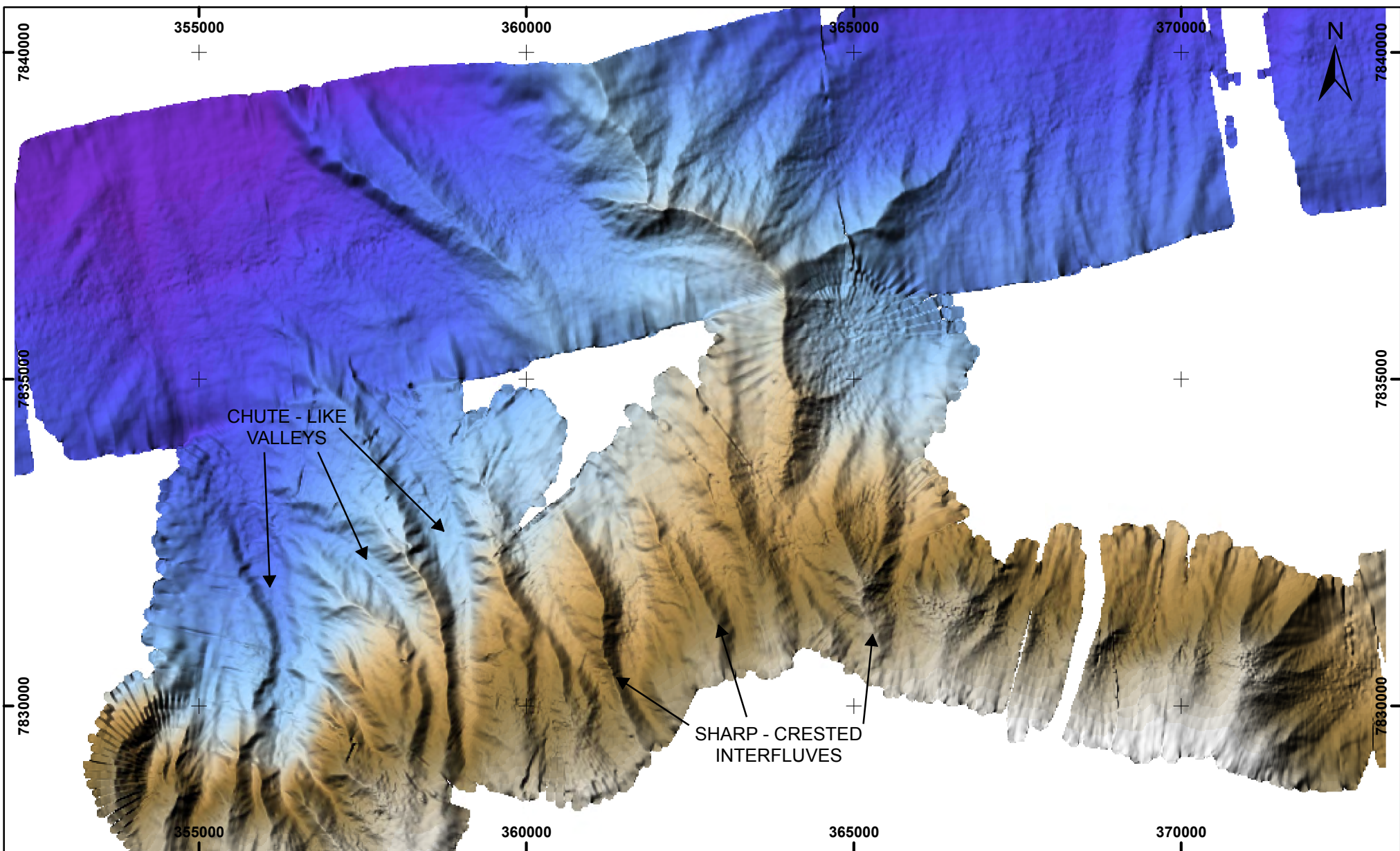
NAD83, UTM ZONE 8

DWG No : 20110068-MBB-DVLY-P524-0
Project No. 20110068



Dendritic valley network, outer Mackenzie Trough. These valleys occur on the continental slope seaward of the Trough between 800m and 1,000 m water depth. The valleys are 5 km to 10 km long, 250 m to 750 m wide and 15 m to 50 m deep with slope angles between 8° and 20°.

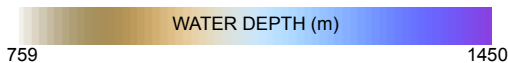




NAD83, UTM ZONE 8



DWG No : 20110068-MBB-CHVLY-P525-0
Project No. 20110068



Chute-like valley network below 1000 m water depth. These valleys are 40 m to 200 m deep and are separated by sharp-crested interfluves, the flanks of which are characterized by small, rill- and gully-like tributaries. At ~1200 m water depth the valleys coalesce and flatten out into a region of meandering, downslope-oriented low relief gullies.



6. GEOLOGIC CONDITIONS AND GEOHAZARD FRAMEWORK: UPPER ~100 M BSF

This section describes the geology and associated geohazards located in the upper ~100 m of section. For each sub-seafloor condition that is described, new interpretations are introduced under separate sub-headings. For ease of description sub-seafloor conditions and associated geohazards in the study area are divided into three general regions: the Continental Slope, Beaufort Shelf and Mackenzie Trough/Yukon shelf.

6.1 Continental Slope

During the Pleistocene glaciation and early deglaciation slope failures were common, and these features can be mapped in the subsurface of the continental slope as buried MTDs from SBP data. There are two principal morphological types of buried MTDs in the investigation area: early sheet-like regional deposits and younger, discrete, downslope-oriented ribbon-like deposits. The morphology of the buried MTDs is different from the scallop-shaped modern seafloor slumps. These, and other buried features and structures are described below.

6.1.1 Sheet-like MTDs

A region-wide interval of acoustically massive to poorly stratified sediments occurs between horizons H4 and H3 in the lower part of slope Unit 2 (Plate 3.7). The interval is generally between 5 m and 25 m thick, and rests on horizon H4, a regional unconformity marking the base of Unit 2 sediments (Plate 3.7). The interval is thickest (15 m to 25 m) beneath the mid-slope region. The upper surface of the deposit is marked by the H3 horizon that has a well-developed hummocky topography expressed at the modern seafloor as downslope-oriented gullies through the overlying Unit 1 and 2 strata, in the mid-slope and bottom slope region. The gullies have widths of 0.5 km to 2 km, and are 2 m to 10 m deep (described in Section 5.1.4). Morphologies resemble type I and type IV gullies described from the glacially influenced continental slope of west Antarctica (Gales *et al.* 2013). These authors relate type I gullies to formation by hyperpycnal flow of sediment-laden subglacial meltwater. Their type IV gullies are interpreted as older features that have been later modified by other processes such as mass wasting. The gullied topography of the buried MTDs can be seen in time slices of 3D seismic data (Plate 6.1A). At the distal ends, some of the gullies flare out into a lobate terminus.

Interpretation

The H3 to H4 interval is interpreted as an erosive and depositional event, or series of events, resulting from regional sheet flows originating at the shelf margin. The poorly stratified deposits suggest they are possible turbidites and because they originate at the shelf margin may comprise coarser glacial shelf sediments. The deposits thus may be more sand-prone than the overlying pelagic silts and clays of Units 1 and 2.

6.1.2 Ribbon-like MTDs

Younger than the sheet-like MTDs beneath, linear MTDs originate immediately seaward of the FEF Zone or in the mid-slope region, and extend downslope, as linear ribbon-like deposits up to 5 km wide, 30 m thick and 40 km long. All have well-defined margins that truncate acoustically well stratified sediments of Unit 2 (Plate 6.2), and are sometimes characterized by positive relief berms. MTD sediments are acoustically structureless, but rarely may preserve a "ghost" stratigraphy in the form of packages of faintly discernible, usually distorted, stratification. The MTDs may occur either as single, ribbon-like deposits (Plate 6.3), or up to four coalescing flows.

The proximal regions of most of the MTDs appear to originate at or be truncated along the northern margin of the paleo-scour zone. Alternatively, the MTDs may have originated farther upslope at the shelf margin, but these regions have been overprinted by the ice keel turbate of the paleo-scour zone.

Overlying, stratified, draped pelagic sediments of Unit 1 mirror the micro-topographic upper surfaces of many buried MTDs such that the general morphologies of the deposits have been propagated upward and are visible at the modern seafloor (Enclosure 1).

In well stratified sediments above the MTDs, partial acoustic wipeouts occur as discrete vertical columns (Plate 6.4). These features are inferred to be vertical zones of gassy sediments. Such gas "pillars" are generally wider than they are tall and may extend upwards 10 m to 20 m from the top of the MTD deposit. Where gas pillars reach the seafloor there is no evidence for the development of fluid escape features.

Interpretation

All ribbon-like MTDs occur within Unit 2 and therefore are of late glacial to early deglacial age. Most of the MTDs originate on the upper slope, and may comprise high proportions of sandy material derived from proximal glacial outwash deposited at the shelf margin. Such sand-prone deposits are expected to have higher porosity and permeability than the pelagic silty clays that envelop them, and may become the locus for gas accumulation, possibly from deeper sources. Gas seepage through the upper MTD surfaces is a potential source for the creation of gas pillars.

If they originate in the paleo-scour zone ice keel turbate it is speculated that initial MTD failures may have been precipitated by ice keel grounding events. Along the eastern Canadian continental margin there is circumstantial evidence that iceberg scour may have been an important process in triggering slope failures and turbidites during Heinrich events (Piper & Campbell 2005).

6.1.3 Seafloor Offsets/Faults

In places, small-scale normal faults offset the modern seafloor (Plate 6.5). In the subsurface these offsets are non-penetrative, are generally confined to Unit 1 and 2 sediments and are non-tectonic in origin. Offset ranges from <1 m to 10 m at the seafloor,

and the amount of offset at the seafloor is generally the same in the subsurface, indicating that they are not growth faults.

There are two types of seafloor offset: those associated with slumped regions, and those associated with subsidence of large-scale slope FEFs (Plate 5.8). Slumped regions are characterized by stepped terraces, and each terrace is bounded on its upslope and downslope margin by a small-scale fault. Slump headwall scarps are exposed fault footwalls with normal throws of 15 m to 20 m. In places, undisturbed seafloor in the region of stratified sediments above the slump terraces may be offset along small-scale faults with throws of <1 m to 3 m. These may represent failure planes of nascent terraces that did not form when the larger terraced slumps formed (Plate 6.5). Seafloor offsets associated with large-scale slope FEFs are characteristically arcuate in plan view, forming concentric, partial ring faults around the FEF (Plate 5.8). Two or more concentric ring faults create stepped terraces of offset seafloor with downthrows of 5 m to 10 m towards the central FEF cone. Faults are related to local FEF subsidence and extend up to 450 m BSF (Plate 6.6).

6.1.4 Mega-Scale Glacial Lineations

Grooves at the base and top of Unit 3 are interpreted as mega-scale glacial lineations (see section 5.1.4) and are observed on SBP profiles (Plate 5.6). The grooves are thought to have been formed by a thick melange of seafloor-touching ice, probably mostly of glacial origin. Possible mechanical reworking of Unit 3 sediments by ice may have altered their physical properties. It is also likely that ice rafted coarse clastic material, originally entrained in the parent ice sheet, may have been deposited within Unit 3 sediments, and lodged or deposited on the grooved surfaces (horizons H5 and H4).

6.1.5 Slope FEFs

The general surface morphology of the large slope FEFs is described in Section 5.1.5. Flat tops of the FEF cones typically show amplitude phase reversals in seismic vertical sections, and acoustic wipeout beneath FEF cones is readily apparent on sub-bottom profiles (Plates 5.9 and 6.7), and in 2D seismic data to considerable depths, indicative of the presence of shallow gas (Plate 6.6). Beneath the FEF margins stratified sediments of Units 1-3 typically are deflected downwards, likely the result of subsidence (see Interpretation below).

Unlike smaller FEFs of the continental margin FEF Zone and shelf FEFs, buried flows of extrusive material are associated with the slope FEFs in the near- and sub-surface. The flows have no surface expression on multibeam imagery but in some cases they are visible as high seafloor amplitude responses in 3DSO data. Flows are easily seen in sub-bottom profiler data as distinct strongly reflective horizons (Plates 5.9 and 6.7). With the exception of two features that are older, extrusive flow material originating from the cones is interbedded with stratified Unit 1 sediments. Flows typically are stacked beneath the sloping flanks of the large FEF cones, and extend upward through Unit 1 sediments to the seafloor (Plate 6.7) suggesting that periodic eruptions may still be occurring. The flow

horizons are discontinuous and not always distinct, but are higher in amplitude and thicker than other Unit 1 reflectors, with which they either tend to interfinger or mask.

Beyond the cone flanks, discrete flows may occur and extend long distances downslope. With sufficient survey line density these flows may be mapped from sub-bottom profiler data as thin, discrete tongue-like lobes. Flows range in length from 3 km to 15 km (Plate 6.8) and in width from 0.3 km to 1.5 km (Plate 6.7). Flows are generally 20 m to 40 m thick close to the FEF source, and thin distally to ~10 m but may be as thin as 1 m before pinching out at the toe (Plate 6.8). The flows were likely quite fluid in order to have flowed down gentle slopes of 1° and 2° over such long distances. 3D seismic data in Plate 6.1 show the development of the FEF associated with these flows. The 72 ms time slice (Plate 6.1 A) shows the gullied topography of sheet-like turbidites in lower Unit 2 before the FEF developed (see section 6.1.1). The FEF cone rests on a prominent reflection in mid-Unit 2 and can be seen, together with its associated flows, on the 40 ms time slice (Plate 6.1B).

Core PC-31 from the summit region of an FEF sampled a buried flow deposit that was mapped from SBP data (Enclosure 3). The flow interval is characterized by massive grey clay that rests in sharp contact on underlying dark green, bioturbated clay (Plates 6.9 and 6.10). The interpreted base of the flow is located at 4.09 m in the core, in close agreement with the SBP and Multi-Sensor Core Logger (MSCL) depth intervals. A C₁₄ date of 4600 cal years BP from immediately below the FEF flow gives the maximum age of the overlying flow deposit (Plates 6.9 and 6.10). A C₁₄ date from immediately above the interpreted flow deposit, at ~3.2 m core depth, gives an age of 3140 cal years BP (Plates 6.9 and 6.10). The 1460 year interval between the top and bottom of the ~90 cm-thick deposit indicates the period of time during which there was extrusive activity. A possible second flow between 1.1 m and the seafloor may be as young as 1000 cal years BP.

6.1.6 Paleo-Scour Zone

The paleo-scour zone on the upper slope was likely formed by deep-drafted icebergs originating from the ice stream in Amundsen Gulf to the northeast (see section 5.1.9). Scouring occurred for a period of at least 3000 years between approximately 15500 cal years BP and 12000 cal years BP. Although they are buried, scour marks on the upper turbate surface roughen the modern seafloor with grooves up to 100 m wide, 3 m deep and side slopes up to 6°. Mechanical reworking by grounding ice keels of sediments within the ice keel turbate likely altered sediment physical properties. Also, there is an increased potential for ice-rafted debris, including cobbles and boulders within the turbate.

6.2 Beaufort Shelf

6.2.1 Acoustic Permafrost

Perhaps the most dominant feature beneath the modern seafloor on the Beaufort Shelf is the presence of frozen or partially frozen sediments, observed in seismic profiles as

acoustic permafrost, or APF. APF is detected on the basis of acoustic and seismic signature in sub-bottom and seismic profiles, not on the basis of temperature. Permafrost is defined on the basis of temperature and it occurs where ground (soil or rock) temperatures have remained at or below 0°C for at least two consecutive years (Permafrost Subcommittee, 1988; van Everdingen, 1998). The upper boundary of permafrost coincides with the upper position of the 0°C isotherm beneath the land surface and is referred to as the permafrost table. Above the permafrost table, seasonal temperature changes at the ground surface may be associated with freeze-thaw cycles. The distribution and occurrence of shallow ice-bearing permafrost in the upper several hundred metres of shelf sediment is spatially discontinuous and is a product of long cyclic periods of subaerial exposure during low sea level associated with glaciation.

Offshore permafrost was first documented in 1970 (Mackay, 1972), and since then its distribution and thermal properties have been well mapped and studied. O'Connor (1981a; 1982) identified three types of APF: hummocky, stratigraphically controlled, and marginally or partially ice-bonded. APF types and distribution were mapped in the top 100 m BSF using sub-bottom profiler data and borehole logs, and results were formally presented in the Marine Science Atlas of the Beaufort Sea (O'Connor and Blasco, 1987a and b). All APF types within the upper 100 m BSF are laterally and vertically discontinuous, and typically only the top surface, mapped as a strong amplitude horizon can be seen on sub-bottom profiler data (Plate 6.11).

Subsea permafrost has been well documented beneath the Beaufort Shelf to depths of ~700 m BSF, and extends seawards to the shelf margin (Fortin and Blasco, 1990). Recent seismic refraction work in the U.S. Beaufort Sea indicates a far more limited extent of subsea permafrost than in the Canadian sector. In their analysis of U.S. legacy multichannel seismic data, Brothers *et al.* (2012) find that permafrost layer refractions (top of permafrost) extend into water depths no greater than 20 m, to a maximum distance of 30 km offshore, and possibly to within 10 km of the shore in Harrison Bay (Ruppel *et al.* 2010). In contrast to the Canadian Beaufort Shelf this restricted region of occurrence implies considerable thawing and accompanying dissociation of intrapermafrost gas hydrate and partial to full dissociation of hydrate beneath the base of permafrost (Brothers *et al.* 2012).

An understanding of permafrost distribution and character within the Beaufort-Mackenzie region has implications for both hydrocarbon exploration and infrastructure development. The presence of permafrost below sea floor can be a hazard to drilling operations. Precise delineation of the permafrost base is needed to identify possible gas hydrates which may accumulate within and near the base of the permafrost zone.

In permafrost-affected sediments decreasing temperature results in increased velocity, and the velocity increase from clays to silts to sands measured from Beaufort Sea samples is significant (King *et al.* 1982; MacAulay and Hunter, 1982). The heterogeneous distribution of clay, silt and sandy facies and variations in temperature with depth results in large vertical and lateral changes in seismic velocity, which in the Beaufort Sea region may range from 2000 m/s to 4000 m/s (King *et al.* 1982; MacAulay and Hunter, 1982).

In general permafrost-affected sandy sediments on the Beaufort Shelf will be imaged in acoustic and seismic surveys if ambient *in situ* temperatures are less than 1.8°C, when they become ice-bonded (Taylor *et al.* 2013). At higher temperatures the pore water is only partially frozen and sediments are termed ice-bearing.

In the nearshore region the top of permafrost is a few metres below seafloor and is marked by the top of shelf Unit C (see section 3.1.3) which extends to the shelf margin. Two lines of evidence suggest that the top of permafrost remains at shallow depth below seafloor near the margin. Firstly, on high resolution 2D seismic profiles the top of Unit C is marked by a high amplitude reflector a few metres below seafloor immediately landward of the FEF zone, and clinoform reflectors are clearly identifiable within the unit (e.g. GSC line CSBS9157F115, not shown here). A seismic refraction line on the outer shelf confirms the presence of shallow permafrost (Morack *et al.* 1983) possibly marking the top of Unit C. Taylor *et al.* (2013) modelled the evolution of offshore permafrost distribution and thickness from 125000 cal years BP to the present and predicted that the outer margin of the permafrost terminates at the edge of the Beaufort Shelf at approximately 95 m water depth. Their results are in agreement with the findings from seismic refraction profiles by Pullan *et al.* (1987), and of the mapped distribution by O'Connor and Blasco (1987a and b).

Hummocky APF exhibits undulose topography. Its subsurface expression is discordant with acoustic stratigraphic horizons. The hummocky surface may be due to irregular partial melting of permafrost.

Stratigraphically controlled APF is observed as strong acoustic reflectors, parallel to stratigraphy and often located at the contact between underlying sands and overlying finer-grained sediments. Pore space between the coarser sediments is thought to allow greater inter-grain ice bonding, while adjacent fine-grained sediments at the same ambient temperatures may not be frozen due to the phenomenon of freezing point depression. Frozen coarse-grained sediments thus enhance the acoustic impedance so that the APF reflector is effectively controlled by vertical and lateral stratigraphic changes in grain size.

Marginally or partially ice-bonded APF is developed in well stratified sediments where alternating strata of sandy and finer-grained sediment occur. APF typically develops in the sandy layers but not in the finer-grained layers, such that sand-prone horizons appear as enhanced reflectors. Typically, only the top surface can be seen on SBP and 2D seismic profiles. Plate 6.12 shows examples of both hummocky and stratigraphically controlled APF on a 2D seismic line north of Pullen Island in the Beaufort Sea (Carr *et al.* 2011).

A government and industry funded study of petroleum systems of the Beaufort-Mackenzie Basin was initiated by the GSC (Hu *et al.* 2013) and as part of that study, permafrost interpretations were re-evaluated and updated as a consequence of the substantial amount of new data available from wells drilled after the 1980's. Judge *et al.* (1987) mapped the base of permafrost using data from 161 wells. Hu *et al.* (2013) updated this work by including data from a total of 265 wells and their revised map shows the depth to

base of fully frozen ice-bearing permafrost (IBPF) in the Beaufort Mackenzie Basin (Plate 6.13). Analyses to construct the map were based on downhole temperature (42 wells), check shot and vertical seismic profile (VSP) surveys (199 wells), Crystal cable surveys (102 wells), and geophysical well logs which included gamma ray, spontaneous potential, caliper, resistivity, sonic transit time, bulk density and neutron porosity (206 wells). Seismic velocity surveys were available for some wells, however the base of the IBPF could only be estimated as a consequence of the much lower resolution of seismic velocity compared to well log data.

Resistivity logs in conjunction with sonic transit time and sonic velocity were identified as being the most useful and reliable mechanisms for accurately identifying permafrost zones and physical properties. When and where available, temperature surveys provide a very direct indication of permafrost zones, however the drilling process typically disturbs permafrost zones from thermal equilibrium. Return to equilibrium may take months to years. Composite plots of various geophysical logs were generated to collectively determine the IBPF zones. Permafrost determinations were quality assessed in terms of their reliability based on the type and quality of data used to constrain the interpretations.

6.2.1.1 Amauligak 3F-24 Borehole and 2D Seismic Correlation

In 1988 a deep geotechnical borehole was drilled at Amauligak 3F-24 with the purposes of collecting *in situ* geophysical data and undisturbed core samples of subsea permafrost-affected sediments (Ruffell *et al.* 1990; Blasco, 2012 and see Plate 6.14 for location). The Amauligak location was chosen because this portion of the shelf in Kugmallit Channel is where subsea permafrost is at its thickest (~700 m BSF). The borehole was drilled to a depth of 468.45 m BSF, with frozen sediment encountered to at least 450 m BSF (Blasco, 2012 and Enclosure 7). At least eight regression/transgression cycles were identified within this interval by Blasco (2012). A total of 309.1 m of 85 mm diameter (core barrel size PQ) frozen core was collected amounting to 65% of the borehole depth (Ruffell *et al.* 1990). The borehole passed through shelf Units A to E (described in Section 3.1.3) and sampled fourteen subsequent lithological units (Units F through S) (Blasco, 2012 and Enclosure 7). Plate 6.11 shows Units A to C in the closest sub-bottom profile to the borehole location.

Downhole slimline tools (supplied by BPB Canada) were deployed to collect continuous downhole compressional and shear wave velocities in the 3F-24 borehole. Chilled drilling muds were used to prevent thermal warming during the drilling process (Blasco, 2012). In addition, 15 sediment samples were collected downcore and maintained in the frozen state during drilling, shipment, storage and during laboratory measurements of compressional (V_p) and shear wave velocities (V_s). The results of the downhole *in situ* and laboratory measurements for V_p and V_s are illustrated in Plate 6.15.

Within ice-bearing permafrost the frozen water content is sensitive to temperature. This is particularly true for coarser-grained sand sediments at $<-3^{\circ}\text{C}$ and for fine-grained silts and clays below 0°C (e.g. Votyakov, 1973). Therefore considerable effort was expended to

maintain the negative thermal regime of the borehole and the recovered sediment samples. Over a period of 23 days *in situ* borehole temperatures were measured from a multithermistor cable to approximately 382 m BSF. Above 67 m BSF temperatures were affected by the setting of a cement plug prior to abandoning the borehole. Within the 67 m to 382 m BSF interval temperatures stabilized over a period of 4 - 5 days between -2°C and -2.5°C . (Taylor *et al.* 1989). *In situ* temperatures must be maintained if accurate V_p and V_s velocity measurements are to be made for both downhole and laboratory conditions. This turned out not to be the case for the Amauligak 3F-24 drilling program for the following reasons:

- Chilled drilling muds used during drilling operations varied from -7 to -1.5°C over the 2 week field program. The impact of temperatures below *in situ* values was to increase the amount of ice in an annular zone immediately surrounding the well bore. It is likely that the acoustic compressional and shear wave pulses of the slimline tool were attenuated in this affected zone and thus did not measure the frozen sediments at ambient temperatures beyond the affected region.
- Recovered frozen sediment samples were also subjected to a colder than *in situ* thermal history during drilling, freezer storage onboard ship, during transport south by aircraft, and storage in the laboratory before velocity measurements were conducted. The thermal history of the samples is not clear. However, once sediments were exposed to colder than the *in situ* temperature of -2.5°C ice content could increase but would not decrease if the thermal regime warmed (up to -1.5°C in this case).
- As a result of the thermal history of the borehole and sediment samples, the ice content of the ensonified *in situ* sediment column and recovered sediment samples were higher than the original undisturbed frozen sediments.

There is a significant difference between downhole *in situ* and laboratory measurements of V_p (Plate 6.15). Downhole values range from <2300 to >2700 m/sec and limited laboratory values ranged from <3000 to >4500 m/sec. The difference between *in situ* and laboratory values is variable down core but with laboratory values consistently higher which is attributed to higher ice contents in the laboratory samples. Similarly there is a significant difference between downhole and laboratory measurements of V_s . Downhole values range from <800 to >1500 m/sec and limited laboratory values range from <1000 to >2700 m/sec. The laboratory values are consistently higher which is also attributed to higher ice contents in the laboratory samples.

The degree to which the downhole measurements of V_p and V_s have been thermally disturbed by cooler than ambient drilling muds is not clear but the values are in line with other studies of subsea permafrost sediment samples from the Beaufort Shelf (e.g. King *et al.* 1982), particularly at the *in situ* temperature of -2.5°C . In addition, compressional wave velocities used to process multichannel seismic reflection data are more in the range of the downhole V_p measurements (e.g. Yelisetti and Dosso, 2015; Brothers *et al.* 2012; Hinz *et al.* 1998; Weaver and Stewart, 1982).

The above discussion does not deal with the variations in velocity due to sediment type (sand, silt, clay) as both down core and laboratory measurements were made on the same sediment types. In general, frozen coarse-grained sediments have higher compressional and shear wave velocities than fine-grained sediments (King *et al.* 1982).

The velocity structure with depth demonstrates two important features of subsea ice-bearing permafrost. Velocity inversions and velocity gradients occur with depth which can adversely affect multichannel seismic data processing and generate significant variation in calculated dynamic moduli.

McGregor Geoscience Limited (MGL 1992b, unpublished) acquired a 2D seismic line passing over the 3F-24 borehole (Plate 6.14) that in conjunction with three other MGL lines and industry seismic lines, linked a continuous regional transect across the Tingmiark Plain, Kugmallit Channel and Akpak Plateau. A series of lines with various recording geometries was also acquired during 1989 and 1990 with differing source and recording parameters (200 and 400 m cables, group intervals of 8.33 m and 16.67 m, varying near trace offsets, 100 and 180 cubic in source arrays).

Seismic datasets were processed through several streams by Calgary based Western Geophysical and formed the basis for comparison with forward modeling using synthetic seismograms. Data quality on the processed sections was described by MGL as being fair in the upper 200 ms and generally coherent laterally with a frequency spectrum of 10-100 Hz. Below 200 ms lateral discontinuity, low frequency (< 50 Hz), variable amplitude, linear and coherent noise characterized the stacked sections. Several regional acoustic boundaries were identifiable on a number of sections as well as indications of the two permafrost layers D5 and D6 at several locations. MGL made the general comment that the use of shallow seismic for geohazard detections may be considered dubious given the poor quality of the data, based on processing techniques then available.

In an effort to correlate the borehole stratigraphy and permafrost characteristics to seismic observations, MGL (1992b, unpublished) conducted a series of investigations to model predicted responses compared to observed data to aid in interpreting the seismostratigraphy along the entire transect. Several investigations were performed with varying parameters using two distinct modeling programs and geophysical and lithology observations from the 3F-24 borehole. The borehole provided continuous sonic and density logs to 390 m BSF and lithology to 500 m BSF (EBA, 1990, unpublished).

Based on the correlations between modelled and field data, MGL (1992b, unpublished) concluded that at the 3F-24 borehole, the primaries and multiples were indistinguishable based upon moveout differences, dip differences on the CMP gathers, frequency differences and the periodicity of the multiples. The synthetic CMP gathers did not resemble the field data. The reflectors on the synthetic had lower moveout and greater coherency. The field data exhibited poor trace to trace coherency, low frequency multiples and poor vertical resolution.

The main velocity/density boundaries at the borehole site could not be resolved as distinct reflectors on the seismic data. The inability to resolve these boundaries was attributed to

the presence of a very shallow, thick, very high velocity layer (permafrost) and the physical limitations it imposed on acoustic energy (as suggested by the work of Poley and Lawton (1991). MGL (1992b, unpublished) concluded that the lateral extension of the velocity/density structure at the borehole could not be resolved with seismic data (acquired in the 1989-1990 datasets).

Poley and Lawton (1991) recommended that future data acquisition should be based on an improved source, decreased source receiver offset, shorter group intervals and maximization of the number of channels. The 1989 and 1990 datasets acquired by MGL were directed towards those objectives; however results suggest that group intervals less than 8.33 m and more than the 24 channels acquired in the 1989/1990 programs will be required to potentially image the shallow APF with 2D seismic.

Technical improvements in acquisition hardware and advances in seismic processing algorithms through 2015 have advanced significantly which suggest that modern high resolution seismic programs and modeling techniques could produce improved results.

6.2.1.2 Recent Examples of Approaches to Permafrost Delineation

Data Acquisition

Ultra high resolution 3D seismic survey systems are now available for shallow investigations and can be configured and operated off mid-sized vessels of opportunity. Geometrics (www.geometrics.com), for instance, offer a complete 3D seismic acquisition system (P-Cable) that can be configured from six to twenty four 300 m streamers with 96 channels per streamer at a group interval of 3.125 m. Real time array positioning and binning are performed aboard the vessel to ensure complete coverage. Examples of very high quality sets collected by this method are shown in Plates 6.16 and 6.17.

Data Processing – 3D Tomography Modeling

Velocity models for near surface features in permafrost environments are a major problem as a consequence of the strong lateral velocity variations and negative velocity gradients caused by higher velocity permafrost overlying lower velocity marginally frozen sediments. The negative gradients prevent the application of conventional refraction and reflection methods to determine near surface velocities and the strong lateral variations can introduce severe static anomalies.

First arrival tomography modeling as described by Zhu *et al.* (2011) has been used to model a grid velocity structure based on first arrival travel times and ray-paths. Each node of the grid is assigned a velocity and the node velocities can vary in an arbitrary fashion capable of modeling strong velocity variations in both vertical and horizontal directions.

Based on a local wavefront tracking and construction algorithm, the method has been shown to be highly accurate and robust in modeling turning waves even for extremely heterogeneous media. In addition to turning waves, the method is also capable of modeling scattered waves, a feature especially important for permafrost velocity calculation as some of the observed first arrivals are not turning waves but waves generated by scattering due to strong lateral variations. Another feature is that Fresnel-zone effects along a geometric ray are included in the tomographic algorithm. This further enhances the ability of the first-arrival tomography in accurately determining a low-velocity layer. Plate 6.18 shows examples of modelled velocity field results for both real and synthetic cases.

Ramachandran *et al.* (2011) have also used first arrival tomography on the first 2 seconds of the 126 km² Mallik 3D survey in the McKenzie River Delta on the coast of the Beaufort Sea. The survey encompassed both land and marine components (Plate 6.19). Four wells on the survey grid and their associated well log products provided groundtruthing to the final velocity model. Their results suggested that a highly heterogeneous permafrost velocity structure exists in the upper 200 m of the subsurface within the 3D volume. Permafrost distribution in the near surface was observed to attenuate signals that affect deeper reflections in the whole seismic volume. Resolution tests with the tomography application indicated good resolution both horizontally and vertically. Zones of strong amplitude blanking and frequency attenuation observed in processed reflection seismic stacked sections correlated with locations of taliks beneath unfrozen lakes (Plate 6.19). Application of the model results provided an estimate of seismic attenuation effects, and provided good control on the near surface static correction required for processing of, and improvement in, the seismic reflection images.

6.3 Mackenzie Trough/Yukon Shelf

6.3.1 Mackenzie Trough Unconformity

The well developed and easily recognizable angular unconformity that defines the buried shape of the Mackenzie Trough formed late in Upper Iperk Sequence time, and was likely excavated to its maximum depth during the early Wisconsinan (Blasco *et al.* 2011; 2007) (Plate 3.2, and Enclosure 4 and 7). On both margins the base of Trough unconformity levels out and becomes parallel with regional Upper Iperk Sequence strata and is either a disconformity or non-depositional unconformity (Enclosure 4). There are no wells or boreholes that sample the angular unconformity beneath the central and outer Mackenzie Trough, and there is scant evidence of its possible age from boreholes located on either of the surrounding continental shelves. There is also considerable uncertainty as to its stratigraphic elevation beneath the shelf regions where it becomes parallel to Upper Iperk Sequence strata. Thus the stratigraphic position and age of the unconformity beneath the central Trough, Beaufort Shelf (Kringalik Plateau) and western Yukon shelf has not yet been resolved (e.g. Blasco *et al.* 1989; 1990; Lewis and Meagher, 1991).

On the Yukon shelf where the unconformity is parallel to Upper Iperk Sequence strata, it may be correlative with an erosional surface marking the base of Unit III, 60 m BSF in a single borehole (GSC-1) located ~60 km west of the Trough's western margin (Enclosure 3). A thermoluminescence date from the top of Unit III gives a wide range between 60000 to 120000 cal years BP, however, the unit may be as old as 180000 cal years BP (Blasco *et al.* 1990). As a result, the unconformity could be from late Middle to early Late Pleistocene in age. Results from the present study suggest that in the transition zone beneath the western Trough margin and eastern edge of the Yukon shelf the unconformity rises to within ~20 m of the seafloor, and is overlain by ice keel turbated sediments of Unit MT2 (see Section 4.2.1 and Plate 4.4).

The unconformity's eastern margin appears to merge and become conformable with strata beneath the Kringalik Plateau of the Beaufort Shelf at about 200 m BSF (e.g. Blasco *et al.* 1990; Carr *et al.* 2011). Downward extrapolation of sedimentation rates based on dated Holocene sediments suggest an absolute minimum age for the unconformity of 70000 to 80000 cal years BP (Blasco *et al.* 1989; 1990), within the age range of the thermoluminescence date beneath the Yukon shelf. Unfortunately no boreholes or wells have retrieved material from this depth, and therefore direct dates have not been obtained, thus its age on the eastern side is inferred.

6.3.2 Shallow Stratigraphy

Unit MT1 appears to pinch out on the Trough's western margin against the Yukon shelf (Blasco *et al.* 1990). Plate 4.4 is part of a legacy sparker sub-bottom profile showing this transition. Multibeam imagery ~6 km south of the sparker profile shows the same transition between the Trough and Yukon shelf (Plate 6.20). Of note are contour-parallel step-like terraces 300 m to 400 m wide between 70 m and 120 m water depth, and the presence of associated subtle, contour-parallel narrow ridges of <1 m to 6 m relief. Similar steps are also visible on the SBP profile (Plate 4.4). At the shelf edge, multibeam imagery shows an abrupt transition in seafloor morphology from the linear, terraced Trough margin to a region ~5 km wide on the Yukon shelf characterized by a rough, hummocky surface (Plate 6.20). The surface is dominated by a number of intersecting linear to curvilinear ridges that typically are a few hundred metres to at least 2 km long, 25 m to 40 m wide with relief of <1.5 m.

Comet-like marks 20 m to 100 m long, 10 m to 20 m wide and with 0.5 m to 1 m relief, cluster along the ridges and on terraces at the western margin of the Trough where MT1a strata are truncated at the seafloor (Plates 6.20 and 6.21). Crag-and-tail morphologies of the comet marks are strongly aligned in a west-northwest to east-southeast orientation, with blunt "upstream" faces to the east-southeast. Fewer, similarly oriented comet marks are seen developed around small mounds of unknown origin on the step-like linear terraces on the upper Trough margin. The ridged MT2 surface is gradually buried beneath a westward-thickening veneer of Holocene sediment, and is completely covered in water depths less than ~50 m where the seafloor is dominated by the grooves of modern scour marks. Comet marks diminish in number and definition westwards as the

ridged surface is obscured beneath the Holocene veneer, and are not seen above ~50 m water depth (Plate 6.20).

Interpretation

For the eastern Mackenzie Trough margin sub-units MT1a and MT1b can be traced and matched reasonably well to Units A and B respectively on the Beaufort Shelf (Plates 4.5 and 4.6). The well defined MT1a/MT1b horizon can be traced from the Trough to the shelf where it merges with the characteristically diffuse stratigraphic Unit A/B horizon at the base of the modern ice keel turbate of the saturated scour zone (see following section). The MT2/MT1b horizon may be equivalent to the hummocky unconformity truncating the clinofold reflectors of Beaufort Shelf Unit C shown in Plate 4.6 but a direct connection cannot be positively proven. Erosion of sediments at the seafloor has occurred along the eastern Trough margin and is seen as low angle truncation of strata in Unit MT1a. However, erosion is not consistent and some apparent truncation may be a function of stratigraphic offlap.

The pinchout of Unit MT1 against the Yukon shelf along the western Trough margin is erosive, not stratigraphic, as shown by a sub-bottom profile across the margin (Plate 4.4). As they are traced upslope towards the Yukon shelf, Unit MT1a strata are progressively truncated at the seafloor and an estimated total of ~55 m of stratigraphic section is missing. Unit MT1b has pinched out against the top of MT2 below the limit of acoustic penetration so that sediments of MT1a rest directly on the MT2 surface in Plate 4.4. Erosion of MT1a has re-exposed the hummocky, ice scoured upper surface of the MT2 ice keel turbate unit at the seafloor on the Yukon shelf.

The flat, smooth, contour-parallel, step-like linear terraces along the Trough/Yukon shelf margin are interpreted to be the result of modern erosion by bottom currents. The narrow ridges associated with the current-swept terraces are interpreted as outcrops of Unit MT1b bedding exposed by current erosion.

In the ~5 km wide region at the edge of the Yukon shelf the top of Unit MT2 is exposed at the seafloor. Exhumed, relict ice keel scour marks are expected on this surface but it is instead characterized by curvilinear, intersecting ridges (Plate 6.21). The ridges have similar shapes and dimensions to ice keel scour marks with the exception that they are positive relief features. The ridges are interpreted as ice keel scour marks of the MT2 surface, their positive relief being accounted for by one of two processes: 1) possible increased cohesion induced by changes to the geotechnical properties of sub-scour soils during the ice scouring events or; 2) post-scour sediment fill in the scour mark troughs, such as fine sand, with greater resistance to erosion than surrounding seafloor soils. The net result of either process is resistance to erosion by bottom currents that have selectively removed non-scour affected sediments.

Comet marks are interpreted as indicators of strong bottom currents with unidirectional flow to the west northwest indicated by well-developed down-current 'tails' (Plate 6.21). Although they are strongly associated with the MT2 surface it is not clear whether the comet marks are relict features related to a period of more regional erosion, and are now blanketed by a veneer of Holocene sediment, or whether bottom-current erosion is a

modern process, restricted to a belt along the western Trough margin. Modern ice keel scouring is an active process on the shelf above ~50 m water depth, and a few new scour marks are superimposed on the relict MT2 ice scoured surface and these appear to be unaffected by comet marks.

6.3.3 Paleo-Scour Zones

Shallow stratigraphy in the outer Mackenzie Trough comprises acoustically well stratified clays and silts of Units MT1 and MT2. These, and deeper Units MT3 to MT5 and the stratigraphy below the basal Mackenzie Trough unconformity are displayed on the SBP legacy profile 80-507 (Enclosure 4).

Unit MT2 is interpreted as a buried ice keel turbate (see section 4.2.2). A second, partially buried ice keel turbate is located along the eastern margin of the Trough within Unit MT1a. This turbate merges with the modern seafloor where active scouring is occurring. Intense mechanical reworking by ice keels has likely altered the original physical sediment properties of both units. Additionally both units may contain coarse-grained ice-rafted debris, possibly ranging from sand to boulders, deposited from floating ice.

6.4 Shallow Water Flow Potential

6.4.1 Background

Shallow water flow (SWF) is defined as water flowing within and around the outside of structural well casing to the seabed (Alberty *et al.* 1997; 1999). SWF can occur during drilling where fluids within highly permeable, typically uncemented sands are at greater than hydrostatic pressure. Disequilibrium occurs when rapidly deposited overburden causes increase in pressure in the underlying sand-prone interval faster than it can be dissipated, resulting in geopressured conditions (Alberty *et al.* 1997; 1999). The upward escape of water from the pressurized sediments can be prevented by an overlying seal composed of fine-grained sediments. Horizontal seals (such as “pinchouts”) can also trap geopressures within isolated, porous sand bodies.

The potential for SWF in the region can be assessed in general terms through analogy with the Gulf of Mexico (GoM) deepwater environment, where SWF has proven to be the most common and costly geohazard encountered to date. Within the GoM, geopressured sands have been encountered as shallow as about 90 m below seafloor. When these sands are penetrated during drilling, the fluids flow out of the formation and up the borehole and drill-string to the seafloor. However, if the overlying seal has been breached by erosion or faulting prior to drilling, the geopressured fluids may escape naturally and in some instances reach the seafloor. In addition, surficial fluid expulsion features may result in some reduction of formation pressure. Evidence of fluid expulsion is commonly seen along the continental slope throughout the northern GoM. However, it should be noted that subsequent fluid recharge can counteract such reductions in fluid pressure. Thus, it is

the mass balance relationship between fluid discharge and recharge that has ultimate bearing on SWF potential.

Although SWF zones cannot be defined with certainty using seismic data alone, the conditions that create overpressure can be assessed. Alberty *et al.* (1997) suggest that composite tophole depositional rates of ~15 cm/ka are enough to produce overpressures within underlying sand-prone intervals. A depositional rate map for the northern GoM was produced to show post-late Pleistocene sedimentation rates. This map was then compared to an in-house SWF database to investigate correlations between SWF and depositional rate. None of the wells that experienced SWF were located within the zone of lowest sedimentation rate (<15 cm/ka). A few significant SWF incidents occurred within the zone of moderate sedimentation rate (15-45 cm/ka). Most of the wells with serious SWF incidents, however, are located in the highest sedimentation rate zone (>45 cm/ka).

Although the geological environments of the GoM and Beaufort Sea are markedly different, both experienced high sedimentation rates of fine-grained sediment during the Quaternary period. The regional distribution on the Beaufort continental slope of variable, but significant thickness of stratified sediments indicates considerable pelagic sediment deposition since the last glacial maximum (~19000 years) and early Holocene. On the Beaufort slope most of the pelagic drape rests directly on MTDs that may be more sand-prone than overlying strata because they originate at or close to the shelf margin. Coarser-grained sediments were being discharged either directly from the margin of a grounded ice sheet at the shelf edge, or from glacial outwash delivered to the slope as sheet flow across the shelf, or as more discrete sources from the cross-shelf Ikit Trough, Kugmallit and Niglik Channels.

6.4.2 Assessment of SWF Potential in the Study Area

As discussed above, the potential for SWF depends on a number of factors, including the presence of porous water-bearing sands with a fine-grained sediment seal, as well as the balance between overburden sedimentation rate and counter-acting dissipation of pressures by erosion, faulting or localized fluid expulsion.

Of interest is the range of, and change in, sedimentation rates across the continental slope since the last glacial maximum (LGM) at approximately 19000 cal years BP when continental glaciers began retreating from the Beaufort Sea region (e.g. Blasco *et al.* 2011). Since the LGM, large outflows of meltwater carried quantities of fine-grained sediment to the shelf margin and into the Beaufort Sea where it was mostly deposited on the slope in the form of well-stratified pelagic rain-out. The LGM is interpreted to be represented by horizon H4 (base of Unit 2), so that all sediments above are of post-glacial age (see Section 4.2.4). Note, in the Geological Survey of Canada model (Plate 4.8) a possible LGM age (~19000 cal years BP) for the base of Unit C beneath the shelf is interpreted. The location of the base Unit C horizon has not yet been identified beneath the slope but may be considerably deeper than H4. Thus sedimentation rates above H4 presented here may be conservative values.

A crude pelagic sedimentation rate may be computed for any core location on the slope where a complete undisturbed Unit 1 and Unit 2 stratigraphy can be identified above H4. Sedimentation rate is calculated using C₁₄ dates obtained from foraminifera sampled from cores at each location. Areas where the stratigraphy above H4 is interrupted by MTDs, turbidites and FEF flows should not be used because these depositional events will introduce aberrations in the calculated pelagic sedimentation rate.

By dividing the vertical distance between horizon H4 and the deepest C₁₄ date in the core by the difference in age between H4 (assumed to be 19000 cal years BP) and the corrected carbon age of the dated horizon, a sedimentation rate is calculated in centimetres per thousand years (cm/kyr). Dividing the depth BSF of the deepest C₁₄ date in the core by the corrected carbon age, provides a sedimentation rate from the sample depth to the modern seafloor (assumed to be 0 years). Plate 6.22 illustrates the method of calculation.

Average sedimentation rates since the LGM have been calculated using C₁₄ dates obtained from foraminifera collected in samples <7 m BSF at 6 different core locations. The cores represent all those that are located on the slope where the complete stratigraphy from horizon H4 to the seafloor is undisturbed. Enclosure 3 shows the location of all cores and boreholes in the study area for which C₁₄ dates are available. The 6 core locations used to calculate post-glacial sedimentation rates are shown in red on Enclosure 3. For each core two average sedimentation rates are calculated: from H4 to the deepest C₁₄ date in the core, and from the deepest C₁₄ date in the core to the seafloor (Table 6.1). Graphs of the continental slope H4 to C₁₄ to seafloor sedimentation rates are presented in Appendix B.

Table 6.1: Cores used for calculating average slope sedimentation rates

Core Number	Year	Location	Water Depth (m)	Sample Depth (cm)	Calibrated C ₁₄ Date	Sedimentation rate (H4 to deepest C ₁₄ date (cm/ka)	Sedimentation rate (deepest C ₁₄ date to seafloor) (cm/ka)
BP10-PC01	2010	upper slope	485	120	1820	326.3	65.9
BP10-PC02	2010	above headwall of slump	684.5	513	14288	117.2	35.9
BP10-PC24	2010	above headwall of slump	909	236	14290	118.1	16.5
2004-804-803	2004	upper slope, NE edge of eroded seafloor	218	224.08	4200*	610.5	53.4



CL01	2009	mid-slope	890	591	12635.5	103.6	46.8
CL25	2009	mid-slope	640	323.25	5320	177.7	60.8

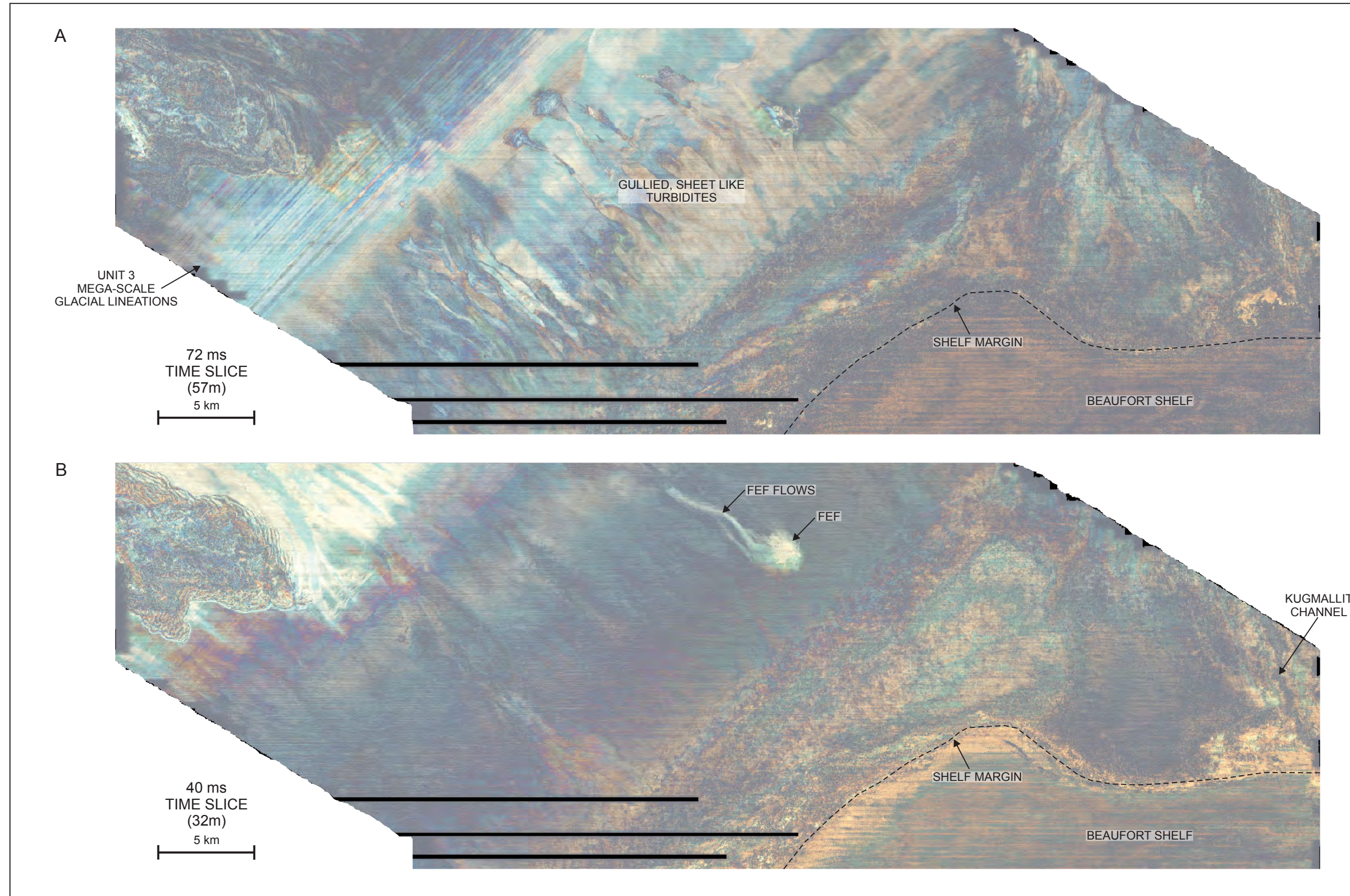
* dates obtained from shells and shell fragments

This two part approach is preferred as some cores contain two or more dates where the sedimentation rates in the intervals between the dates show variations that are considered to be anomalous. For example, core 2004-804-803 contains four dates tightly clustered within a 5 cm vertical section of the core, the interval between the uppermost date and the seafloor is 219 cm thick. Rates of <1.5 cm/ka are calculated for the three deeper intervals between four C₁₄ dates, but a rate of 326 cm/ka is derived for the interval between the uppermost date and the seafloor.

Reasons for these large interval variations are not clear but may be due to a number of factors including: reworking and mixing of older with younger datable material; possible hiatuses in sedimentation within an interval or possible pulses in sedimentation due to minor turbidite deposition; or variations in accuracy of C₁₄ dates depending on sample size. Reworking of older foraminifera is a known potential problem for C₁₄ dating and tends to increase the derived age. Heier-Nielsen *et al.* (1995) proposed a method to reduce or eliminate the error from such contamination by establishing a control curve, based on dates from *in situ* shells, against which the foraminifera dates can be correlated. The establishment of a control curve from shells is not available for the Beaufort Slope cores.

On the continental slope average post-LGM sedimentation rates from horizon H4 to the deepest C₁₄ dates all exceeded 100 cm/ka, and at one location exceeded 600 cm/ka (2004-804-803). At the core sites, H4 is generally less than 50 m BSF. These relatively high interval rates are in contrast to sedimentation rates between the deepest C₁₄ dates and the seafloor which range from approximately 16 to 66 cm/ka (see Table 6.1). H4 to deepest C₁₄ sedimentation rates significantly exceed those observed in areas prone to serious SWF incidents in the GoM, and four of the six C₁₄ to seafloor sedimentation rates also exceed the GoM rate. However, experience in the GoM shows SWF problems are generally not encountered at burial depths less than ~100 m, and sediment thickness above H4 on most of the Beaufort Slope is less than this. It should be noted that Unit 1 sediments rest above a number of buried MTDs, and the total thickness of fine-grained Unit 1 deposits that cap the youngest buried MTDs is generally less than 30 m, and the maximum thickness of Unit 1 and 2 sediments above the older buried MTDs seldom exceeds 40 m.

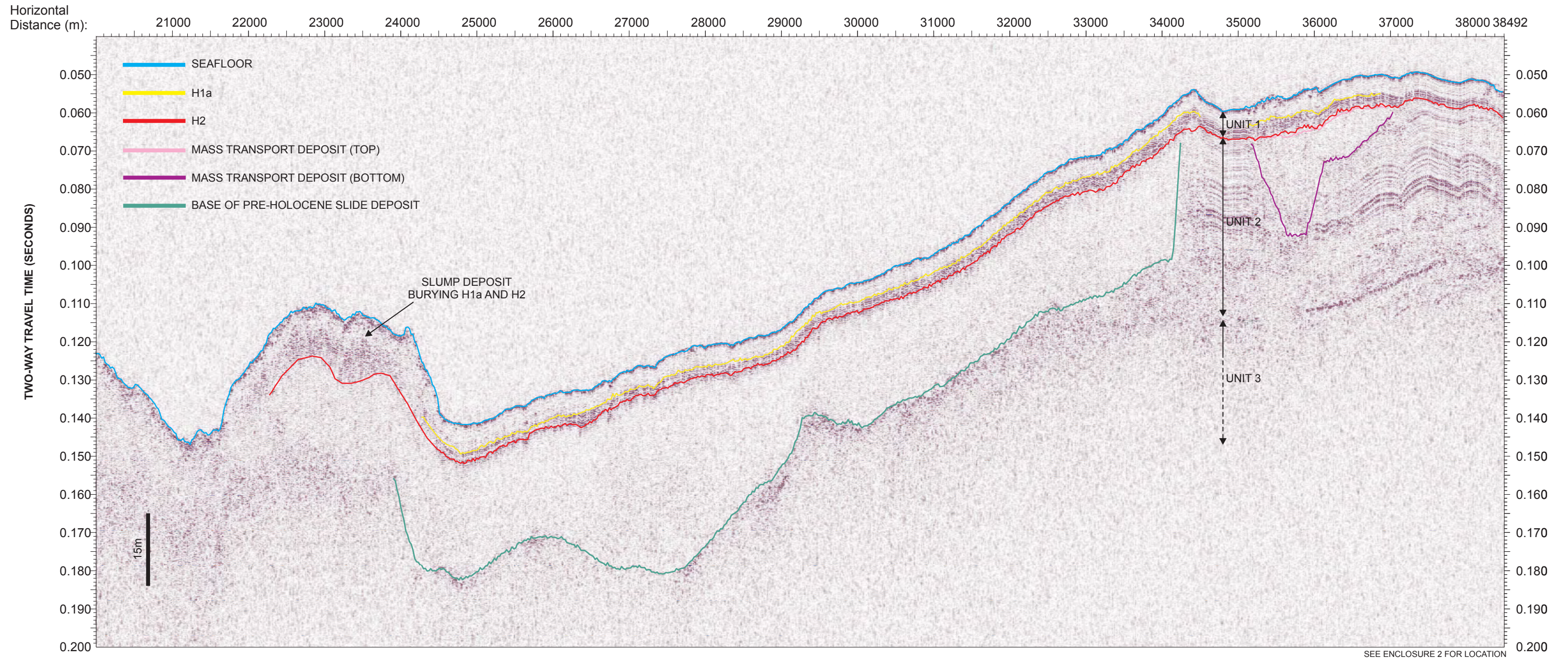
If it is assumed that the MTDs are potentially more sand-prone and porous than overlying Unit 1 clays, it may be possible for over-pressuring to develop within them. Shallow overpressures have not been encountered in most wells on the Beaufort Shelf; however, wellbore stability problems due to SWF forced abandonment of the Kopanoar D-14 well after penetrating overpressured saturated sand at 503 m BSF. It is recommended that potential for SWF be considered during well-planning, and that prospective wellsites be evaluated on a site-specific basis, with attention given to the possible presence of buried sand-prone deposits, and proximity to sources of fluid/gas charging.



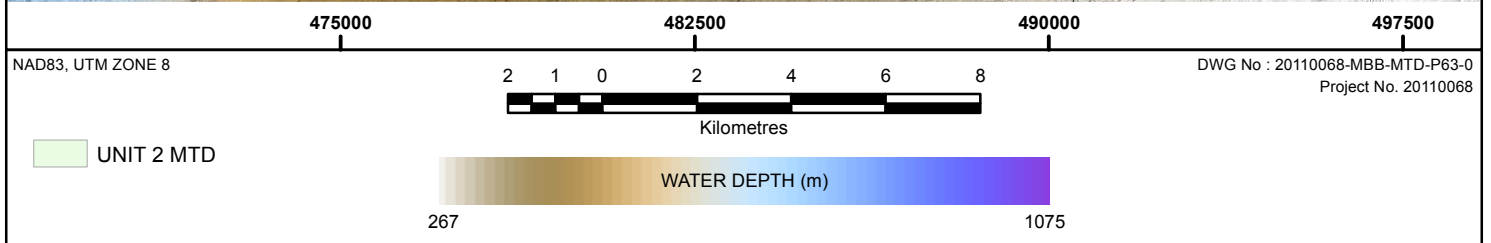
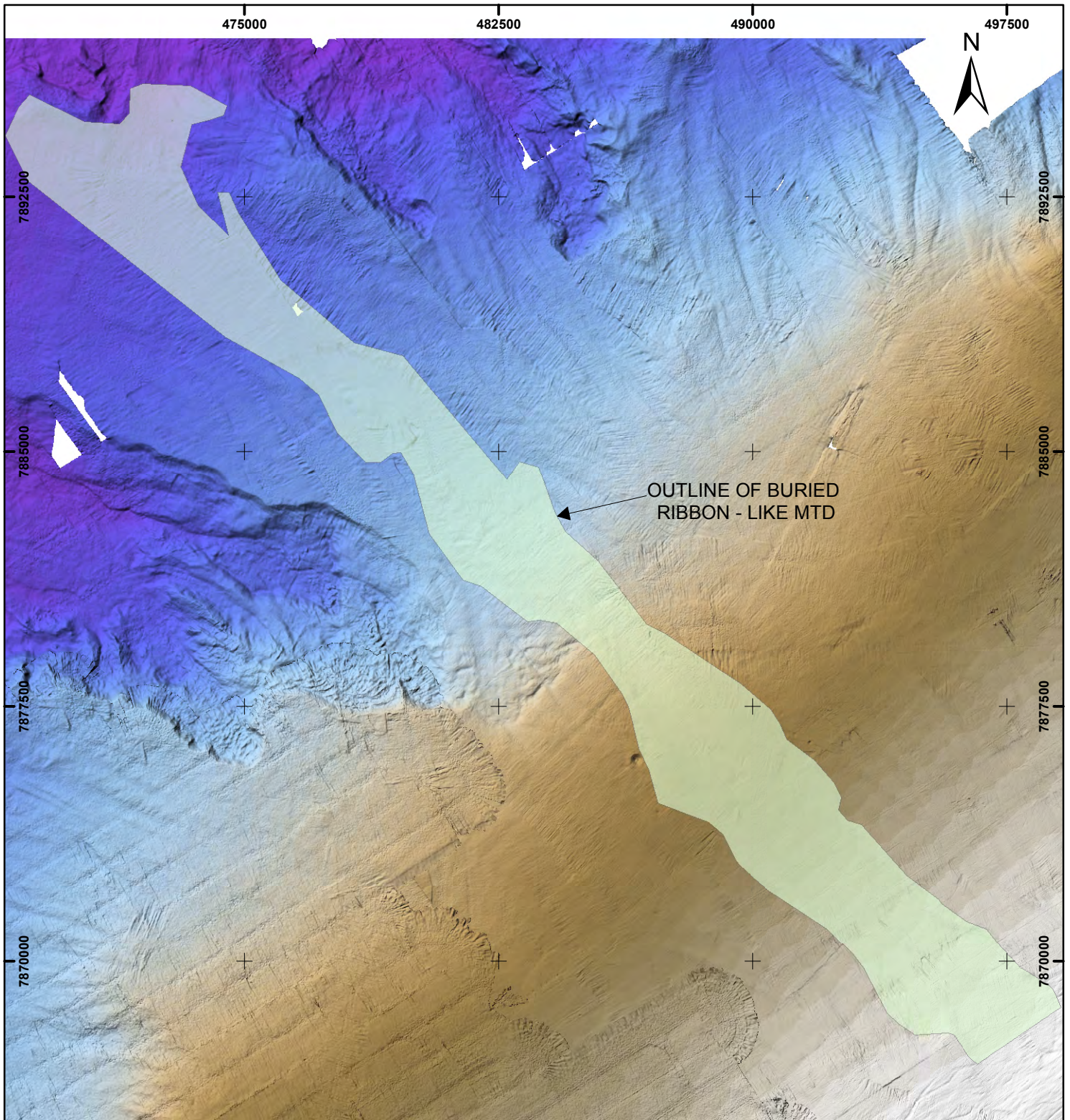
TIME SLICES OF 3D SEISMIC DATA. A: GULLIED TOPOGRAPHY OF UNIT 2 SHEET-LIKE TURBIDITES AND SLIGHTLY OLDER MEGA-SCALE GLACIAL LINEATIONS. B: A FEF AND ITS ASSOCIATED FLOWS HAS DEVELOPED IN YOUNGER SEDIMENTS ABOVE THE TURBIDITES. LICENSE BLOCK EL477 (IMAGES COURTESY OF BP EXPLORATION COMPANY).

SW

NE

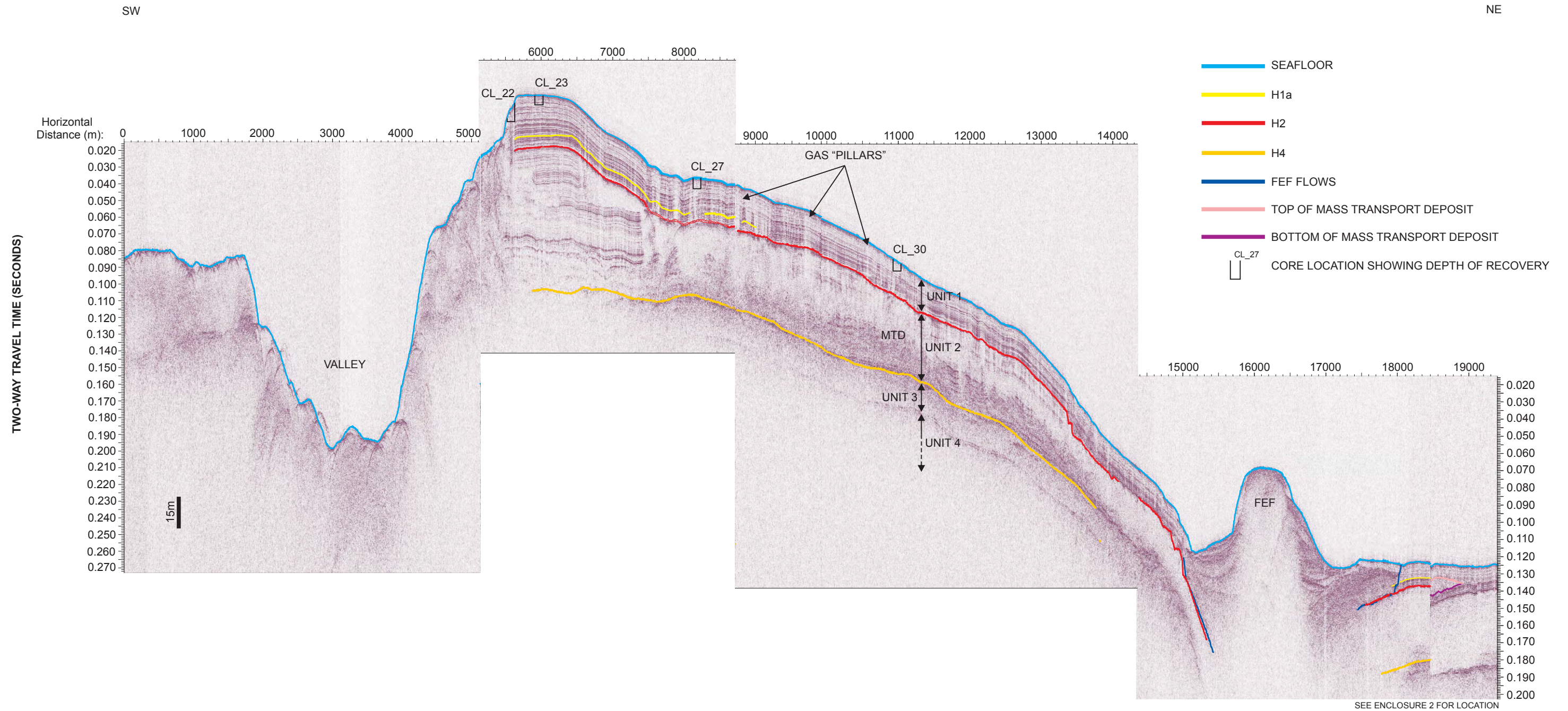


Sub-bottom Profile (Line 092780111) showing an example of buried MTDs. The cross-section of a ribbon-like MTD is shown on the right, beneath horizon H2 (red). A regional sheet-like MTD occurs beneath H2 in the central part of the profile.

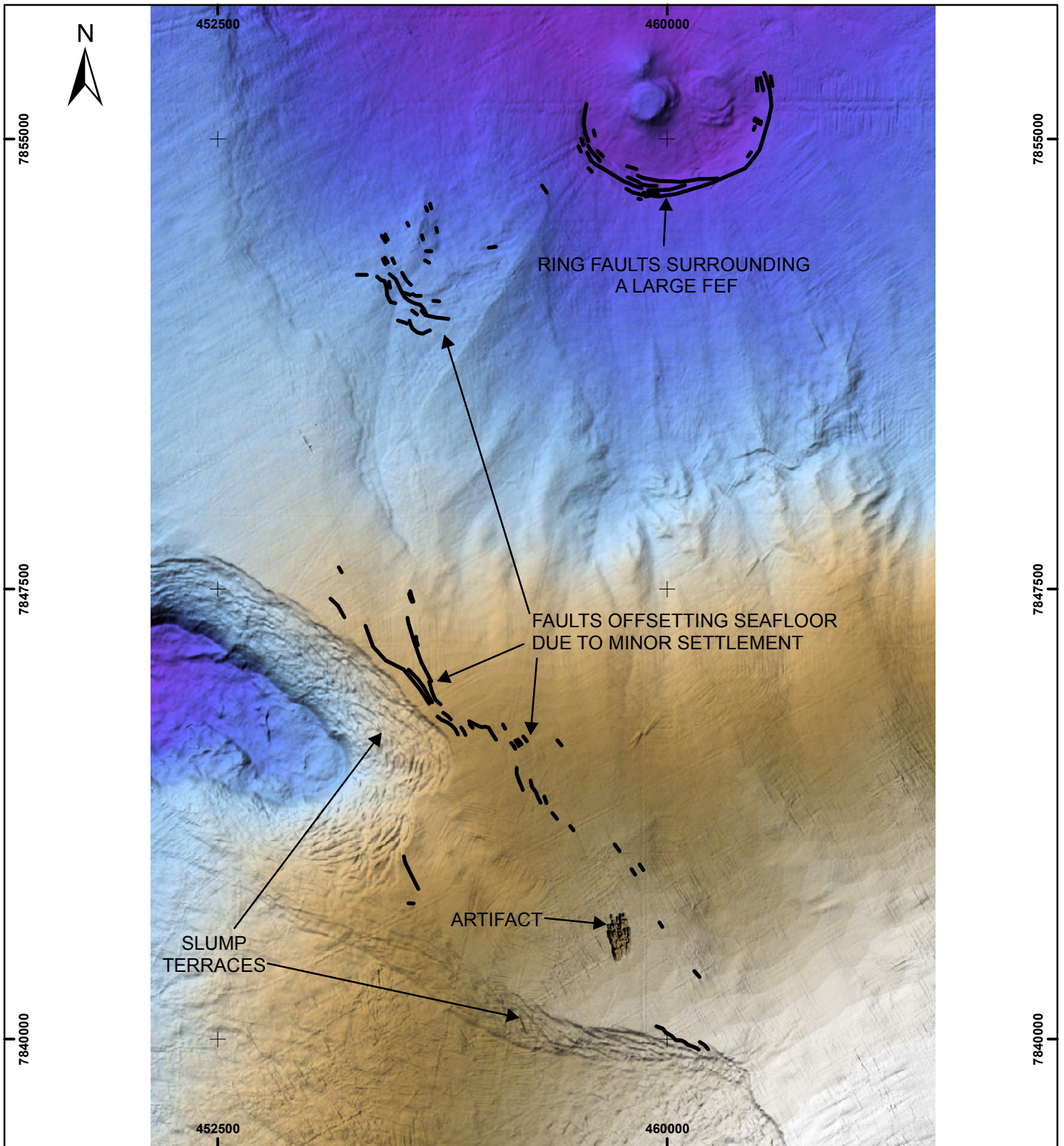


Example of a single, ribbon-like buried MTD in Unit 2 sediments. The MTD ranges in thickness from ~30 m to 3 m at its distal end (NW).



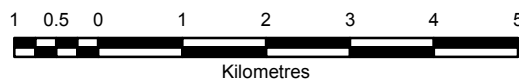


Sub-bottom Profile (Lines 092571339 & 092571436) showing gas pillars above a buried MTD.



NAD83, UTM ZONE 8

DWG No : 20110068-MBB-SFFLT-P65-0
Project No. 20110068

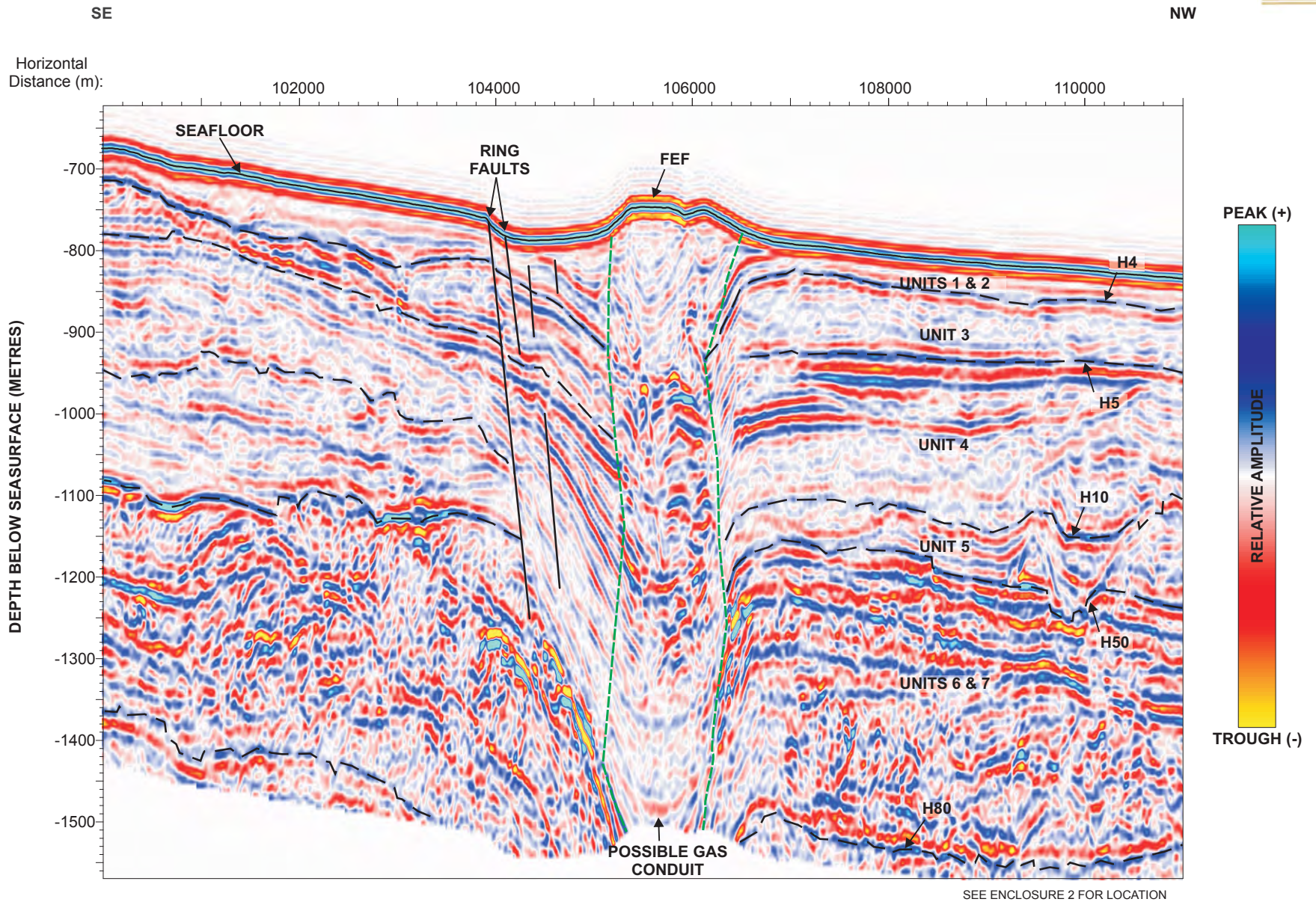


— SEAFLOOR OFFSETS

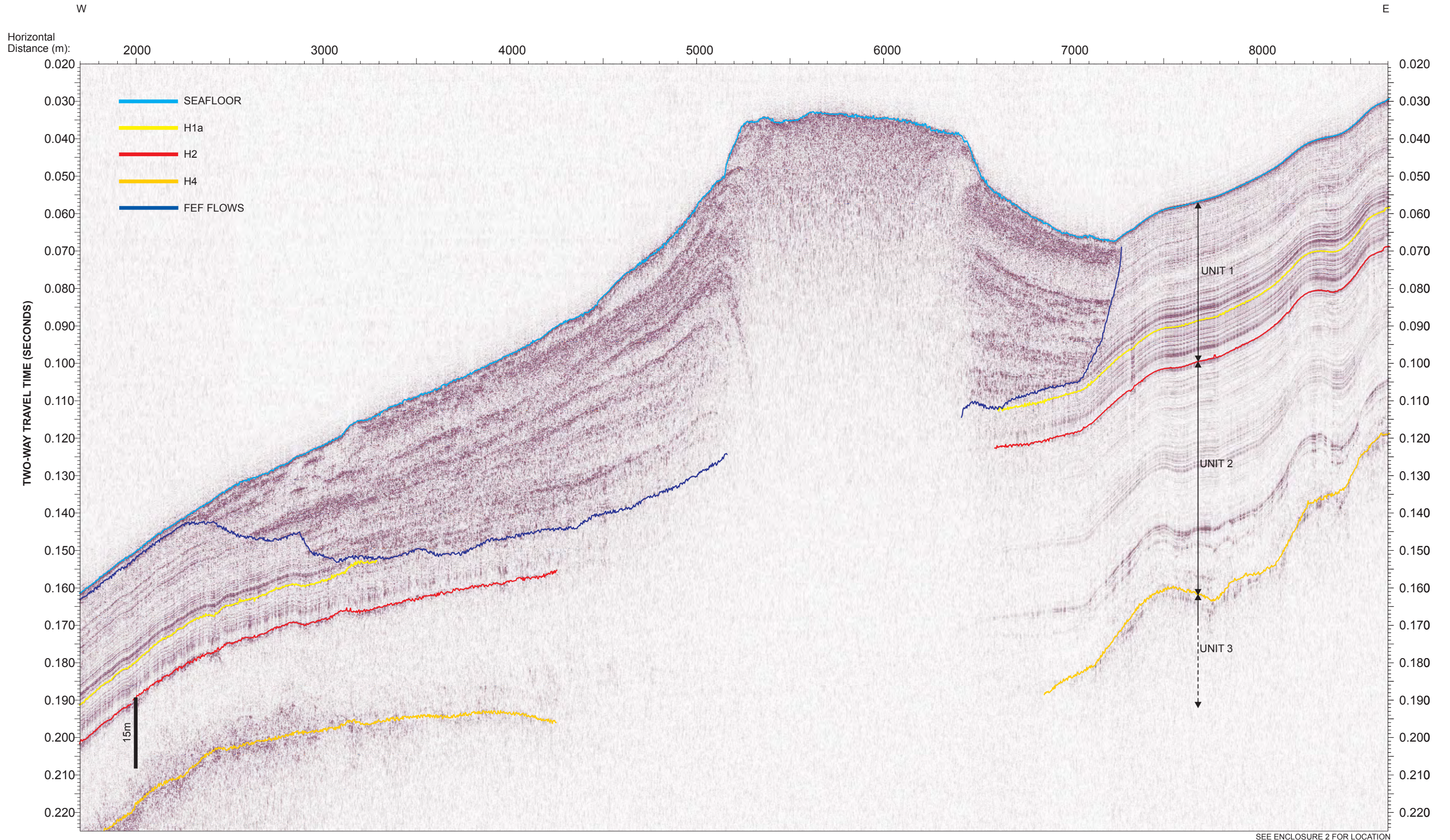


Illustration of small-scale faults that offset the seafloor. Faults associated with minor settlement generally offset the seafloor <1 m to 3 m. Ring faults around the FEF have offsets of 5 m to 10 m. Faults are mapped from sub-bottom profiler data.

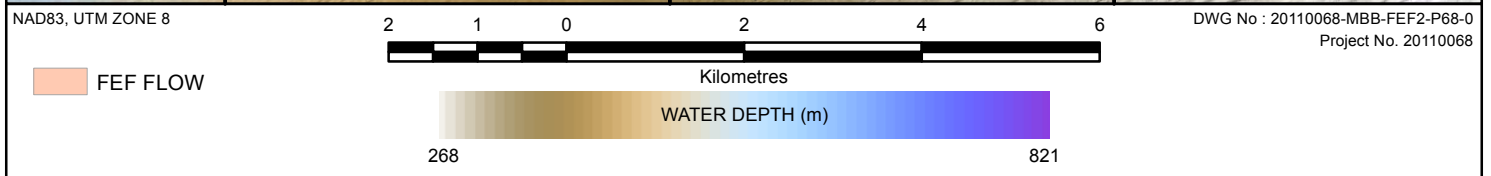
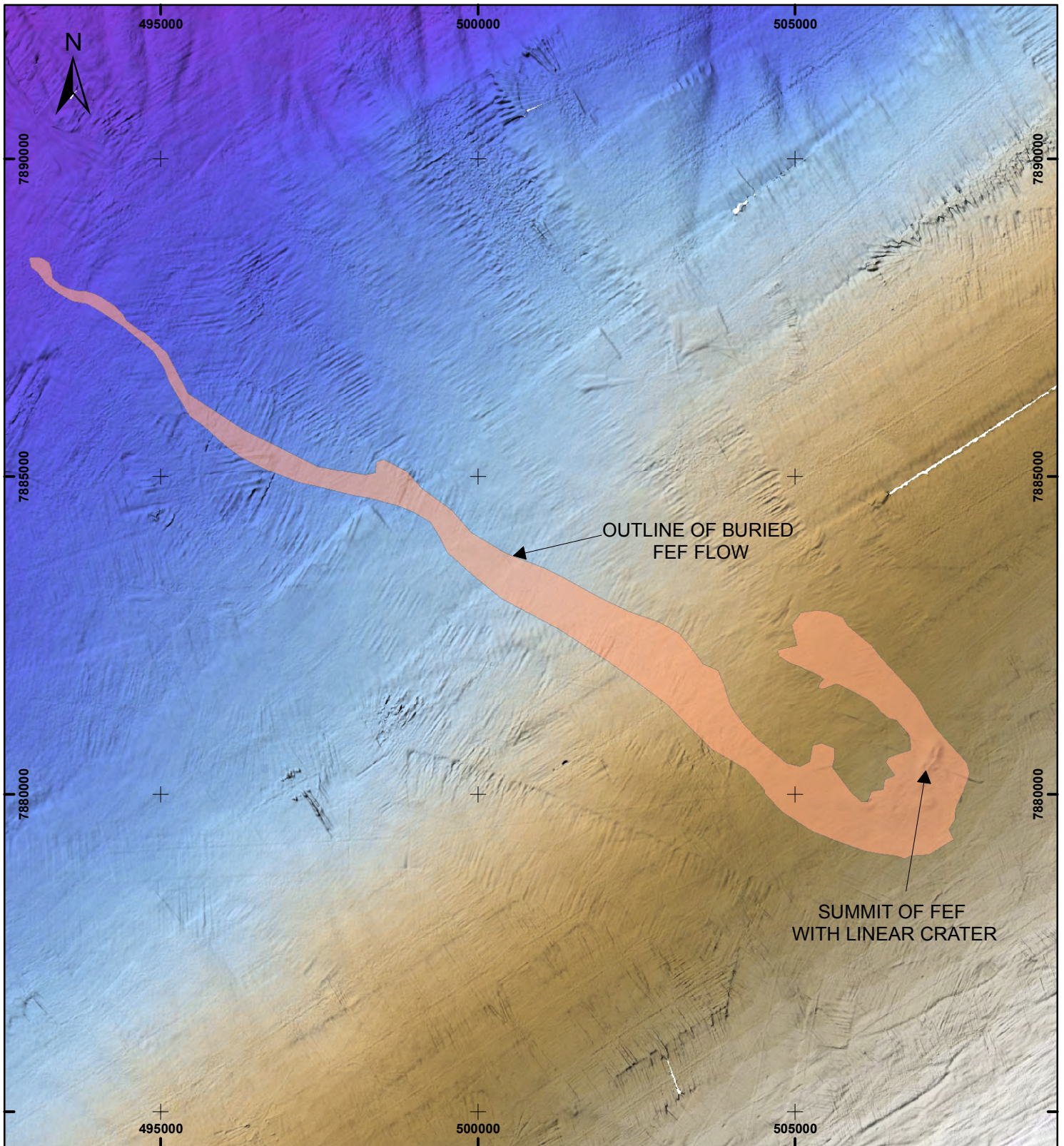




2D seismic profile through a large FEF. This is the same feature as illustrated in Plate 5.9. Note the column of possible gas extending to at least 750 m BSF beneath the FEF, and ring faults that extend to ~450 m BSF. Beaufort SPAN Line BE1-4200, courtesy of ION Geophysical Corporation.

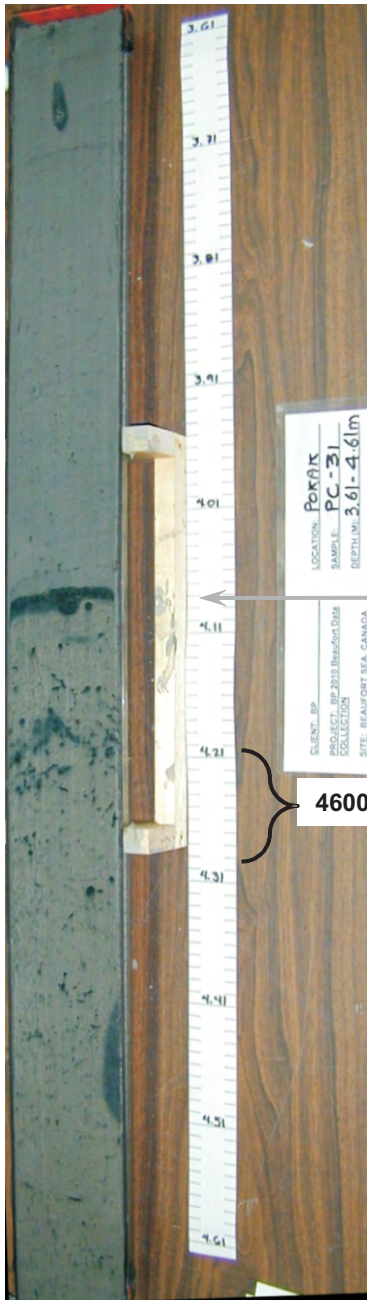


Sub-bottom Profile (Line 092580826) through a slope FEF. A stacked series of flows can be clearly seen as high amplitude reflectors surrounding the flank of the cone. The dark blue line marks the base of the flows. Note a flow very close to the modern seafloor on the left side of the profile suggesting recent eruptive activity.

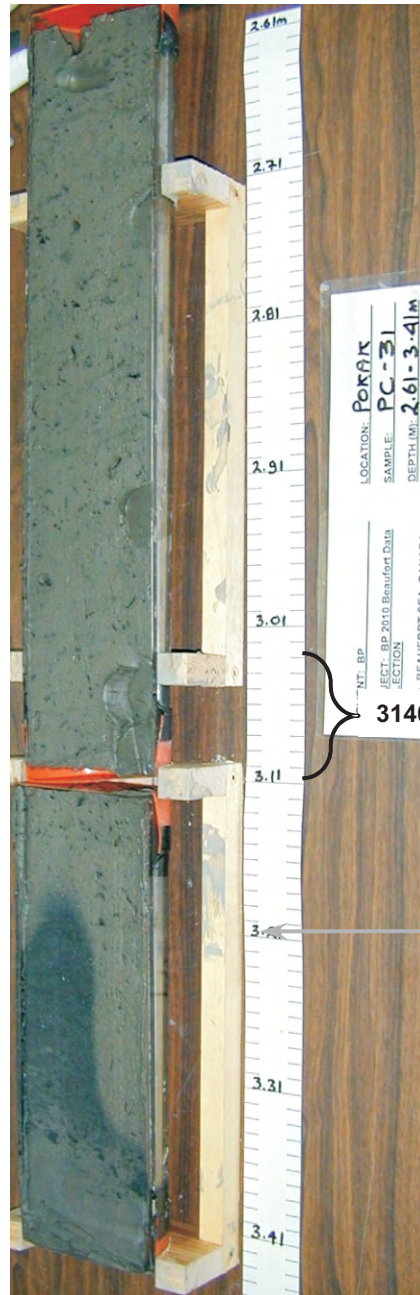


Example of buried FEF flows around a slope FEF. There are two branches oriented downslope to the northwest. One is 3 km long, 0.5 km to 1 km wide and extends from the northeastern margin of the FEF, and a longer flow extends from the southwest side of the FEF. The longer slightly meandering flow is 0.5 km to 1 km wide and 15 km long. The flow is no thicker than ~1 m, suggesting it may be the result of a single effusive event.





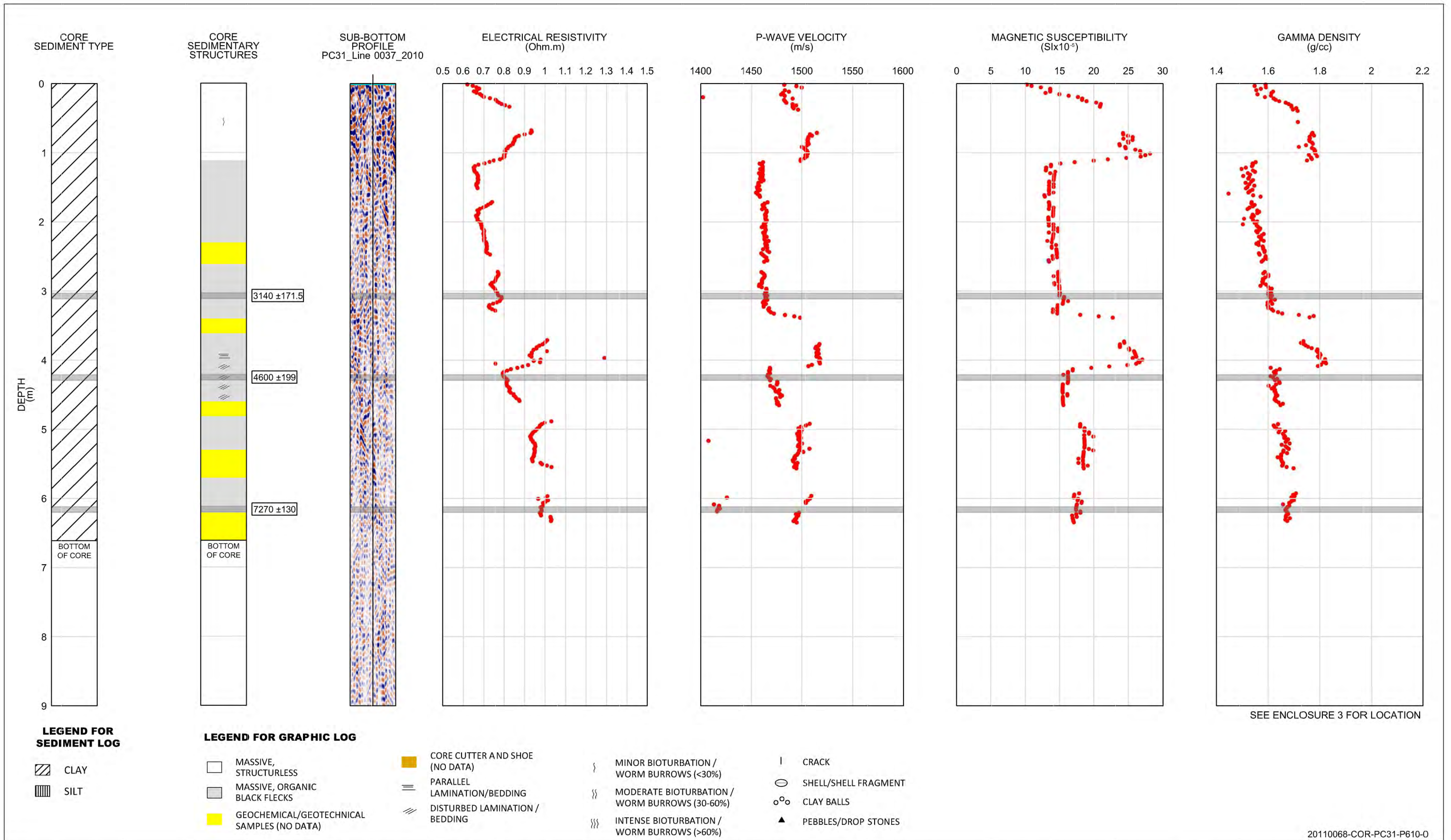
FEF flow



FEF flow

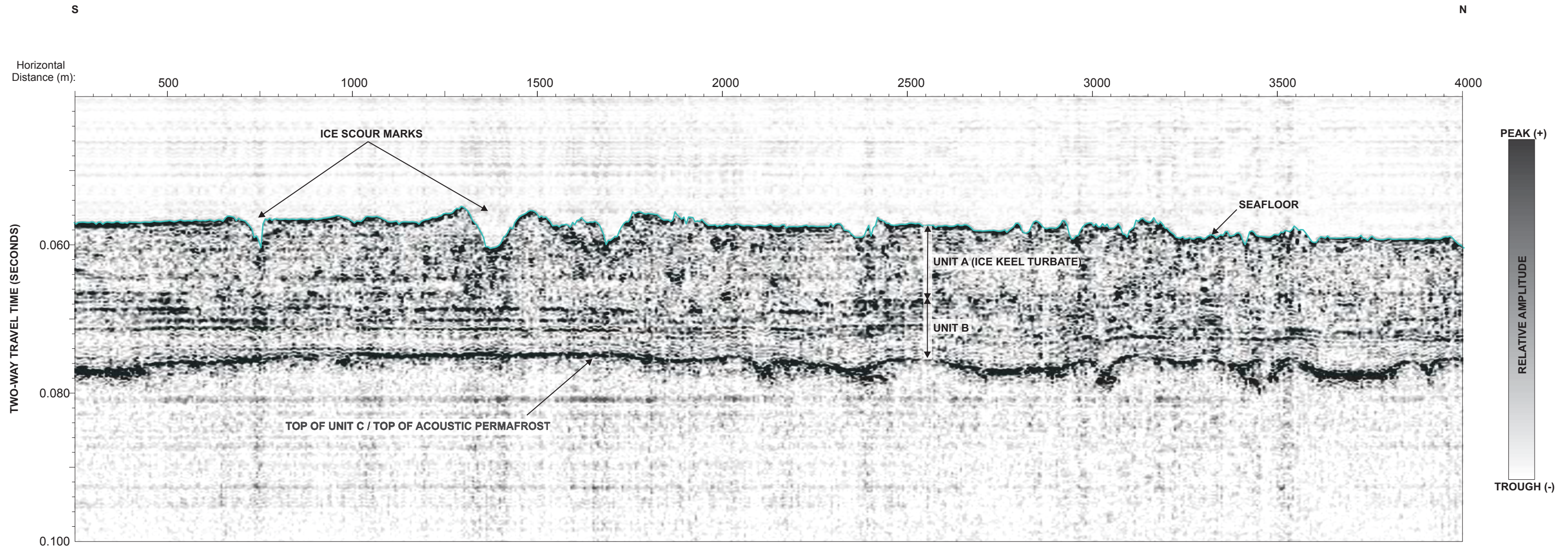
SEE ENCLOSURE 3 FOR LOCATION

Photographs of core PC-31. The left and right images show, respectively, the interpreted lower and upper boundary of an FEF flow from a slope FEF. Bounding C_{14} dates of 4600 ± 199 years BP and 3140 ± 171.5 years BP indicate an approximately 1460 year interval in which deposition of the FEF flow occurred.

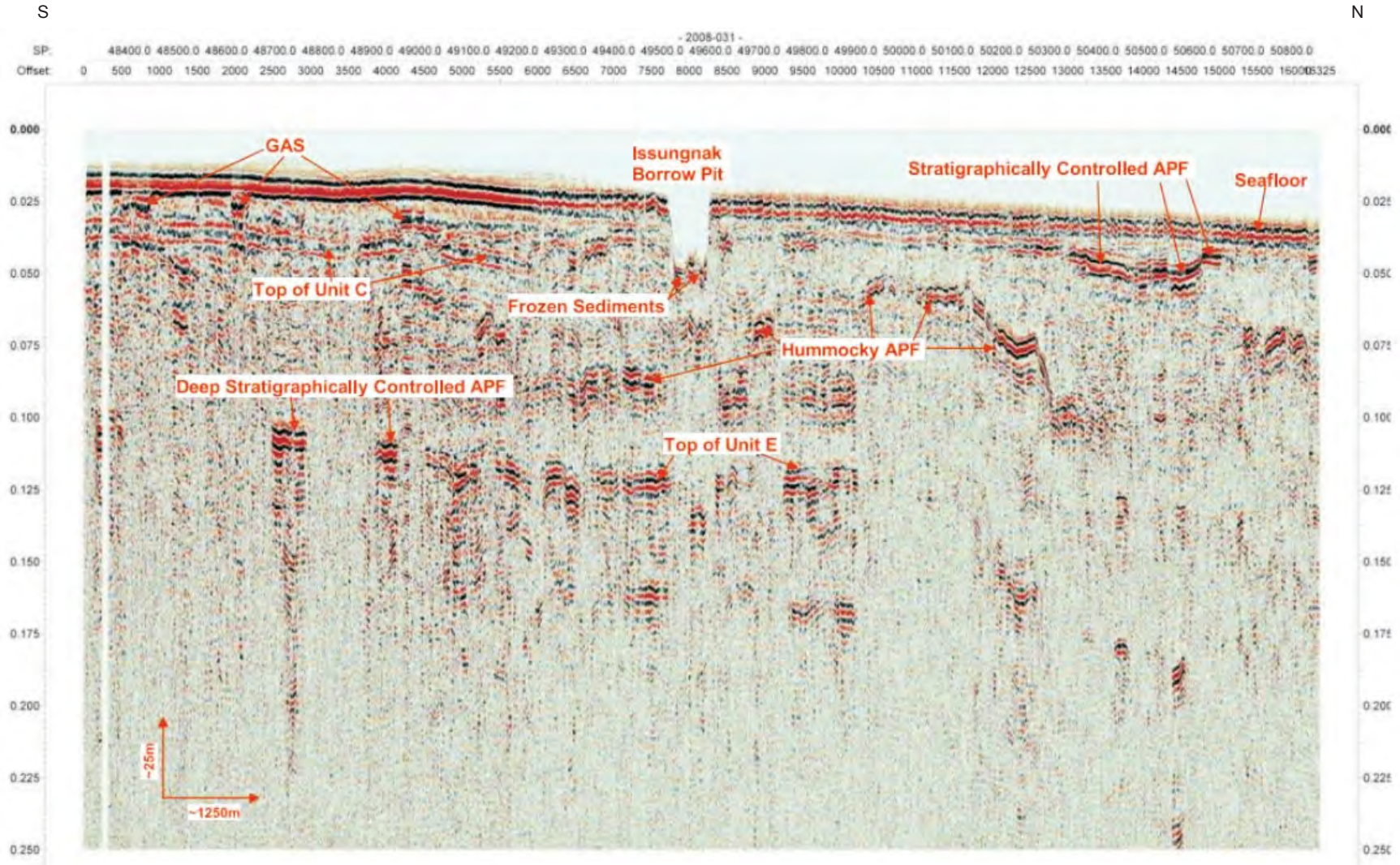


Log of core PC-31. The dated FEF flow between 4.06 m and ~3.2 m is clearly shown by peaks in electrical resistivity, p-wave velocity, magnetic susceptibility and gamma density. Another series of peaks between 1.1 m and the seafloor suggest the presence of a younger flow, the base of which is possibly as young as ~1000 years BP.

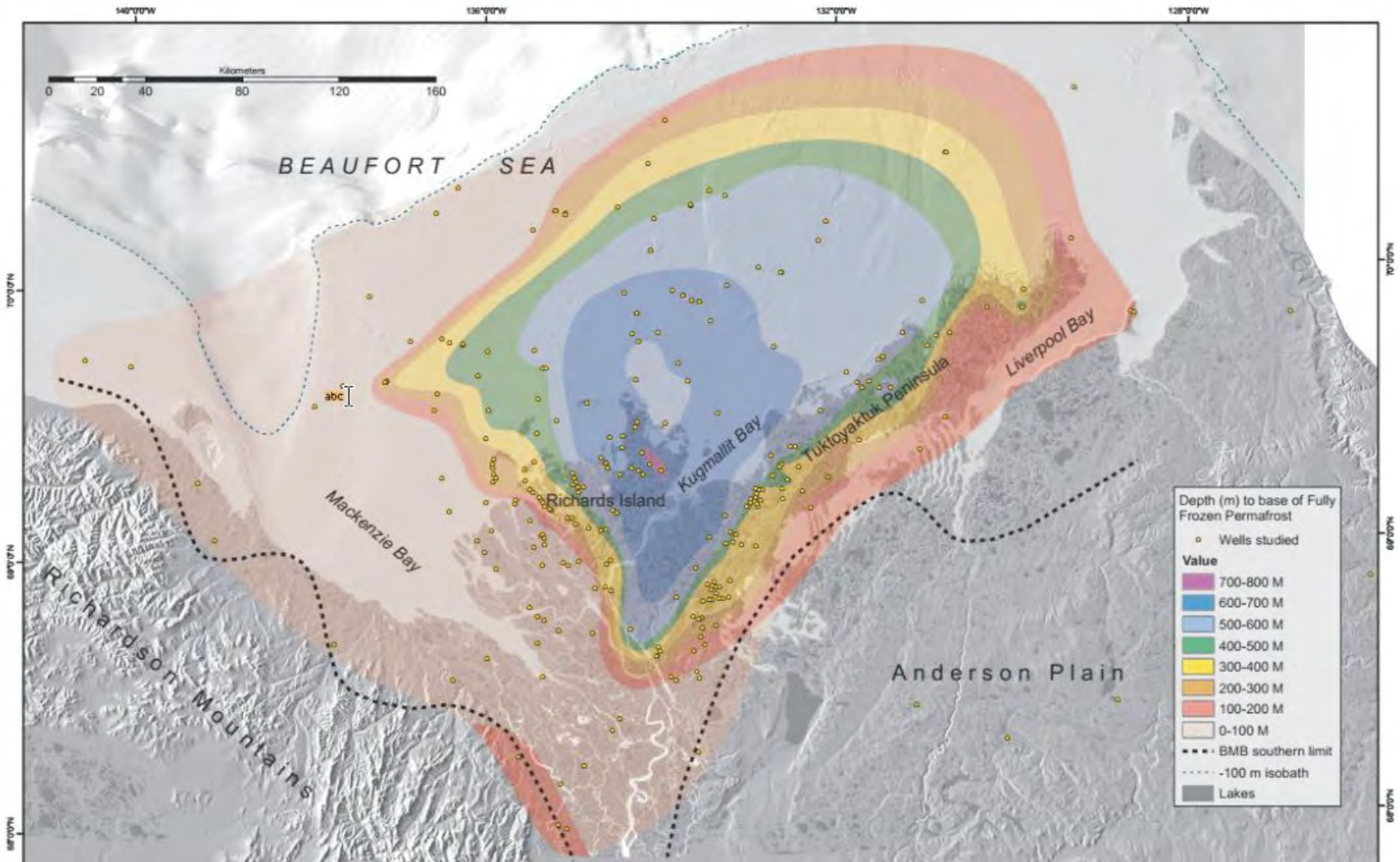




SBP profile north of Amauligak borehole 3F-24. This section shows massive Unit A and stratified Unit B sediments resting on the eroded, hummocky surface of Unit C. No structure is seen in the APF-affected sediments of Unit C. Line 0060_2010_232_1125_LF_utm.



High resolution multichannel seismic profile showing acoustic permafrost in the vicinity of the Issungnak Borrow Pit (Fig. 6.5.6 of Carr *et al.* 2010).



Map of depth to fully frozen ice-bearing permafrost in the BMB (Beaufort Mackenzie Basin) (Hu *et al.* 2013).

500000

550000

600000






780000

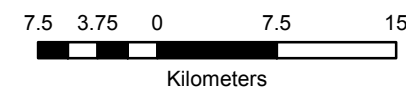
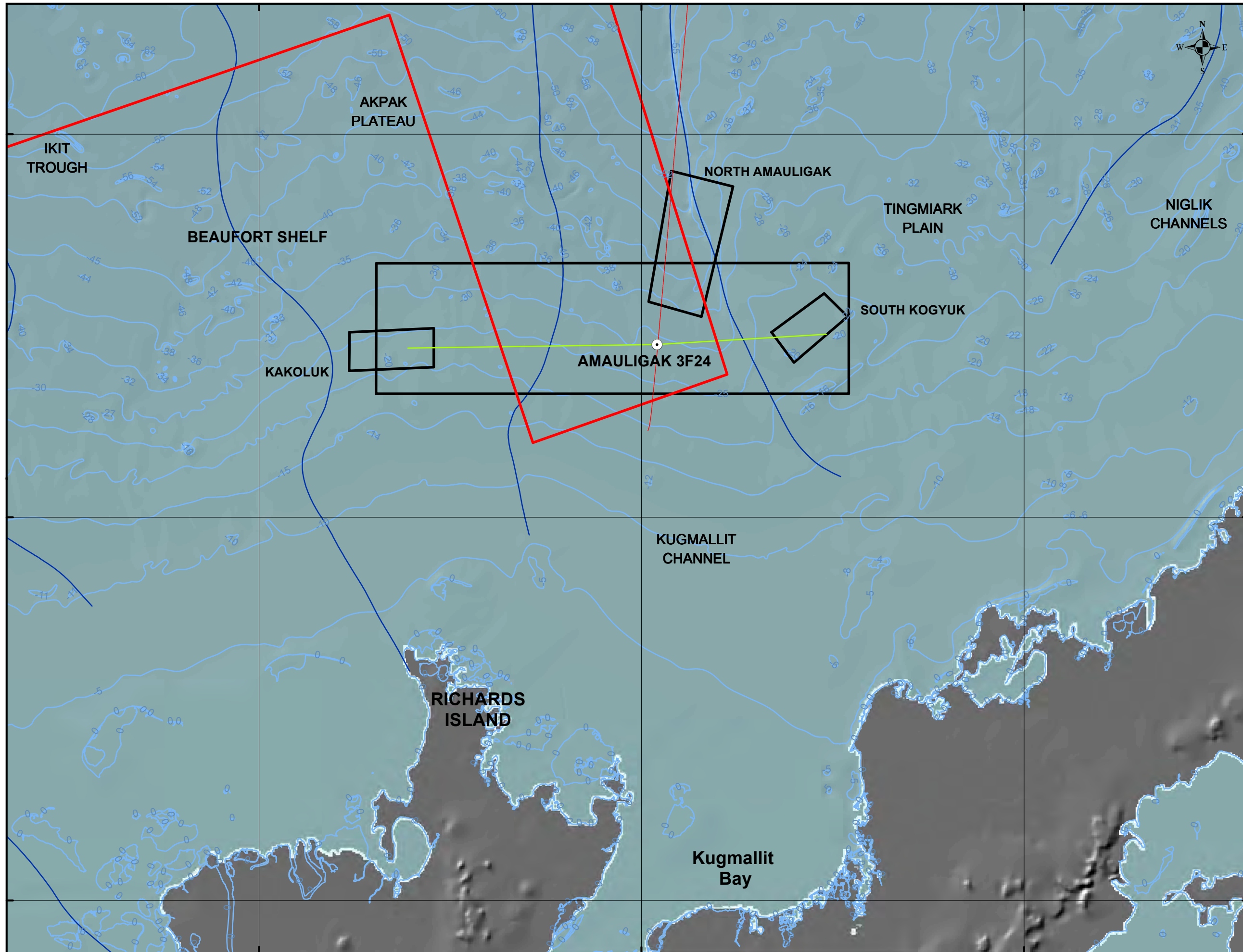
775000

770000

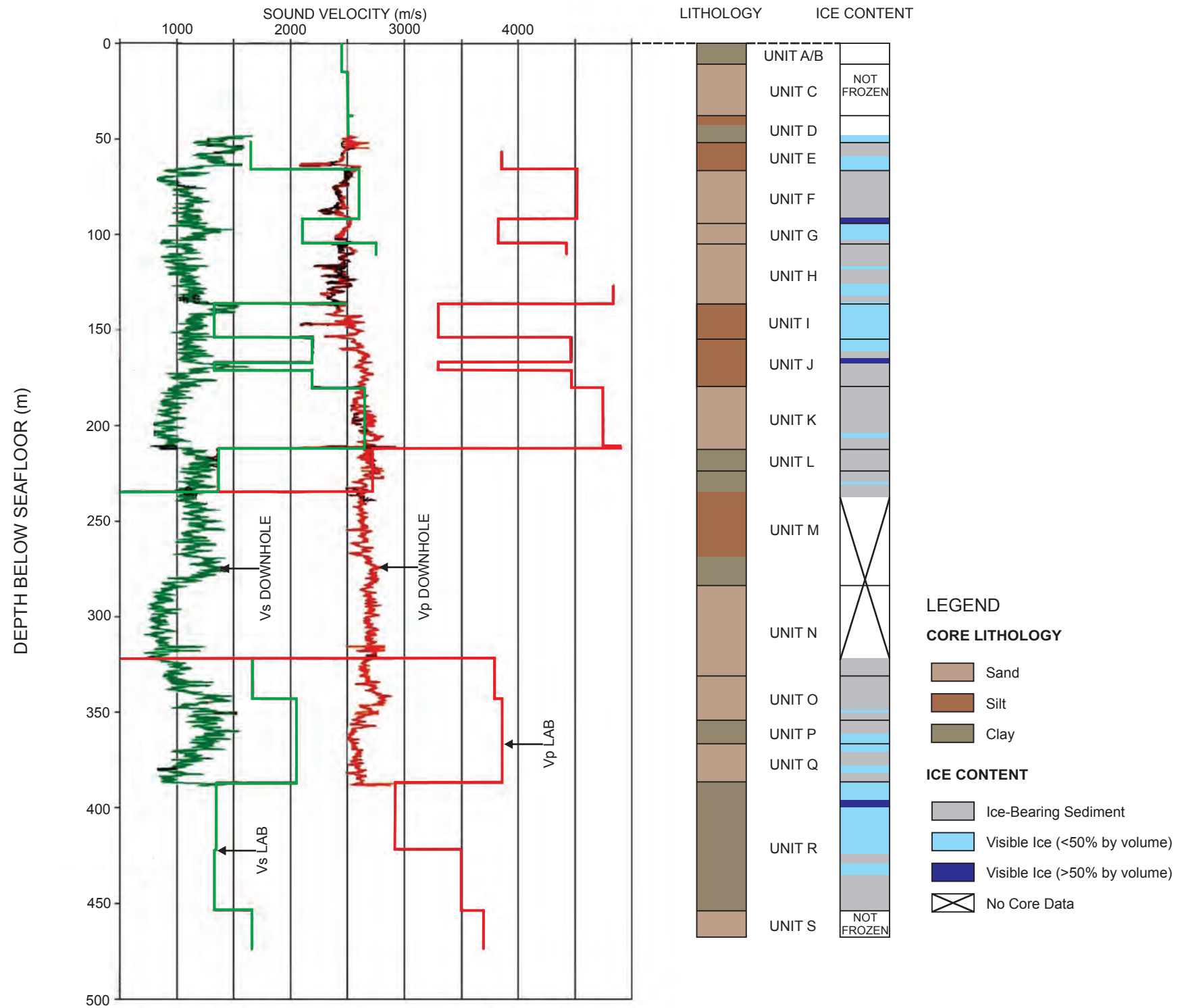


Legend

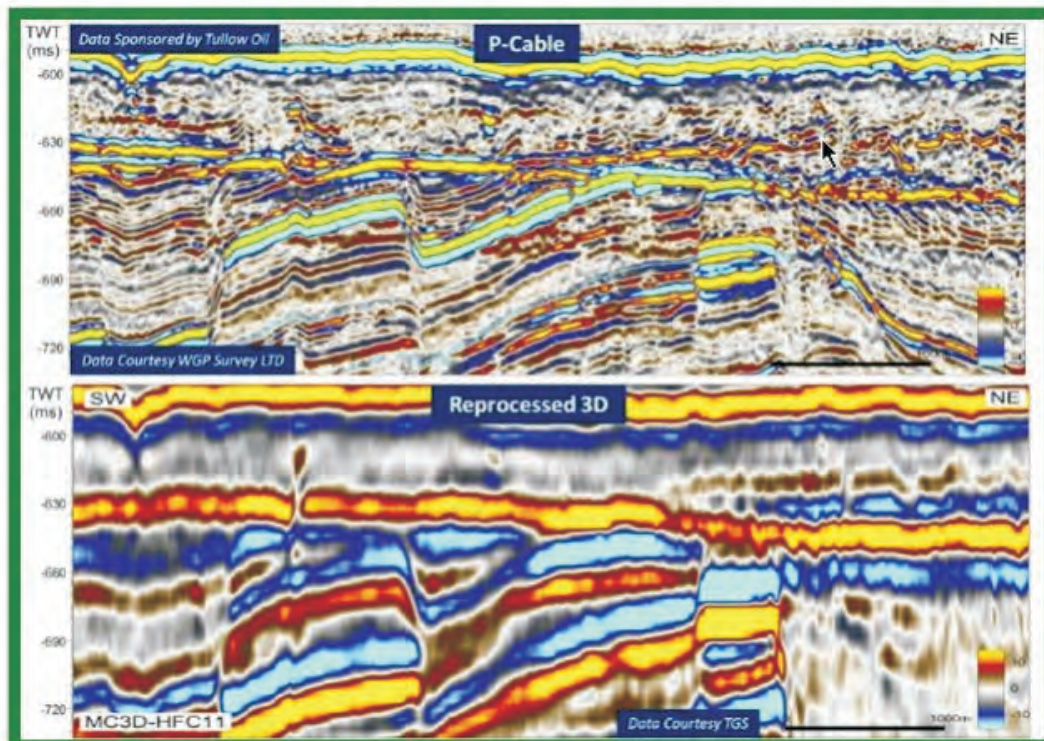
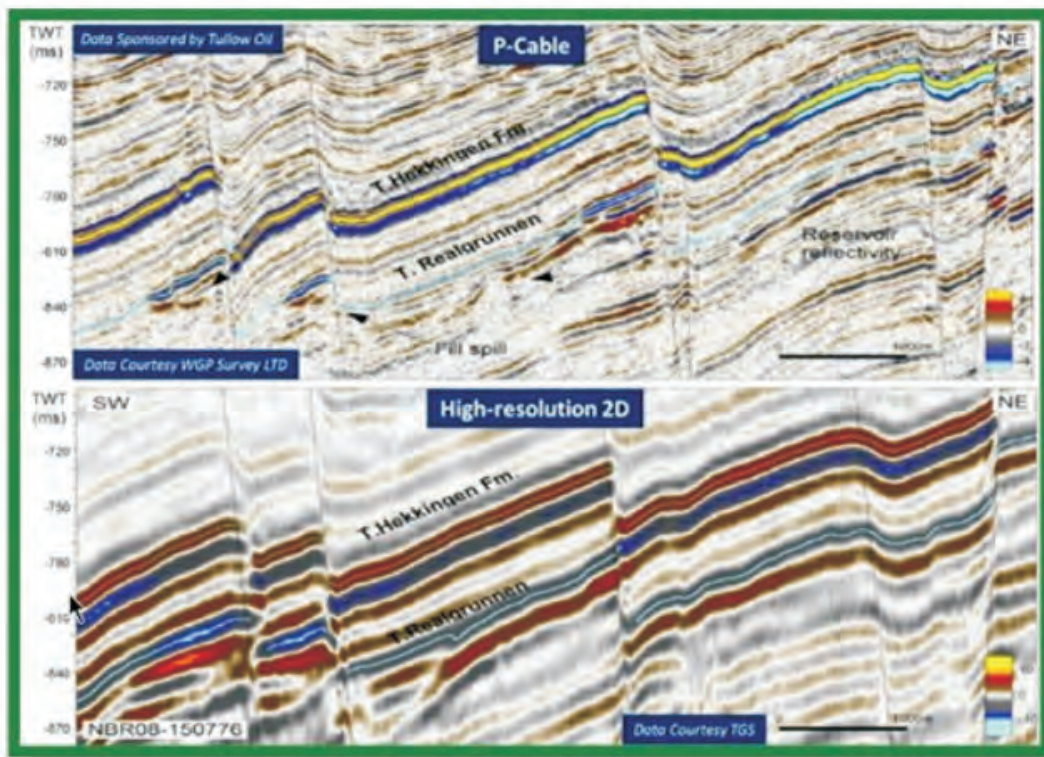
-  2-D SEISMIC LINE REPORTED IN MCGREGOR (1992b)
-  2D BEAUFORTSPAN SEISMIC LINE (BE3-3950)
-  WELLSITE SURVEY AREA (MCGREGOR 1992b)
-  STUDY
-  BOREHOLE LOCATION



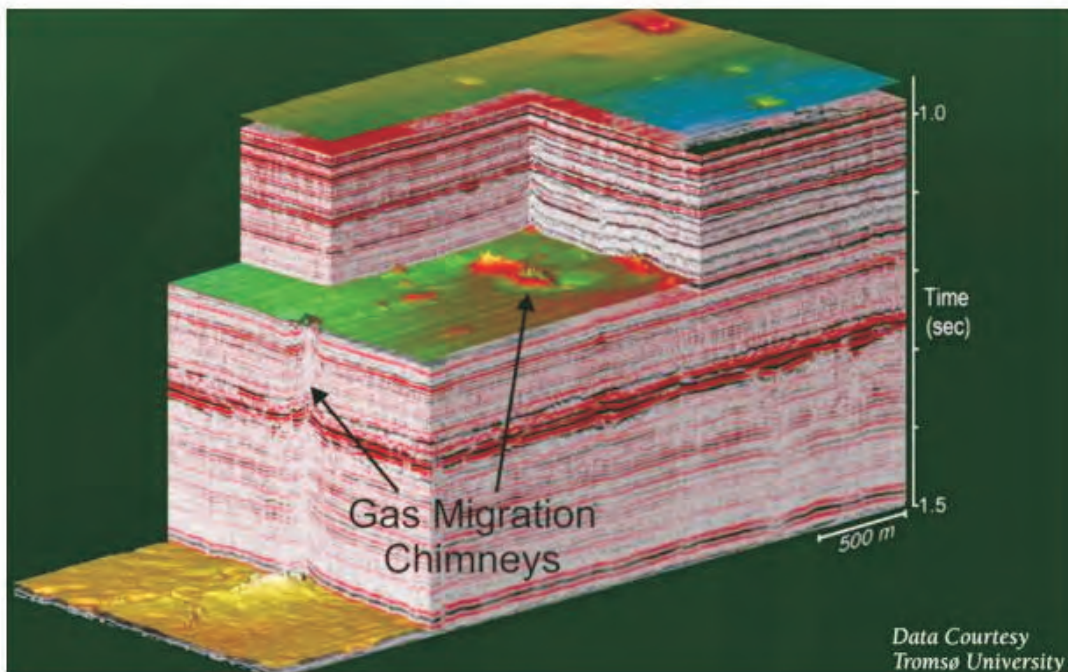
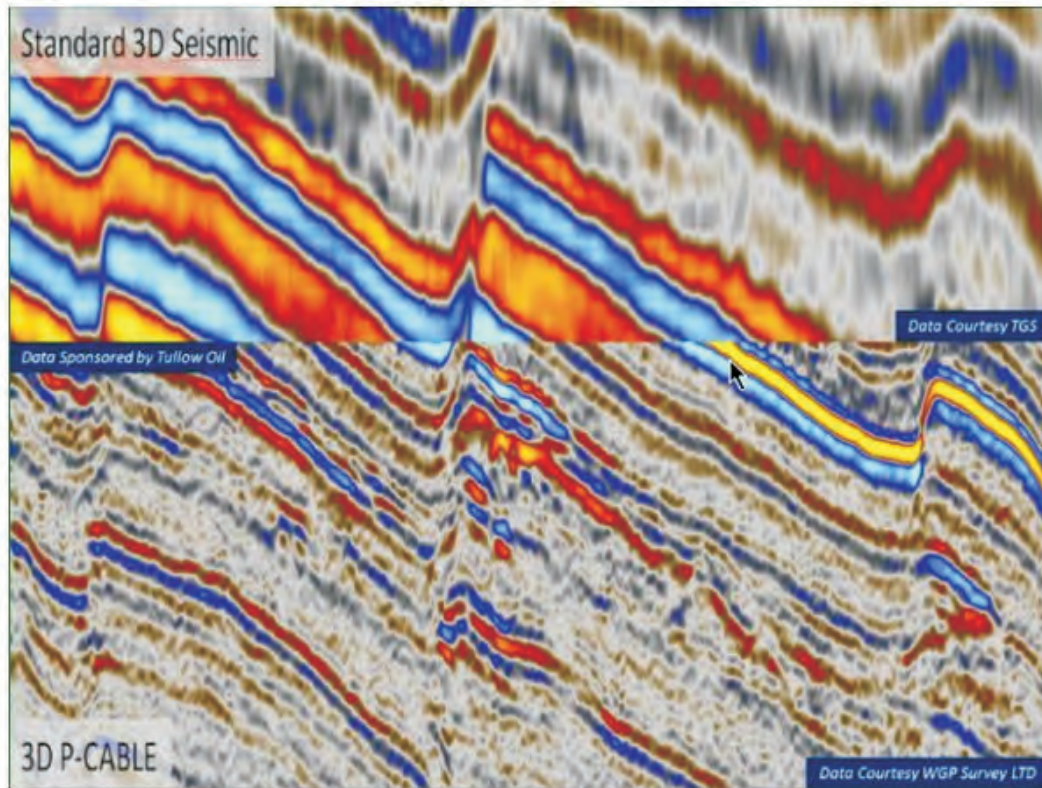
LOCATION OF GSC
 AMAULIGAK 3F-24 BOREHOLE
 AND REGIONAL 2D SEISMIC LINES



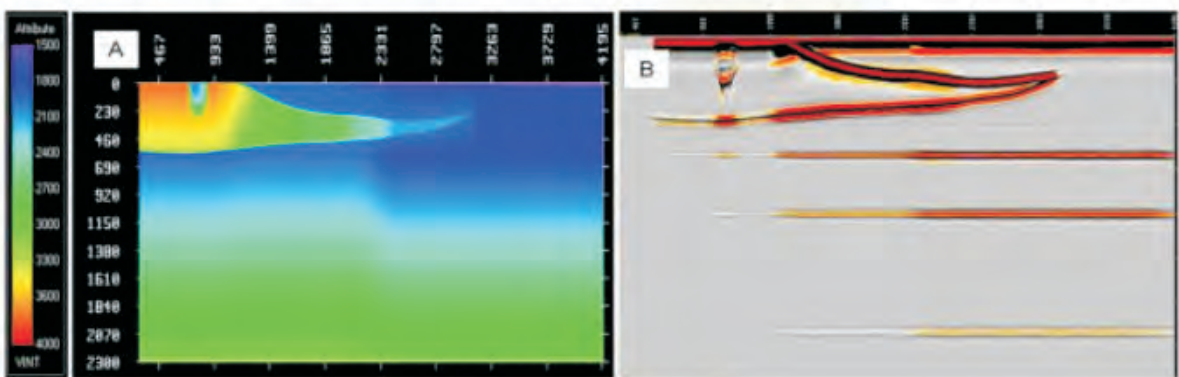
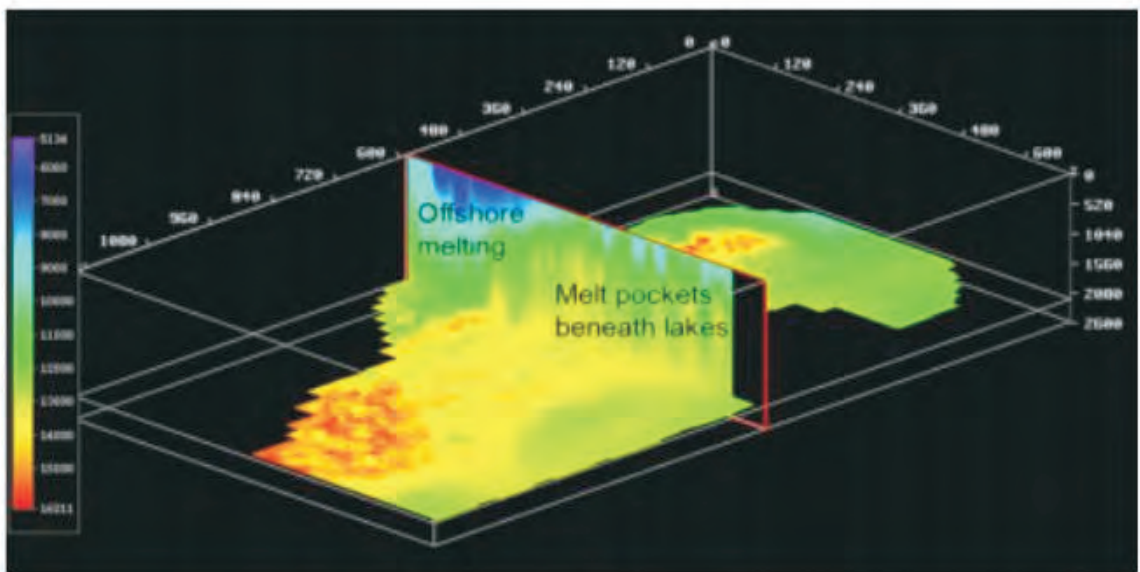
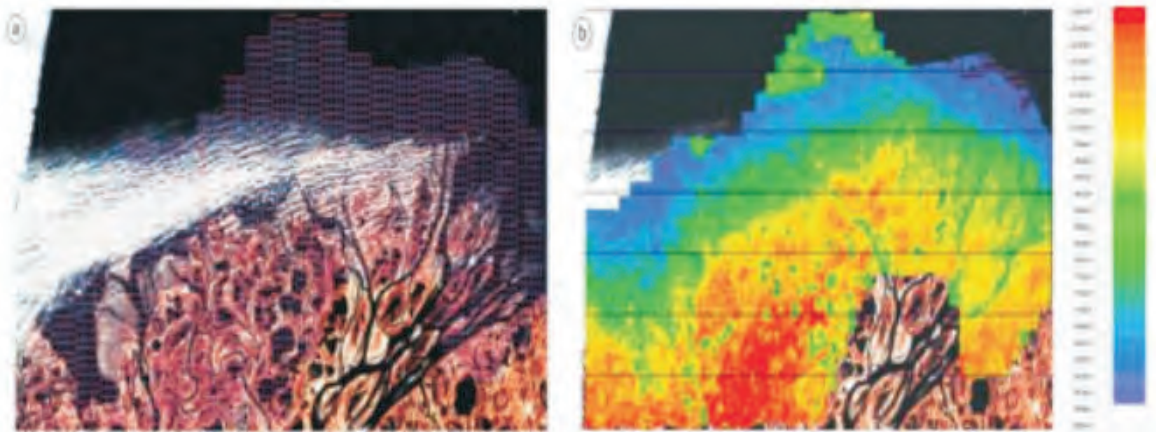
VELOCITY LOGS, LITHOLOGY AND ICE CONTENT OF THE AMULIGAK 3F-24 BOREHOLE.



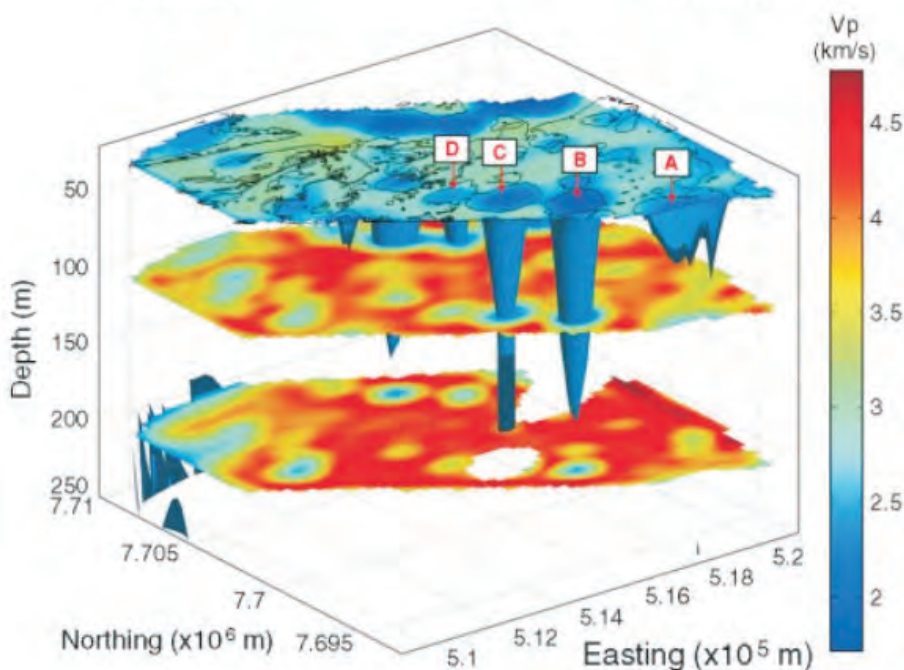
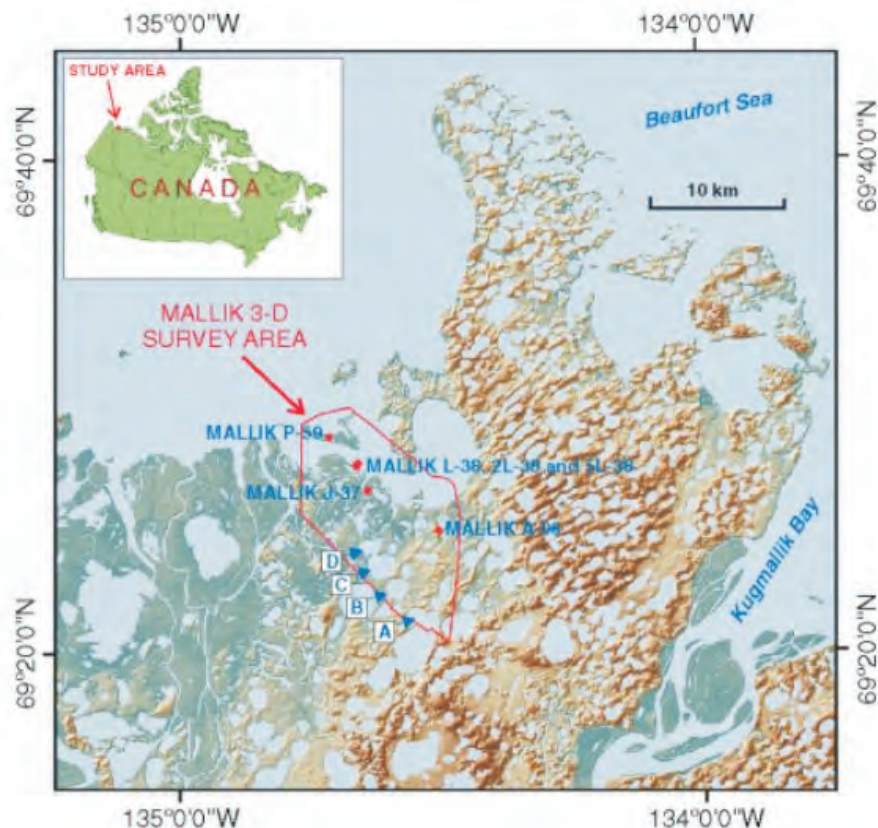
Examples of P-cable data comparisons with High Resolution 2D and reprocessed 3D data. (Geometrics web site)



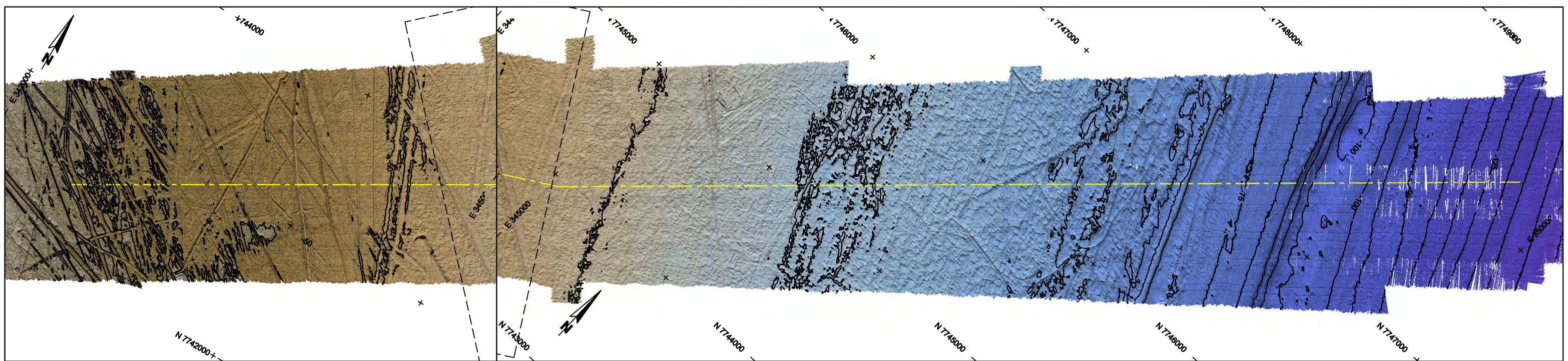
Top Image - P-cable data comparison to a standard 3D. Bottom image - P-cable 3D volume. (Geometrics web site)



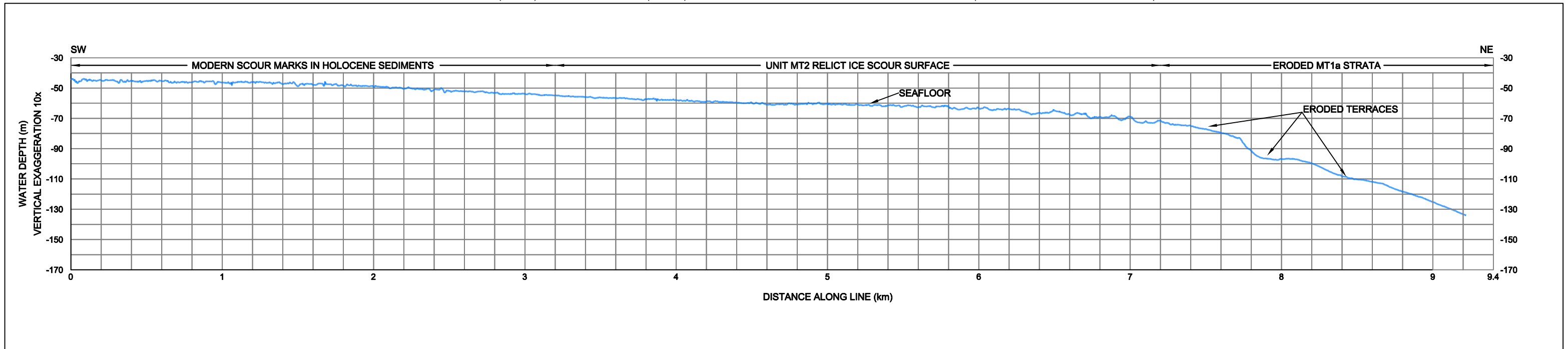
Sample images from Zhu *et al.* (2011). The top image to the left is an aerial photo from a coastal Canadian Arctic survey. The image immediately to its right is the tomographic velocity model at a depth slice of 60m overlaid on the aerial photo. The middle image is a cross section of the velocity field from North to South. The bottom images are a synthetic example of a transition zone between land and water with a high velocity permafrost zone. To the left is the synthetic model, to the right the prestack depth image as determined by the calculated velocity model. Excellent correlations are present in each example.



Location map of the Mallik 3D survey. Lakes labelled A and B are fresh water lakes; C and D are connected to the ocean by a small channel. Lower image - velocity model plunge view to the NE showing 3 velocity slices at 25 m, 100 m and 200 m. Unfrozen water in lakes B and C is observed to extend deeper than lakes A and D. Seismic amplitude blanking and strong frequency reduction were observed over all lakes (after Ramachandran 2011).



MULTIBEAM IMAGE (ABOVE) AND SEABED PROFILE (BELOW) OF THE MACKENZIE TROUGH TO YUKON SHELF TRANSITION (SEE SECTION 6.3.2 FOR DESCRIPTION)

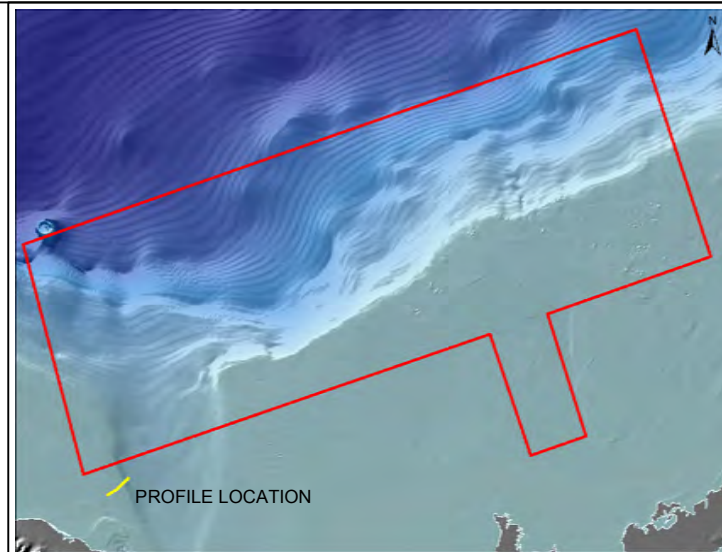
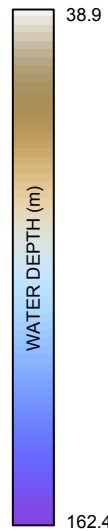


LEGEND

- LOCATION OF SEAFLOOR PROFILE
- 50** MAJOR CONTOURS (25m INTERVAL)
- MINOR CONTOURS (5m INTERVAL)

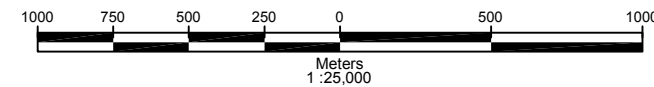
RENDERING PARAMETERS

AZIMUTH=315°
ELEVATION=45°
EXAGGERATION = 10

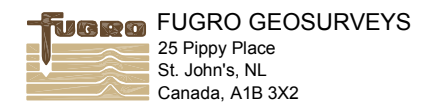


MAP PROJECTION DETAILS

GRS 80 ELLIPSOID
NORTH AMERICAN DATUM (NAD) 1983
UNIVERSAL TRANSVERSE MERCATOR PROJECTION; ZONE 8
CENTRAL MERIDIAN; 135° WEST
SCALE FACTOR AT CENTRAL MERIDIAN; 0.9996
FALSE EASTING; 500,000m
FALSE NORTHING; 0m

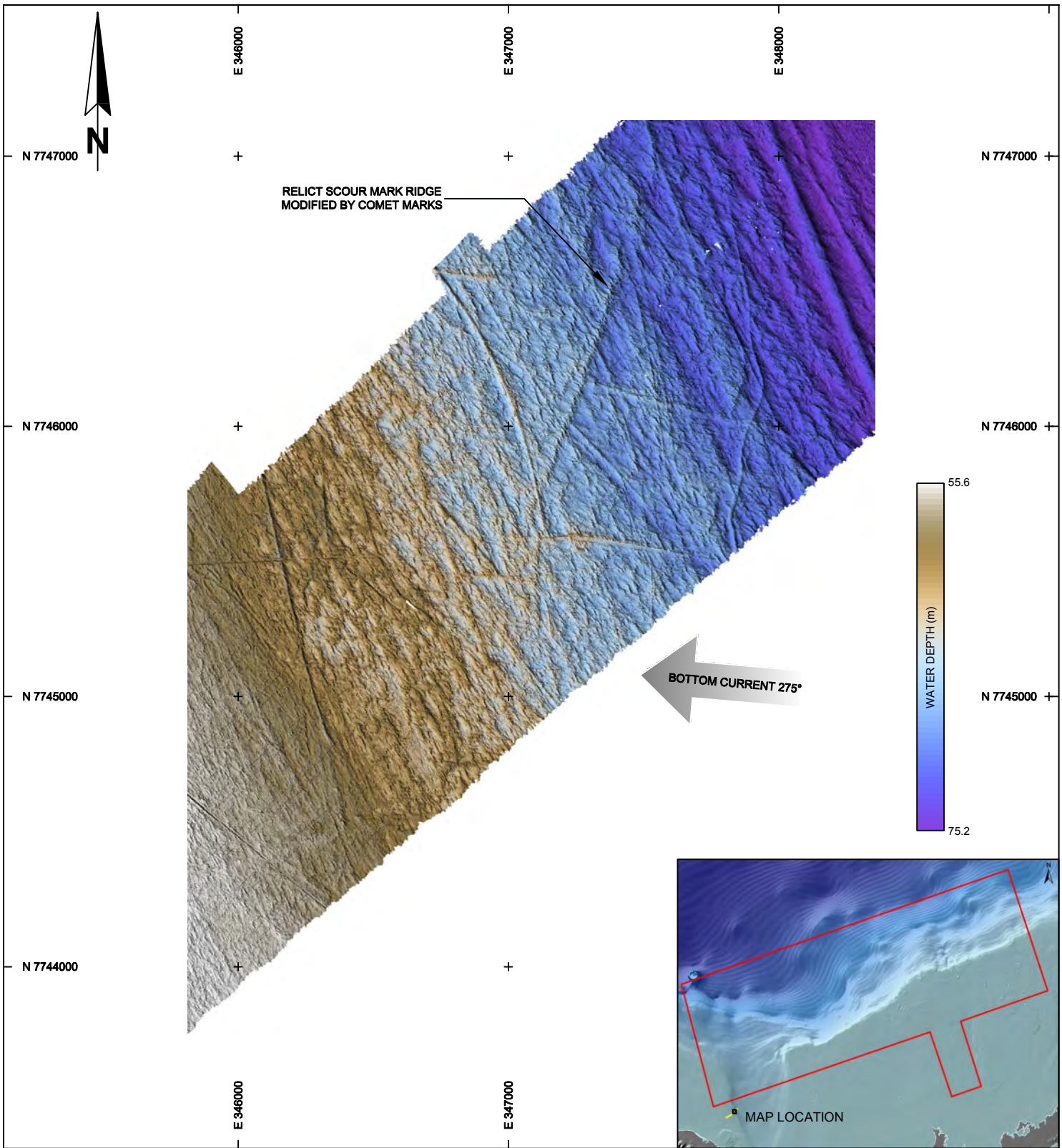


REVISIONS					
REV.	DATE	DESIGNATION	DRAWN	CHECK'D	APPR'D
4					
3					
2					
1	DEC. 03/15	SEE CRN No. 918 FOR CHANGES	AC	CWL	EC
0	SEP. 09/15	ISSUED FOR FINAL REPORT	CS	CWL	EC
DRAFT C	MAR. 30/15	DRAFT C SUBMISSION FOR REVIEW	AC	CWL	EC



TITLE
**MACKENZIE TROUGH/YUKON SHELF
MULTIBEAM BATHYMETRY AND PROFILE**

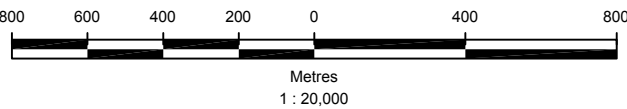
DWG No. : 20110068-RTE-MACT1-P620-1	PLATE 6.20	REV. 1
PROJ. No. : 20110068		
SURVEY DATE : N/A		
DRAWING DATE : DECEMBER 3, 2015		



NAD83, UTM ZONE 8

RENDERING PARAMETERS

AZIMUTH = 245°
 ELEVATION = 45°
 EXAGGERATION = 10

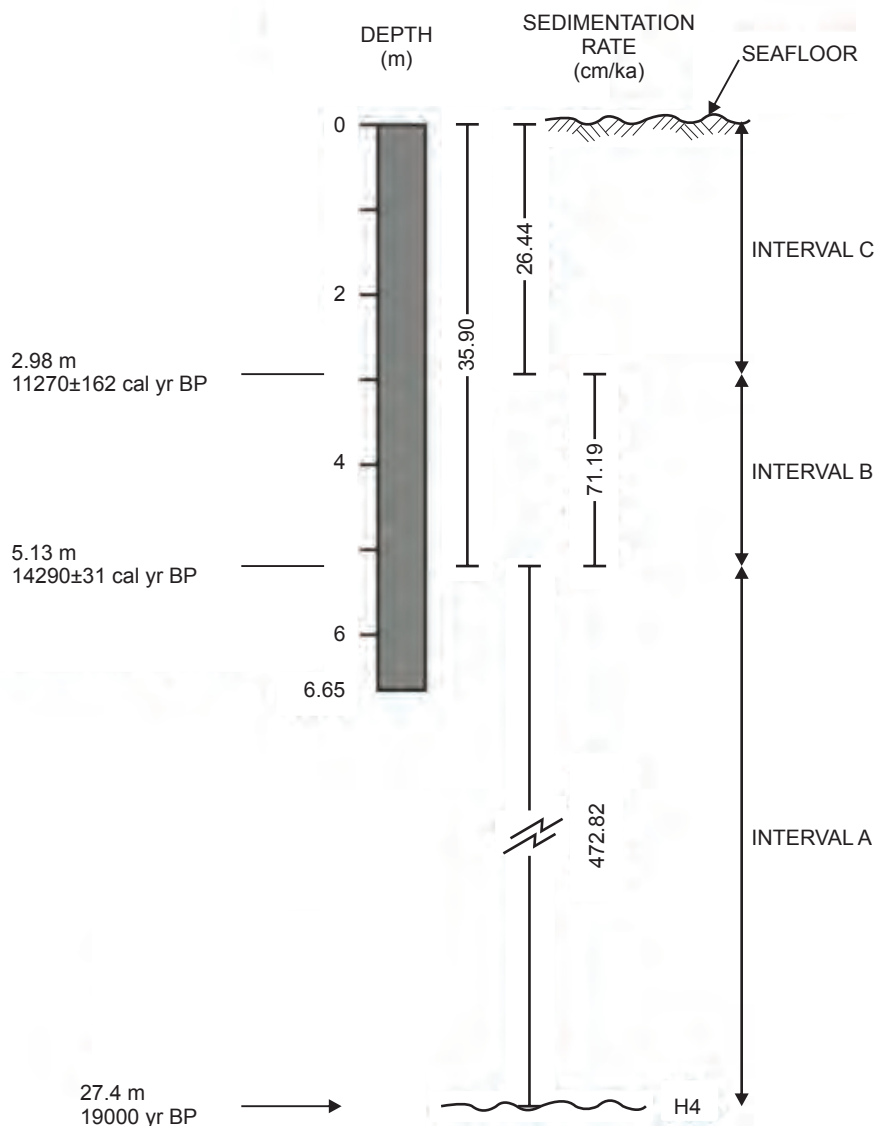


Dwg. No : 20110068-RTE-MACT2-P621-1
 Project No. 20110068

Current-formed comet marks affect the Unit MT2 relict ice scour surface. The comet marks are 20 m to 100 m long, 10m to 20 m wide and 0.5m to 1 m high and are particularly well developed on one of the relict ice scour mark ridges (arrowed). Zoomed in portion of multibeam image illustrated in Plate 6.20.



BP10-PC02



Example of the calculation of sedimentation rates (core BP10-PC02). Sedimentation rate in centimetres per thousand years (cm/ka) is calculated by dividing the depth in the core of the dated sample (assumed to be depth BSF) by the corrected carbon age. In this example, two corrected C_{14} dates and assumed ages for horizon H4 (19,000 yr BP) and the seafloor (0 yr BP) are available. Using these dated elevations three sedimentation rates may be calculated: A. 27.4 m (H4) to the deepest C_{14} date in the core at 5.13 m; B. 5.13 m to 2.98 m (the elevation of the two C_{14} dates); and C. 2.98 m to 0 m (seafloor). For the purposes of this study, where two or more dates are available in a core, only two sedimentation rates are calculated: H4 to the deepest core date, and from the deepest core date to the seafloor.

7. GEOLOGIC CONDITIONS AND GEOHAZARD FRAMEWORK: ~100 m to ~1000 m BSF

This section describes the geology and associated geohazards located deeper than ~100 m BSF, as interpreted from selected and available GSC and ION GXT multichannel seismic data. A 3D seismic volume from the mid- to upper slope was provided by Imperial Oil for comparison with overlapping 2D seismic data. Enclosure 8 shows four representative seismic profiles, including two BeaufortSPAN lines, a recent GSC 2D line and a GSC 2D legacy line. These are paired with matching arbitrary lines from the 3D volume. The two BeaufortSPAN lines are almost identical to the 3D arbitrary lines, capturing the same details of sedimentary architecture that can be used in identifying and mapping potential geohazards in the 100 m to 1000 m BSF interval. Resolution of the 3D data appears slightly better, with finer detail in stratification evident. The recent GSC profile lacks the fine resolution of strata seen in the 3D data, and the legacy line is of much coarser resolution.

For ease of description, deep sub-seafloor conditions and geohazards are discussed in terms of three geographic regions: the Continental Slope, Beaufort Shelf and Mackenzie Trough/Yukon shelf.

Throughout the Pliocene and Pleistocene the continental shelf was continually accreting by progradation of the continental slope into the Canada Basin, and by vertical aggradation of the continental shelf. These margin-building processes are exemplified by the Iperk Sequence as sedimentation kept pace with regional subsidence (e.g. Dixon *et al.* 1992; Blasco *et al.* 1990; Dietrich *et al.* 2011), evidence of which can be seen in cross-shelf seismic sections (Plate 7.1). As the shelf advanced the continental slope was similarly prograding northwards and aggrading, marked by continuous sedimentation and slope failure. Much of the sediment associated with these failures flowed north out of the study region and across the Canada Basin as turbidites, forming strata up to 4 km thick of equivalent age to the Iperk Sequence (horizon H10 to seafloor of Mosher *et al.* 2011; 2012).

7.1 Continental Slope

Throughout the Pleistocene glaciation and early deglaciation slope failures were common, and evidence of their occurrence can be mapped in the subsurface as buried MTDs, topographic unconformities and disconformities. Slope Units 1 to 3 identified and described from SBP data represent a late glacial to deglacial sediment package, characterized by continuous pelagic sedimentation during which three different phases of slope failure occurred leading to three distinct types of mass transport deposits: sheet-like, finger-like and broad, and retrogressive slump failures (described in Sections 6.1.1, 6.1.2 and 5.1.1, respectively).

In 2D seismic data, MTDs are characterized by poorly stratified, chaotic or structureless intervals, often with irregular basal and upper surfaces. MTDs are typically sandwiched between, and often truncate, well to poorly stratified sediments. The close association of

facies indicates that pelagic sedimentation and slope failure were synchronous, as documented in surficial slope Units 1 to 3. MTD/stratified sediment packages may represent glacial and interglacial/interstadial cycles, but this cannot be stated with confidence, due to the complexity of slope stratigraphy and because of difficulties in correlating shelf and slope sequences.

Unconformities and disconformities mark the erosional basal surfaces of slope failures and of channels that served as conduits for MTDs and more fluidized flows. Many unconformities preserve original rugged seafloor topography of significant relief from as little as 20-30 m over distances of ~600 m but ranging up to nearly 500 m over distances of 6 km (e.g. Plates 7.2 to 7.4). Buttress unconformities occur where stratified sediments lap against the steep walls of buried channels or steep failure surfaces, and can be hard to distinguish where the stratified fill of younger sediments is parallel to older, truncated strata (Plates 7.2 and 7.5).

Large vertical and horizontal variations in deposit type and style suggest that tophole prognoses for potential exploratory well locations on the continental slope will exhibit significant vertical differences in sediment facies and sediment type between nearby sites. Large vertical variability means that sediments are not likely to be normally consolidated, and changes in the pre-consolidation pressures of the soils may be expected across boundaries between stacked MTDs and between stratified sediments and overlying and underlying MTDs. Four arbitrary vertical profiles shown in Plate 7.3 illustrate the vertical variation in seismic facies.

7.1.1 Buried Mass Transport Deposits

Throughout Units 4 to 7, 2D seismic data show a thick sequence of laterally discontinuous and truncated packages of MTDs sandwiched between well to poorly stratified pelagic sediments. Stratified sediments are similarly discontinuous and truncated by unconformities.

The relatively thin MTDs identified in surficial Units 2 and 3 from SBP data are barely discernible in seismic profiles due to relatively coarser vertical resolution. As a result, thick underlying MTD intervals identified in seismic profiles could potentially represent multiple events that are not resolved (e.g. Plates 7.2 and 7.3). MTDs are typified by vertical intervals of distorted to chaotic, low to moderate amplitude reflectors (Plates 7.2 to 7.5). In slope-parallel seismic profiles they range in thickness from approximately 150 m to 425 m and 5 km to >40 km in horizontal extent, and in downslope profiles from 80 m to 450 m thick and 10 km to 85 km long.

Globally, seafloor regions affected by slope failures often have gravitational spreading recognized immediately downslope of terraced headwall regions. Here 'ridge and trough' morphologies are formed by trapezoid-shaped spreading blocks as a result of extension and thinning (e.g. Micallef *et al.* 2009; 2007a,b; Kvalstad *et al.* 2005; Quinn *et al.* 2007). Spreading blocks have been recognized on the Norwegian slope notably in the Storegga slide, and also in the Trænadjupet, Nyk and Hinlopen slides, and from the Mediterranean

Sea in the BIG'95 and Nuna slides and Eivissa Channel slides (Micallef *et al.* 2007; Lastras *et al.* 2006). Features that appear to be spreading blocks have been identified in the near-surface portion of Unit 3 on the Yukon continental slope (Plate 7.6).

7.1.2 Stratified Sediments

Stratified pelagic sediments are typically eroded and truncated by MTDs, however in places thick sequences of undisturbed strata do occur (e.g. Plates 7.2 and 7.3). In slope-parallel seismic profiles the stratified packages may range from 30 m to 480 m thick and extend laterally from 8 km to 68 km (e.g. Plate 7.3). On downslope profiles thicknesses of between 60 m and 500 m are observed and lateral extents range from 21 km to 35 km (e.g. Plate 7.2). The majority of these packages occur within slope Units 6 or 7, and several may be continuously traced upwards from Unit 6 into Unit 7. If these strata were deposited at similar sedimentation rates to those computed for Units 1 and 2 (see Section 6.4.2) then areas/intervals where there is more than ~100 m thickness may be overpressured and thus there is potential for shallow water flow when drilling in these intervals.

7.1.3 Faults

Large scale faults related to Early Pliocene tectonic movements affect Tertiary sediments and are generally truncated by the Early Pliocene unconformity that marks the base of the Iperk Sequence. Rarely, faults may penetrate the unconformity to affect basal Iperk strata (Plate 7.1; Blasco *et al.* 1990; Fortin and Blasco, 1990). Large scale tectonic faults were not identified in the upper 750 m of slope deposits observed on seismic data analyzed in this study.

Small-scale normal faults can be observed in places within individual seismic slope units. These faults are non-tectonic in origin and are most likely the expressions of previous regressive slope failure events (e.g. Plates 7.2 and 7.6). Other small-scale faults are possibly linked to subsidence caused by sediment compaction and range in vertical extent from 50 m to 280 m.

7.1.4 Slope FEFs

The seafloor and shallow sub-seafloor structure of FEFs is described in Sections 5.1.5 and 6.1.5, respectively. The FEF illustrated in Plate 5.9 is also shown on a 2D seismic profile (Plate 6.6). The ring faults partially surrounding the collapse zone around the FEF are apparent, and extend up to 450 m BSF.

Imaged directly beneath the FEF cone is a well defined vertical zone comprising chaotic, acoustically attenuated reflections which exhibit velocity effects (pull-down or sag) resulting from potentially gas-charged sediments. This zone, interpreted as a possible gas chimney, is approximately 500 m in diameter and may be a conduit for fluids rising to the seafloor. The feature extends beyond 750 m BSF, the vertical limit of seismic data, implying a deeper source for the migrating fluids. Plate 7.3 illustrates a similar columnar

pull-down extending to at least 750 m BSF that may also indicate the presence of a conduit for ascending fluids.

7.1.5 Amplitude Anomalies

2D volume attribute extractions were performed on the selected and available ION GXT BeaufortSPAN data from a series of 100 m thick, incremental depth windows extending from seafloor to depth limit of investigation (~750 m BSF). Amplitude extractions were performed using an algorithm that auto-picks the maximum negative (trough) amplitude at every trace within the specified depth intervals. Anomalies were assessed for indicators of shallow gas, including polarity, phase reversals, amplitude gradients, tuning effects, transmission losses, frequency effects and velocity effects (e.g. pull-downs).

The majority of anomalies occur on the slope between approximately 200 m and 500 m BSF (Plates 7.7 and 7.8). These anomalies exhibit trough-over-peak reflection pairings, indicating a decrease in seismic velocity and impedance, consistent with free-phase gas. The anomalies have sharp lateral gradients, apparent frequency loss and may exhibit velocity pull-downs beneath them. Velocity effects can be difficult to discern relative to the complex seismic reflection character of the host mass transport deposits.

7.1.6 Gas Hydrates

Gas hydrates are a solid form of light gasses compressed within an ice-like matrix of water molecules, forming when escaping gasses are of the proper chemistry, under sufficient hydrostatic pressure, typically in water depths greater than 300 to 500 m, and within the proper temperature regime (Kvenvolden and Barnard, 1983; Milkov *et al.*, 2000; Judd and Hovland, 2007). Escaping gasses can produce hydrates at or below the seafloor and, in many instances, be recognized or inferred by the subtle mounding of the seafloor at the site of venting (Neurauter and Bryant, 1989; Brooks and Bryant, 1985) or through the presence of a Bottom-Simulating Reflector (BSR) below the seafloor (Judd and Hovland, 2007).

The geophysical expression of gas hydrates is a Bottom-Simulating Reflector (BSR), which often corresponds with the base of the hydrate stability zone, and mimics the seafloor topography. In appearance, a BSR is highly reflective and represents a change in acoustic impedance due to a relatively dense/rigid hydrate-bearing layer overlying sediment containing free gas. It is noted that care should be taken in the identification and interpretation of apparent BSRs, which can be difficult where bedding is highly conformable, or data artifacts such as residual seafloor multiple reflections exist. Confidence in the interpretation of gas hydrates increases where a BSR clearly cross-cuts 'real' shallow stratigraphic reflections that dip away from seafloor. While a BSR is a common indicator of gas hydrates, its presence does not necessarily mean the occurrence of gas hydrates nor does the absence of a BSR mean the absence of gas hydrates.

Fortin and Blasco (1990) report the presence of a possible BSR in upper slope sediments, deepening from ~200 m BSF (0.25 s TWT) at 400 m water depth to ~440 m BSF (0.55 s TWT) at 750 m water depth. However, inspection of the seismic data available for the present study did not display any potential BSRs beneath the continental slope. Despite this, conditions are thought to be favourable for gas hydrate development on the slope. If hydrates are present, they are probably localized within small sand-prone lenses and/or disseminated within fine-grained sediments.

7.2 Beaufort Shelf

The stratigraphy of the upper approximately 50 m of the Beaufort Shelf is well known (see Section 3.1.3; Blasco *et al.* 2011 and references therein). In particular a complete stratigraphy from seafloor to 468.45 m BSF has been compiled from data collected in the 3F-24 borehole (Ruffell *et al.* 1990; Blasco, 2012).

7.2.1 Permafrost

In their analysis of borehole and seismic data Fortin and Blasco (1990) were able to define the complete vertical extent of APF in six units (in descending order, D6 to D1) from the near-seafloor to ~700 m BSS. However, developing a seismic stratigraphy for the deeper section is greatly complicated by a series of velocity inversions caused by discontinuous acoustic permafrost layers (section 6.2.1). Permafrost-affected sediments present a complex challenge for stratigraphic investigations using acoustic and seismic methods. Plate 7.9 illustrates the difficulties in tying borehole to seismic stratigraphy (see also Enclosure 7). These challenges, and potential solutions, are discussed in section 6.2.

Recent 2D seismic investigations by the Geological Survey of Canada between 2006 and 2008 have focused on mapping APF distribution (e.g. Carr *et al.* 2011; Blasco *et al.* 2011). Seismic velocity analysis within a 13 km x 16 km test site on the Akpak Plateau, west of Kugmallit Channel, showed velocity ranges from 1450 m/s to 2200 m/s. Using a mean velocity of 1800 m/s these authors have attempted to map the top surfaces of stratigraphically-controlled and hummocky APF to a depth of approximately 200 m BSF.

7.2.2 Gas Hydrates

The maximum depth to which hydrates remain stable is up to 1.4 km in the Mackenzie delta/Beaufort Sea (e.g. Judge *et al.* 1994; Judge and Majorowicz, 1992). The hydrate stability zone is between 0.2 km and 1.4 km thick, and the inferred thickness in permafrost-affected sediments is between 0.2 km and 0.5 km where the hydrate layer typically occurs between 0.7 km and 1.4 km BSF (Majorowicz and Osadetz, 1999). Majorowicz and Hannigan (2000) suggest that permafrost and the hydrate stability zone form the only traps preventing upward migration of gas since the Sangamonian glaciation. Elevated gas content in porous sand/sandstone was commonly encountered beneath the base of permafrost in exploration wells drilled on the Beaufort Shelf (see Section 2.4).

Although their presence at depth is inferred, no samples of gas hydrate have been recovered from Beaufort Shelf sediments (Weaver and Stewart, 1982; Smith and Judge, 1993; Osadetz and Chen, 2010; Blasco *et al.* 2011). From wireline and mud-gas logs Weaver and Stewart (1982) interpret the presence of gas hydrates in fine-grained sands between 700 m and 740 m BSF at Kopanoar and between 1150 m and 1250 m at Ukalerk.

Fortin and Blasco (1990) tentatively identified a reflector at approximately 700 m BSF from a seismic profile collected across the Kopanoar wellsites that they interpreted as the possible upper boundary of the hydrate zone. Laterally restricted high amplitude reflectors are observed at this depth on two orthogonal BeaufortSPAN lines that intersect over the Kopanoar wellsites (Lines BE1-4200 and BE2-5150), however it is not conclusive whether gas hydrates are present.

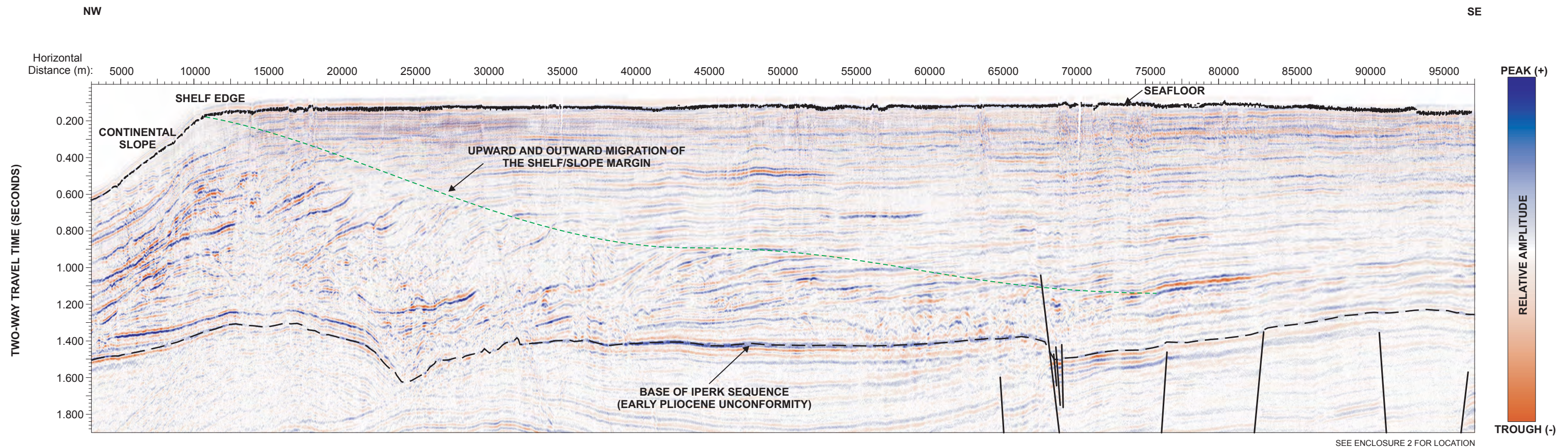
7.3 Mackenzie Trough/Yukon Shelf

The angular unconformity defining the base of the Mackenzie Trough is clearly identified as a high amplitude reflector on 2D seismic profiles (e.g. Plates 7.7, 7.8, 7.10 and Enclosure 4). Trough units thin progressively distally so that the unconformity approaches the seafloor to within ~50 m and appears to be truncated at the Trough to slope margin. At the outermost Trough margin on the Yukon slope the unconformity, although still a strong reflector, has become a disconformity and is mostly parallel with the underlying Iperk Sequence strata (Enclosure 4). Unit MT4 sediments rest directly on the disconformity (Plate 7.8) and overlying MT2 and MT1 sediments have a combined thickness of ~30 m.

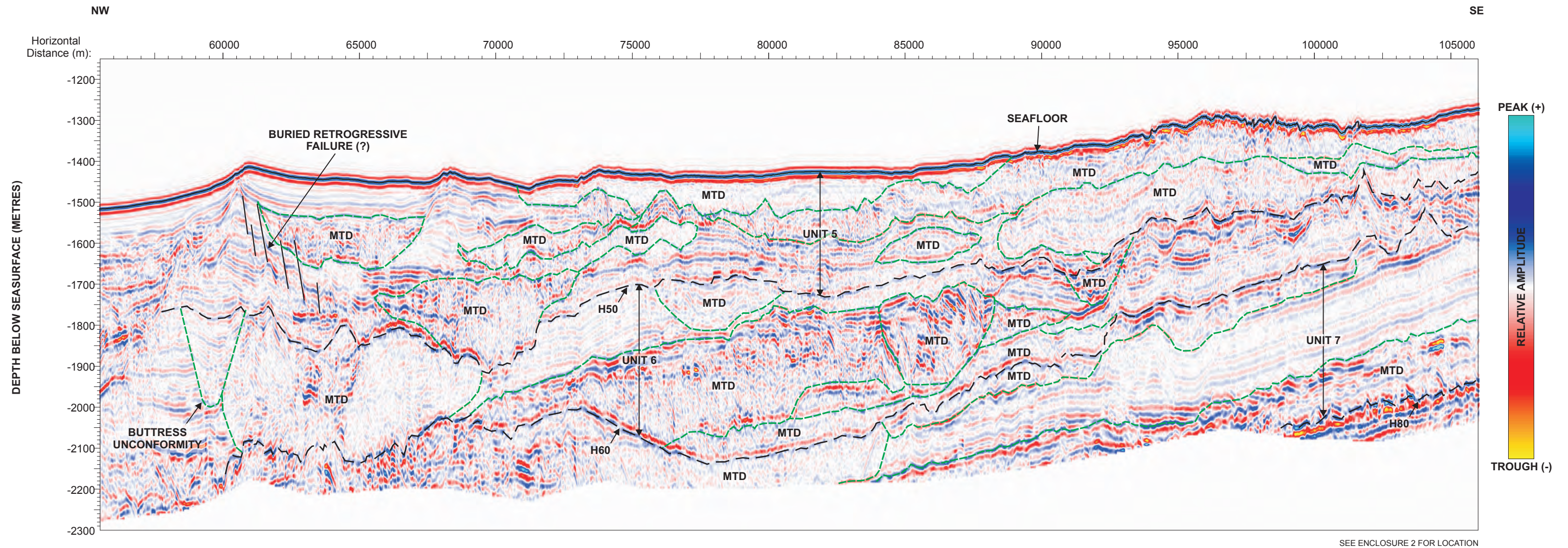
Unit MT4 thickens from the slope towards the Yukon shelf in the form of a prismatic wedge of prograding sediments resting on the Trough unconformity (Plate 7.8). Large scale clinoform reflectors within the wedge are truncated at an elevation of ~150 m BSS (90 m to 100 m BSF) and are overlain by horizontal topsets. The prograding edge of the MT4 clinoforms dips seaward to a pinchout on the Trough disconformity at ~460 m BSS. From the southwest, where it pinches out against the Trough disconformity, to beneath the modern break in slope to the northeast, the prograding wedge has extended the shelf margin by a distance of ~9 km.

7.3.1 Amplitude Anomalies

MGL (1987; 1992a) reported phase-reversal amplitude anomalies, interpreted as free gas, associated with the Base of Trough unconformity and in younger sediments filling the Trough. MGL (1992a) suggested that the anomalies may be the seismic expressions of petrogenic hydrocarbons which have migrated upward from underlying Tertiary anticlines. Examples of high amplitude anomalies in Iperk Sequence strata beneath the unconformity are seen in Plates 7.7 and 7.8.



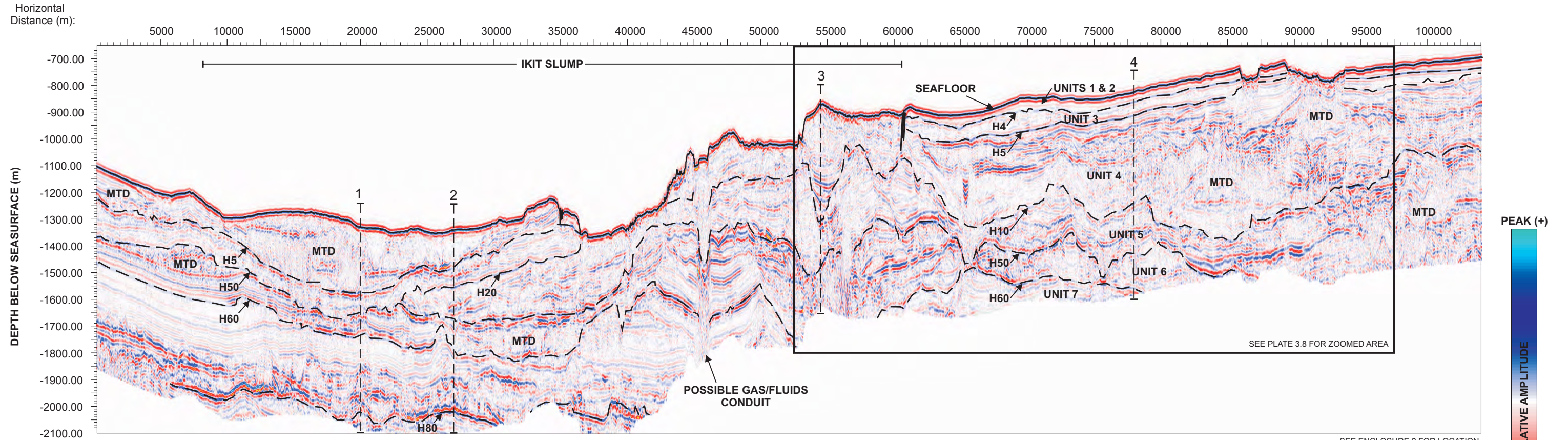
Cross-shelf 2D seismic profile. This profile illustrates the development of the modern continental shelf through both aggradation and progradation at the migrating shelf/slope margin during the Pliocene and Pleistocene. The green dashed line marks the approximate trace of the shelf to slope transition through time. Approximately 65 km of progradation and 1 km of vertical accumulation (1.3 - 1.5 s TWT) is seen in this profile, although up to 120 km of progradation is evident elsewhere (e.g. Dietrich *et al.* 2011). Line FGP_87_2, Geological Survey of Canada Frontier Geoscience Program.



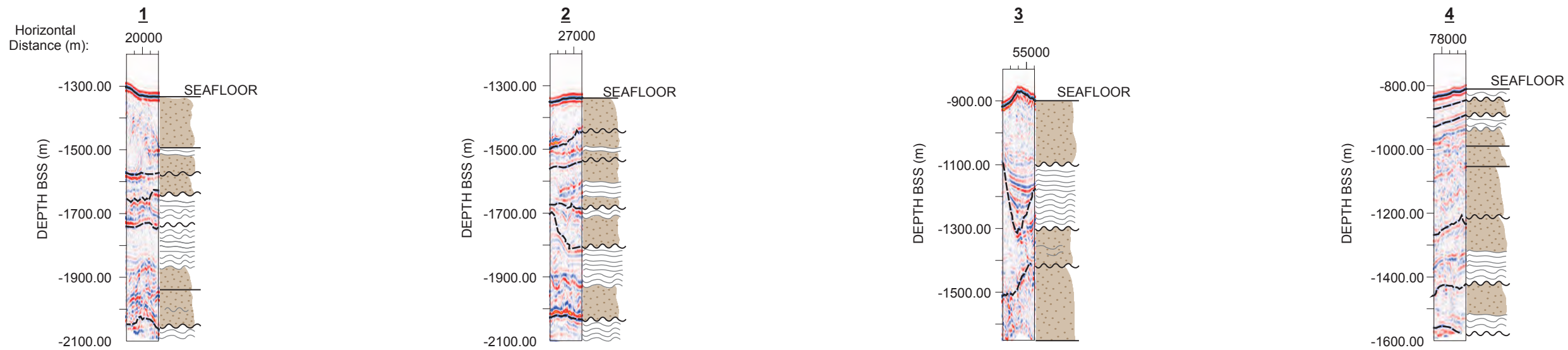
Downslope seismic profile. This profile shows complex, sequential stacking of MTDs. At least 19 MTDs can be seen in this cross-section, with thick ones likely comprising multiple events. Irregular top surfaces are mirrored by draped pelagic strata where these strata are preserved. Note the buried paleo-valley (~240 m deep) which is marked by a buttress unconformity that cuts into stratified sediments on its NW flank, and into a thick MTD complex on its SE flank. A possible buried retrogressive failure (left) is marked by small faults and terraces in Unit 5 strata. BeaufortSPAN Line BE3-4125, courtesy of ION Geophysical Corporation.

SW

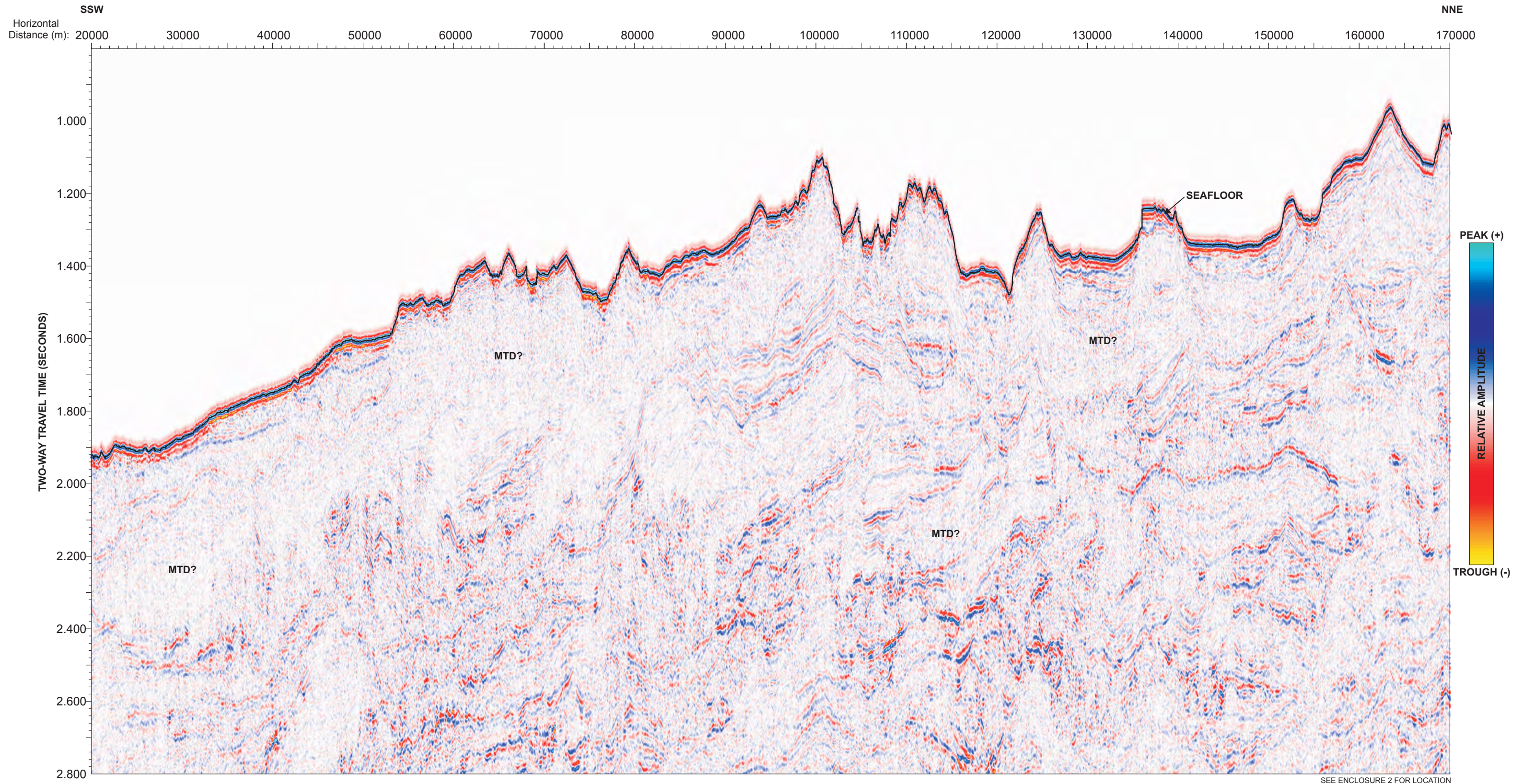
NE



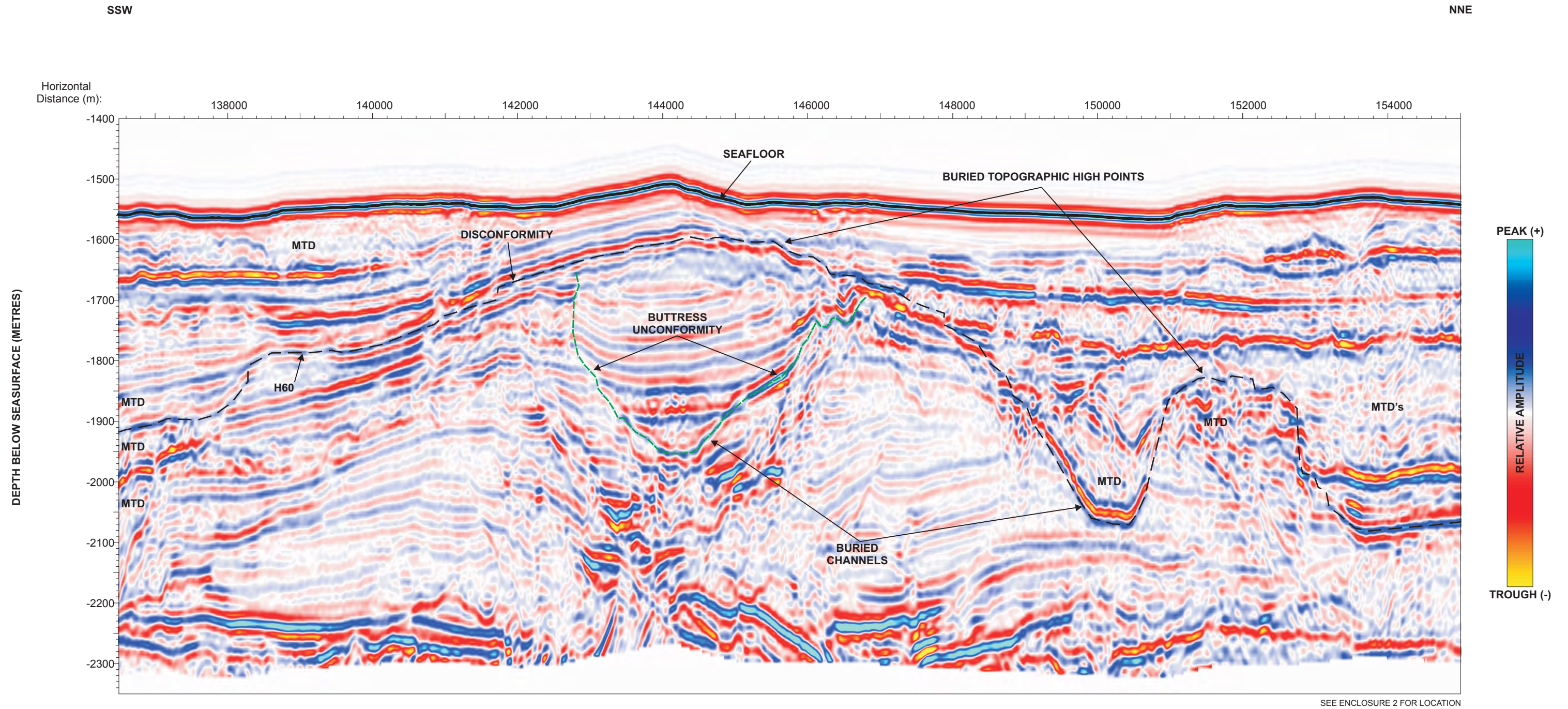
SEE ENCLOSURE 2 FOR LOCATION



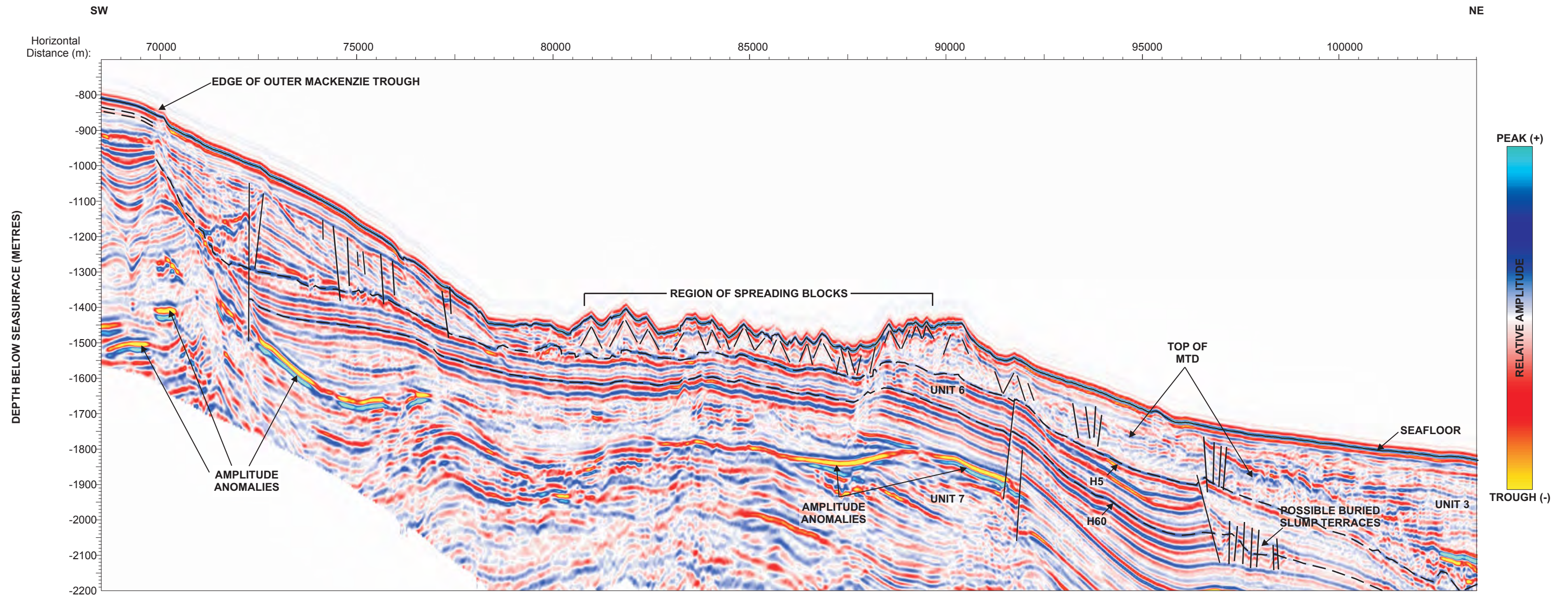
2D cross-slope seismic profile. This profile illustrates the variation in stratigraphy that can be expected over short horizontal distances. Four arbitrary sections and stratigraphic interpretations are shown. The Ikit Slump across which the surficial stratigraphy cannot be traced and matched is shown between 8 km and 60 km. BeaufortSPAN Line BE2-5450 courtesy of ION Geophysical Corporation.



Example of a recent cross-slope 2D seismic profile. This line is between 15 km and 35 km north of the profile shown in Plate 7.3. Although of good quality data it lacks sufficient resolution to map regional slope units identified in BeaufortSPAN data. Line ISI1023, Geological Survey of Canada.

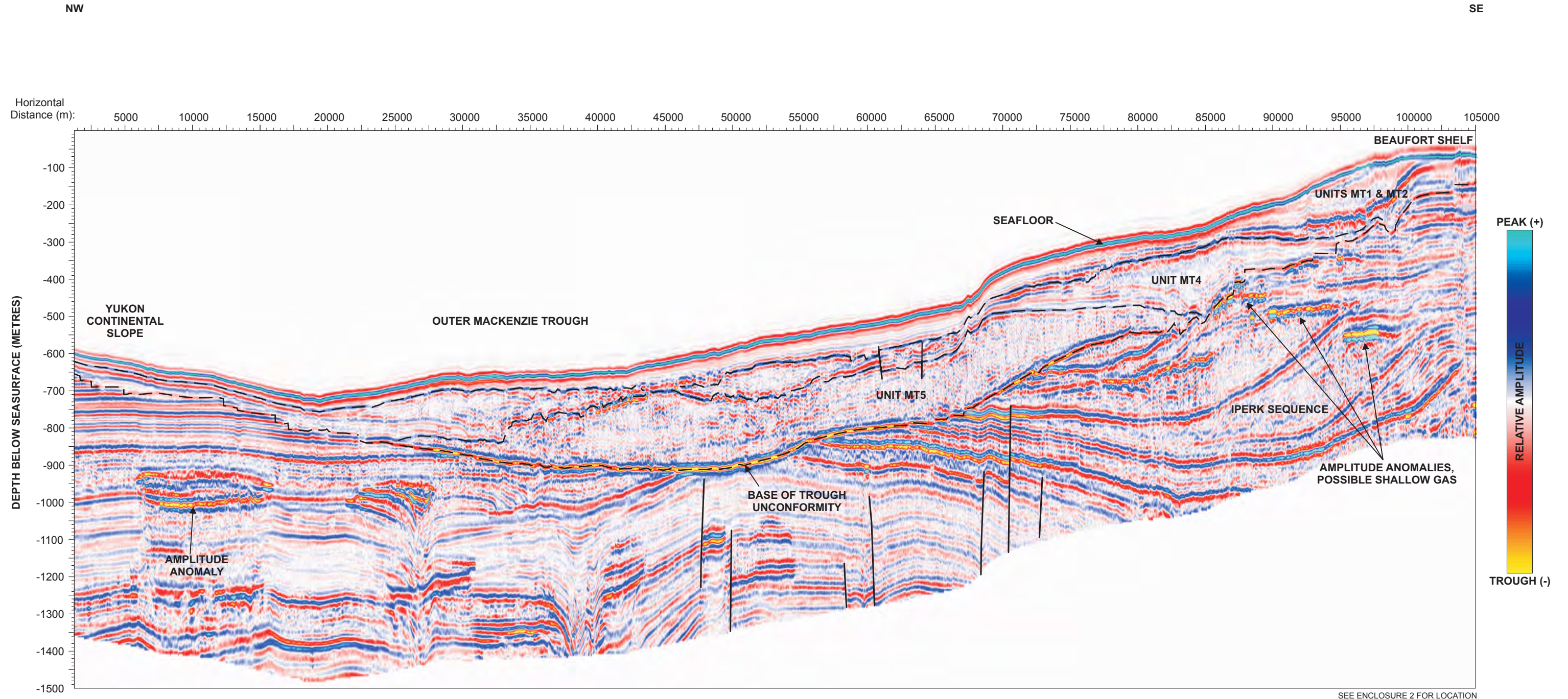


Unconformities and buried topography. This 2D Seismic Profile illustrates the variety of unconformities and buried topography commonly seen in slope sediments. **Buttress unconformities**, as shown in the buried channel (centre) where stratified fill is parallel to older strata truncated by the channel, make it difficult to trace erosion surfaces. The channel, truncated by horizon H60, is ~280 m deep. The channel to the right, filled with mass transport deposits, is easier to distinguish. Topographic relief on H60 from the truncated top of the central channel to the base of the MTD-filled channel is ~470 m. BeaufortSPAN Line BE4-3325, courtesy of ION Geophysical Corporation

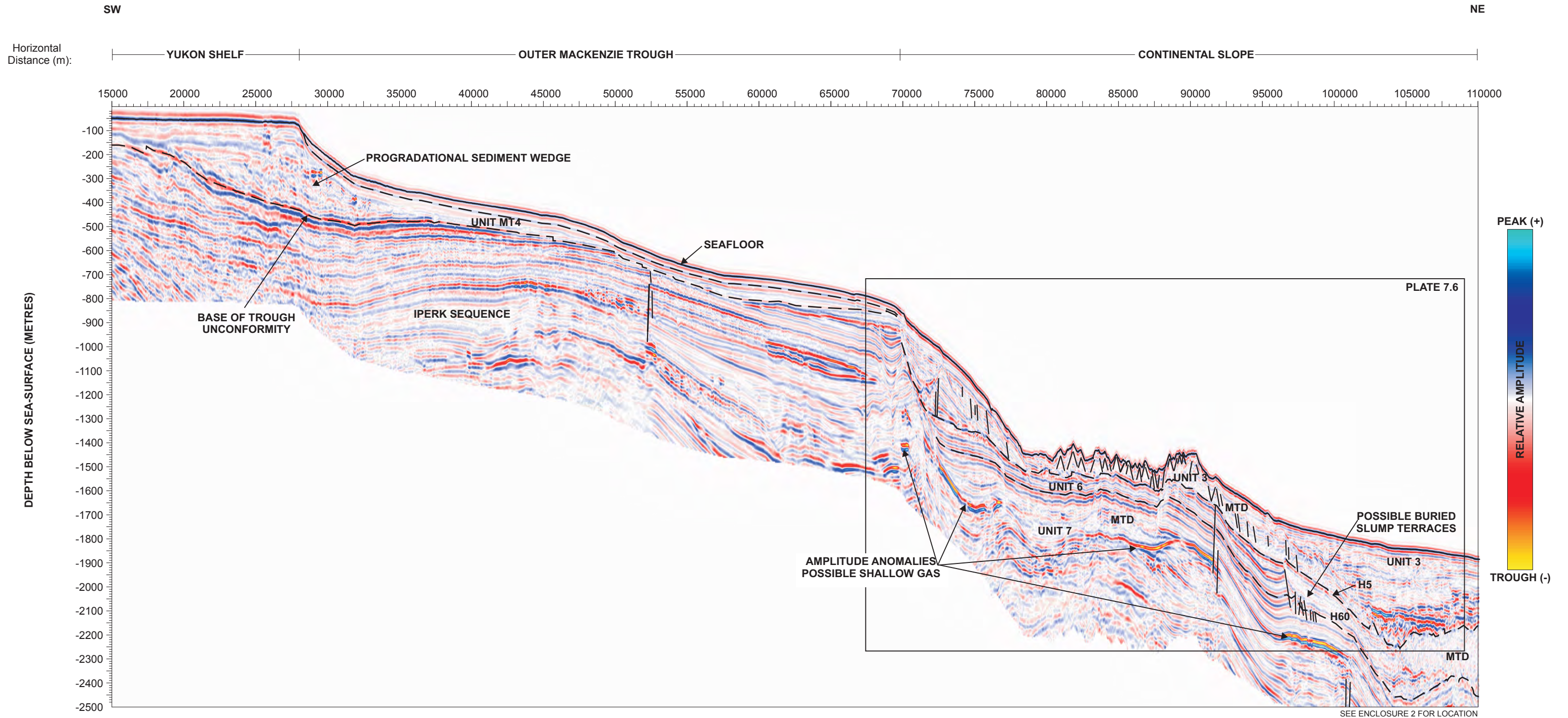


SEE ENCLOSURE 2 FOR LOCATION

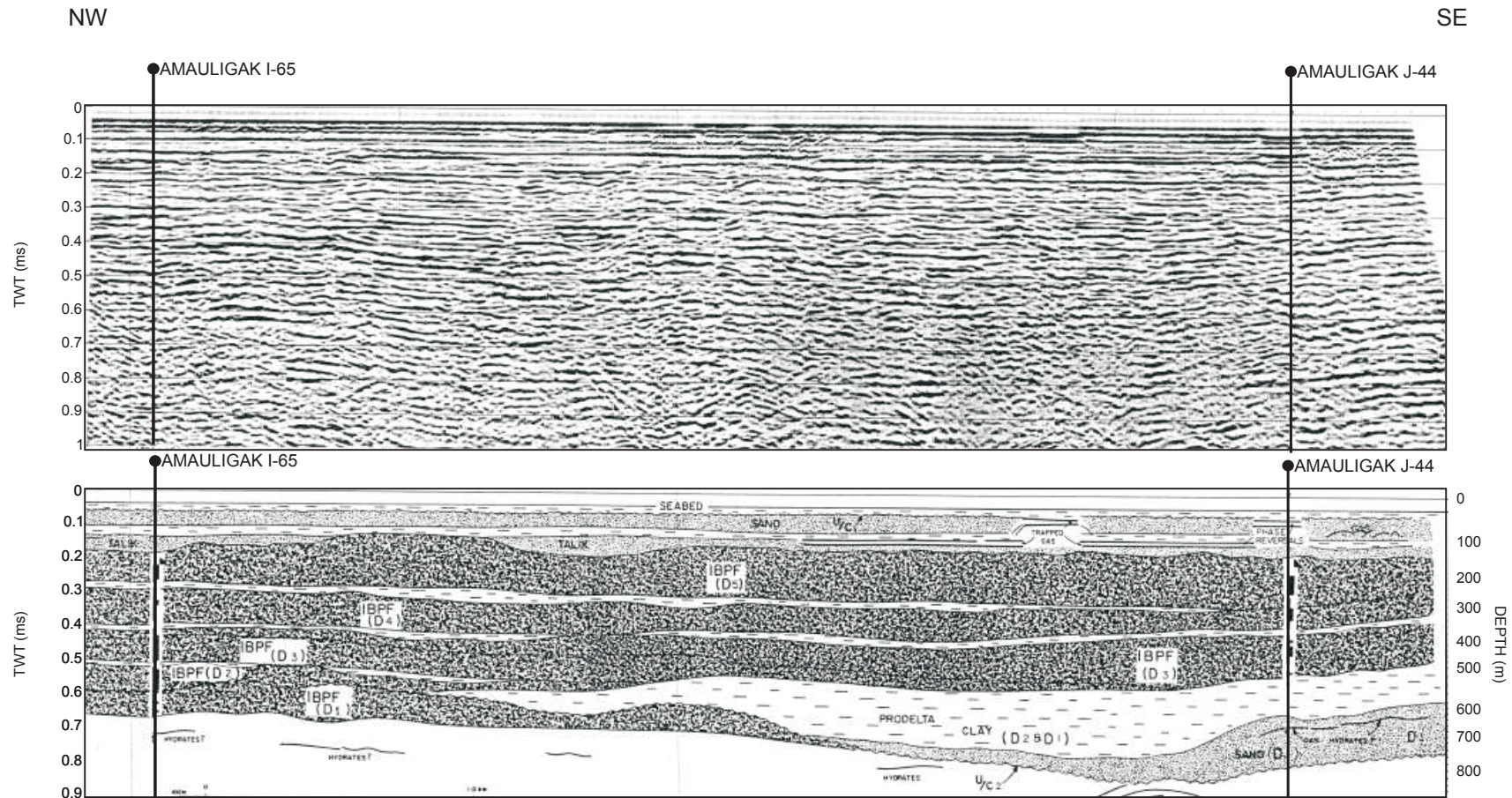
2D Seismic Profile showing possible spreading blocks in a near-surface MTD. Prismatic sharp-crested spreading blocks have been documented from other submarine landslides and are indicative of retrogressive failure (Micallef *et al.* 2008; Kvalstad *et al.* 2005; Quinn *et al.* 2007). The blocky region has been mobilized on the H5 surface and passes downslope into disrupted MTD sediments in Unit 3. A cluster of small-scale faults affecting the H60 horizon (right) may represent buried retrogressive failure terraces. BeaufortSPAN Line BE4-3200, courtesy of ION Geophysical Corporation.



2D seismic profile across Outer Mackenzie Trough. This profile illustrates the geometry of interpreted units from the edge of the Beaufort Shelf (Kringalik Plateau) in the southeast, across the Outer Mackenzie Trough and onto the Continental Slope off the Yukon Shelf in the northwest. Unit MT5 is up to 225 m thick in this profile. The unconformity marking the base of the Mackenzie Trough is readily apparent, truncating faulted strata of the underlying Iperk Sequence. Potential gas-related amplitude anomalies on the SE trough margin occur between 200 m and 450 m BSF. Beaufort SPAN Line BE2-5100W, courtesy of ION Geophysical Corporation.

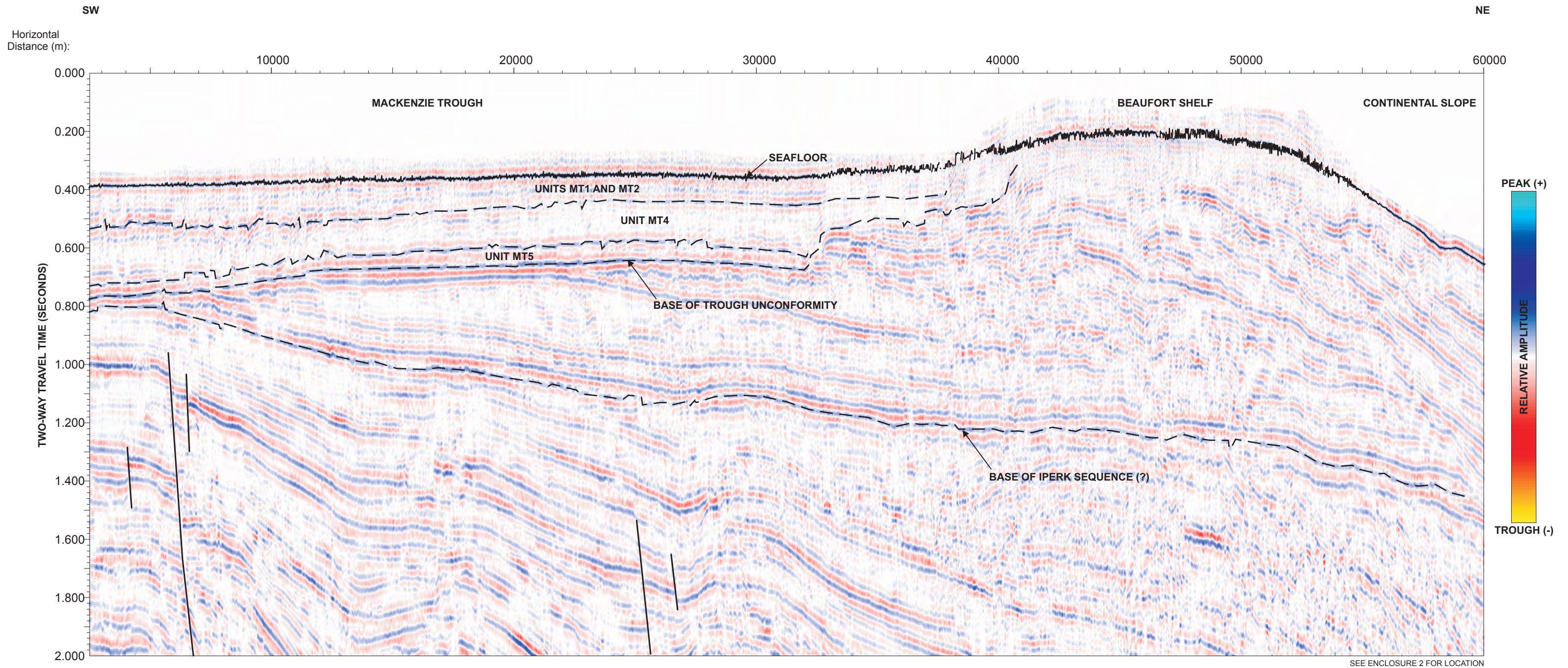


2D seismic profile from Yukon Shelf to Continental Slope. This profile illustrates the geometry of interpreted units from the Yukon Shelf to the Continental Slope. Unit MT4 rests directly on the unconformity marking the base of the Mackenzie Trough. Unit MT4 includes a shelf-extending progradational wedge of sediments. The Trough/Slope boundary is sharp and marks the transition between well stratified sediments of the Iperk Sequence to a sequence of mass transport deposits that pass laterally into and are overlain by pelagic drape sediments. In this interpretation, disrupted MTD sediments of Unit 3 rest directly on Unit 5 implying the removal of Unit 4 by mass transport processes. A number of amplitude anomalies, possibly indicating the presence of gas occur mostly within slope sediments between 225 m and 450 m BSF. BeaufortSPAN Line BE4-3200, courtesy of ION Geophysical Corporation.



SEE ENCLOSURE 2 FOR LOCATION

2D seismic profile in the Amauligak discovery region. This profile illustrates the difficulties with interpreting seismic data in regions of permafrost-affected sediments. The interpreted permafrost stratigraphy (D5 to D1) in this section is largely based on data from two Amauligak wells (I-65 and J-44). Figure 44 of Fortin and Blasco (1990).



Example of scanned 2D seismic profile from the Mackenzie Trough. Although the quality is not as good as BeaufortSPAN data this legacy profile is useful for regional correlations. Legacy line SU-79-141.

8. GEOHAZARD OVERVIEW

The following summarizes potential geohazards that have been identified in the southern Beaufort Sea, as discussed in previous sections.

8.1 Slope Failure

Three different types of slope failure and associated MTDs have been identified on the continental slope. Each type is related to temporal changes in slope processes since the LGM. Large portions of seafloor on the continental slope show morphological evidence of slope failure in a series of irregular, downslope oriented channels and valleys tens of kilometres wide and up to 65 km long, or more, that merge downslope into large, continuous regions of deformed seafloor sediments, the single largest feature being the Ikit Slump (Enclosure 1). Seafloor topography in these regions is typically hummocky in cross-slope profiles, and smoother in downslope profiles. Large slumps, characterized by a sequence of terraces beneath the headwall regions, are generally interpreted to represent changes in process from retrogressive rotational slumping, to debris flow and turbidity currents during a single failure event. Slumps affect sediments from a wide range of slope deposits including stratified pelagic silts and clays, sheet-like and ribbon-like MTDs, the paleo-scour zone, and possible FEFs and FEF flows. In addition, where slumped material has been completely evacuated from the failure zone, older possibly more consolidated sediments may be exposed at the seafloor (e.g. the flat valley floor shown in Plate 5.2). As a consequence a range of geotechnical properties may be expected in slumped regions. Slope failure regions are shown on Enclosures 1 and 6.

The earliest identified slope failure mechanism is linked to sheet-like MTDs in lower Unit 2. These poorly stratified gully deposits are found slope-wide and may comprise sand-prone turbidites that originated from the shelf margin during early deglaciation. Geotechnical properties of these sediments may be different from well stratified silts/clays of the overlying pelagic drape in Units 1 and 2.

Ribbon-like MTDs occur stratigraphically higher than the sheet-like MTDs and represent a different failure process involving debris flow in confined channels. Overprinting by the paleo-scour zone masks the upper reaches of these deposits that may have originated close to the shelf margin and thus may contain coarse shelf-derived glacial sediments including sands and gravels. Alternatively the MTDs may have originated in the paleo-scour zone triggered by the action of scouring ice keels. In this case the MTDs may also contain ice-rafted debris, from sand to boulders, transported by floating ice.

Stratified sediments and buried MTDs, topographic unconformities and disconformities point to continuous pelagic sedimentation and numerous slope failure events throughout the Pleistocene. MTD intervals up to 450 m thick and 85 km long are identified in seismic profiles and probably represent multiple events.

Large vertical and horizontal variations in deposit type and style mean that significant vertical differences in sediment facies and sediment type are likely between nearby sites

illustrated by the four seismo-stratigraphic profiles on Plate 7.3. Vertical variability means that sediments are not likely to be normally consolidated, and changes in the pre-consolidation pressures may be expected across boundaries between stacked MTDs and between stratified sediments and overlying and underlying MTDs.

8.2 Shallow Water Flow

SWF is a potential geohazard when drilling through overpressured strata. Overpressure may be induced where sedimentation rate exceeds the ability of pore pressures to dissipate in underlying strata, typically uncemented sands. An analysis of sedimentation rates at six core locations on the continental slope indicates that average post-LGM sedimentation rates all exceeded 100 cm/ka, and at one location exceeded 600 cm/ka, the rate dropping significantly towards the seafloor. Sedimentation rates of >45 cm/ka may be linked to serious SWF incidents. However, these incidents generally only occur where such rapidly accumulated sediment is more than ~100 m thick, and on most of the Beaufort Slope sediment thickness of undisturbed strata seldom exceeds 30 m to 40 m above possibly sand prone MTDs.

In the deeper section beneath the continental slope thick sequences of undisturbed strata can be seen on 2D seismic profiles. These stratified packages may range from 30 m to 500 m thick and extend laterally from 8 km to 68 km. If these strata were deposited at similar sedimentation rates to those computed for Units 1 and 2 (see Section 6.4.2), then where they exceed ~100 m in thickness, sediments may be overpressured and as a result there is potential for shallow water flow when drilling through these intervals.

8.3 Faults

Small-scale non-tectonic faults with offsets of a few metres affect the seafloor and near-surface strata on the continental slope. Faults are associated with slumped regions and with subsidence around large scale FEFs (Plates 5.8, 5.9 and 6.6). Slump headwall scarps are the exposed footwalls of normal faults and may have throws of 15 m to 20 m. Small-scale faults with throws of <1 m to 10 m may occur elsewhere in regions of undisturbed seafloor above the slump terraces. Small-scale normal faults are also observed in 2D seismic profiles. These are likely the expressions of previous regressive slope failure events (e.g. Plates 7.2 and 7.5). Other small-scale faults exist, ranging from 50 m to 280 m in vertical extent and are possibly the result of sediment compaction. Ring faults associated with slope FEFs have seafloor displacements between 5 m and 10 m and extend up to 450 m BSF (Plate 6.6).

Large scale deep-seated faults seen in 2D seismic data are related to Early Pliocene tectonic movements which affect Tertiary sediments. Most faults are truncated by the Early Pliocene unconformity that marks the base of the Iperk Sequence. They rarely penetrate the unconformity and are not observed in the upper 750 m of slope deposits based on the seismic data used in the present study.

8.4 Seafloor Gradient

A seafloor gradient map, based on the existing multibeam data is given in Enclosure 5. In summary, most of the seafloor on the continental shelf and slope has gradients of $<2^\circ$ (generally $<0.5^\circ$ on the shelf). Gradients $>6^\circ$, exceptionally $>20^\circ$, are generally concentrated along headwall and sidewall scarps of slumped regions, and along the margins of the Kugmallit Channel on the continental slope. Individual FEF mounds on the shelf margin in the FEF Zone are characterized by convex slopes with angles between 15° and 20° , occasionally approaching 30° . The FEF Zone is approximately 1.5 km to 5 km wide and at least 130 km long. Small (40 m to 50 m diameter) pockmarks on the upper slope have sidewall gradients between 2° and 4° (Plate 5.12).

8.5 Fluid Escape Features

With the exception of pockmarks, FEFs are positive relief, conical seafloor mounds that occur as isolated features on the continental shelf and as tightly grouped, often coalesced features in the FEF Zone at the shelf margin (Plate 5.14). They also occur as single, relatively large features on the continental slope (Plate 5.8). FEFs on the shelf and in the FEF Zone are likely the result of upward extrusion of sediment under pressure from escaping gas through overlying weaknesses in sub-seafloor permafrost. A small number of pockmarks on the upper slope are negative relief indicators of fluid expulsion (Plate 5.12).

Water column plumes possibly related to seafloor fluid and/or gas expulsion, were observed in multibeam data in a region of relatively smooth seafloor at the shelf margin above the Ikit Slump headwall. The absence of water column anomalies in multibeam data above FEFs in the FEF Zone or the upper slope pockmarks suggest that these features may no longer be active.

Slope FEFs are considerably larger than in the shelf margin FEF Zone, and their origin is linked to the vertical migration of overpressured fluids from depth. Beneath the FEFs 2D seismic profiles indicate the presence of well defined vertical columns of disrupted strata which can exhibit velocity effects (pull-down or sag) indicating the potential presence of gas-charged sediments (e.g. Plates 7.3 and 6.6).

The slope FEFs are likely still active with fluids and gas permeating the cone sediments and escaping into the water column from the flat-topped summit regions. Eruptive flows associated with the FEFs are mostly accretionary and confined to the flanks of the FEF cones (Plates 5.9 and 6.7). However, FEF flows can be mapped in the subsurface (Plate 6.8) indicating eruptive periods in the past when fluids and sediments, likely brought to the surface from considerable depth, flowed onto the seafloor and downslope.

The geotechnical and geochemical properties of FEFs is likely to be significantly different from seafloor sediments that surround them. Slope FEFs appear to be long-lived features and may comprise a wide variety of sediment types and grain size derived from considerable depth. Long FEF flows were probably quite fluid when they were erupted

and may consist of better sorted sediment. Fluids contained in the flows are presently stable at present water and burial depths but *in situ* disturbance could cause exsolution of constituent phases causing instability. Phase change was particularly noticeable in cores retrieved from FEF summit regions. Once the core liners were cut open the reduction in ambient pressure between seafloor and sea surface resulted in sample expansion caused by the liberation of gas bubbles.

FEFs on the shelf and in the FEF Zone probably comprise a mixture of extruded material originating from permafrost-affected sediments (e.g. Units C, D and E) and from unfrozen Units A and B and thus may include a range of grain sizes including gravel, sand and silt. Gas hydrates in the sediment matrix may be stable at shelf depths but *in situ* disturbance could cause exsolution resulting in instability.

8.6 Seafloor Erosion

Continental slope Unit 1 strata are truncated at very low angles at the seafloor immediately seaward of the FEF zone (Plate 5.11). The presence of eroded strata in water depths below the influence of the modern shelf margin jet suggests that active erosion of upper Unit 1 strata during the Holocene transgression is a likely explanation (see section 5.1.7). Streamlined FEFs on the upper slope are thought to be the result of modern shelf jet currents depositing sediment on the east-facing lee slopes (Plate 5.10).

On the western margin of the Mackenzie Trough a region of seafloor erosion has exposed the MT2 surface and resulted in the development of current-formed comet marks (Plate 6.21). It is uncertain whether the eroded surface is relict or modern.

8.7 Ice Keel Turbates

Five ice keel turbates have been identified. A thick, regional turbate, the paleo-scour zone, is located on the upper slope (Plate 4.8). Two others are located in the Mackenzie Trough, one at the top of Unit MT2 and a thin ice keel turbate developed in Unit MT1a on the northeast margin of the Trough (Enclosure 4). A relict saturated paleo-scour zone (SPZ) is located below 60 m in deep water on the Beaufort Shelf, and the modern saturated scour zone (SSZ) is in shallower water above 60 m water depth. Uneven, hummocky seafloor topography exists in the regions of relict scour marks on the upper continental slope, in deeper shelf waters and on the western margin of the Mackenzie Trough. The mechanical reworking of these sediments by ice keels may alter physical properties.

8.8 Boulders and Ice-Rafted Debris

There is potential for isolated cobbles and boulders at the seafloor and in the shallow subsurface within the study area. Large clasts (if present) consist of ice-rafted debris (IRD), shed by melting icebergs during Pleistocene glacial phases. IRD was interpreted in ten piston cores located on the Beaufort Shelf and slope. Coarse-clastic IRD may occur in association with the deeply buried mega-scale glacial lineations identified on horizons 4

and 5 in Unit 3. IRD may be expected within ice scour turbate deposits, particularly in the upper slope paleo-scour zone where scour marks may have been created by icebergs. Gravel, cobbles and boulders within the turbated unit and in contemporary sediments elsewhere on the slope may be expected.

8.9 Acoustic Permafrost

Although acoustic permafrost is the most dominant feature there is a wide range in the amount of ice in sediments beneath the Beaufort Shelf. There are significant challenges for acoustic and seismic imaging of APF because of large vertical and lateral changes in seismic velocity between frozen and unfrozen sediments. However, advances in ultra high resolution 3D seismic surveys make data acquisition of heterogeneous permafrost regions a relatively inexpensive method for mapping offshore permafrost distribution. Recent advances in 3D tomographic modeling have overcome many of the problems associated with negative velocity gradients encountered with traditional seismic reflection profiling and proven to be a robust method for mapping deep permafrost.

8.10 Shallow Gas and Hydrate Potential

Amplitude anomalies observed on 2D seismic profiles are indicators of possible shallow gas and occur on the slope between approximately 200 m and 500 m BSF (Plates 7.7 and 7.8). These anomalies exhibit trough-over-peak reflection pairings, indicating a decrease in seismic velocity and impedance, consistent with free-phase gas. It is not known whether the possible shallow gas occurrences are over-pressured.

Depending on a number of factors the base of the gas hydrate stability zone in continental slope sediments in other parts of the world may be observed on seismic profiles as a reflective interface, typically mimicking the seafloor topography. Such bottom-simulating reflectors (BSRs) may be proxy indicators of the presence of the base of the gas hydrate stability zone. No BSRs were observed in the seismic data used for this study, however, the absence of BSRs is not necessarily an indication of the absence of gas hydrate. Conditions are thought to be favourable for gas hydrate development in the Beaufort Sea region.

8.11 Wellbore Instability and Tight Spots

Wellbore stability problems, due to shallow water flow, lost circulation or mechanical difficulties possibly corresponding with the presence of subsurface permafrost-bearing sand, caused the abandonment of several wells located mostly landward of the study area (Section 2.4, Table 2.3). There is also potential for well kicks and tight hole conditions.

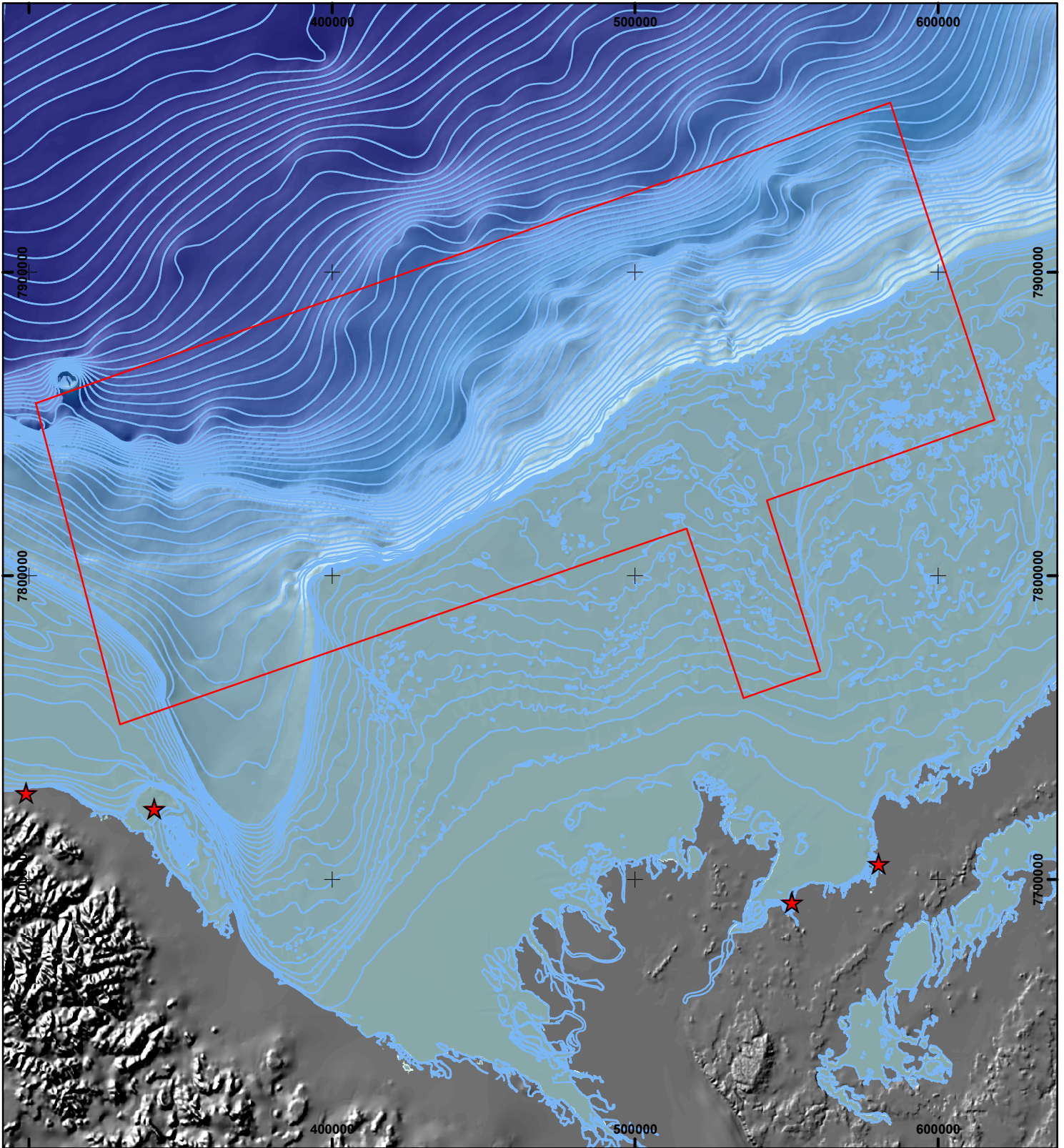
8.12 Seismicity and Tsunamis

The southern Beaufort Sea is seismically active with small to moderate earthquakes occurring within historical times (Plate 3.9). How these affect modern slope stability is not known, however, earthquakes and gas hydrate decomposition are two processes that

have been implicated as conditioners for failure of the Ikit Slump and for slope failures elsewhere around the world. It is possible that the Ikit Slump failure had the capacity to create a tsunami but no evidence has been found of such an event.

8.13 Anthropogenic Features

A request was made to the Department of National Defence Unexploded Ordnance (UXO) and Legacy Sites Program regarding the potential presence of submerged UXO within the study area. Their analysis indicated that there are no UXO-bearing wrecks or dumpsites in the survey area (Plate 8.1).



NAD83, UTM ZONE 8

DWG No : 20110068-DND-BEAU-P81-0

Project No. 20110068

- ★ LEGACY SITES
- BATHYMETRY CONTOURS
- STUDY AREA

**DND LEGACY SITES
SOUTHERN BEAUFORT SEA**



9. DISCUSSION AND RECOMMENDATIONS

Since 1970 a number of geohazards in the southern Beaufort Sea have been discovered and documented. With the benefit of a large amount of high quality sub-bottom profiler, multibeam, 2D seismic and supporting core sample data collected largely since 2004, a number of new geohazards have been identified, mostly from the shelf margin and on the continental slope. Based on existing data a number of data gaps are identified below.

9.1 Data Gaps

- **Multibeam and sub-bottom profiler coverage.** Much of the central and outer Mackenzie Trough, the continental slope west of Easting 430000 (NAD83, CSRS, UTM Zone 8) and the region east of Kugmallit Channel.

Recommendation: Conduct a survey of the central and outer Mackenzie Trough and the continental slope along and across the Trough parallel to existing multibeam lines collected in 2002 in order to extend bathymetric coverage and to collect sub-bottom profiler data. Collect piston and box cores as appropriate.

- **Mackenzie Trough/Slope stratigraphy.** Attempts to extend the slope stratigraphy developed in this study from the large sub-bottom dataset in the central part of the study area to the outer Mackenzie Trough has not been possible. The difficulty is related to the Ikit Slump, a wide region of disturbed seafloor on the slope which separates the two regions, that has destroyed all original acoustic stratigraphy in this region.

Recommendation: Conduct a survey across the upper slope in front of Ikit Trough in an attempt to find possible undisturbed upper slope stratigraphy above the Ikit Slump that connects the central slope and outer Mackenzie Trough. Collect piston and box cores as appropriate.

Recommendation: Collect piston cores from the Unit MT2 ice keel turbate, where it has been exhumed on the Yukon shelf/Mackenzie Trough margin, to establish its age in comparison with the continental slope paleo-scour zone.

- **Ikit Slump.** The full extent of the Ikit Slump that extends along the shelf margin southwest of the area of main data coverage is not mapped along the mouth of Ikit Trough and margin of the adjacent Kringalik Plateau.

Recommendation: Conduct a survey extending along the edge of Kringalik Plateau into Mackenzie Trough. Collect piston and box cores as appropriate.

- **Lower Slope.** There are no data for the slope region in water depths >1500 m in the northwest portion of the study area.

Recommendation: Conduct a regional survey with tie lines. Collect piston and box cores as appropriate.

- **Shelf to slope stratigraphy.** Shelf to slope stratigraphy is poorly constrained because the transition is masked by the FEF Zone. The extent of the paleo-scour and FEF zones northeast of Kugmallit Channel are unknown.

Recommendation: Conduct a survey line along the upper slope and shelf margin to the east of Kugmallit Trough with appropriate tie lines from the shelf to upper slope. This should investigate the potential of finding a "gap" in the FEF Zone across which undisturbed shelf to slope stratigraphy may be observed on acoustic and seismic profiles, and to map the northeastern extents of the FEF and paleo-scour zones. Collect piston and box cores as appropriate.

- **Kugmallit Channel.** The slope portion of Kugmallit Channel is partially mapped but the Channel passes obliquely out of the region of survey coverage to the north.

Recommendation: Conduct a survey to fill in gaps between existing survey coverage north of Kugmallit Channel. Collect piston and box cores as appropriate.

- **SBP data quality.** The quality of existing sub-bottom profiler data to the east of the slope portion of Kugmallit Channel is often poor due to ice and/or other poor survey conditions.

Recommendation: Conduct a regional survey to fill in gaps between existing coverage. Collect piston and box cores as appropriate.

- **Boreholes for Stratigraphy, Permafrost and Hydrate Identification.** A slope stratigraphy has been established and linked to the continental shelf, and more speculatively to the Mackenzie Trough. Surficial sediments on the slope have been sampled from several piston cores but beyond ~10 m BSF knowledge of sediment type, geotechnical properties and age is speculative, and primarily based on geophysical interpretations. A single deep borehole (Amauligak 3F-24) sampling stratigraphy and permafrost is the only one drilled on the Beaufort Shelf.

Recommendation: Geotechnical boreholes with full sampling to at least 100 m BSF on the upper, middle and lower slope should be considered. An upper slope borehole should sample completely through the paleo-scour zone to at least H4 and preferably to H5 if it can be identified. Two mid-slope boreholes would be useful: one that penetrates at least one buried MTD to at least H5 and one that samples undisturbed stratigraphy to at least H5. A lower slope borehole should sample a slump-affected region.

Recommendation: Hydrates have not been identified from offshore borehole or well samples. One or more boreholes at the shelf margin in the vicinity of the FEF

Zone are recommended with the goal of determining the presence of hydrate and associated permafrost.

Recommendation: Future drilling on the Beaufort Shelf should take into account stability problems encountered in permafrost where previous experience has shown that the use of chilled muds maintained at *in situ* temperatures may mitigate these problems. Downhole velocity logging requires a clear understanding of the travel path and distance of signal penetration within the sediments adjacent to the borehole. Ideally signal travel path must be through thermally undisturbed sediments. Recovered sample velocity measurements should be made onboard ship in a refrigerated laboratory as samples are retrieved from the borehole.

- **Deep geohazards.** The identification of deeper geohazards is limited by the amount of 2D and 3D seismic data coverage available for this study.

Recommendation:

Access and include further existing 2D and 3D seismic data for an integrated and detailed analysis of deeper geohazards across the study area.

10. REFERENCES

Adams, J. and G. Atkinson. 2003. Development of seismic hazard maps for the proposed 2005 edition of the National Building Code of Canada. *Canadian Journal of Civil Engineering*, 30: 255-271.

Alberty, M.W., M.E. Hafle, J.C. Minge and T.M. Byrd. 1999. Mechanisms of Shallow Water flows and Drilling Practices for Intervention. *SPE Drilling and Completion*, 14 (2): 123-129.

Alberty, M.W., Hafle, M.E., Minge, J.C., and Byrd, Tom M., 1997. Mechanisms of Shallow Water flows and Drilling Practices for Intervention. *Proceedings Offshore Technology Conference*, OTC Paper No. 8301.

Batchelor, C.L., J.A. Dowdeswell and J.T. Pietras. 2012. Variable history of Quaternary ice-sheet advance across the Beaufort Sea margin, Arctic Ocean. *Geology*, doi:10.1130/G33669.1.

Bard, E., B. Hamelin and D. Delanghe-Sabatier. 2010. Deglacial Meltwater Pulse 1B and Younger Dryas Sea Levels Revisited with Boreholes at Tahiti. *Science*, 327: 1235-1237. DOI: 10.1126/science.1180557.

Blasco, S. 2012. Origin and engineering implications of deep ice-bearing permafrost, Canadian Beaufort Shelf. GSC-A reference No. sb1330. Poster presented at the Tenth International Conference on Permafrost, Salekhard, Russia, 25-29 June 2012

Blasco, S., R. Bennett, T. Brent, M. Burton, P. Campbell, E. Carr, R. Covill, S. Dallimore, E. Davies, J. Hughes-Clarke, D. Issler, L. Leonard, K. MacKillop, S. Mazzotti, E. Patton, G. Rogers, J. Shearer and M. White. 2011. State of Knowledge: Beaufort Sea Seabed Geohazards Associated with Offshore Hydrocarbon Development. *Geological Survey of Canada Open File 6989*: 307 pages.

Blasco, S.M., M. O'Connor, R. Bennett, T. Lapierre, E. Davies, J. Shearer and K. Blasco. 2007. Origin and evolution of the Mackenzie Trough, Canadian Beaufort Shelf. *Canadian Arctic Shelf Exchange Study (CASES) 2006/2007 Annual Meeting*, Quebec City, Quebec, April 30 to May 2.

Blasco, S.M., G. Fortin, P.R. Hill, M.J. O'Connor, M.J. and J. Brigham-Grette. 1990. The late Neogene and Quaternary stratigraphy of the Canadian Beaufort Continental Shelf, in Grantz, A., Johnson, L., Sweeney, J.F., eds., *The Arctic Ocean region: Boulder, Colorado*, Geological Society of America, *The Geology of North America*, v. L: 491-502.

Blasco, S.M., J. Brigham-Grette and P.R. Hill. 1989. Offshore constraints on the late Pleistocene glacial history at the mouth of the Mackenzie River. In: *Late Cenozoic history of the interior basins of Alaska and the Yukon* (eds. Carter, L.D., T.D. Hamilton and J.P. Galloway). *United States Geological Survey Circular 1026*: 15-17.

Brigham-Grette, J. 2013. A fresh look at Arctic ice sheets. *Nature Geoscience*, 6: 807-808.

Brooks, J. M., and Bryant, W. R., 1985. "Geological and Geochemical Implications of Gas Hydrates in the Gulf of Mexico", Final Report, Department of Energy, Morgantown Energy Technology Center, p 131.

Brothers, L.L., P.E. Hart, and C.D. Ruppel. 2012. Minimum distribution of subsea ice-bearing permafrost on the U.S. Beaufort Sea continental shelf. *Geophysical Research Letters*, 39, L15501, doi:10.1029/2012GL052222, 2012

Burden, E. 1986. Mid and Late Wisconsinan through Holocene biostratigraphic zonation of Beaufort Sea shelf sediments from Herschel Island to the Mackenzie Trough. Draft report for the Geological Survey of Canada: 20 pages plus 12 figures.

Carr, E., M. Burton, M. White, P. Campbell, and S. Blasco. 2011. 2008 Beaufort Seabed Mapping Program Geological Analysis and Geohazard Assessment. Draft Report prepared by Canadian Seabed Research Ltd. for the Geological Survey of Canada. 132 pages plus appendices.

Carr, E., C. Breton, M. White, P. Campbell, and S. Blasco. 2010. 2008 Beaufort Sea Ice Scour Repetitive Mapping Program. Draft Report prepared by Canadian Seabed Research Ltd. for the Geological Survey of Canada.

Chappell, J. and N.J. Shackleton. 1986. Oxygen isotopes and sea level. *Nature*, 324: 137-140.

Christensen, J.P. and H. Melling. 2010. Mesoscale Distribution of Springtime Waters and Nutrients near the Continental Shelf Break, Beaufort Sea, Alaska. *The Open Oceanography Journal*, 4: 115-136.

Clark, C.D. 1993. Mega-scale glacial lineations and cross-cutting iceflow landforms. *Earth Surface Processes and Landforms* 18: 1-29.

Comfort, G., G. Gilbert and C. Ferregut. 1990. Analysis of subscour stresses and probability of ice scour-induced damage for buried submarine pipelines, Volume 1, database of key ice scour parameters. Report submitted to the Geological Survey of Canada. Canada Oil and Gas Lands Administration (COGLA) File No. 0825-25-6-4.

Coulthard, R.D., M.F.A. Furze, A.J. Pieńkowski, F.C. Nixon and J.H. England. 2010. New marine ΔR values for Arctic Canada. *Quaternary Geochronology*, 5: 419-434.

Dietrich, J., Z. Chen, G. Chi, J. Dixon, K. Hu and D. McNeil. 2011. Petroleum Plays in Upper Cenozoic Strata in the Beaufort-Mackenzie Basin, Arctic Canada. Search and Discovery Article #10300 (2011) Posted February 14, 2011. Adapted from a poster presentation at AAPG International Conference and Exhibition, Calgary, Alberta,

September 12-15, 2010.

http://www.searchanddiscovery.com/documents/2011/10300dietrich/ndx_dietrich.pdf

Dinkelman, M., N. Kumar, J. Helwig, P. Emmet and J. Granath. 2008. Highlights of Petroleum and Crustal Framework of the Beaufort-Mackenzie Basin: Key Results from BeaufortSPAN East Phases I and II Surveys. Canadian Society of Exploration Geophysicists, Recorder, September: 22-25.

Dixon, J. 1996. Geological atlas of the Beaufort-Mackenzie area/Atlas géologique de la région de Beaufort-Mackenzie. Geological Survey of Canada, Miscellaneous Report 59: 173 pages.

Dixon, J., J. R. Dietrich, and D. H. McNeil. 1992. Upper Cretaceous to Pleistocene Sequence Stratigraphy of the Beaufort-Mackenzie and Banks Island areas, northwest Canada: Geological Survey of Canada Bulletin 407: 90p.

Dixon, J., D.H. McNeil, J.R. Dietrich, J.P. Bujak and E.H. Davies. 1984. Geology and biostratigraphy of the Dome Gulf and others, Hunt Kopanoar M-13 well, Beaufort Sea. Geological Survey of Canada Paper 82-13: 28 pages.

Dixon, J., and L.R. Snowdon. 1979. Geology and organic geochemistry of the Dome Hunt Nektoralik K-59 well, Beaufort Sea. In, Current Research, Part C, Geological Survey of Canada Paper 79-1C: 85-90.

Dome Hunt 1979. Well History Report, Dome Hunt Kenalooak J(N)-94.

Dome Petroleum Ltd. 1977. Well History Report, Dome Hunt Nektoralik K-59.

Dome Petroleum Ltd. 1979. Well History Report, Dome Gulf Hunt Kopanoar L-34.

Dome Petroleum Ltd. 1980. Well History Report, Dome Kopanoar I-44.

Dome Petroleum Ltd. 1982. Well History Report, Dome Aiverk I-45.

Dome Petroleum Ltd. 1982. Well History Report, Dome Aiverk 2I-45.

Dome Petroleum Ltd. 1982. Well History Report, Dome Hunt Irkaluk B-35.

Dome Petroleum Ltd. 1982. Well History Report, Dome Nerlerk M-98.

Dome Petroleum Ltd. 1983. Well History Report, Dome Natiak O-44.

Dome Petroleum Ltd. 1984. Well History Report, Dome Nerlerk J-67.

EBA Engineering Consultants Ltd. 1990. Correlation of Acoustic and Physical Properties of Deep Permafrost, Canadian Beaufort Sea. Draft Report.

Edmonds, A.D. 1973. *Voyage to the edge of the world*, Toronto, McClelland and Stewart. ISBN 0771030673: 254 pages.

Engels, J.L., Edwards, M.H., Polyak, L., Johnson, P.D. 2008. Seafloor evidence for ice shelf flow across the Alaska-Beaufort margin of the Arctic Ocean. *Earth Surface Processes and Landforms*. 33. 1047-1063.

Evans, R. J., S. A. Stewart and R. J. Davies. 2008. The structure and formation of mud volcano summit calderas. *Journal of the Geological Society*, 165: 769–780.

Forest, A., M. Babin, L. Stemmann, M. Picheral, M. Sampei, L. Fortier, Y. Gratton, S. Belanger, E. Devred, J. Sahlin, D. Doxaran, F. Joux, E. Ortega-Retuerta, W. H. Jeffrey, J. Martín, B. Gasser, and J. C. Miquel. 2012. Ecosystem function and particle flux dynamics across the Mackenzie Shelf (Beaufort Sea, Arctic Ocean): an integrative analysis of spatial variability and biophysical forcings. *Biogeosciences Discussions*, 9: 10883–10960, 2012 doi:10.5194/bgd-9-10883-2012.

Fortin G. and S.M., Blasco. 1990. *Regional Geological Framework for the Late Neogene/Quaternary Strata Beneath the Canadian Beaufort Continental Shelf*. Report submitted to the Geological Survey of Canada: 180 pages.

Gales, J.A., R. D. Larter, N. C. Mitchell and J. A. Dowdeswell. 2013. Geomorphic signature of Antarctic submarine gullies: Implications for continental slope processes. *Marine Geology*, 337: 112-124. <http://dx.doi.org/10.1016/j.margeo.2013.02.003>.

Gulf 1984-1985. Well History Report, Akpak P-35.

Gulf 1985. Well History Report Akpak 2P-35.

Gulf Canada Corporation 1986. Gulf *et al.* Aagnerk E-56 End of Well History Report, Gulf Canada Corporation.

Gulf Canada Resources Inc. 1982. Well History Report for Gulf *et al.* North Issungnak L-86. Drilling Authority No. 978.

Gulf Canada Resources Ltd. 1988. Well History Report Gulf *et al.* Amauligak 2F-24.

Gulf Canada Resources Ltd. 1988. Well History Report Gulf *et al.* Amauligak 2F-24A.

Gulf Canada Resources Ltd. 1988. Well History Report Gulf *et al.* Amauligak 2F-24B.

Gulf Canada Resources Ltd. 1988. Well History Report Gulf *et al.* Amauligak 2F-24BST.

Gulf Canada Resources Ltd. 1989. Gulf Canada Resources Limited Drilling Program. Gulf *et al.* Immiugak N-05.

Hafliðason, H., H. P. Sejrup, A. Nygard, J. Mienert, P. Bryn, R. Lien, C. F. Forsberg, K. Berg and D. Masson. 2004. The Storegga Slide: architecture, geometry and slide development. *Marine Geology*, 213: 201–234.

Hasegawa, H. S., C. W. Chou, and P. W. Basham. 1979. Seismotectonics of the Beaufort Sea. *Canadian Journal of Earth Sciences*, 16: 816-830.

Heier -Nielsen, K. Conradsen, J. Heinemeier, K. L. Knudsen, H. L. Nielsen, N. Rud and A. E. Sveinbjornsdottir. 1995. Radiocarbon dating of shells and foraminifera from the Skagen core, Denmark: evidence of reworking. *Proceedings of the 15th International 14C Conference* (eds: G. T. Cook, D. D. Harkness, B. F. Miller and E. M. Scott). *Radiocarbon*, 37 (2): 119-130.

Helwig, J., N. Kumar, P. Emmet and M. G. Dinkelman. 2011. Regional Seismic Interpretation of Crustal Framework and Petroleum Potential, Canadian Arctic Passive Margin, Beaufort Sea. Chapter 35 in, *Arctic Petroleum Geology* (eds. Spencer A.M., A. Embry, D. Gautier, A. Stoupakova and K. Sorensen). *Geological Society Memoir No. 35*: 527-543. doi:10.1144/M35.35.

Hill, P.R., Hequette, A., and Ruz, M-H. 1993. Holocene sea-level history of the Canadian Beaufort Shelf. *Canadian Journal of Earth Sciences*, 30: 103-108.

Hill, P.R., Hequette, A., Ruz, M-H. and Jenner, K.A., 1991. Geological Investigations of the Canadian Beaufort Sea Coast. Hill Geoscience Research Project No: 88-1. Geological Survey of Canada Open File Report 2387.

Hill, P.R., J.P. Mudie, K. Moran and S.M. Blasco. 1985. A sea-level curve for the Canadian Beaufort Shelf. *Canadian Journal of Earth Sciences*, 22: 1383-1393.

Hill, P.R., K.M. Moran and S.M. Blasco. 1982. Creep deformation of slope sediments in the Canadian Beaufort Sea, *Geo-Marine Letters*, 2: 163-170.

Hinz, K, G. Delisle and M. Block. 1998. Seismic evidence for the depth and extent of permafrost in shelf sediments of the Laptev Sea, Russian Arctic. *Proceedings: Permafrost - Seventh International Conference, Yellowknife, Collection Nordicana 55*: 453-457.

Hu, K., D.R. Issler, Z. Chen and T.A. Brent. 2013. Permafrost investigation by well logs, and seismic velocity and repeated shallow temperature surveys, Beaufort-Mackenzie Basin. Geological Survey of Canada, Open File 6956: 33 p.

Hunt International Petroleum 1979. Well History Report, Dome Hunt Kopanoar M-13.

Hyndman, R D; Cassidy, J F; Adams, J; Rogers, G C; Mazzotti, S. 2005. *Canadian Society of Exploration Geophysicists, Recorder vol. 30, May, 2005*: 9 pages.

Jakobsson, M. L. Polyak, M. Edwards, J. Kleman and B. Coakley. 2008. Glacial geomorphology of the Central Arctic Ocean: The Chukchi Borderland and the Lomonosov Ridge. *Earth Surface Processes and Landforms*, 33: 526-545.

Jenner, K.A. and S.M. Blasco In prep. Piston cores from MR02-K05 RV Mirai, Mackenzie Trough, Beaufort Sea: data and interpretations. Geological Survey of Canada Open File.

Jones, P.B., J. Braches and J.K. Lentin. 1980. The geology of the 1977 offshore hydrocarbon discoveries in the Beaufort -Mackenzie basin, N.W.T. *Bulletin of Petroleum Geology*, 28: 81-102.

Judd, A. and Hovland, M., 2007. *Seafloor Fluid Flow: The Impact on Geology, Biology and the Marine Environment*. Cambridge University Press.

Judge, A. S. and J. A Majorowicz. 1992. Geothermal conditions for gas hydrate stability in the Beaufort-Mackenzie area – the global change aspect. *Paleogeography Paleoclimatology and Paleoecology*, Global and Planetary Change Section, 98: 251–263.

Judge, A.S., S.L. Smith and J.A. Majorowicz. 1994. The current distribution and thermal stability of natural gas hydrates in the Canadian Polar margin. In, *Proceedings of the IVth International Offshore and Polar Engineering Conference*, Osaka. The International Society of Offshore Polar Engineering, VI: 307-314

Judge, A. S., B.R. Pelletier and I. Norquay. 1987. Permafrost base and distribution of gas hydrates. In, *Marine Science Atlas of the Beaufort Sea: Geology and Geophysics*, Geological Survey of Canada Miscellaneous Report 40 (ed. B. R. Pelletier): page 39 doi:10.4095/126940.

King, M. S., B. I. Pandit, J. A. Hunter, and M. I. Gajtani. 1982. Some seismic, electrical and thermal properties of sub-seabottom permafrost samples from the Beaufort Sea. 4th Canadian Permafrost Conference, Ottawa: 268–273.

Kvalstad, T. J., L. Andresen, C. F. Forsberg, K. Berg, P. Bryn and M. Wangen. 2005. The Storegga slide: evaluation of triggering sources and slide mechanics. *Marine and Petroleum Geology*, 22: 245–256. doi:10.1016/j.marpetgeo.2004.10.019.

Kvenvolden, K. A. and Barnard, L. C., 1983. Hydrates of Natural Gas in Continental Margins. In *Studies in Continental Margin Geology*. Edited by G. S. A. Drake and C. L. Watkins. American Association of Petroleum Geologists Memoir 34: 631-640.

Laberg, J.S. and T.O. Vorren. 2000. The Trænadjupet Slide, offshore Norway - morphology, evacuation and triggering mechanisms. *Marine Geology*, 171: 95-114.

Lakeman, T.R., B. MacLean, S. Blasco, R. Bennett and J.E. Hughes Clarke. 2012. Chronology and dynamics of the Amundsen Gulf Ice Stream in Arctic Canada during the

last glacial-interglacial transition Geophysical Research Abstracts Vol. 14, EGU2012-12907-1, 2012.

Lamar Hunt 1976. Well History Report, Hunt Dome Kopanoar D-14.

Lane, L.S. 2002. Tectonic evolution of the Canadian Beaufort Sea-Mackenzie delta region: A brief review. Recorder, Canadian Society of Exploration Geophysicists, 27 (2): 49–56.

Lane, L.S. 1997. Canada Basin, Arctic Ocean: Evidence against a rotational origin. Tectonics, 16 (3): 363-387.

Lastras, G., M. Canals, D. Amblas, M. Ivanov, B. Dennielou, L. Droz, A. Akhmetzhanov and TTR-14 Leg 3 Shipboard Scientific Party. 2006. Eivissa slides, western Mediterranean Sea: morphology and processes. Geo-Marine Letters, 26 (4). <http://dx.doi.org/10.1007/s00367-006-0032-4>.

Lemmen, D.S, A. Duk-Rodkin and J.M. Bednarski. 1994. Late glacial drainage systems along the northwestern margin of the Laurentide ice sheet. Quaternary Science Reviews, 13: 805–828.

Leonard, L. J., R.D. Hyndman, and G.C. Rogers. 2010. Towards a national tsunami hazard map for Canada: tsunami sources. In, Proceedings of the 9th U.S. National and 10th Canadian Conference on Earthquake Engineering, July 25-29, 2010, Toronto. Paper No. 1844: 10 pages.

Lewis, J. and L. Meagher. 1991. Upper Tertiary and Quaternary Geology and morphology of the Western Beaufort (Yukon) Continental Shelf and Slope. Report submitted to Department of Supply and Services Canada.

MacAulay, H. A., and J. A. Hunter. 1982. Detailed seismic refraction of ice-bonded permafrost layering in the Canadian Beaufort Sea: 4th Canadian Permafrost Conference: 256–267.

MacKay, J. R. 1972. Offshore Permafrost and Ground Ice, Southern Beaufort Sea. Canadian Journal of Earth Sciences, 9 (11): 1550-1561.

MacLean, B., S. Blasco, R. Bennett, T. Lakeman, J. Hughes-Clarke, P. Kuus and E. Patton. 2015. New marine evidence for a Late Wisconsinan ice stream in Amundsen Gulf, Arctic Canada. Quaternary Science Reviews, 114: 149-166.

Majorowicz, J.A. and P.K. Hannigan. 2000. Natural Gas Hydrates in the Offshore Beaufort-Mackenzie Basin - Study of a Feasible Energy Source II. Natural Resources Research, 9 (3): 201-214.

Majorowicz, J.A. and K. Osadetz. 1999. Basic geological and geophysical indications of gas-hydrate distribution and volume in Canada. Geological Survey of Canada Open File 3780: 21 pages plus 16 figures.

Mathis, J.T., R.S. Pickart, D.A. Hansell, D. Kadko and N.R. Bates. 2007. Eddy transport of organic carbon and nutrients from the Chukchi shelf into the deep Arctic basin. *Journal of Geophysical Research* 112. doi:10.1029/2006JC00389.

McNeil, D.H., N.S. Ioannides and J. Dixon. 1982. Geology and biostratigraphy of the Dome Gulf *et al.* Ukalerk C-50 well, Beaufort Sea. Geological Survey of Canada Paper 80-32: 17 pages.

McNeely R., A. S. Dyke and J. R. Southon. 2006. Canadian marine reservoir ages, preliminary data assessment. Open File 5049, Geological Survey Canada.

MGL (McGregor Geoscience Ltd.). 1992a. Seismo-stratigraphic analysis and geohazard evaluation - Mackenzie Trough. DSS File No. 23420-0-M568/01-OSC. Volume 1: pages 1-174; Volume 2: pages 175-262. Submitted to the Geological Survey of Canada.

MGL (McGregor Geoscience Ltd.). 1992b. Processing and modeling of seismic data at the Amauligak 3F24 borehole site - implications for geological interpretation. Three volumes. Submitted to Dept. of Energy Mines and Resources. Dept. of Supply and Services Number 23420-0M567/01-OSC.

MGL (McGregor Geoscience Ltd.). 1987. Surficial geology of the Mackenzie Trough, Canadian Beaufort Sea. DSS File No. 10SC.23420-6-M549. 85 pages plus appendices. Submitted to the Geological Survey of Canada.

Micallef, A., D. G. Masson, C. Berndt and D.A.V. Stow. 2009. Development and mass movement processes of the north-eastern Storegga Slide. *Quaternary Science Reviews*, 28 (5-6): 433-448. <http://dx.doi.org/10.1016/j.quascirev.2008.09.026>.

Micallef, A., C. Berndt, D. G. Masson and D.A.V. Stow. 2007a. Submarine spreading: dynamics and development. In: Lykousis, V., Sakellariou, D., Locat, J. (Eds.), *Advances in Natural and Technological Hazards Research*. Springer, Netherlands: 119–128.

Micallef, A., C. Berndt, D.G. Masson and D.A.V. Stow. 2007b. A technique for the morphological characterization of submarine landscapes as exemplified by debris flows of the Storegga Slide. *Journal of Geophysical Research* 112, F02001.

Milkov, A.V., R. Sassen, I. Novikova and E. Mikhailov, 2000. *Gulf Coast Association of Geological Societies Transactions*, Volume L: 217-224.

Morack, J. L., H. A. MacAulay, and J. A. Hunter. 1983. Geophysical measurements of subbottom permafrost in the Canadian Beaufort Sea. In, *Proceedings, Permafrost, Fourth International Conference*: 866–871. National Academy Press, Washington, D. C.

Moran, K.M., P.R Hill and S.M. Blasco. 1989. Interpretation of piezocone penetrometer profiles in sediment from the Mackenzie Trough, Canadian Beaufort Sea. *Journal of Sedimentary Petrology*, 59 (1): 88-97.

Mosher, D. C. 2009. International Year of the Planet Earth 7. Oceans: Submarine Landslides and Consequent Tsunamis in Canada. *Geoscience Canada*, 36 (4): 179-190.

Mosher, D. C., J. Shimeld, D. Hutchinson, N. Lebedeva-Ivanova and C. Borden Chapman. 2012. Submarine landslides in Arctic sedimentation: Canada Basin. In, *Submarine Mass Movements and their Consequences. Advances in Natural and Technological Hazards Research*, Volume 31 (2): 147-157 . DOI: 10.1007/978-94-007-2162-3_13.

Mosher, D.C., Shimeld, J., Hutchinson, D., Lebedeva-Ivanova, N., and Chapman, C.B., 2011. Submarine Landslides in Arctic Sedimentation: Canada Basin. In: Yamada, Y., Kawamura, K., Ikehara, K., Ogawa, Y., Urgeles, R., Mosher, D., Chaytor, J. And Strasser, M. (eds). *Submarine Mass Movements and Their Consequences V, Advances in Natural and Technological Hazards Research*, Vol 29.

Murton, J. B., M. D. Bateman, S. R. Dallimore, J. T. Teller & Z. Yang. 2010. Identification of Younger Dryas outburst flood path from Lake Agassiz to the Arctic Ocean. *Nature, Letters*, 464: 740-743. doi:10.1038/nature08954.

Murton, J.B., M. Frechen and D. Maddy. 2007. Luminescence dating of Mid- to Late Wisconsinan aeolian sand as a constraint on the last advance of the Laurentide Ice Sheet across the Tuktoyaktuk Coastlands, western Arctic Canada. *Canadian Journal of Earth Sciences*, 44: 857–869.

NEB (National Energy Board). 1998. Probabilistic estimate of hydrocarbon volumes in the Mackenzie Delta and Beaufort Sea discoveries January 1998. 8 pages. ISBN 0-662-27455-5.

Neurauter, T. W. and Bryant, W. R. 1989. Gas Hydrates and Their Association with Mud Diapir/Mud Volcanoes on the Louisiana Continental Slope. *Offshore Technology Conference Proceedings, Twenty-First Annual Offshore Technology Conference*, OTC Paper No. 5944: 599-607.

Niessen, F., J.K. Hong, A. Hegewald, J. Matthiessen, R. Stein, H. Kim, S. Kim, L. Jensen, W. Jokat, S. Nam and S. Ka. 2013. Repeated Pleistocene glaciation of the East Siberian continental margin. *Nature Geoscience*, 6: 842-846.

Nikolopoulos, A., R.S. Pickart, P.S. Fratantoni, K. Shimada, D.J. Torres and E.P. Jones. 2009. The western arctic boundary current at 152W: structure, variability, and transport. *Deep Sea Research II*, 56: 1164–1181.

O'Connor, M.J . 1982. A Review of the Distribution and Occurrence of Shallow Acoustic Permafrost in the southern Beaufort Sea: a report prepared for the Geological Survey of Canada, Contract No . 078C-23420-2M562.

O'Connor, M.J. 1981a. Distribution of shallow acoustic permafrost: a report on the southern Beaufort Sea prepared for the Geological Survey of Canada, Contract No . 08SC .23420-0-M531.

O'Connor, M.J. 1981b. Morphology of the shelf edge : a report on the southern Beaufort Sea prepared for the Geological Survey of Canada, Contract No . 08SC .23420-0-M531: 70 pages.

O'Connor, M.J. 1980. Development of a proposed model to account for the surficial geology of the southern Beaufort Sea: a report prepared for the Geological Survey of Canada, Contract No. OSC79-00212. Geological Survey of Canada Open File Report No. 954: 128 pages.

O'Connor, M.J. and S.M. Blasco. 1987a. Subsea acoustically defined permafrost (APF types). In, Marine Science Atlas of the Beaufort Sea: Geology and Geophysics (B.R. Pelletier, ed.). Geological Survey of Canada Miscellaneous Report 40: page 35.

O'Connor, M.J. and S.M. Blasco. 1987b. Subsea acoustically defined permafrost (APF distribution). In, Marine Science Atlas of the Beaufort Sea: Geology and Geophysics (B.R. Pelletier, ed.). Geological Survey of Canada Miscellaneous Report 40: page 36.

O'Connor, M.J. and S.M. Blasco. 1986. Surficial geology of the Mackenzie Trough. Report prepared for the Geological Survey of Canada, 1985. Job No. 10-154.3. 188 pages.

O'Connor, M.J. and S.M. Blasco. 1984. Geotechnical characteristics of the shallow sediments of the Akpak Plateau, Kringalik Plateau and Tingmiark Plain regions of the Canadian Beaufort Shelf: a report prepared for the Geological Survey of Canada, Job No. 60-564. 363 pages. Revised version, December 1987.

O'Connor, M.J. and S.M. Blasco. 1984. Distribution and occurrence of frozen subseabottom sediments: a comparison of geotechnical and shallow seismic evidence from the Canadian Beaufort Sea. Report submitted to the Geological Survey of Canada.

O'Connor, M.J. and S.M. Blasco. 1982. An evaluation of the regional surficial geology of the southern Beaufort Sea. Job No. 10-127: 188 pages.

O'Connor, M.J. and Blasco, S.M., March 1980. An Evaluation of the Regional Surficial Geology of the Southern Beaufort Sea, 188 pages 98 accessions, 1 map.

Osadetz, K.G. and Z. Chen. 2010. A re-evaluation of Beaufort Sea-Mackenzie Delta basin gas hydrate resource potential: petroleum system approaches to non-conventional gas resource appraisal and geologically-sourced methane flux. Bulletin of Canadian Petroleum Geology, 58 (1): 56-71; DOI: 10.2113/gscpgbull.58.1.56

Parker, G. 1982. Conditions for the ignition of catastrophically erosive turbidity currents . *Marine Geology*, 46: 307--327.

Paull, C., S. Dallimore, John Hughes-Clarke, S. Blasco, E. Lundsten, W. Ussler III, D. Graves, A. Sherman, K. Conway, H. Melling, S. Vagle, and T. Collett. 2011. Tracking the decomposition of submarine permafrost and gas hydrate under the shelf and slope of the Beaufort Sea. Paper 328 in the Special Session - Gas Hydrates & Global Climate Change, 17-21 July 2011, Edinburgh, Scotland.

Paull, C.K, W. Ussler, S.D. Dallimore, S.M. Blasco, T.D. Lorenson, H. Melling, B.E. Medioli, F.M. Nixon and F.A. McLaughlin. 2007. Origin of pingo-like features on the Beaufort Sea Shelf and their possible relationship to decomposing methane gas hydrates. *Geophysical Research Letters*, 34: 1-5.

Pelletier, B.R. 1987a. *Marine Science Atlas of the Beaufort Sea: Geology and Geophysics* (B.R. Pelletier, ed.). Geological Survey of Canada Miscellaneous Report 40: 39 pages.

Pelletier, B.R. 1987b. Late Quaternary Glaciation and Sea Level History. In, *Marine Science Atlas of the Beaufort Sea: Geology and Geophysics* (B.R. Pelletier, ed.). Geological Survey of Canada Miscellaneous Report 40: page 28.

Pelletier, B.R. 1984. *Marine Science Atlas of the Beaufort Sea: Sediments* (B.R. Pelletier, ed.). Geological Survey of Canada Miscellaneous Report 38: 26 pages.

Peltier, W.R. 2002. On eustatic sea level history: Last Glacial Maximum to Holocene. *Quaternary Science Reviews* 21: 377–396.

Peltier, W.R. and R.G. Fairbanks. 2006. Global glacial ice volume and Last Glacial Maximum duration from an extended Barbados sea level record. *Quaternary Science Reviews* 25: 3322–3337.

Permafrost Subcommittee. 1988. *Glossary of Permafrost Terms and Related Ground-Ice Terms*. National Research Council of Canada Technical Memorandum No. 142: 156 pages.

Picard, K., A. Wickert and Hill, Philip R. 2012. Insights into the timing of submarine landslide events on the Beaufort slope from sea level and stratigraphic modeling. Abstract in, ArcticNet 2012 Annual Meeting, Vancouver, B.C. Programme: page 139.

Pickart, R.S., D.J. Torres and P.S. Fratantoni. 2004. Shelfbreak circulation in the Alaskan Beaufort Sea: mean structure and variability. *Journal of Geophysical Research*, 109. doi:10.1029/2003JC001,912.

Piper, D. 2012. How geological framework explains the distribution of geohazards, geoconstraints and geoinsights for offshore development in the deep-water eastern

Canadian margin. Abstract, Geological Association of Canada - Mineralogical Association of Canada joint annual meeting, St. John's, Newfoundland, May 27-29.

Piper D.J.W. 2005. Late Cenozoic evolution of the continental margin of eastern Canada. *Norwegian Journal of Geology*, 85: 305-318.

Piper D.J.W. & D.C. Campbell. 2005. Quaternary geology of Flemish Pass and its application to geohazard evaluation for hydrocarbon development. GAC Special Paper 43: 29-43.

Piper D.J.W., P. Cochonat and M. Morrison. 1999. Sidescan sonar evidence for progressive evolution of submarine failure into a turbidity current: the 1929 Grand Banks event. *Sedimentology*, 46: 79-97.

Poley, D.F. and D.C. Lawton. 1991. A model study of multichannel reflection seismic imaging over shallow permafrost in the Beaufort Sea continental shelf. *Canadian Journal of Exploration Geophysics*, 27 (1): 34-42.

Pullan, S., H. A. MacAulay, J. A. M. Hunter, R. L. Good, R. M. Gagne, and R. A. Burns. 1987. Permafrost distribution determined from seismic refraction. In, *Marine Science Atlas of the Beaufort Sea: Geology and Geophysics*, Misc. Rep. 40, 39 p. (page 37). Edited by B. R. Pelletier. Geological Survey of Canada, Ottawa, Canada, doi:10.4095/126940.

Quinn, P., M. S. Diederichs, D. J. Hutchinson and R. K. Rowe. 2007. An exploration of the mechanics of retrogressive landslides in sensitive clay. *OttawaGeo2007: The Diamond Jubilee: 60th Canadian Geotechnical Conference and 8th Joint CGS/IAH-CNC Groundwater Conference: Conference Proceedings*, October 21-25, 2007, Ottawa, Canada: 721-727.

Ramachandran, K., G. Bellefleur, T. Brent, M. Riedel, and S. Dallimore. 2011. Case History: Imaging permafrost velocity structure using high resolution 3D seismic tomography. *Geophysics*, 76 (5): B187–B198.

Rankin, S., E. Carr, P. Campbell and S. Blasco. 2013. 2011 Beaufort Seabed Mapping Program – Geological Analysis and Geohazard Assessment. Draft Report prepared by Canadian Seabed Research Ltd. for the Geological Survey of Canada Atlantic. CSR Project No. 13150: 121 pages.

Rankin, S., E. Carr, P. Campbell and S. Blasco. 2011. 2010 Beaufort Seabed Mapping Program – Geological Analysis and Geohazard Assessment. Draft Report prepared by Canadian Seabed Research Ltd. for the Geological Survey of Canada Atlantic. CSR Project No. 10173: 81 pages.

Rankin, S., E. Carr, P. Campbell and S. Blasco. 2010. 2009 Beaufort Seabed Mapping Program – Geological Analysis and Geohazard Assessment. Draft Report prepared by

Canadian Seabed Research Ltd. for the Geological Survey of Canada Atlantic. CSR Project No. 10152: 84 pages.

Reimer, P. J., M. G. L. Baillie, E. Bard, A. Bayliss, J. W. Beck, P. G. Blackwell, C. Bronk Ramsey, C. E. Buck, G. S. Burr, R. L. Edwards, M. Friedrich, P. M. Grootes, T. P. Guilderson, I. Hajdas, T. J. Heaton, A. J. Hogg, K. A. Hughen, K. F. Kaiser, B. Kromer, F. G. McCormac, S. W. Manning, R. W. Reimer, D. A. Richards, J. R. Southon, S. Talamo, C. S. M. Turney, J. van der Plicht and C. E. Weyhenmeyer. 2009. Intcal09 and Marine09 radiocarbon age calibration curves, 0-50,000 years cal BP. *Radiocarbon*, 51: 1111-1150.

Rohling, E. J., M. Fenton, F. J. Jorissen, P. Bertrand, G. Ganssen and J. P. Caulet. 1998. Magnitudes of sea-level lowstands of the past 500,000 years. *Nature*, 394, 9 July 1998: 162-165.

Richardson, S. E. J., R. J. Davies, M. B. Allenn and S. F. Grant. 2011. Structure and evolution of mass transport deposits in the South Caspian Basin, Azerbaijan. *Basin Research*, 23: 702–719, doi: 10.1111/j.1365-2117.2011.00508.x.

Robertson, A.H.F. and A. Kopf. 1998. Tectonic setting and processes of mud volcanism on the Mediterranean ridge accretionary complex: evidence from leg 1601. Chapter 50, in: *Proceedings of the Ocean Drilling Program, Scientific Results*, Vol. 160 (Robertson, A.H.F., Emeis, K.-C., Richter, C., and Camerlenghi, A., Eds.): 665-680.

Ruffell, J.P., T.R. Murphy, and C. Graham. 1990. Planning and execution of a 500m corehole through permafrost, *Proceedings. Proceedings of the Fifth Canadian Permafrost Conference, Collection Nordicana No. 54. l'Université Laval, Québec: 271-282.*

Ruppel, C., P Hart, and C. Worley. 2010. Degradation of subsea permafrost and associated gas hydrates offshore of Alaska in response to climate change. *Sound Waves Volume FY 2011, Issue No. 128, October/November 2010: 1-3.*

Saint-Ange, F., P. Kuus, S. Blasco, D. J.W. Piper, J. Hughes Clarke and K. MacKillop. 2014. Multiple failure styles related to shallow gas and fluid venting, upper slope Canadian Beaufort Sea, northern Canada. *Marine Geology* 355: 136–149.

Sawyer, D. E., P. B. Flemings, B. Dugan, and J. T. Germaine. 2009. Retrogressive failures recorded in mass transport deposits in the Ursa Basin, Northern Gulf of Mexico. *Journal of Geophysical Research*, 114 (B10102): 20 pages. doi:10.1029/2008JB006159.

Schell, T.M., Scott, D.B., Rochon, A. and Blasco, S. 2008. Late Quaternary paleoceanography and paleo sea-ice conditions in the Mackenzie Trough and Canyon, Beaufort Sea. *Canadian Journal of Earth Sciences*, 45, 1399-1415, doi:10.1139/E08-054.

Scott, D.B., Schell, T., St-Onge, G., Rochon, A. and Blasco, S. 2009. Foraminiferal assemblage changes over the last 15,000 years on the Mackenzie-Beaufort Sea slope and Amundsen Gulf, Canada: implications for past sea ice conditions. *Paleoceanography*, 24, PA2219, doi:10.1029/2007PA001575.

Shearer, J.M. 1971. Preliminary interpretation of shallow seismic reflection profiles from west side of Mackenzie Bay, Beaufort Sea. In, Report of Activities, Part B, Geological Survey of Canada, Paper 71-1: 131-138.

Smith, S.L. and A.S. Judge. 1993. Gas hydrate database for Canadian Arctic and selected East Coast wells. Geological Survey Canada, Open File Report 2746: 120 pages.

Spall, M.A., R.S. Pickart, P.S. Fratantoni and A.J. Plueddemann. 2008. Western Arctic shelfbreak eddies: formation and transport. *Journal of Physical Oceanography*, 38: 1644–1668.

Spagnolo, M., C. D. Clark, J. C. Ely, C. R. Stokes, J. B. Anderson, K. Andreassen, A. G. C. Graham and E. C. King. 2014. Size, shape and spatial arrangement of mega-scale glacial lineations from a large and diverse dataset. *Earth Surface Processes and Landforms*, 39: 1432–1448.

Stokes, C. R., C. D. Clark and M. C. M. Winsborrow. 2006. Subglacial bedform evidence for a major palaeo-ice stream and its retreat phases in Amundsen Gulf, Canadian Arctic Archipelago. *Journal of Quaternary Science*, 21(4): 399–412.

Stuiver, M., P. J. Reimer and R. W. Reimer. 2005. CALIB 5.0. [WWW program and documentation].

Stuiver, M. and P.J. Reimer. 1993. Extended 14C data base and revised CALIB 3.0 14C age calibration program. *Radiocarbon*, 35: 215-230.

Taylor, A. E., S. R. Dallimore, P. R. Hill, D. R. Issler, S. Blasco and F. Wright. 2013. Numerical model of the geothermal regime on the Beaufort Shelf, arctic Canada since the Last Interglacial. *Journal of Geophysical Research: Earth Surface*, 118: 1–15. doi:10.1002/2013JF002859.

Taylor, A., A. Judge, and V. Allen. 1989. Recovery of precise offshore temperatures from a deep geotechnical hole, Canadian Beaufort Sea. In, Current Research Part D, Geological Survey of Canada, Paper 89-1D: 119–123.

Törnqvist, T. E. and M. P. Hijma. 2012. Links between early Holocene ice-sheet decay, sea-level rise and abrupt climate change. *Nature Geoscience*, 5: 601-606.

van Everdingen, R. 1998. Multi-language glossary of permafrost and related ground-ice terms. Boulder, Colorado, National Snow and Ice Data Center. Revised May 2005.

Votyakov, I.N. 1973. Structural transformations in frozen soils on variation of the ground temperature. In, Permafrost: USSR Contribution to the International Conference (edited by F.J. Sanger with assistance of P.J. Hyde). Published in 1978, National Academy of Sciences, Washington, D.C.: 264 – 267.

Weaver, J.S., and J.M. Stewart. 1982. In situ hydrates under the Beaufort Sea Shelf. In Proceedings, Fourth Canadian Permafrost Conference (editor H.M. French), Ottawa. National Research Council of Canada: 312-319.

Weber, W.S., P.W. Barnes, and E. Reimnitz. 1989. Data on the Characteristics of Dated Gouges on the Inner Shelf of the Beaufort Sea, Alaska; 1977-1985. USGS Open-File Report 89-151.

Werner, F., G. Unsold, B. Koopman, and A. Stefanon, 1980. Field observations and flume experiments on the nature of comet marks. *Sedimentary Geology* 26, 233-262.

Yelisetti, S. and S. Dosso. 2015. New Seismic Studies in the Beaufort Sea Contract Report No. 3000566280 for Natural Resources Canada, Geological Survey of Canada Pacific, Sidney Subdivision: 43 pages.

Zhu, T., Y. Yan and J. Downton J. 2011. Near-surface velocity model building and statics in permafrost regions. Canadian Society of Petroleum Geologists, Canadian Society of Exploration Geophysicists, Canadian Well Logging Society (CSPG, CSEG, CWLS) "Recovery" Convention.



A Methodology: Radiocarbon Age Calibration

A total of 98 radiocarbon (C_{14}) dates, from 47 cores, boreholes and wells were calibrated to assist in constraining the age relationship between stratigraphies on the shelf, slope and in Mackenzie Trough. These C_{14} ages were compiled from samples collected during previous expeditions within the Beaufort Sea and were converted to cal years BP to obtain the sample's true age.

Calibration was completed using CALIB 6.0.0 software developed at the Quaternary Isotope Lab, University of Washington, initially published in 1986 (Stuiver and Reimer, 1993; Stuiver *et al.* 2005). CALIB converts the C_{14} date to calibrated calendar years, considered to be the sample's true age, by calculating a probability distribution for that sample (Stuiver and Reimer, 1993; Stuiver *et al.* 2005).

A calibration dataset, chosen based on the type of sample used and location, is input into the software for the age conversion. A number of calibration datasets are available, and it was decided to use the Marine09 calibration dataset for C_{14} dates of marine samples, such as shells, within the present study area (Stuiver and Reimer, 1993; Stuiver *et al.* 2005).

The Marine09 calibration dataset (Reimer *et al.* 2009) represents the "global" ocean and uses a default Mean Global Reservoir Correction (408 years) during the age calibrations to account for the varying degrees of C_{14} exposure. A local reservoir correction (ΔR) was calculated to accommodate local effects of radiocarbon exposure and used for the calibration of Beaufort Sea samples (Stuiver and Reimer, 1993).

The local reservoir correction (ΔR) for the study area was determined from six reference samples collected along the Arctic Ocean coastal region between Prince Patrick Island (Northwest Territories), Dolphin & Union Strait (Nunavut) and Point Barrow (Alaska) (McNeely *et al.* 2006; Coulthard *et al.* 2010). Reservoir corrections for the reference samples range from 180 years to 560 years, with a mean value of 428.5 years. The calculated local mean reservoir correction agrees with the correction value of 420 years used by Jenner and Blasco (in prep.). Taking into consideration the variation in reservoir corrections from six samples, a local reservoir correction (ΔR) of 420 ± 40 years was used for the region investigated in this study.

Ages were calibrated using a reference date of 1950 as a calibrated year zero since any sample formed since the mid-1950s would have high initial C_{14} levels due to nuclear testing. A standard deviation is provided for each calibrated C_{14} age based on the uncertainty associated with ΔR ; the ΔR uncertainty is assumed to be independent for each sample (Stuiver and Reimer, 1993; Stuiver *et al.* 2005).

As suggested by Stuiver and Reimer (1993), results for samples with standard deviation in the radiocarbon age >50 years are rounded to the nearest 10 years (e.g., 8015 ± 63 cal years BP = 8020 ± 63 cal years BP). Samples with standard deviation less than 50 years are unchanged. Radiocarbon ages for Beaufort Sea samples, including uncalibrated ages, calibrated ages and rounded calibrated ages, are presented in Table B.1 of Appendix B.



B Calibrated C₁₄ Dates and Sedimentation Rates

Table B.1: C₁₄ dates for cores located within the Beaufort Sea. Age calibrations were completed using the radiocarbon calibration program 'Calib Rev 6.0.0'.

Well/Borehole/Piston Core	Year	Easting (NAD83 Z8)	Northing (NAD83 Z8)	Water Depth (m)	Core Length (cm)	Sample Type	Sample Depth (cm BSF)	Uncalibrated C ₁₄	Calibrated Age (Year BP ±1σ)	Calibrated Age (Rounded If σ >50 Years)	Lab No.
Uviluk P-66	1983	601305.74	7797412.09	30	-	Wood, herb frag.	94-114	21620 ±630	25894 ±867	25890 ±867	B-6276
Tarsiut N-44	1981	454194.67	7754828.99	12	-	Peat	14100	27380 ±470	31622.5 ±430.5	31620 ±430.5	B-5069
750 or 2004804_0015	2004	533808.86	7899965.51	1087	586	Foraminifera	179-180	10865 ±30	11522.5 ±139.5	11520 ±139.5	UGAMS-27757
750 or 2004804_0015	2004	533808.86	7899965.51	1087	586	Foraminifera	381	12450 ±90	13479 ±121	13480 ±121	BETA-206657
2004-804-912A	2004	385043.82	7711485.72	54	-	Shell	93	1420 ±40	1316 ±25	1316 ±25	BETA237046
Kopanoar I-44 Borings 2,3	1980	474542.67	7821776.51	58	-	-	~80	18400	-	-	-
Kopanoar I-44 Borings 2,3	1980	474542.67	7821776.51	58	-	-	~125	28000	-	-	-
2004-804-803	2004	467421.80	7836694.79	218	-	Yoldia myalis	219.08	1530 ±40	672 ±48	672 ±48	-
2004-804-803	2004	467421.80	7836694.79	218	-	Buccinum sp.	221.32	3000 ±40	2249 ±70	2250 ±70	-
2004-804-803	2004	467421.80	7836694.79	218	-	Shell fragments	222.18	3540 ±40	2896 ±80	2900 ±80	-
2004-804-803	2004	467421.80	7836694.79	218	-	Shell fragments	224.08	4560 ±40	4204.5 ±91.5	4200 ±91.5	-
GSC-1	1985	292784.67	7790797.19	41	-	Sediment	46	>53000	Thermoluminescence	-	-
GSC-1	1985	292784.67	7790797.19	41	-	Sediment	54	66000-96000	Thermoluminescence	-	-
GSC-1	1985	292784.67	7790797.19	41	-	Sediment	73	78000-117000	Thermoluminescence	-	-
2009804_0013PC	2009	464606.05	7828387.01	-	300	Mollusc	242	8070 ±35	8100.5 ±64.5	8100 ±64.5	OS-94755
2009804_0013PC	2009	464606.05	7828387.01	-	300	Mollusc	230	7980 ±35	8015 ±63	8020 ±63	OS-94756
2009804_0013PC	2009	464606.05	7828387.01	-	300	Mollusc	191	6490 ±35	6496 ±96	6500 ±96	OS-94757
2009804_0013PC	2009	464606.05	7828387.01	-	300	Mollusc	186	6370 ±35	6351.5 ±56.5	6350 ±56.5	OS-94758
2009804_0013PC	2009	464606.05	7828387.01	-	300	Mollusc	163	6000 ±30	5961 ±64	5960 ±64	OS-94759
2009804_0013_PC	2009	464606.05	7828387.01	-	300	Mollusc	141	5360 ±30	5281.5 ±72.5	5280 ±72.5	OS-94761
2009804_0013PC	2009	464606.05	7828387.01	-	300	Mollusc	55	3230 ±30	2574 ±89	2570 ±89	OS-94762
2009804_0019PC	2009	461342.13	7832237.71	-	-	Mollusc	270	7730 ±35	7768.5 ±64.5	7770 ±64.5	OS-94763
2008802_0038	2008	508413.64	7864403.20	-	-	Mollusc	2	7390 ±35	7467 ±47	7467 ±47	OS-94764
2008802_0038	2008	508413.64	7864403.20	-	-	Mollusc	14	7430 ±35	7505 ±48	7505 ±48	OS-94765
2008802_0038	2008	508413.64	7864403.20	-	-	Mollusc	20	7510 ±35	7564.5 ±51.5	7560 ±51.5	OS-94766
2008802_0038	2008	508413.64	7864403.20	-	-	Mollusc	22	7520 ±30	7581 ±49	7581 ±49	OS-94767
2008802_0038	2008	508413.64	7864403.20	-	-	Mollusc	33	7540 ±35	7600.5 ±48.5	7600.5 ±48.5	OS-94875
2008802_0038	2008	508413.64	7864403.20	-	-	Mollusc	43	7400 ±35	7475 ±48	7475 ±48	OS-94891
2009804_0040PC_A	2009	472100.78	7831896.30	-	-	Mollusc	114	5830 ±30	5791 ±66	5790 ±66	OS-94879
2009804_0040PC	2009	472100.78	7831896.30	-	-	Mollusc	71	4610 ±40	4292 ±87	4290 ±87	OS-94880
2009804_0040PC	2009	472100.78	7831896.30	-	-	Mollusc	91	5600 ±30	5532.5 ±51.5	5530 ±51.5	OS-94892
2009804_0040PC	2009	472100.78	7831896.30	-	-	Mollusc	109	5480 ±30	5393.5 ±69.5	5390 ±69.5	OS-94893
2009804_0040PC_B	2009	472100.78	7831896.30	-	-	Mollusc	114	5860 ±35	5814.5 ±65.5	5810 ±65.5	OS-94894

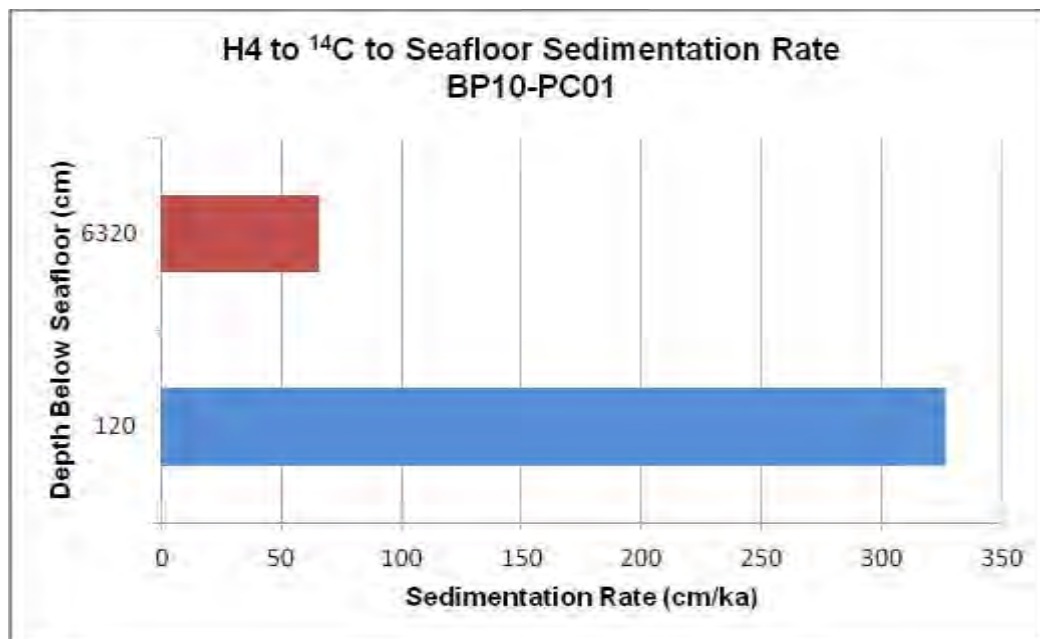
2009804_0026PC	2009	457105.28	7837294.01	-	-	Mollusc	179	7050 ±45	7167.5 ±74.5	7170 ±74.5	OS-94895
2008802_0046	2008	521155.21	7847282.66	-	-	Mollusc	49	1830 ±25	957 ±52	960 ±52	OS-94896
2008-801_0073A	2008	508937.31	7864540.65	-	-	Mollusc	8	9100 ±40	9359 ±67	9360 ±67	OS-94897
2008-801_0073A	2008	508937.31	7864540.65	-	-	Mollusc	15	9130 ±40	9388.5 ±64.5	9390.5 ±64.5	OS-94898
2008-801_0073A	2008	508937.31	7864540.65	-	-	Mollusc	23	9160 ±40	9423.5 ±58.5	9420 ±58.5	OS-94899
2008-801_0073A	2008	508937.31	7864540.65	-	-	Mollusc	25	9170 ±35	9434 ±52	9430 ±52	OS-94906
2008-801_0075_GC	2008	508937.76	7864537.31	-	-	Mollusc	0	40 ±30	40 ±30	40 ±30	OS-94907
2008-801_0078_GC	2008	510888.44	7860355.75	-	-	Mollusc	68	7520 ±40	7578.5 ±54.5	7580 ±54.5	OS-94969
2008-801_0078_GC	2008	510888.44	7860355.75	-	-	Mollusc	77	7250 ±35	7356 ±51	7360 ±51	OS-94970
2002MR_K05_PC01	2002	338854.04	7816399.12	671	1993.5	Foraminifera	704.5-705.5	10480 ±90	11044 ±136	11040 ±136	Keck-UCIAMS 22606
2002MR_K05_PC01	2002	338854.04	7816399.12	671	1993.5	Foraminifera	1000.5-1005.5	10690 ±30	11239 ±47	11239 ±47	Keck-UCIAMS 22607
2002MR_K05_PC02	2002	370409.10	7761125.90	223	1582	Small shell fragment; unknown species	135.0-136.0	3420 ±130	2785 ±177	2790 ±177	Beta-176604
2002MR_K05_PC02	2002	370409.10	7761125.90	223	1582	Small shell fragment; unknown species	560.0-561.0	6670 ±50	6703 ±79	6700 ±79	Beta-176605
2002MR_K05_PC02	2002	370409.10	7761125.90	223	1582	Tiny valve; unknown species	813.0-814.0	8110 ±40	8140.5 ±80.5	8140 ±80.5	Beta-176606
2002MR_K05_PC03	2002	388105.06	7719619.34	57.5	736.5	2 valves; unknown species	27.0-28.0	1060 ±40	310 ±73	310 ±73	Beta-176607
2002MR_K05_PC03	2002	388105.06	7719619.34	57.5	736.5	cf. <i>Mya arenaria</i> (one valve)	20.0-21.0	1090 ±40	327.5 ±61.5	330 ±61.5	Beta-176608
2002MR_K05_PC03	2002	388105.06	7719619.34	57.5	736.5	cf. <i>Mya arenaria</i> (2 valves in life position)	156.5-157.5	2400 ±40	1537.5 ±78.5	1540 ±78.5	Beta-176609
2002MR_K05_PC03	2002	388105.06	7719619.34	57.5	736.5	cf. <i>Mya arenaria</i> (2 valves)	369.0-370.0	3770 ±40	3224.5 ±80.5	3220 ±80.5	Beta-176610
2002MR_K05_PC03	2002	388105.06	7719619.34	57.5	736.5	cf. <i>Macoma</i> sp. (3- 4 fragments of a single valve)	480.5-481.5	4600 ±50	4268.5 ±96.5	4270 ±96.5	Beta-176611
2002MR_K05_PC03	2002	388105.06	7719619.34	57.5	736.5	1 valve; unknown species	550.5-551.5	4890 ±40	4657 ±78	4660 ±78	Beta-176612
2002MR_K05_PC03	2002	388105.06	7719619.34	57.5	736.5	1 valve; unknown species	634.0-635.0	6760 ±50	6805.5 ±81.5	6810 ±81.5	Beta-176613
BP10-PC01	2010	490591.80	7867483.67	484.73	-	B&P forams	116-124	2640 ±130	1819.5 ±166.5	1820 ±166.5	-
BP10-PC02	2010	496431.27	7890418.45	684.66	-	B&P forams	294-302	10670 ±140	11266 ±162	11270 ±162	-
BP10-PC02	2010	496431.27	7890418.45	684.66	-	B&P forams	509-517	13360 ±100	14288 ±31	14288 ±31	-
BP10-PC08	2010	508156.47	7866219.71	141.45	-	B&P forams	414-420	6810 ±120	6864 ±158	6860 ±158	-
BP10-PC08	2010	508156.47	7866219.71	141.45	-	B&P forams	681-687	8220 ±110	8266 ±116	8270 ±116	-
BP10-PC21	2010	480096.74	7877546.92	705.61	-	B&P forams	96-104	14150 ±240	15701.5 ±32.5	15701.5 ±32.5	-
BP10-PC22	2010	479078.63	7893662.92	953.77	-	B&P forams	111-119	14130 ±180	16305.5 ±431.5	16310 ±431.5	-



BP10-PC24	2010	481512.33	7893248.81	908.72	-	B&P forams	127-135	10010 ±220	10444.5 ±274.5	10440 ±274.5	-
BP10-PC24	2010	481512.33	7893248.81	908.72	-	B&P forams	227-245	13320 ±90	14294.5 ±51.5	14290 ±51.5	-
BP10-PC25	2010	531408.17	7873751.23	194.38	-	B&P forams	621-629	11190 ±100	12185 ±192	12190 ±192	-
BP10-PC26	2010	500199.78	7861715.44	104.83	-	B&P forams	75-83.5	12890 ±70	13912 ±92	13910 ±92	-
BP10-PC28	2010	527566.53	7866186.96	83	-	B&P forams	0	10260 ±110	10745.5 ±172.5	10750 ±172.5	-
BP10-PC31	2010	507095.32	7880483.02	432.63	-	B&P forams	303-311	3720 ±130	3141.5 ±171.5	3140 ±171.5	-
BP10-PC31	2010	507095.32	7880483.02	432.63	-	B&P forams	421-429	4830 ±150	4597 ±199	4600 ±199	-
BP10-PC31	2010	507095.32	7880483.02	432.63	-	B&P forams	612-620	7140 ±120	7267 ±130	7270 ±130	-
2004-804-0008	2004	403425.32	7829130.54	-	-	-	51.0-52.0	7495 ±40	7552.5	7550 ±53.5	-
2004-804-0008	2004	403425.32	7829130.54	-	-	-	71.0-72.0	7860 ±50	7898.5	7900 ±64.5	-
2004-804-0008	2004	403425.32	7829130.54	-	-	-	111.0-112.0	7950 ±55	7993	7990 ±74	-
2004-804-0008	2004	403425.32	7829130.54	-	-	-	151.0-152.0	11875 ±40	12971.5	12970 ±111.5	-
2004-804-0008	2004	403425.32	7829130.54	-	-	-	201.0-203.0	8360 ±30	8397.5	8400 ±51.5	-
BH34+00	1985	516587.40	7738517.53	-	-	Peat	23.6	5580 ±80	6355 ±59	6360 ±59	-
BH34+00	1985	516587.40	7738517.53	-	-	Wood fragments	23.75	6210 ±100	7125 ±123	7130 ±123	-
BH38+00	1985	519383.22	7741382.58	-	-	Plant debris	12.55	9470 ±100	10688.5 ±112.5	10690 ±112.5	-
BH15+00	1985	510712.15	7742386.58	20.5	-	Wood in marine seds	20.5	3530 ±80	3800.5 ±103.5	3800 ±103.5	B-9501
87NAH-39	1987	471157.04	7730661.65	-	-	Marine bivalve	7.3	1520 ±60	663 ±66	660 ±66	-
87NAH-48	1987	475423.43	7732267.37	-	-	Marine bivalve	8.4	1460 ±50	604 ±51	600 ±51	-
87NAH-60	1987	482336.21	7734901.02	-	-	Marine bivalve	10.8	2360 ±60	1481 ±88	1480 ±88	-
87NAH-75	1987	493893.62	7734247.39	-	-	Marine bivalve	8.6	1850 ±50	980 ±68	980 ±68	-
87NAH-81	1987	492741.46	7737020.67	-	-	Marine bivalve	8.6	1600 ±50	721.5 ±60.5	720 ±60.5	-
CL01	2009	456015.40	7863563.30	890	623	Foraminifera	590-592	11570 ±40	12635.5 ±49.5	12635 ±49.5	UGAMS# 6057
CL03	2009	457098.80	7837297.80	469	-	Foraminifera	125-129.5	2190 ±25	1314.5 ±43.5	1314 ±43.5	UGAMS# 6051
CL03	2009	457098.80	7837297.80	469	-	Foraminifera	140-142	7750 ±30	7791 ±63	7790 ±63	UGAMS# 6049
CL03	2009	457098.80	7837297.80	469	-	Foraminifera	142-144	7640 ±30	7680.5 ±57.5	7680 ±57.5	UGAMS# 6050
CL04	2009	461338.67	7832236.83	202	-	Foraminifera	93-100	2200 ±25	1322 ±44	1322 ±44	UGAMS# 6052
CL04	2009	461338.67	7832236.83	202	-	Foraminifera	135-139	8040 ±30	8079.5 ±60.5	8080 ±60.5	UGAMS# 6053
CL07 152	2009	464590.90	7828387.90	76	-	Shell	152	5380 ±40	5332 ±80	5330 ±80	Beta - 273329
CL07 262	2009	464590.90	7828387.90	76	-	Shell	262	6090 ±40	6079 ±78	6080 ±78	Beta - 273330
CL09	2009	473995.80	7840761.40	647	444	Foraminifera	421-423	8740 ±40	8813 ±16	8813 ±16	UGAMS# 6103
CL25	2009	458952.80	7848718.70	640	-	Foraminifera	322.5-324	5370 ±40	5316.5 ±86.5	5320 ±86.5	Beta - 273325
CL25	2009	458952.80	7848718.70	640	-	Foraminifera	75-81	2620 ±30	1794.5 ±64.5	1790 ±64.5	UGAMS# 6048
CL41	2009	438796.40	7848440.80	1253	422	Foraminifera	39-41	5800 ±40	5760 ±78	5760 ±78	UGAMS# 6055
CL41	2009	438796.40	7848440.80	1253	422	Foraminifera	200-202	9820 ±40	10237.5 ±62.5	10240 ±62.5	UGAMS# 6054
CL41	2009	438796.40	7848440.80	1253	422	Foraminifera	344-346	7420 ±30	7499 ±47	7500 ±47	UGAMS# 6056

Table B.2: Sedimentation rates for cores located within undisturbed strata.

Core Number	Year	Water Depth (m)	Sample Depth BSF (cm)	Depth of H4 BSF (cm)	Calibrated C ₁₄ Date	Sedimentation Rate: H4 (19000 years) to C ₁₄ Date (cm/ka)	Sedimentation Rate: C ₁₄ Date to Seafloor (cm/ka)
BP10-PC01	2010	485	120	6320	1820	326.3	65.9
BP10-PC02	2010	684.5	513	2740	14288	117.2	35.9
BP10-PC24	2010	909	236	2480	14290	118.1	16.5
2004-804-803	2004	218	224.08	11600	4200*	610.5	53.4
CL01	2009	890	591	2560	12635.5	103.6	46.8
CL25	2009	640	323.25	3700	5320	177.7	60.8



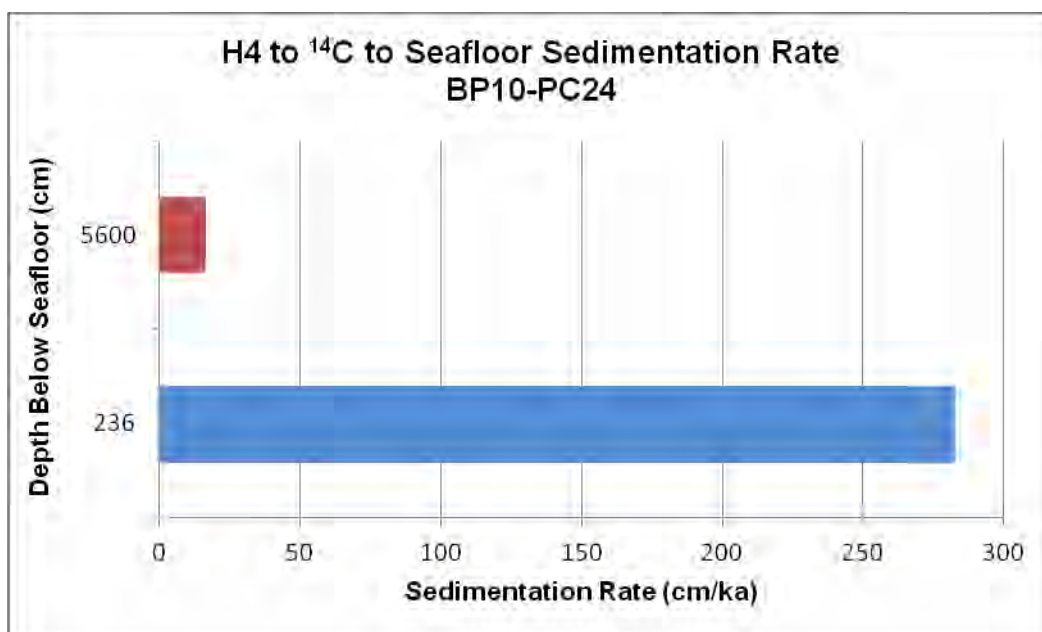
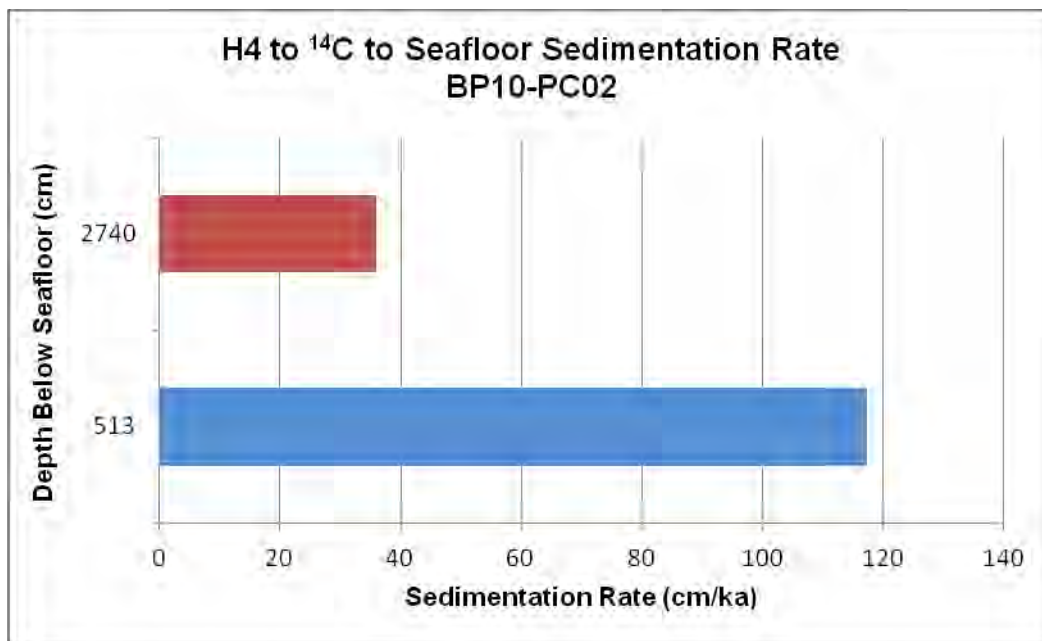
Legend



¹⁴C Date to
Seafloor



H4 to ¹⁴C
Date



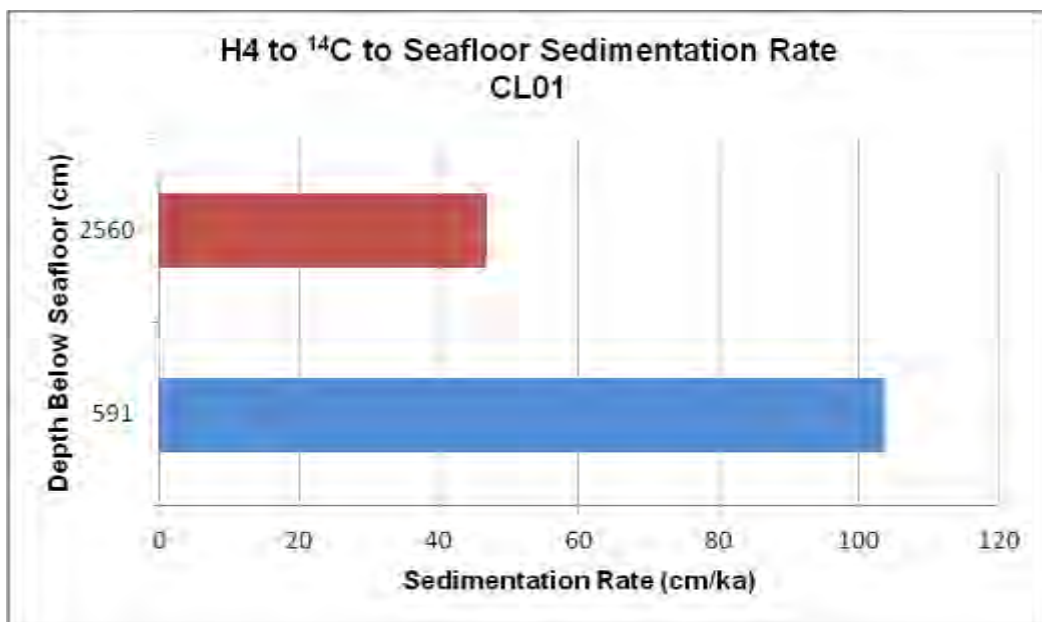
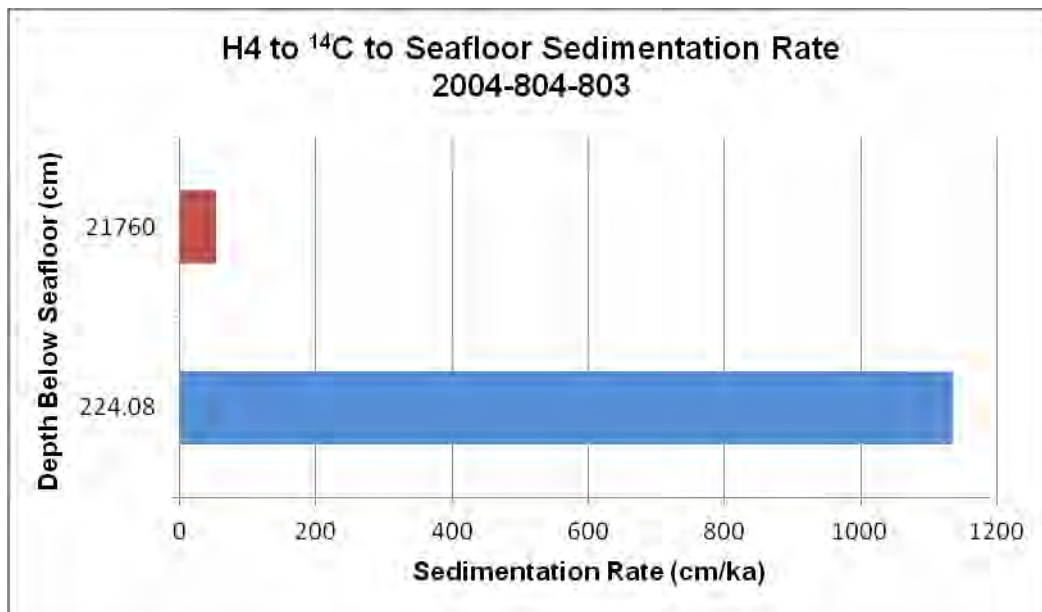
Legend



**¹⁴C Date to
Seafloor**



**H4 to ¹⁴C
Date**



Legend



¹⁴C Date to Seafloor



H4 to ¹⁴C Date

